Multi-omics based characterization of various stress responses in *Bacillus subtilis*

I n a u g u r a l d i s s e r t a t i o n

zur

Erlangung des akademischen Grades
Doktor rerum naturalium (Dr. rer. nat.) an der Mathematisch-Naturwissenschaftlichen Fakultät

der

Ernst-Moritz-Arndt-Universität Greifswald

Vorgelegt von

Praveen Kumar Sappa

geboren am 05.08.1986
in Tadepalligudem – India

Greifswald, 2013

Dekan: Prof. Dr. rer. nat. Klaus Fesser

1. Gutachter: Prof. Dr. rer. nat. Uwe Völker

2. Gutachter: Prof. Dr. Oscar Kuipers

Tag der Promotion: 24.04.2014

1. TABLE OF CONTENTS

1. Table of Contents 3
2. Summary 7
3. Introduction 11
3.1 Stress responses 12
3.2 Central carbon metabolism 13
3.2.1 Regulation of CCM 18
3.3 Osmoprotection 20
3.4 Genomics and Proteomics 25
3.5 Aim of the study 30
4. Materials and methods 33
4.1 List of abbreviations 33
4.2 Strains used in the study 34
4.3 Biphasic batch fermentation (performed by Dr. Beate Knoke, Stuttgart) 34
4.4 Growth conditions for transcriptome analysis by tiling arrays 35
4.4.1 Growth at 37°C 35
4.4.2 Growth in the presence of 1.2 M NaCl 36
4.4.3 Growth at 16°C 37
4.4.4 Growth at 51°C 37
4.4.5 Growth in M9 37
4.5 Experiments for optimizing trypsin digestion of protein samples from sporulating *B. subtilis* 39
4.5.1 Growth in DSM media 39
4.5.2 Calculation of percentage of heat resistant endospores (heat kill assay) 39
4.6 Chemostat based cultivations (performed by Michael Kohlstedt, Braunschweig) 39
4.7 Sample harvesting for transcriptome analysis 40
4.8 RNA preparation 40
4.9 Gene expression profiling 41
4.9.1 Relative gene expression analysis 41
4.9.2 Tiling array design 43
4.9.3 Statistical and functional data analysis in Genedata Analyst 44
4.10 Protein isolation and estimation 44
4.10.1 Sample harvesting and preparation of protein lysate by cell disruption 44
4.10.2 Determination of protein concentrations by Ninhydrin assay 45
4.10.3 Determination of protein concentrations by Bradford assay 45
4.11 Proteolysis and purification of proteome samples 46
4.11.1 Proteolysis by trypsin 46
4.11.2 Purification and in-gel digestion of the proteins 46

4.11.3 Desalting of peptides by ZipTip® 47
4.12 Mass spectrometry 47
4.12.1 MS parameters –LTQ Velos Orbitrap 47
4.12.2 MS parameters –TSQ Vantage 48
4.12.3 Data analysis 48
4.13 Absolute protein quantification by Multiple Reaction Monitoring (MRM) 49
4.13.1 Design of the QconCATs 49
4.13.2 MRM method development 49
4.14 Enzyme activity assays (performed by Michael Kohlstedt, Braunschweig) 57
4.15 Metabolome analysis (performed by Hanna Meyer, Greifswald) 57
4.16 13C Metabolic flux analysis (performed by Michael Kohlstedt, Braunschweig) 59
4.16.1 Visualization of multi-omics data sets and pathway mapping. 59
5. Results 60
5.1 Trypsin digestion optimization for the samples obtained from sporulating *B. subtilis* 60
5.2 Multi-omics profiling of *B. subtilis* during the transition from growing to non-growing state 64
5.2.1 Transcriptome profiling of *B. subtilis* in tri-phase fed-batch fermentation 64
5.2.2 Multi-omics analysis of *B. subtilis* in bi-phase batch fermentation 67
5.3 Whole-transcriptome analysis of *B. subtilis* at high temperature, low temperature, high salt and during glucose starvation 76
5.4 Multi-omics study of osmostressed- and osmoprotected *B. subtilis* under glucose limiting conditions 80
5.4.1 Analysis of transcriptional changes 82
5.4.2 Multi-omics investigation of the central carbon metabolism 85
5.4.3 Effect of glycine betaine during exponential growth and osmoprotection 93
5.4.4 Comparative analysis of the central carbon metabolism during osmostress and osmoprotection at high and low glucose 103
5.4.5 Effect of ProH and ProJ over-expression and glutamate supplementation onto the osmo-adaptation of *B. subtilis* 107
5.4.6 The effect of glutamate supplementation on osmoadaptation of *B. subtilis* 112
6. Discussion 114
6.1 Multi-omics profiling of *B. subtilis* during the transition from growing to non-growing state. 114
6.2 Multi-omics analysis of *B. subtilis* cultivated in bi-phase batch fermentation 117
6.3 Whole-transcriptome analysis of *B. subtilis* at high temperature, low temperature, high salt and during glucose starvation 122
6.4 Multi-omics study of osmostressed and osmoprotected *B. subtilis* in glucose limiting conditions 125
6.4.1 Multi-omics investigation of central carbon metabolism 128
6.4.2 Effect of glycine betaine during exponential growth and osmoprotection 133
6.4.3 The effect of ProH, ProJ over-expression and glutamate supplementation 136
7. References 140
8. Supplementary tables 151

9. Affidavit / Erklärung 211
10. Curriculum Vitae 213
11. Scientific contributions 214
11.1 Publications 214
11.2 Posters 215
12. Acknowledgements 216

2. SUMMARY

The soil bacterium *Bacillus subtilis* is capable of surviving most of the ensuing environmental stress conditions. The dynamic nature of the soil habitat is manifested with varying amounts of nutrients, frequent flooding and drying and variation of other growth parameters like temperature, acidity, aeration etc. In order to survive through the wide range of challenges posed by the environment, *B. subtilis* has evolved to employ very effective and complex adaptational responses. These adaptational responses are often multi-faceted and rely on well-orchestrated regulatory and metabolic networks involving changes in gene expression, control of protein synthesis and modification and adjustments of cellular metabolism. Hence comprehensive understanding of the adaptational responses requires generation and integration of data on multi-omics level. In the current study two major stress conditions were extensively investigated: 1) energy limitation/starvation which is achieved by limiting glucose in the growth medium, 2) osmostress resulting from frequent drying out of soil which is simulated by adding 1.2 M NaCl to the growth medium. In addition to osmostress, the naturally available osmoprotectant glycine betaine (GB) was supplemented to understand the simultaneous influence of osmostress and osmoprotection on cellular physiology.

Under conditions of hyperosmotic stress, *B. subtilis* produces high amounts of proline as an osmoprotectant via ProH, ProA and ProJ enzymes from glutamate that is replenished from the tricarboxylic acid cycle (TCA), whereas ProB, ProA and ProI satisfy the anabolic requirement of proline. In both pathways ProA is the common enzyme. As the central carbon metabolism (CCM) plays an important role for osmoadaptive synthesis of proline, the main aim of this study was the multi-omics based elucidation of the regulation of CCM during osmostress (NaCl) and osmoprotection (NaCl and GB) under glucose limiting conditions in chemostat cultures. To measure absolute protein abundances by mass spectrometry, a targeted approach (SRM –single reaction monitoring) using stable heavy isotope labeled artificial standard proteins known as QconCATs was optimized and implemented in the current study. The SRM technique in combination with QconCAT provided absolute quantitative data with high dynamic range for the 45 targeted CCM proteins across all the conditions measured. The resulting data were integrated with the other omics data sets obtained by transcriptome (microarray), metabolome and flux studies.

The analysis of global transcriptional changes during osmostress and osmoprotection revealed major changes including the down regulation of genes involved in utilization of specific carbon sources and chemotaxis during osmostress, which are partially or completely restored during osmoprotection. Other changes include the induction of the general stress response and the response to iron limitation during osmostress which was further increased during osmoprotection.

The multi-omics analysis of molecules involved in the CCM revealed differences between normal growth, osmostress and osmoprotection at mRNA, protein and metabolite levels. As expected, high amounts of proline were synthesized during osmostress. This was achieved by the significant increase in flux towards proline from the TCA and an increase of ProJ and ProH in both mRNA and protein amount, whereas ProA mRNA and protein remained almost unchanged. Though ProA was not regulated, the ProA protein was always present in higher amounts compared to the other proline metabolic enzymes and was thus sufficient to sustain proline synthesis during osmostress condition. However during osmoprotection all enzymes of proline biosynthesis were present in higher amounts, whereas the mRNA levels remained unchanged. This observation could be explained by the biophysical properties of GB that can promote protein stabilization by enhancing protein aggregation/complex formation. Similar observations could be made in a proteome analysis of a corresponding shake flask experiment under glucose excess conditions, in which 45 proteins previously described as unstable were stabilized in the presence of GB either during standard growth or at high osmolarity.

Detailed analysis of the CCM during simultaneous glucose limitation and osmostress revealed an upregulation of most of the genes and proteins involved in glycolysis. The part of the TCA cycle from oxaloacetate to 2-oxoglutarate, which supplies glutamate for proline biosynthesis was up-regulated, whereas the rest of the TCA cycle was either unchanged or down regulated. Though the protein concentrations of many enzymes increased, the flux through the core CCM was unaffected, a phenomenon that could be explained by the reduced catalytic activity of the enzymes at high intracellular ion (K^+) concentration due to osmostress. Furthermore, the levels of many of the measured proteins further increased when GB was added to salt-stressed cells. This observation can be explained by the biophysical properties of GB and was most pronounced for the proteins known to interact within the CCM (e.g., CitZ, Icd, Mdh, PckA). On the other side during osmostress in the presence of excess glucose, proteins of the core CCM were not up-regulated in contrary to the observation during osmostress at low glucose. During osmostress at

high glucose the proteins of the CCM were already present at higher abundance to catalyze the degradation of excess glucose available; therefore the loss of catalytic activity of the CCM proteins due to osmostress was compensated with higher protein abundances. But the influence of osmostress on proline biosynthetic enzymes was similar whether the glucose concentration was low or high.

Osmostressed *B. subtilis* grew four times slower compared to normal growth conditions, even in the presence of excess glucose. Therefore, the limiting factors like the levels of ProH and ProJ and the glutamate availability were investigated. The overexpression of ProH and ProJ enzymes did not enhance growth of *B. subtilis*; furthermore the osmoadaptive production of proline did not increase to the same extent as the ProH and ProJ enzyme concentrations. This observation suggested that glutamate availability or the activity of these enzymes or ProA, the third enzyme involved in proline biosynthesis, might be the limiting factor. Supplementation of excess glutamate during osmostress could partially improve the growth rate, but the amount of the osmoprotective enzymes ProJ and ProH remained unchanged, whereas the anabolic route of proline biosynthesis (ProB and ProI) was up-regulated indicating a feed forward regulation.

As part of a joint study conducted by the BaCell-SysMO and BaSysBio consortia which aimed for the genome wide mapping of transcription units and previously unannotated RNAs of *B. subtilis* by means of tiling array hybridizations, we provided mRNA samples from growth at high and low temperatures (51°C and 16°C) and in the presence of 1.2 M NaCl, shake flask experiments during transition from exponential growth to the stationary phase, and high density batch fermentation. The results showed that glucose starvation influenced the highest number of genes compared to all other stress conditions, which was mainly due to strong upregulation of sporulation genes, which were not severely affected by the other stress conditions. Furthermore, there was very little overlap between the regulated genes in each of the tested conditions pointing to the diversity of the adaptational strategies employed by *B subtilis.*

Time course analysis of exponentially growing *B. subtilis* and the transition to stationary phase was investigated in detail by high cell density fed-batch fermentation (glucose limitation) and batch fermentation (glucose exhaustion) with glucose as a limiting factor. Transcriptome analysis of the cells experiencing glucose limitation and glucose starvation revealed major differences and some similarities as well. Strong and transient upregulation of the SigB regulon mediating the general stress response was observed immediately after the onset of glucose

starvation whereas during glucose limitation the SigB regulon showed a rather weak and gradual increase. Sporulation response at transcriptome level was initiated within 150 to 180 minutes regardless of whether the cells entered glucose limitation or glucose starvation. A multi-omics analysis of the CCM for the batch fermentation was performed and the time course data was integrated and visualized. This analysis provided valuable insights into the dynamic changes between mRNA, proteins and metabolites.

In conclusion, pathway based multi-omics data were generated, integrated and visualized as a prerequisite for systems biology approaches and for a better understanding of the complex adaptational responses of *B. subtilis*.

3. INTRODUCTION

Bacillus subtilis is a non-pathogenic, rod shaped Gram-positive bacterium belonging to the most ubiquitous and diverse genus *Bacillus* that was discovered in 1872 (Cohn F.E, 1872). *B. subtilis* is an omnipresent bacterium found in a various habitats like water, soil, air, decomposing plant residue, intestinal tract of animals [11]. The type strains for *B. subtilis* are the Marburg strain NCTC3610 (National Collection of Type Cultures, London, GB) and ATCC6051 (American Type Culture Collection, Rockville, USA). Subsequent mutations to the strain ATCC6051 by ultraviolet and X-ray radiations led to the development of the strain commonly used laboratory strain 168 which is auxotrophic for tryptophan [12].

B. subtilis was the first nonpathogenic microorganism which was genetically transformed by Spizizen *et al.*[13] in 1961. Therefore, *B. subtilis* evolved to be a model organism for Gram-positive bacteria and holds an equivalent status as that of *Escherichia coli* which is a model organism for Gram-negative bacteria. The analysis of the complete genome of *B. subtilis* containing approximately 4200 genes started after the publication of the complete genome sequence by Kunst and coworkers in 1997 [14], which was recently updated by Barbe *et al.* 2009 [15] and Belda *et al* 2013 [16]. Analysis of several knock out mutants identified 271 genes to be essential for *B. subtilis* [17]. These studies also helped to raise interesting biological questions that subsequently led to understanding several genetic aspects of *B. subtilis*.

In addition to the scientific interests, the metabolic diversity of the members of the genus *Bacillus* led to profound usage in industrial processes like the production of carbohydrates, proteases and other enzymes. The most industrially prominent bacteria of the genus *Bacillus* are *B. licheniformis, B. pumilus, B. amyloliquefaciens* and *B. mojavensis* [18-20]. *B. subtilis* is one of the preferred workhorses among other bacteria because of its ability to acquire natural competence for the uptake of plasmid as well as the chromosomal DNA. This genetic property is exploited to understand and characterize the molecular phenotype and for the production of various extracellular enzymes like α-amylase, dextranase, bio-surfactants and antibiotics etc. [21, 22] that have a high commercial importance. *B. subtilis* is also widely used in probiotic food products and in food processing industries leading to the approval of GRAS (generally regarded as safe) status by the US food and Drug Administration (FDA).

3.1 STRESS RESPONSES

B. subtilis has a complex lifecycle as it often encounters wide range of environmental stress conditions. In order to sustain in different conditions in its habitat, *B. subtilis* exhibits a very sophisticated network of adaptational responses. Depending on the availability of the nutrients *B. subtilis* can enter into one of the three main different genetic programs. These responses include entry into the stationary phase, which is comparable to the laboratory shake flask culture where a large number of stress dependent genes are regulated including morphological changes like motility. The second response is the development of competence which involves the binding, processing and internalizing of exogenous high molecular weight DNA[23]. When the two main alternative strategies fail, *B. subtilis* can enter the third and last ultimate response known as sporulation which is a highly organized process of the vegetative cell differentiating into dormant, dry and tough endospore resistant to most of the environmental stress conditions[24]. Apart from these, other kind of stress responses includes biofilm formation, antibiotic production and cannibalism etc.

All the above mentioned response strategies adopted by *B. subtilis* are a result of well-orchestrated global gene expression network controlled by various sigma factors associated to its core RNA polymerase. The sigma factor A (σ^A) functions as general and housekeeping sigma factor and the rest of the sigma factors are considered as alternate sigma factors with specialized functions. The major alternate sigma factors in *B. subtilis* are SigB. SigD, SigH, SigL, SigW, SigE, SigF, SigG, and SigK[25]. The last four sigma factors (SigE, F, G and K) and SigH (early sporulation genes) are mainly involved in sporulation. SigL is involved in expression of degradative enzymes and metabolism of alternate carbon sources. SigD is involved in motility and chemotaxis. SigW along with few other sigma factors provide resistance to antimicrobial compounds [26]. SigB is the factor controlling the general stress response and receives signal cues from both energy and environmental stress responses[4].

Apart from these sigma factors there are several other DNA binding proteins that induce or repress the expression of their target genes in a given condition. The major pleiotropic transcriptional regulators in *B. subtilis* are CcpA, CcpN, TnrA and CodY. While CcpA and CcpN play an important role in carbon metabolism, TnrA regulates the nitrogen metabolism (discussed later in detail). CodY regulates branched chain amino acid synthesis, degradation of histamine and asparginine, competence, motility and sporulation [27]. The stringent factor RelA (ribosomal associated protein) indirectly regulates several genes involved in protein translation

and amino acid biosynthesis [28]. Accumulation of uncharged tRNAs at A site of ribosomes triggers the RelA dependent synthesis of (p)ppGpp that binds to RNA polymerase and inhibit the transcription of several genes that mainly code for components of the translational apparatus (rRNA, tRNA, elongation factors etc.) which is known as stringent response [28, 29].

3.2 CENTRAL CARBON METABOLISM

The central carbon metabolism (CCM) is an important fundamental component of metabolic network in all-living organisms. CCM consists of glycolysis, pentose phosphate pathway, tricarboxylic acid (TCA) cycle and other anaplerotic reactions that replenish the consumed metabolic intermediates. The major role of the CCM is to harnesses the chemical energy stored in carbohydrates for the production of precursors required for the biosynthesis of macromolecules (proteins, peptidoglycans, DNA, RNA, lipids etc.,) and for the production of energy currency of the cell i.e. ATP and NADH.

Glycolysis involves sequential conversion of glucose into pyruvate. Two German biologists Hans and Eduard Buchner brothers in 1897 using yeast lysate mentioned a first indication of glycolysis. Later in 1905, Harden and Young together reported ethanol production and proved that phosphate is required for the fermentation process using Yeast lysate. By 1940 all of the reactions of the glycolysis pathway were known from the research of Embden, Meyerhof, Parnas and Warburg, thus glycolysis is also known as the Embden-Meyerhof pathway as well. In 1937 Hans Krebs discovered a cyclic sequence of reactions that explained the oxidation of an unidentified ‘triose’ derived from glycolysis in pigeon breast muscle[30]. This pathway was later named as Krebs cycle or Citric acid cycle or Tri-Carboxylic Acid cycle (TCA cycle).

Glucose is the preferred source of carbon for most of the living organism including *B. subtilis*, as glucose can enter CCM directly without any further modifications. But availability of free glucose in natural habitat is often a rare scenario, so *B. subtilis* is able to secrete extracellular enzymes like amylase, gluconases etc., to degrade polysaccharides like amylase, glucans etc., into more simple monosaccharaides like glucose. Glucose and other simple carbohydrates are then transported into the cells via an active and bifunctional transport system known as phosphoenol pyruvate-dependent sugar phosphotransferase (PTS) system [31, 32]. The PTS system is responsible for conversion and import of extracellular free glucose to glucose-6-phosphate (Glu-6-P). Intracellular glucose generated from degradation of di- or oligosaccharides

is converted to Glu-6-P by glucose kinase [33]. Glucose-6-phosphate isomerase (Pgi) performs a reversible isomerization of Glu-6-P to fructose-6-phospahte which is then phosphorylated to fructose-1,6-bis-phosphate (FBP) by 6-phosphofructokinase (PfkA) (Figure 1). One molecule of FBP is then split into two C-3 molecules, dihydroxyacetone phosphate (DHAP) and glyceraldehyde-3-phosphate (GAP) by fructose-bisphophate aldolase. Isomerization/interconversion of DHAP to GAP is done by triose-phosphate isomerase (TpiA).

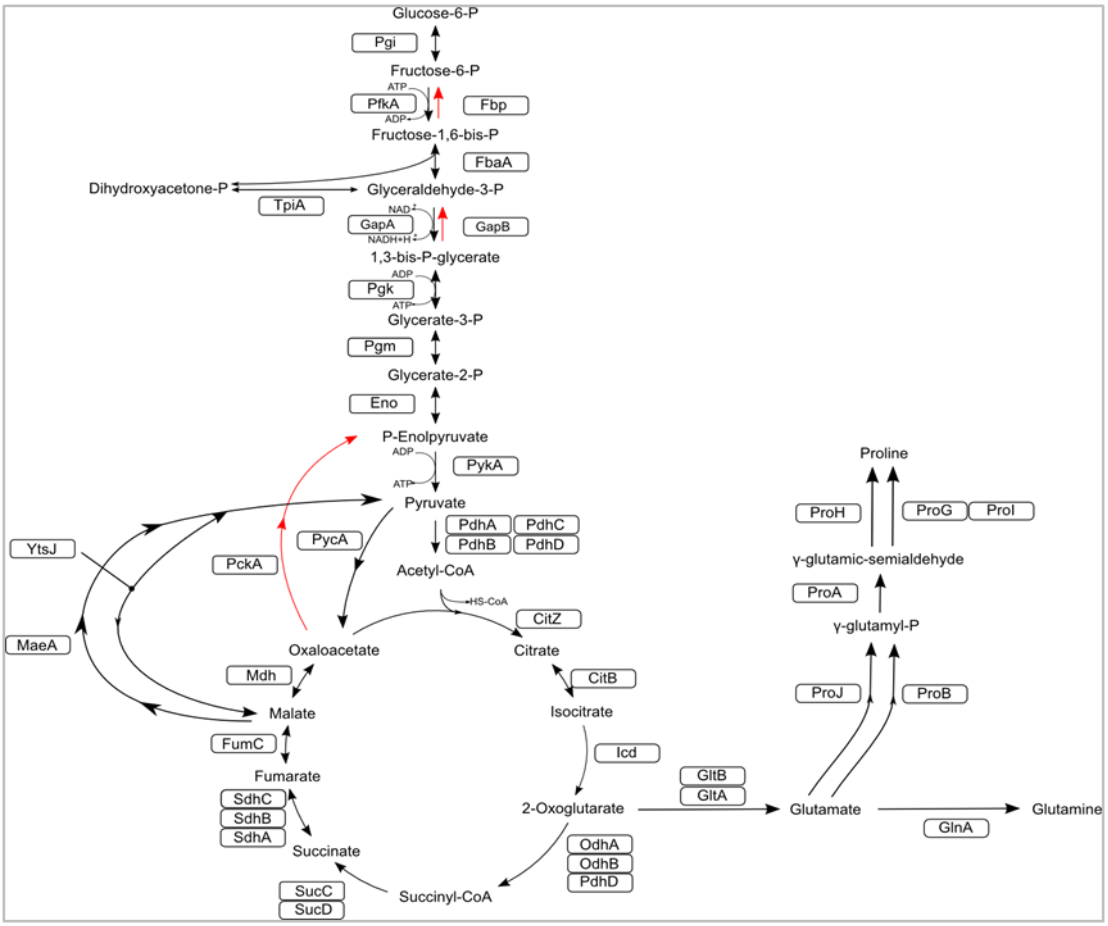

Figure 1 : Schematic representation of glycolysis, gluconeogenesis, TCA cycle and proline biosynthetic proteins in *B. subtilis*.

Subsequent enzymes required for the conversion of GAP to phosphoenol pyruvate (PEP) are encoded in a single operon *(cggR-gapA-pgk-tpi-pgm-eno)*. The first gene product of *cggR* (central glycolytic genes regulator) [34] is the repressor of this operon. This repression effect by CggR is antagonized by FBP that increases during glycolytic growth conditions[35]. Apart from CggR all other members of this operon are glycolytic enzymes, which are present in high abundance. This differential abundance is achieved by RNase Y an endoribonuclease that cleaves between mRNA of *cggR* and *gapA* generating two mature transcripts with different stabilities (Figure 2). While the transcript of *cggR* is unstable, the transcript of *gapA* is stabilized

due to the presence of stem-loop at the 5´end[36]. The final step of glycolysis involves the conversion of PEP to pyruvate mediated by pyruvate kinase. The net energy yield of glycolysis is 2 molecules of ATP and NADH for each glucose molecule.

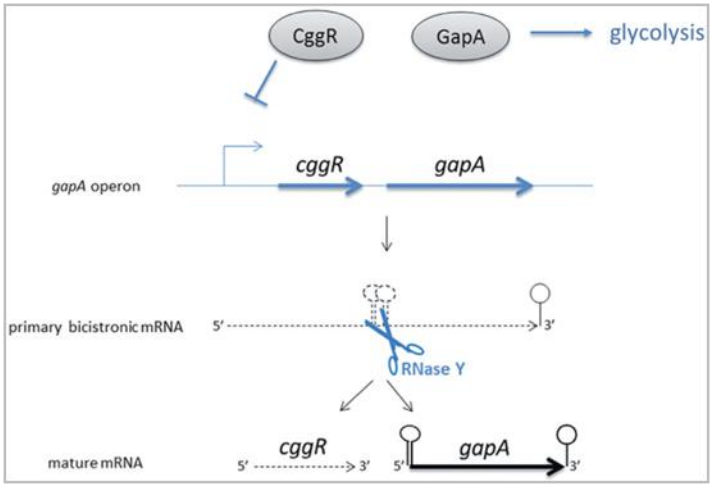

Figure 2: Stabilization mechanism of gapA mRNA. Processing of *cggR* and *gapA* transcript by RNase Y [10]. RNaseY cleaves the bicistronic transcript inbetween the two hairpin loop structures leaving behind the less stable *cggR* transcript and much stable transcript *gapA* which is protected on both ends by the hairpin structures (figure obtained from Martin *et al* 2012 [10])

When required *B. subtilis* can synthesize glucose from TCA cycle intermediates like oxaloacetate (OAA) and malate, this process is known as gluconeogenesis. Gluconeogenesis is important for *B. subtilis* when growing on TCA intermediates as the only carbon source [34, 37]. The main purpose of gluconeogenesis is to generate intermediates for anabolic growth such as glucose-6-phosphate to generate peptidoglycans (cell wall biosynthesis), also production of ribose-5-phosphate and glycerol-3phosphate via pentose-phosphate shunt pathway [38]. All the enzymes that catalyze reversible reactions of glycolysis are part of gluconeogenesis, except for the irreversible enzymes like GapA, PfkA and PykA. Conversion of OAA to PEP is catalyzed by phosphoenolpyruvate carboxykinase (PckA) (Figure 1). When malate is supplied as the only carbon source to *B. subtilis* leads to induction of gluconeogenesis via four malic enzymes that generate pyruvate[39]. Among the four malic enzymes the malate dehydrogenase(Mdh) and the NADP –dependent malic enzyme(YtsJ) are essential for the growth of *B. subtilis* when malate is the only carbon source[40]. The other two enzymes are malic enzymes (MaeA and MleA), of which MaeA is known to be expressed only in the presence of malate[39]. Catalysis of glyceraldehyde-3-phosphate is performed by glyceraldehyde-3-phospate dehydrogenase (GapB) which acts in exact opposite manner to GapA [34]. GapA is required when cell grow in glycolytic conditions, whereas GapB is required during gluconeogenic growth conditions. This differentiation is achieved for GapA and GapB by having different cofactor dependencies. While

GapA is only dependent on the co-factor NAD, whereas GapB is 50 fold more effective in presence of NADP compared to NAD [41]. De-phosphorylation of fructose-1,6-bisphosphate to fructose-6phosphate is catalyzed by fructose-1,6-bisphosphatase(fbp)[42].

Pyruvate from glycolysis has two fates: pyruvate is reduced to lactate catalyzed by lactate dehydrogenase (Ldh), with the simultaneous oxidation of one molecule of NADH[43] or the conversion of pyruvate to acetyl-CoA by pyruvate dehydrogenase complex(PdhA, PdhB, PdhC, PdhD) encoded by two operons *pdhAB* and *pdhCD*. This step generates one NADH molecule. Acetyl-CoA is then either converted to acetate by the enzyme acetate kinase (AckA), which is a part of overflow metabolism (discussed later) or enters into TCA cycle.

The first enzyme of TCA cycle is the citrate synthase (CitZ) that converts acetyl CoA and oxaloacetate from the cycle to citrate. This is an irreversible process; hence this is the rate limiting step of TCA cycle. Aconitase (CitB) catalyzes the conversion of citrate to isocitrate that is further reversibly converted to 2-oxoglutarate by isocitrate dehydrogenase (Icd). CitB is also known to be a RNA binding protein regulating iron metabolism [44].

The inter-conversion of 2-oxoglutarate to glutamate reversibly is marked as a key link between carbon and nitrogen metabolism, which is forward catalyzed by glutamate synthase (GltA and GltB known as GOGAT)[45]. Expression of GOGAT is facilitated by the binding of GltC, a transcription factor activated in the presence of glucose[46]. Repression of GOGAT is achieved in presence of the global nitrogen metabolism regulator TnrA which is activated in the absence of glutamine[47]. The reverse catalyzes of glutamate to 2-oxoglutarate is independently performed by two glutamate dehydrogenases- RocG and GudB (Figure 3A). However, *in vivo* only RocG is functionally active whereas GudB is enzymatically inactive[48]. Interestingly functional inactivation of RocG leads the *B. subtilis* to acquire spontaneous mutations that produce functional GudB[49] by an unknown mechanism. This regulatory mechanism signifies the role of glutamate in cellular metabolism. *In vivo* RocG expression is induced by the presence of nitrogen sources like arginine via two transcription factors AhrC and RocR along with the sigma factor SigL. CcpA represses RocG in presence of glucose. As glutamate is also generated by catabolism of several amino acids (including arginine, ornithine, histidine and proline), conversion of glutamate to 2-oxoglutarate creates the entry point for several amino acids into the TCA. Biosynthesis of proline is marked as the key protective mechanism when *B. subtilis* encounters hyperosmolar conditions (see below).

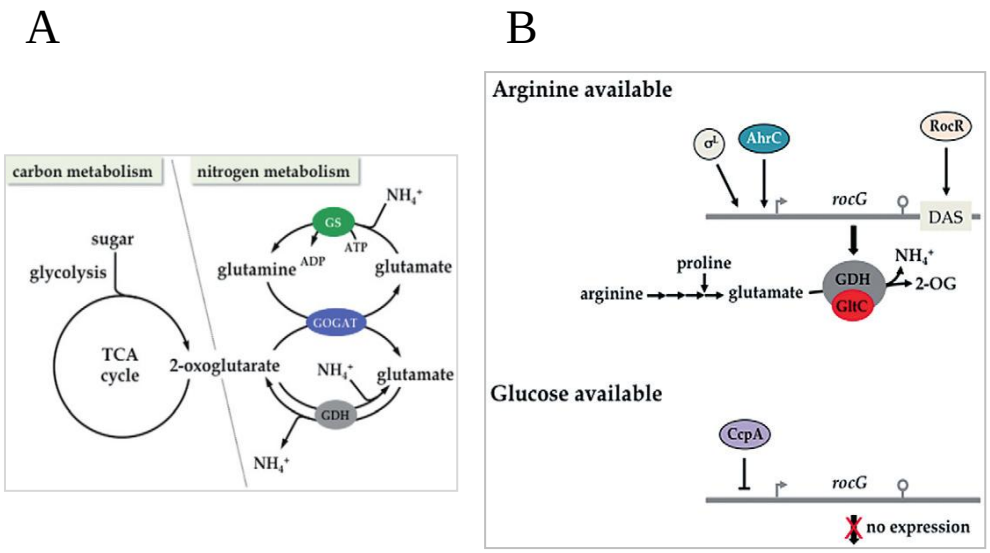

Figure 3: Regulation of nitrogen metabolisms in *B. subtilis*. A) The link between central carbon metabolism and nitrogen metabolism. B) Regulation of the gene glutamate dehydrogenase (rocG) in presence of arginine and glucose (Figure obtained from Katrin *et al* 2012 [3]).

Conversion of 2-oxoglutarate to succinyl-CoA is catalyzed by a complex of 3 subunits i.e., 2-oxoglutarate dehydrogenase (E1 subunit-OdhA and E2 subunit-OdhB) and PdhD(dihydrolipoamide dehydrogenase or E3 subunit of pyruvate dehydrogenase). Succinyl-CoA is dephosphorylated to succinate by SucC and SucD (succinyl-CoA synthase beta and alpha subunits) generating a GTP. Succinate is oxidized to fumarate by a complex of succinate dehydrogenase(SucA, SucB and SucC) generating a $FADH_2$. Fumarate is hydrated to malate by fumarase (CitG). Malate is oxidized to oxaloacetate by malate dehydrogenase (Mdh) generating a $NADH_2$ there by completing the cycle. To summarize the TCA cycle, one molecule of acetyl-coA is completely oxidized to two molecules of CO_2, yielding three molecules of NADH, one molecule of NADPH, FADH and GTP. Reducing equivalents like NADH and FADH are oxidized via oxidative phosphorylation for the production of ATP whereas NADPH is used in the anabolic reactions.

As the TCA cycle intermediates are also used for other metabolic processes, to maintain a steady state within the pathway there are several ways to replenish the metabolic intermediates. This process is known as anaplerosis. The main anaplerotic step that branches from glycolysis and replenishes OAA for sustained TCA cycle involves the conversion of pyruvate to OAA by pyruvate carboxylase (PycA) with the consumption of one ATP[50]. Oxaloacetate (OAA) is also generated from transamination of aspartate. Succinyl-CoA which is a product of β-oxidation of fatty acids is also an anaplerotic step for TCA cycle.

3.2.1 Regulation of CCM

Central carbon metabolism is a robust process which is stringently controlled depending on the extracellular nutrition and intracellular energy levels. Presence of glucose in the growth medium leads to the accumulation of fructose-1,6-bis-phosphate which is an activator of CcpA which in turn shuts down the expression of all the genes responsible for utilization of secondary carbon source, this phenomenon is termed as carbon catabolite repression(CCR)[35]. CcpA is a pleiotropic global regulator of carbon metabolism which interacts with phosphorylated forms of ATP dependent HPr(component of PTS system) and its paralogue Crh. This binding leads to strengthening the affinity of CcpA for *cre* sites (12-base pair sequence preceding promoter of target genes) and regulating the target genes. Both HPr and Crh are phosphorylated on serine by HPr kinase/phosphorylase in the presence of fructose-1,6-bis-phosphate (FBP) [32, 51]. Unlike Hpr, Crh cannot be phosphorylated on His-15 which acts as a phosphate donor during glucose import and hence Crh is not a part of phospho transfer system[52]. Glucose-6-phosphate and FBP are also known to interact directly to CcpA and affect its activity. Both the non-phosphorylated forms of Hpr and Crh (that are accumulated during gluconeogenic growth) can bind to GapA (glyceraldehade-3-phosphate) and are able to inhibit GapA activity. In addition, the non-phosphorylated form of Crh has an inhibitory role for methylglyoxal synthase (MgsA) that catalyzes the conversion of dihydroxyacetone phosphate to methylglyoxal. This step creates a bypass from glycolysis to relieve the cells from sugar-phosphate stress under surplus glucose availability which may lead to a condition where a carbohydrate uptake rate exceeds the capacity of the lower branch of the glycolysis [53].

Genes that encode CitZ, Icd together with one more gene *mdh/citH* which encodes malate dehydrogenase (Mdh) are present in one operon[54] that is repressed by CcpA, however, the aconitase gene(*citB*) is encoded elsewhere on the chromosome[55]. Transcription from the *citZ* and *citB* promoters is repressed by CcpC, a member of the LysR family of regulatory proteins. CcpC is repressed by accumulation of citrate[56]. *citB* is also repressed by CodY and by AbrB in the early stationary phase [57]. Activity of CodY is in turn dependent on cellular GTP and branched chain amino acids. To summarize, three regulatory proteins CcpC, CcpA and CodY which depend in their corresponding four metabolites citrate, FBP, GTP or isoleucine or valine respectively function together to determine the extent to which pyruvate and acetyl CoA enter the TCA cycle [58].

A recent study by Meyer *et al.* 2011[59] revealed that the proteins CitZ, Icd and Mdh that are expressed from a single operon interact with each other and from the core of the TCA cycle metabolon. A metabolon is defined as a group of enzymes from a specific pathway that might form complexes. Formation of metabolon prevents the escape of substrates and intermediates by diffusion resulting in higher efficiency of the pathways[60]. Mdh also interacts with PEP carboxy kinase (PckA) and NADH dehydrogenase, this metabolon is prominent during gluconeogenesis. Isocitrate dehydrogenase (Icd) also interacts with glutamate synthase (GltA and GltB), this interaction leads to the channeling of 2-oxoglutarate from Icd to GltA and GltB[59]. Glycolytic enzymes like PfK, Pgm and Eno are also known to from a metabolon[61].

Presence of Glucose in the growth medium also leads to overflow metabolism caused by the repression of TCA cycle. This leads to accumulation of pyruvate and acetyl CoA which are converted to lactate, acetate and acetoin and excreted into the extracellular environment[58]. Conversion of acetyl-CoA to acetate by phosphotransacetylase and acetate kinase generates an additional ATP. However, *B. subtilis* cannot survive with acetate as the sole carbon source due to the absence of glyoxylate pathway[62]. Conversion of pyruvate to lactate by the enzyme lactate dehydrogenase regenerates the co factor NAD^+ required by the glycolytic enzymes for substrate oxidation; this process is also familiar in humans for causing muscle fatigue during rapid exercise. Later when the glucose is depleted both lactate and acetate are reimported and introduced to TCA cycle for the production of more NADH and ATP. Thus, the main advantage of the overflow metabolism is to replenish NAD^+ and sustain continued glycolysis during two possible conditions; availability of excess glucose and nitrogen[63], unavailability of terminal electron acceptors like oxygen and nitrogen[43]. In *B. subtilis* overflow metabolism is regulated by the global regulators CcpA and CodY. Mutants of TCA cycle enzymes are able to grow vegetatively with reduced growth rate but sporulation efficiency is significantly decreased. The decrease in sporulation is due to the reduced energy supply, availability of intermediates and phosphorylation of Spo0A is effected which is a key regulatory protein for sporulation [64, 65].

Enzymes that exclusively participate in gluconeogenesis are repressed in the presence of glucose. Expression of PckA and GapB is strongly repressed in the presence of glucose by the regulator CcpN as the expression of these two gluconeogenic enzymes is futile to the glucose flux. As CcpN is constitutively expressed, it can sense the energy charge state of the cell by sensing the ATP/ADP levels thereby enhancing/decreasing the repression effect over its target genes[66]. CcpN competes with RNA polymerase there by inhibits expression of its target genes. A change in the confirmation in the presence of ADP can relieve CcpN from RNA polymerase and

activating its target genes expression. Hence CcpN is very essential in maintaining carbon flux through CCM.

The other important enzyme of gluconeogenesis Fbp(fructose-1,6-bis phosphatase) is a constitutively expressed protein and is not subjected to catabolite repression[42]. Interestingly, an *fbp* mutant strain of *B. subtilis* is able to grow on gluconeogenic carbon sources such as glycerol and malate, however, no paralogue of Fbp enzyme has been found till date[42]. Adding to this, the *fbp* gene from *B. subtilis* has no orthologs in any other species [42].

3.3 OSMOPROTECTION

High salinity and fluctuating temperature are common conditions encountered by *B. subtilis* being a soil bacterium. Exposure of microorganisms to an environment of high salinity will result in excessive water efflux and destruction of the positive turgor (Figure 4) that is generally regarded as the driving force for cell growth and division[67]. Unlike eukaryotes, bacteria cannot actively transport water to maintain this turgor balance[68]. Thus, maintaining cytoplasmic hydration for the unhindered physiological activity is of great importance, this is accomplished by accumulating compatible solutes either by biosynthesis or by active uptake. Compatible solutes accomplish osmoprotection and do not interfere with cell physiology, even at a high concentration in the cytoplasm. Osmoprotectants, such as glycine betaine, proline, proline betaine, ectoine, carnitine besides maintaining cellular turgor pressure also function as kosmotropes, compounds that stabilize the conformations of biological macromolecules [69]. In addition to their role in osmoprotection, compatible solutes were identified to possess multifaceted functions, including thermoprotection, and stabilization of proteins and cell components against the denaturing effects of high ionic strength [70, 71].

The majority of the uptake of osmoprotectants or its precursors in *B. subtilis* is realized by specific transporters (osmoprotectant uptake systems) OpuA, OpuB, OpuC, OpuD and OpuE. These transporters are either multi-component import systems in case of OpuA (OpuAA, OpuAB, OpuAC), OpuB (OpuBA, OpuBB, OpuBC, OpuBD) and OpuC (OpuCA, OpuCB, OpuCC, OpuCD) or single-component transporters for OpuD and OpuE (Figure 5A). OpuD is responsible for only glycine betaine import and OpuE is responsible for proline import alone. OpuE is highly similar to that of proline inducible PutP permeases in *E. coli* which is used to import proline as carbon and nitrogen source but not for osmoprotection, which signifies the

evolutionary conservation for the same function[68]. Deletion of OpuE leads to inability of *B. subtilis* to use exogenously provided proline during high osmolar conditions[72]. The ability to import wide range of osmoprotectants by *B. subtilis* imparts the unique flexible adaptation to various high osmolality ecological niches.

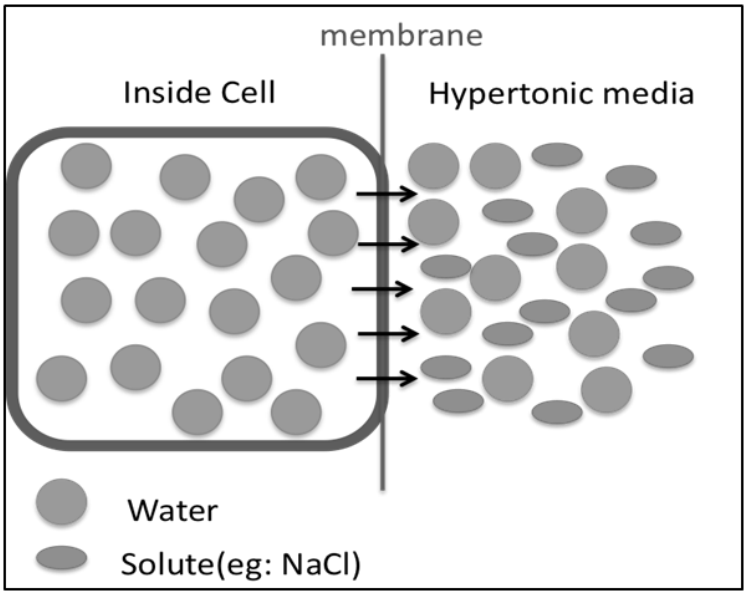

Figure 4: When the bacterial cells encounter high osmolar environment, to maintain the turgor pressure on either side of the cell membrane, cells loose water due to exo osmosis resulting in plasmolysis. To avoid plasmolysis cells accumulate osmoprotectants such as proline and glycine betaine

In vivo, the primary osmotic stress response in *B. subtilis* is to rapidly accumulate K^+ ions from the environment via two different K^+ uptake systems (KtrAB and KtrCD)[73]. However uptake of K^+ is a short-term response because high intracellular ionic strength is deleterious to cellular physiology [74, 75]. Subsequently, accumulation of K^+ ions is followed by long-term accumulation of compatible osmoprotectants like proline[76]. Proline/other osmoprotectants like glycine betaine are either imported or synthesized intracellular from glutamate in order to decrease the K+ intracellular concentration. Synthesis of proline takes place in two different ways: for anabolic synthesis and for osmoprotection [77](Figure 5B). Anabolic synthesis involves synthesis of proline from glutamate that involve three enzymes: γ-glutamyl kinase (ProB), the γ-glutamyl-phosphate reductase (ProA) and the Δ-pyrroline-5-carboxylase reductase (ProI) (Figure 5B) [78]. The activity of the ProB enzyme from *B. subtilis* is subjected to feedback control by proline [77]. The anabolic biosynthetic pathway involving *proB–proA* operon and that of the *proI* gene is regulated through a proline-responsive T-box regulatory system (RNA-based regulatory switches that regulate the levels of amino acids via

charged/uncharged tRNA) [77]. This pathway ensures that enough amount of intra cellular proline levels are maintained as building block for protein synthesis.

In addition to the anabolic pathway involving ProB–ProA–ProI enzymes, the second route for proline biosynthesis accounts for production of the large amounts of proline as an osmoprotectant[79]. This osmoadaptive proline biosynthetic route is formed by the ProJ– ProA–ProH enzymes, and relies on isoenzymes for the first and last steps. Therefore, the expression of the *proHJ* operon is strongly up-regulated in response to either sustained osmotic stress or sudden osmotic upshift, whereas that of the *proBA* operon (Figure 5C) or that of the *proA* gene alone is not osmotically induced [80, 81]. In addition to the ProI and ProH enzymes, the ProG protein also possesses D1-pyrroline-5-carboxylase reductase activity although the precise physiological regulation of the ProG protein has not been resolved yet. Data from two independent studies have shown that ProA was both cytosolic and membrane bound protein [2, 81], however the rest of the enzymes involved in the proline biosynthesis were not found in the membrane bound fraction. Steil *et al.* (2003) [80] for the first time reported the genome wide transcriptional analysis of a *sigB* mutant of *B. subtilis* during sudden osmotic upshift and adaptation to prolonged growth at high osmolarity. The authors have indicated that adaptation to sudden osmotic upshift and continuous growth at high osmolarity require different physiological adaptations by the *B. subtilis* cells as both the adaptations shared limited number of commonly regulated genes. Hahne *et al.* (2010) [81] have performed a comprehensive time course proteomic and transcriptomic analysis of *B. subtilis* during osmotic upshift. The authors reported the expression profiles for 590 proteins and 3961 mRNAs. The authors indicated that about 500 genes were up-regulated in response to osmotic upshift suggesting a dynamic physiological adaptation of *B. subtilis* towards osmotic stress.

Proline can act as a nutrient, where proline is catabolized to glutamate that is at the center of carbon and nitrogen metabolism (see above). In *B. subtilis* and other microorganisms the oxidation of proline to glutamate is catalyzed by PutB PRODH and the monofunctional PutC Δ^1pyrroline-5-carboxylate dehydrogenase (PD5CD) [82, 83] that are products of the gene cluster *putBCP*. The last gene in the gene cluster *putP* encodes for the L-proline transporter PutP [84]. PutP has high affinity for extracellular proline intake compared to OpuE. Unlike other microorganisms the regulation of *putBCP* gene cluster in *B. subtilis* is under control of the proline-responsive PutR protein encoded by the gene *putR* [83]. It was shown recently by Moses *et al.* (2012) [83] that L-proline generated as a result of osmoprotection by the ProJ-ProA-ProH pathway does not induce *putBCP,* indicating that *B. subtilis* can somehow sense the difference between *de novo* synthesized L-proline and imported extracellular L-proline.

Glycine betaine is one of the important osmoprotectants next to proline that can be imported or synthesized *de novo* in the presence of choline. Glycine betaine is a prominent osmoprotectant that is available readily in the habitat of *B. subtilis* the soil, as it is one of the products released due to degradation of the plant tissues and roots [85]. The transporters OpuA, OpuC and OpuD import glycine betaine into the cell. Mutants of these transporters were not able to import glycine betaine suggesting that these are the only transporters that can import glycine betaine in *B. subtilis* [86]. OpuA and OpuC are multicomponent transporters that belong to ABC (ATP binding cassette) type super family, whereas OpuD is a single-component transporter. All these three transporters have low Km signifying high affinity towards glycine betaine giving *B. subtilis* the ability to import glycine betaine even at very low extracellular concentrations. Even though these three transporters are expressed during osmotic upshift, OpuA contributes to the majority of the imported glycine betaine due to its high V_{max} over OpuC and OpuD [86].

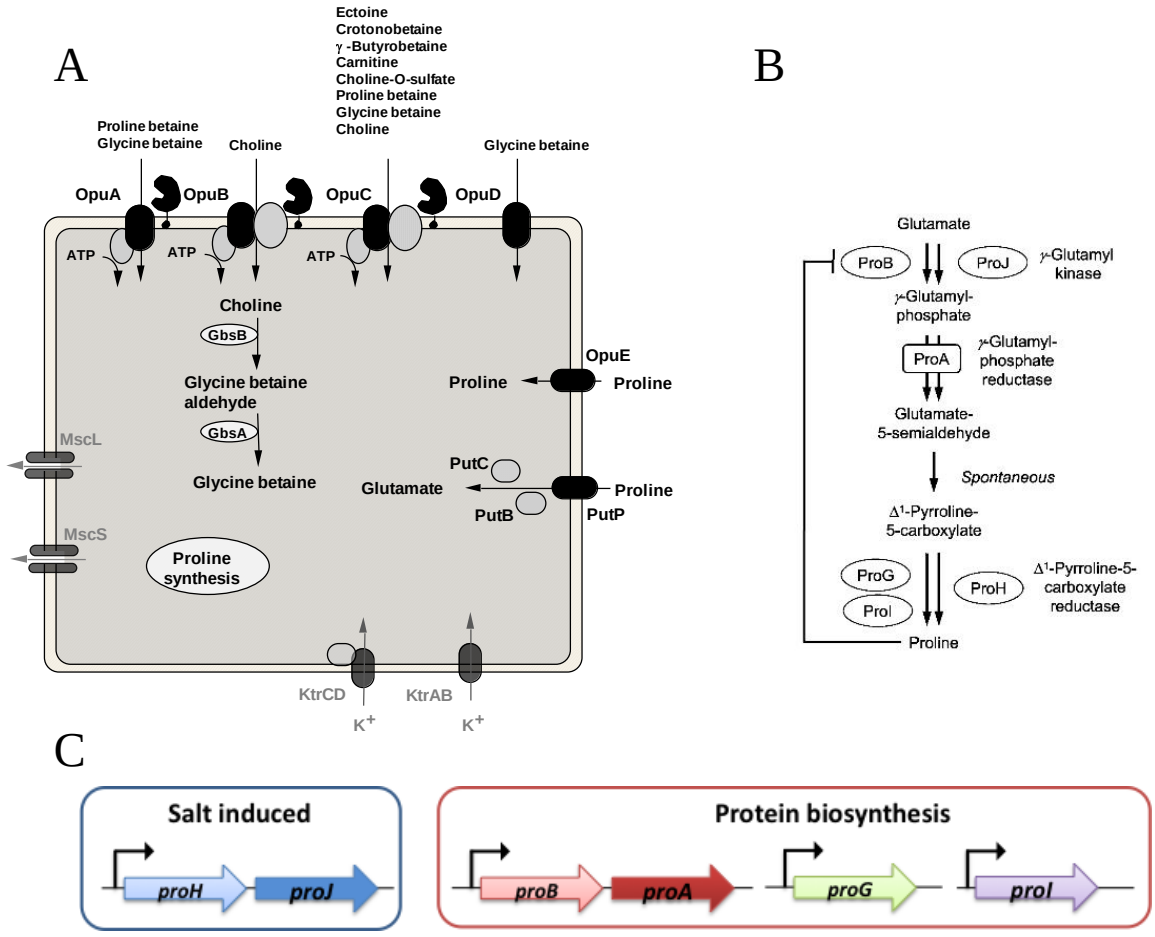

Figure 5: Osmoprotectants import mechanisms and proline biosynthetic proteins. A) Different types of transporters of osmoprotectants into the cell during osmotic stress (figure modified from Bremer *et al.* 2002 [8]). B) Enzymes involved in proline biosynthesis as a result of osmotic stress and protein biosynthesis (figure obtained from Brill *et al.*2011 [9]. C) Genetic arrangement of proline biosynthetic enzymes.

De novo synthesis of glycine betaine takes place in the presence of extracellular choline which is imported by the transporters OpuB and OpuC (Figure 5A). Imported choline is oxidized to glycine betaine in two steps that involves GbsB (choline dehydrogenase) and GbsA (glycine betaine synthesis) with glycine betaine-aldehyde as an intermediate [85]. The transcription of the operon *gbsA-gbsB* is enhanced under the presence of choline [87]. It has been shown that glycine betaine apart from being an osmoprotectant, can also offer thermo-protection at 52°C [70] and cold-protection at 13°C [88].

During osmotic down shock conditions like a rain fall or a washout, presence of intracellular osmoprotectants at high concentrations leads to influx of water into the cell there by increasing the turgor pressure inside the cells which can lead to cell lysis. *B. subtilis* overcomes this problem by employing two mechanosensitive channels MscL (large conductance) and MscS (small conductance). These channels are located on the cell membrane and they respond to changes in the tension of lipid bilayer which leads to the formation of transient aqueous pore through which solutes and solvents are released into the environment [75, 89]. This phenomenon allows *B. subtilis* to reduce the intracellular turgor and avoid cell lysis. Hoffmann *et al.*[89] have shown that the protein MscL prevents the lysis of *B. subtilis* that are osmotically down shocked during the early and mid-log phase growth period, whereas MscS is responsible for prevention of cell lysis during late log phase growth.

3.4 GENOMICS AND PROTEOMICS

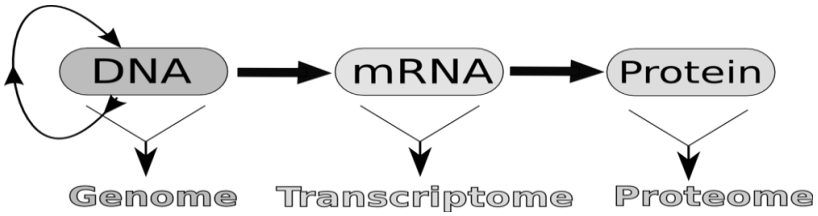

Discovery of DNA structure in 1953 by Watson and Crick and invention of DNA sequencing technique by Fredrick Sanger in 1975 laid the foundation for the development of Genomics. The term ‘omics’ is often used when a large scale and holistic approach in understanding biological mechanism of life is addressed. Transcriptomics and proteomics are two of the several omics technologies available today.

The transcriptome is the set of total messenger RNA and their quantity in a tissue type or cell type for a developmental or physiological condition and transcriptomics is the term used for studying the transcriptome. There are different methods to study transcriptomics like DNA microarrays and more advanced recent RNA-seq (next generation sequencing); considering the past two decades the most popular and established method is the DNA microarray. A DNA microarray is defined as an orderly arrangement of thousands of identified sequenced genes (probes) printed on an impermeable solid support, usually glass, silicon chips or nylon membrane. There are different types of probes used in microarray, such as fragment of genomic DNA, cDNAs, PCR products or chemically synthesized oligonucleotides (up to 70mers). A single DNA microarray slide/chip may contain thousands of probes each representing a known single gene and collectively the entire genome of an organism. Oligonucleotide DNA microarray has an advantage over cDNA and PCR based microarray due to automation, speed of manufacturing and reproducibility. DNA microarrays works on the principle of hybridization, where a fluorescently labeled cDNA is hybridized onto a custom-made microarray or commercial high-density oligo microarray [90, 91].

The latest in the series of microarray technologies is the genome-wide tiling arrays which is a high-density oligo microarray. Unlike other DNA microarrays, tiling arrays contain probes that map the whole genome or region of interest including complete sense and anti-sense strands giving this technique many advantages like mapping non-protein-coding RNAs (ncRNAs), transcription unit mapping (genome annotation), mapping of DNA methylation sites (methylome) and comparative genome hybridization [92]. Recent tiling array analysis in

B. subtilis by Rasmussen *et al.* (2009) [93] showed 3662 transcriptional active regions (TARs) and newly identified 84 non-coding RNAs and 127 antisense transcripts; this signifies the importance of tiling array in modern day transcriptomics.

While genomics represents the genotype of an organism, the other omes (transcriptome, proteome and metabolome) measure how the genome is utilized under a particular situation, which is shaped by both the genotype and the environmental conditions of the organism. The proteome is the sum of proteins expressed in an organism, tissue type or cell under any specific condition and proteomics is the term for studying the proteome. Two major methods are being used for proteomic studies: the well-established two-dimensional gel electrophoresis (2DE) developed in 1975 (Klose, O'Farrell 1975) and more modern liquid-chromatography assisted mass spectrometry methods (LC-MS/MS).

Mass spectrometry has its roots in 1912 when JJ Thomson a British physicist analyzed isotopes of Neon by the instrument "parabola spectrograph" which later became much prominent during world war II for enrichment of Uranium isotopes [94]. With the invention of MALDI (matrix-assisted laser desorption/ionization) [95] and ESI (electro spray ionization)[96] in the 1980s mass spectrometry became indispensable for the development of proteomics and other "Omics" platforms. In the context of proteomics, both MALDI and ESI convert peptides and proteins into gaseous phase as the mass spectrometers work with vacuum. The ESI (electro spray ionization) is more prominent among shotgun proteomics work flow (a complex mixture of peptides sprayed simultaneously into a mass spectrometer). In a classical 'bottom up' shot gun proteomics approach; a complex mixture of proteins from a sample is digested to peptides by a sequence specific enzyme such as trypsin. The resulting peptide mixture is separated with a binary gradient of aqueous/organic solvent in a high-performance liquid chromatography (HPLC) equipped with a C18 based reverse phase columns, the gradient lasting about one to several hours to reduce the complexity of peptides entering the mass spectrometer at any given time. On the other side top down proteomics describes the analysis of intact proteins with mass spectrometry [97], which is currently a flourishing field.

The data obtained from the mass spectrometry based proteomics can be broadly used and classified into three categories; posttranslational modifications (PTMs), protein interactions (network biology/interactome) and much extensively used expression proteomics [98]. Expression proteomics deals with the relative or absolute amounts of the proteins in a sample

and can be compared to transcriptome data, but also unique information about subcellular protein localization can be obtained using expression proteomics.

Quantification in proteomics is of central importance and is of two kinds; relative and absolute quantification. Though relative quantification delivers enough data to differentiate and compare two or several different conditions, it cannot deliver absolute value/copy number of proteins per cell- an important input for systems biology. Absolute quantification in MS can be performed by spiking in stable isotope labeled peptide/protein standards (stable isotope dilution mass spectrometry: SID-MS) into the sample and by label free approach (spectral counting[99] and intensity based). Label free approaches are more error prone compared to the label-based approach due to sensitivity and reproducibility issues[98]. Stable isotope based absolute quantification involves spiking of standards like AQUA (absolute quantification) peptides [100], absolute SILAC proteins [101] and QconCAT (Quantification concatemers)[102]. Spiking-in of heavy isotope labeled reference peptides eliminates the ion suppression effect in MS measurements due to the identical retention times and fragmentation patterns of the reference peptide and the analyte peptide [103]. Quantification of multiple proteins of interest requires several heavy labeled AQUA peptides and proteins, this also introduces multiple pipetting steps during sample processing and sometimes this may result in inappropriate estimation of protein concentration. Furthermore, AQUA peptides are added at the end of the sample processing which implies that unlike the native peptides the AQUA peptides do not undergo the same treatment procedure leading to a biased estimation of protein concentrations. This problem can be avoided by using AQUA proteins, but the AQUA proteins are very expensive and laborious to produce compared to the AQUA peptides. On the other hand, the QconCAT based absolute quantification is a more cost effective and more accurate method due to involvement of less pipetting steps while performing multiplexed quantification for several proteins.

The QconCAT strategy relies on a heavy labeled artificial protein that is an assembly of signature Qpeptides derived from multiple proteins of interest. Qpeptides are designed to end with arginine or lysine at the C terminus as they represent and will be internal standards for tryptic peptides derived from digestion of the analyte proteins [102, 104]. Known concentrations of QconCATs are spiked to a complex mixture of analyte proteins and digested with trypsin to release both the stable isotope-labeled peptide and the native peptide from the analytes. From the known concentration of spiked QconCAT in to the analyte, absolute quantification of the target analyte proteins can be achieved.

Among the available MS techniques MRM (multiple reaction monitoring) is the best approach for targeted proteomics. MRM is performed by analyzing a predefined set of unique peptides of the corresponding proteins with optimized parameters. MRM performed in combination with stable isotope dilution on a triple quadrupole mass spectrometer is a very robust method for absolute quantitative measurement of target proteins [105]. Targeted mass spectrometry always has an advantage in terms of sensitivity over discovery proteomics. A comprehensive study by Picotti *et al.* (2009) [106] in yeast proved the sensitivity and dynamic range of MRM based absolute quantification for ~100 proteins ranging from 50 to 200000 copies/cell in a single MS analysis without the need for extensive prefractionation. Costenoble *et al.* (2011) had pushed the upper limit of MRM by performing absolute quantification of 228 proteins accounting for 95% of the central carbon metabolism including isoenzymes in budding yeast [107].

After whole genome sequencing of *B. subtilis* was performed in 1997 [14], several proteome and transcriptome studies were performed in the past but only a few targeted transcriptome and proteome studies were performed simultaneously to understand the intricate physiological mechanisms adopted by *B. subtilis* to survive in various stress conditions. For the first time a comprehensive characterization of proteome and transcriptome of *B subtilis* was first done by Eymann *et al.* 2004[108] reporting a total 876 proteins and 2515 genes expressed in exponentially growing cells. Hahne *et al.* [109] performed a comprehensive studies comparing membrane proteome profiling of exponentially growing *B. subtilis*. The authors reported 527 integral membrane proteins covering up to 66% of the predicted membrane bound proteins. A recent comprehensive proteomic and transcriptome profiling of *B. subtilis* by Otto *et al.* 2010[2] reported 2142 proteins by extensive pre-fractionation of intracellular and membrane bound proteins in glucose starved *B. subtilis*.

In *B. subtilis* a large scale phosphoproteome study was performed by Macek *et al.* [110] identifying 103 protein phosphorylation sites; 54 on serine, 16 on threonine and 8 on tyrosine. Complementing the above study Elsholz *et al.* (2012) [111] demonstrated protein phosphorylation on arginine residues for 86 proteins. This study suggests the importance of the protein arginine kinase and phosphatase, MscB and YwiE respectively as regulators.

Development of techniques to analyze global scale gene and protein expression patterns provided great insight into complex cellular network organization. From the perspective of systems biology it is of great importance to have absolute quantitative data for any of the considered data sets (transcriptome, proteome, metabolome). Technological improvements to generate large scale quantitative data sets and multidisciplinary approaches during the last

decade has driven the increased interest in systems biology, a discipline encompassing data based mathematical modeling and simulation that help to understand the dynamic interactions of cells and components within cells[112]. Interest in the understanding of robust signaling networks that help *B. subtilis* to survive under changing environmental conditions has motivated numerous studies that involve mathematical modeling. A studies by Kleijn *et al.* (2010) [113] has shown through mathematical modeling of central carbon metabolism that malate is the second preferred carbon source which is co-utilized with glucose as well as the preferred gluconeogenic carbon source. The co-utilization of glucose and malate is a rare phenomenon among microorganisms as both carbon sources exert carbon catabolite repression against other carbon sources but not against each other. However, it is unclear how malate represses the uptake of other carbon sources. In a follow up multidisciplinary study, Buescher *et al.* (2012) [114] reported that adaptability of *B. subtilis* towards utilization of malate was faster primarily due to post-transcriptional regulation. On the other hand adaption towards glucose is slower primarily due to transcriptional regulation involving approximately regulation of half of the genes. The authors used comprehensive omics-based platforms such as transcriptome, proteome, metabolome, fluxome, promoter activity assays and finally integrated all the above-mentioned data to fit into a mathematical model.

Ferguson *et al.* (2012) had demonstrated the absolute quantification of promoter activity for the genes *cggR, gapB, pckA* and *ccpN*, as these genes primarily control the carbon flux in CCM [115]. The authors showed that the negative feedback regulation for strong promoters like *cggR* is not achieved by reduced transcriptional noise, rather it depends on burst size (number of mRNA molecules produced in one burst) which is proportional to the active state of the operator at the promoter. Contrarily, *ccpN* in order to maintain its repressive mechanism over *gapB* and *pckA* under glycolytic conditions has evolved to limit bursting and not allowing the RNA polymerase to escape from promoter leading to strong catabolite repression.

To summarize, advent of more sophisticated techniques in analyzing the transcriptome, proteome and metabolome in combination with mathematical modeling in recent years have enabled a deeper understanding of biological systems. Hence, in this study a combination of transcriptome, proteome and metabolome analysis will be applied to gain deeper understanding of the physiological adaptational mechanisms of *B. subtilis*. To my knowledge this is the first pathway targeted multi-omics study targeting the central carbon metabolism in *B. subtilis*.

3.5 AIM OF THE STUDY

B. subtilis is one of the best studied model organisms among Gram positive bacteria. Being a soil bacterium, the adaptational responses employed by *B. subtilis* are very complex often involving multiple regulatory networks that involve regulation of gene expression, protein expression and metabolite levels. Hence, comprehensive understanding of the complex adaptational responses deployed by *B. subtilis* requires generation and integration of data on multi-omics level. In the past only few studies have tried to understand the adaptational responses of *B. subtilis* at multi-omics level. Therefore, in the current study a multi-omics approach will be employed for a systems biology study.

Energy limitation or starvation for carbon is one of the key challenges faced by *B. subtilis* in its natural environment the soil. Hence, the time-resolved transition of *B. subtilis* from exponential phase to stationary phase will be investigated in high cell density fermentation where glucose will be the growth limiting factor.

When challenged with osmostress *B. subtilis* produces high amount of proline as an osmoprotectant from glutamate. Glutamate is mainly replenished from 2-oxoglutarate from the TCA cycle. Hence, central carbon metabolism and glucose play a crucial role during the osmostress. Therefore, a workflow for measuring mRNA, proteins and various metabolites involved in the central carbon metabolism and proline biosynthesis will be established and the data will be integrated for the better understanding of the adaptational responses. As a proof of concept, two major stress conditions will be simultaneously investigated in a controlled chemostat based cultivations. The conditions that are going to be investigated are 1) energy limitation which will be achieved by limiting glucose in the growth medium, 2) osmostress resulting from frequent drying out of soil will be achieved by adding 1.2 M NaCl to the growth medium. In addition to osmostress, the effect of naturally available osmoprotectant glycine betaine (GB) under simultaneous influence of osmostress and osmoprotection on cellular physiology will be investigated. Influence of high glucose concentration during osmostress and osmoprotection will also be investigated.

Information about the absolute protein abundances with in a pathway will contribute to a better understanding of the adaptational mechanisms of *B. subtilis*. Hence, a method to quantify

absolute concentrations for the proteins involved in the central carbon metabolism and proline biosynthesis will be developed and implemented.

Complementing these experiments, global transcriptome analysis of other major stress conditions like growth at high temperature, low temperature, high salinity and late stationary phase will be performed to understand the transcriptional plasticity under different stress conditions in general.

4. MATERIALS AND METHODS

4.1 LIST OF ABBREVIATIONS

ACN	Acetonitrile
ANOVA	Analysis of variance
ATP	Adenosine triphosphate
BSA	Bovine serum albumin
CCM	Central Carbon Metabolism
CCR	Carbon Catabolite Repression
cDNA	copy DNA
Cy3/Cy5	Fluorescent dyes of the cyanine dye family
Dnase I	Deoxyribonuclease I
DTT	Dithiothreitol
EDTA	Ethylenediaminetetraacetic acid
FBP	Fructose-1,6-bisphosphate
FWHM	Full Width at Half Maximum (Resolution)
GB	Glycine Betaine
GTP	Guanosine TriPhosphate
IAA	Indoleacetic acid
LC-MS	Liquid Chromatography–Mass Spectrometry
PAGE	Polyacrylamide gel electrophoresis
PCA	Principal component analysis
QconCAT	Quantification concatamer
QQQ	Triple quadrupole mass spectrometer
SDS	Sodium dodecyl sulfate
Sig	RNA polymerase sigma factor
SRM/MRM	Selected Reaction Monitoring / Multiple Reaction Monitoring
TCA cycle	Tricarboxylic acid cycle
TE	Tris-EDTA
TPP	Trans-Proteomic Pipeline
UTP	Uridyl triphosphate

4.2 STRAINS USED IN THE STUDY

Table 1 : *B. subtilis* strains used in the current study.

Strain	Genotype	Construction	Phenotype	Reference
BSB1		Trp^+ derivative of *B. subtilis* 168	Trp+	[114, 116]
MO1027	*trpC2 pheA1 spoIVCB::erm*		Trp^- Spo^-	P. Stragier
BSG 112	*spoIVCB::erm*	Transformation of BSB1 with chromosomal DNA of MO1027	Trp^+ Spo^-	Current study
JH642	*trpC2 pheA1*		Trp^-	Laboratory stock (E. Bremer, Marburg)
MDB22	*trpC2 pheA1 ΔproHJ amyE::P(proHwt)-proH-proJ*	Details in results section 5.4.5	Trp^-	Current study (Marburg)
MDB28	*trpC2 pheA1ΔproHJ amyE::P(proH-M10)-proH-proJ*	Details in results section 5.4.5	Trp^-	Current study (Marburg)

4.3 BIPHASIC BATCH FERMENTATION (PERFORMED BY DR. BEATE KNOKE, STUTTGART)

Precultures with 100 mL of LB medium (erythromycin – 1 µg/mL) was inoculated with the *Bacillus subtilis* strain-BSG112 and incubated for 4h at 37°C at 130 rpm orbital shaking. The batch fermentation was carried out in a 30 L bioreactor (Bioengineering AG) using minimal medium according to Hardiman *et al.* 2007 [117] but without thiamin-HCl, a reduced calcium concentration (7% [w/v]) and addition of 0.6 mg l^{-1} sodium molybdate (Na2MoO4 * $2H_2O$). The following process parameters were applied: dissolved oxygen concentration > 50% saturation, pH 7, pressure of 0.5 bar, temperature of 37°C. The gas inflow (*V*G =10 l min^{-1}) was monitored by a mass flow meter (Bioengineering AG) and foam formation was suppressed by the addition of polypropylene glycol P 2000 (Sigma–Aldrich) when necessary. Samples were taken at mid-log phase (OD600nm 1.7; t0) and 1.5 h and 5 h after glucose exhaustion (t1 and t2, respectively).

BM5 (batch medium): (10x per liter)

BM5 (10x)	**Quantity**
Na_2SO_4 * 10 H_2O	20 g
$(NH_4)_2SO_4$	26.8 g

$N1H_4Cl$	10 g
$NaH_2PO_4.2H_2O$	40.2 g
K_2HPO_4	146 g

Autoclave and store at RT.

Trace elements (100x per liter):

Trace elements(10x)	Quantity
$CaCl_2.2H_2O$	1.0 g
$FeCl3.\ 6H_2O$	16.7 g
Na_2 – EDTA	20.1 g
$ZnSO_4.7H_2O$	0.18 g
$MnSO_4.H_2O$	0.1 g
$CuSO_4.5H_2O$	0.16 g
$CoCl_2.6H_2O$	0.18 g
$Na_2MoO_4.2H_2O$	0.2 g

BM5 (1x) (1000 mL)	
H_2O HPLC	870 mL
BM5 10 x stock	100 mL
trace salts 100x stock	3 mL
Glucose 20% (w/v)	25 mL
1 M $MgSO_4$	2 mL

4.4 GROWTH CONDITIONS FOR TRANSCRIPTOME ANALYSIS BY TILING ARRAYS

4.4.1 Growth at 37°C

Cultivations were performed as mentioned by Steil *et al.* (2003) [80]. Briefly, *B. subtilis* was grown for 24 h on a LB plate at 37°C and used to inoculate 100 mL of overnight Spizizen's minimal medium (SMM) media in a 500 mL-Erlenmeyer bacterial culture flask. Flasks were aerated by shaking at 220 RPM at 37°C in an orbital shaker (Innova 4230, New Brunswick, USA). A fresh 100 mL SMM (pre-culture) was inoculated to an optical density (OD) of 0.1 at 578 nm from the overnight cultures. After these pre-culture reached an OD_{578} of 0.5, a fresh pre-warmed (37°C) 100 mL of main culture was inoculated with the pre-culture to a final OD_{578} of 0.1 and the growth curve was followed. Samples for RNA isolation were harvested (as described in section 4.7) at OD_{578} 1.0.

SMM (5x)	Quantity
$(NH_4)_2SO_4$*	5.0 g
K_2HPO_4*	35.0 g

KH_2PO_4*	15.0 g
Na_3-Citrate x 2 H_2O*	2.5 g
$MgSO_4$ x 7 H_2O*	0.5 g
deion. H_2O	*ad* 475 mL

*Sigma. Taufkirchen

Trace Elements for SM-Medium

Trace Elements (100x)	Quantity
$CaCl_2$*	0.055 g
$FeCl_3$ x 6 H_2O**	0.0135 g
$MnCl_2$ x 4 H_2O**	0.01 g
$ZnCl_2$**	0.017 g
$CuCl_2$ x 6 H_2O**	0.0043 g
$CoCl_2$ x 6 H_2O**	0.006 g
Na_2MoO_4 x 2 H_2O**	0.006 g
deion. H_2O	*ad* 100 mL

*Sigma. Taufkirchen. **Merck. Darmstadt

1x SM-Medium

SM-Medium (100 mL)	Quantity
SMM 5x	20.0 mL
Trace Elements x 100	1.0 mL
Glucose* (50 %)	1.0 mL
Phenylalanine(5 mg/ mL)	0.74 mL
deion. H_2O	*ad* 100 mL

*Sigma. Taufkirchen

4.4.2 Growth in the presence of 1.2 M NaCl

Cultivations were performed as mentioned by Steil *et al.* (2003) [80]. Briefly, *B. subtilis* was grown for 24 h on a LB agar plate at 37°C and used to inoculate 100 mL of Spizizen's minimal medium (SMM) media containing 1.2M NaCl in a 500 mL-Erlenmeyer bacterial culture flasks. The flasks were aerated overnight by shaking at 220 RPM at 37°C in an orbital shaker (Innova 4230, New Brunswick, USA). A pre-culture of fresh 100 mL 1.2 M NaCl-SMM was inoculated to an OD_{578} of 0.1 with the overnight cultures. After these pre-culture reached an OD_{578} of 1.0 they were used to inoculate to a pre-warmed main culture of 100 mL SMM containing 1.2 M NaCl to a final OD_{578} of 0.1. The growth curve was recorded and samples for RNA isolation were harvested (as described in section 4.7) at OD_{578} 1.0.

4.4.3 Growth at 16°C

Cultivations were performed according to Budde *et al.* 2006 [118]. Briefly, *B. subtilis* was grown for 24 h on a LB plate at 37°C and used to inoculate 100 mL of overnight Spizizen's minimal medium (SMM) in a 500 mL-Erlenmeyer bacterial culture flasks. The flasks were aerated by shaking at 220 RPM at 37°C in an orbital shaker (Innova 4230, New Brunswick, USA). A fresh 100 mL SMM (pre-culture) was inoculated to an optical density (OD) of 0.1 at 578 nm from the overnight cultures. After the pre-cultures reached an OD_{578} of 0.5, a 100 mL of pre-cooled (16°C) SMM main culture were inoculated to a final OD_{578} of 0.1. The main cultures were grown at 16°C at 220 rpm in an orbital shaker. The growth curve was recorded and samples for RNA isolation were harvested (as described below in section 4.7) at OD_{578} 1.0.

4.4.4 Growth at 51°C

Cultivations were performed as mentioned by Holtmann *et al.* (2004) [119]. Briefly, *B. subtilis* was grown for 24 h on a LB plate at 37°C and used to inoculate 100 mL of overnight Spizizen's minimal medium (SMM) in a 500 mL-Erlenmeyer bacterial culture flasks. The flasks were aerated by shaking at 220 RPM at 37°C in an orbital shaker (Innova 4230, New Brunswick, USA). A fresh 100 mL SMM (pre-culture) was inoculated to an optical density (OD) of 0.1 at 578 nm from the overnight cultures. After the pre-cultures reached an OD_{578} of 0.5, a 100 mL of pre-warmed (51°C) SMM main culture were inoculated to a final OD_{578} of 0.1. The main cultures were grown by shaking at 160 linear strokes/minute (stroke length 18cm) at 51°C in a water bath (OLS 200, Grant Instruments. Cambridge Ltd.). The growth curve was recorded and samples for RNA were harvested (as described in section 4.7) at OD 1.0.

4.4.5 Growth in M9

B. subtilis 168 Trp^+ was grown in 5 mL of LB for 4 hours at 37°C and used to inoculate 100 mL of overnight culture with three different dilutions (1:10000, 1:20000, 1:40000). These overnight cultures were allowed to grow for 12 to 14 hours at 37°C in an orbital shaker at 300 rpm of vigorous shaking (to avoid oxygen limitation during stationary phase). From the overnight cultures, an exponentially growing culture was used to inoculate the 200 mL of main culture to a final OD at 600nm of 0.05. The main culture was allowed to grow and three samples for RNA were harvested to reflect three growth states of the growth curve, they are exponential phase (OD_{600} at 0.4), early stationary phase (at OD_{600} 1.3 which is approximately 90 min after exponential phase) and late stationary phase (at OD_{600} at 1.0 which is approximately 180 min after entry into stationary phase).

5x M9 minimal medium

M9 5x(1000 mL)	**Quantity**
$Na_2HPO_4.2H_2O$**	42.5 g
KH_2PO_4 **	15 g
NH_4Cl *	5.0 g
NaCl **	2.5 g

HPLC H_2O* **	ad 1000 mL

*Sigma. Taufkirchen, **Merck. Darmstadt,***J.T Baker
Adjusted to pH 7.0 using 4M NaOH
100x Trace elements solutions:

Trace Elements (100x)	**Quantity**
$MnCl_2 \cdot 4H_2O$ **	0.1 g
$ZnCl_2$ **	0.17 g
$CuCl_2 \cdot 2H_2O$ **	0.043 g
$CoCl_2 \cdot 6H_2O$ **	0.06 g
$Na_2MoO_4 \cdot 2H_2O$ **	0.06 g

**Merck. Darmstadt
Solution is Filter-sterilized and stored at RT.

Stock solutions (100 mL)	**Quantity**
100 mM $CaCl_2 \cdot 2H_2O$ *#	1.47 g
1M $MgSO_4 \cdot 7H_2O$ *#	24.6 g
50%(w/v) Glucose($C_6H_{12}O_6$) *#	50 g
50%(w/v) Malate($C_4H_6O_5$) *#	50 g
50 mM $FeCl_3 \cdot 6H_2O$ *##	1.35 g
100 mM $Na_3C_6H_5O_7 \cdot 2H_2O$	2.94 g

*Sigma. Taufkirchen. **Merck. Darmstadt, #Autoclaved and stored at RT,
##Filter sterilize and store in the dark at 4°C.

M9 (1x) (1000 mL)	
H_2O HPLC	783 mL
M9 5x stock	200 mL
trace salts 100x stock	10 mL
Glucose 50% (w/v)	2 mL
Malate 50% (w/v)	2 mL
1 M $MgSO_4$	1 mL
100 mM $CaCl_2$	1 mL
50 mM $FeCl_3$ in 100 mM citric acid	1 mL

4.5 EXPERIMENTS FOR OPTIMIZING TRYPSIN DIGESTION OF PROTEIN SAMPLES FROM SPORULATING *B. SUBTILIS*

4.5.1 Growth in DSM media

Exponentially growing *B. subtilis* was inoculated to DSM (Difco Sporulation Medium) to an optical density (OD) of 0.1 at 600 nm and the flasks were aerated by shaking at 220 RPM at 37°C in an orbital shaker (Innova 4230, New Brunswick, USA). Samples for protein isolation and heat kill assay were harvested by taking equivalent volume for 15 OD units starting at exponential phase (OD_{600nm} - 1) followed by every hour until 6 hours into stationary phase.

4.5.2 Calculation of percentage of heat resistant endospores (heat kill assay)

Frequency of heat resistant endospore formation was calculated from the number of CFU's (colony forming units) before and after heat treatment (20 min at 80°C), which was determined by plating various dilutions (10^{-5},10^{-6} & 10^{-7}) on agar plates. Non-heated samples with the same dilutions were considered as the controls and were set as 100% of CFU's.

4.6 CHEMOSTAT BASED CULTIVATIONS (PERFORMED BY MICHAEL KOHLSTEDT, BRAUNSCHWEIG)

All experiments were performed with the tryptophan prototroph wild-type *B. subtilis* 168 Trp^+ [13]. Cells from glycerol stocks were grown overnight on LB agar plates composed of: 10 g L^{-1} tryptone, 10 g L^{-1} NaCl, 5 g L^{-1} yeast extract and 15 g L^{-1} agar. Subsequently a single colony was transferred into a 500-mL baffled shake flask filled with liquid LB medium. After 2 hours cells were harvested via centrifugation, washed with deionized water and transferred into M9 minimal medium supplemented with 3,4-dihydroxybenzoic acid as chelating agent and grown up to an optical density of 1. The M9 medium contained: 5 g L^{-1} glucose, 8.5 g L^{-1} $Na_2HPO_4 \cdot 2H_2O$, 3 g L^{-1} KH_2PO_4, 1 g L^{-1} NH_4Cl, 0.5 g L^{-1} NaCl, 246 mg L^{-1} $MgSO_4 \cdot 7H_2O$, 30 mg L^{-1} 3,4-dihydroxybenzoic acid, 14.7 mg L^{-1} $CaCl_2 \cdot 2H_2O$, 13.5 mg L^{-1} $FeCl_3 \cdot 6H_2O$ and 10 mL of a trace element solution with the following components: 0.17 g L^{-1} $ZnCl_2$, 0.1 g L^{-1} $MnCl_2 \cdot 4H_2O$, 0.06 mg L^{-1} $CoCl_2 \cdot 6H_2O$, 0.06 mg L^{-1} $Na_2MoO_4 \cdot 2H_2O$ and 0.043 g L^{-1} $CuCl_2 \cdot 2H_2O$. Precultured cells served as inoculum for 4 simultaneous bioreactor cultivations in a parallel 1 L bioreactor system (dasGIP, Jülich, Germany) with a working volume of 300 mL of M9 minimal medium each with the same composition as described above but with only 1 g of glucose per liter. In the 4th reactor naturally labeled glucose was replaced by >99% [1-^{13}C]-glucose (Euriso-top, Gif sur Yvette, France) for metabolic flux analysis. The cultivation was started in batch mode and before substrate depletion chemostat mode was initiated by starting feed and harvest pumps at a fixed pump rate of 30 mL h^{-1} to keep the reactor volume and the growth rate of 0.1 h^{-1} constant. Aeration rate, agitation speed, temperature and pH were kept constant at 0.5 vvm, 1,000 rpm, 37°C and 7.1 respectively. Offgas CO_2 formation was monitored by a mass spectrometer (Pfeiffer Vacuum, Asslar, Germany). Chemostat cultures were run until metabolic and isotopic steady-state were reached which was defined as at least 5 volume changes, as well as stable

optical density, CO_2 exhaust gas concentration and an invariant extracellular metabolite profile. When steady-state was reached, sampling for transcriptome, metabolome, proteome and fluxome analysis was performed at the same time.

4.7 SAMPLE HARVESTING FOR TRANSCRIPTOME ANALYSIS

Sample harvesting and RNA extraction was performed as previously described (Eymann et al, 2002 [29]). Briefly, 15 optical density units (OD units) of cells were harvested by centrifugation (6,700 x g, 10 min, 4 °C) after addition of ½ volume of frozen killing buffer (20 mM Tris-HCl adjusted to pH 7.5, 5 mM MgCl2, 20 mM NaN3) to the culture sample. After discarding the supernatant, the obtained cell pellets were frozen in liquid nitrogen for RNA extraction.

4.8 RNA PREPARATION

Lysis solution:	
guanidine-thiocyanate (4 M)*	118.16 g
3 M Na-acetate, pH 5.2 (0.025 M)*	2.08 mL
10 % N-lauroylsarcosinate (0.5 %)***	12.5 mL
deionized water.	ad 250 mL

Killing buffer:	
Tris-HCl,pH-7.5(Stocksolution:1 M)***	20 mM
$MgCl_2$ (Stock solution: 1 M)**	5 mM
NaN_3 (Stock solution: 2 M)*	20 mM

*Merck. Darmstadt, **Roth. Lauterbourg, ***Sigma –Aldrich.

Bacterial cell pellets were resuspended in 200 µL of ice cold killing buffer and flash frozen using liquid nitrogen cooled Teflon vessels. Then, the Teflon vessels were closed with the disruption ball and frozen in liquid nitrogen for 1 min and were then subjected to mechanical shaking at 2600 rpm for 2 min in a bead mill (Mikrodismembrator S, B. Braun Biotech International GmbH, Melsungen, Germany). The resulting lysate was resuspended in 4 mL lysis buffer by repeated pipetting and then aliquoted at 1 mL each to a 2 mL microcentrifuge tubes which were flash frozen in liquid nitrogen. Acid phenol (Roth, Lauterbourg) was added to the frozen lysate in a 1:1 ratio and mixed on a thermomixer (Eppendorf, Germany) until completely thawed, and then for additional 5min. Organic and aqueous phase were separated by centrifugation (12000 x g, 15 min RT) and the supernatant (maximum 850 µL) was carefully transferred (without disturbing DNA and protein containing interphase) into a fresh microcentrifuge tube. To the

supernatant collected, one volume of acid phenol was added and then mixed on a thermomixer and centrifuged (12000 x g, 15 min). The resultant supernatant (maximum 700 µL) was again transferred into a fresh microcentrifuge tube to which equal volume of chloroform/IAA was added, mixed and centrifuged as above mentioned. Supernatant was transferred into a fresh microcentrifuge tube to which 1/10 volume of 3 M Na-Acetate, pH-5.2 and 1 mL of isopropanol was added, mixed well and the RNA was precipitated overnight at -20°C. After centrifugation (15000 x g 15 min) the resultant supernatant was discarded and the RNA pellet was washed with 70% ethanol and the pellet was vacuum dried (LTF Labortechnik, Germany). The RNA pellet was dissolved in an appropriate volume (50-100 µL) of nuclease-free water (Ambion Inc., Austin, TX, USA, now part of Applied Biosystems, Foster City, CA, USA) for 3 hours on ice and then for 30 min at room temperature.

The concentration was determined photometrically (NanoDrop ND-1000, NanoDrop Technologies, Wilmington, DE, USA), and the RNA quality was checked with an Agilent-Nano chip on an Agilent 2100 Bioanalyzer (Agilent Technologies, Santa Clara, CA, USA).

For further processing of RNA for microarray hybridization, RNA had to be pure without DNA contamination. For this reason DNase treatment was performed and RNA was purified using the RNA Clean-Up and Concentration Kit (Norgen Biotek Corp., Thorold, ON, Canada; distributed by BioCat GmbH, Heidelberg, Germany). The concentration after cleanup was determined photometrically, and the quality was checked again with an Agilent 2100 Bioanalyzer.

The purified mRNA was used for the subsequent gene expression profiling for either relative expression profiling with Agilent customized microarray or with NimbleGen Tiling array technology (see below).

4.9 GENE EXPRESSION PROFILING

Two different kinds of gene expression profiling were performed in this study, they are relative gene expression profiling (Agilent customized microarray) and intensity based high density Tiling array (NimbleGen Tiling array)

4.9.1 Relative gene expression analysis

Relative gene expression analysis was performed by the dual dye hybridization method, where mRNA of the samples of interest was hybridized against the mRNA of a reference pool. The reference pool was prepared by mixing equal amounts of mRNA from all samples in the corresponding experiment.

Chemicals	Company
Random Primer	Promega
Agilent Two-Color RNA Spike-In Kit	Agilent
dNTPs	Roche

Cy5-dCTP	GE Healthcare
Cy3-dCTP	GE Healthcare
CyScribe GFX Purification Kit	GE Healthcare
Superscript II	Invitrogen
RNase H	Invitrogen
Gene Expression Hybridization Kit	Agilent
Gene Expression Wash Buffer 1	Agilent
Gene Expression Wash Buffer 2	Agilent
Hyb Gasket Slides , 4 arrays per slide	Agilent

10 µg (20.5 µL) of resultant RNA with high purity and quality was mixed with 2.5 µL of random primers and 1 µL of each Spike-Mix A to the reference (pool) and Spike-Mix B to the sample. The tubes were incubated at 70°C (heat block) for 10 min and then on ice for 5 min, 22.5 µL of master mix(mentioned below) and 1.25 µL of Cy3(for reference pool) and Cy5(for sample) was added and mixed well(these steps are performed in low light as Cy-dyes are light sensitive). Reverse transcription was done by adding 2 µL of superscript-II to the above solution and incubated for 42°C (60 min), then at 70°C (for 10min) and then onto ice (5 min, all the incubations were performed in the dark). After the cDNA was synthesized, remaining RNA was degraded by adding 1 µL of RNaseH (room temperature, 30min).

Master mix composition

	1X (for one reaction)
Nuclease-free water	7 µL
5x 1st Strand Buffer	10 µL
0.1 M DTT	5 µL
10 mM dNTP Mix, 2.5 mM dCTP	0.5 µL

The resultant cDNA was purified by CyScribe GFX purification kit, cDNA concentration and Cy-Dye concentration were measured with a NanoDrop. The incorporation rate of the Cy-dyes was calculated with the following formula:

Incorporation rate= 1000* concentration of Cy3 (or) Cy5 / concentration of cDNA

0.4 µg of Cy3-labelled cDNA and 0.4 µg of Cy5-labelled cDNA were mixed and total volume was adjusted to 44 µL with nuclease-free water and incubated at 95°c for 2 min and then placed onto ice. 11 µL of preheated (60°C, 30 min) 10x blocking agent and 60 µL of 2x GEx Hybridization buffer were added to the cDNA mix and centrifuged at 13000 x g for 1min. 100 µL of the mix was added on the Agilent gasket slide and combined together with microarray slide with the help of an Agilent hybridization chamber. Hybridization was performed for 17 hours at 65°C in an Agilent hybridization oven.

After hybridization, non-specific probes were removed by washing with Agilent wash buffers according to the manufacturer´s guidelines. Scanning was performed with a Agilent Technologies Scanner G2505C US45103079 in accordance with "Two-Colour Microarray-based Gene Expression Analysis manual, version 5.5"

Data were extracted and processed using the Feature Extraction software (version 9.5, Agilent Technologies). For each gene on the microarray, the error-weighted average of the log ratio values of the individual probes was calculated using the Rosetta Resolver software (version 7.2.1, Rosetta Biosoftware).

4.9.1.1 Data analysis – relative gene expression analysis

A reference pool was prepared by mixing equal amounts of RNA isolated from each of the samples in the experiment. The individual samples of interest were labeled with Cy5, whereas the reference pool was labeled with Cy3, equal amounts of Cy5 and Cy3 labeled cDNA were hybridized onto an Agilent custom microarray. For each gene on a microarray, the error-weighted average of the log ratio (Cy5/Cy3) values of the individual probes was calculated using the Resolver software (version 7.2.1, Rosetta Biosoftware, Seattle, USA). As this is dual dye hybridization, the common reference pool was used for experimental normalization to reduce the influence of technical errors within the experiment. The normalized ratio data represent the relative gene expression levels for the corresponding sample and these data were imported into the software Genedata Analyst for the subsequent analysis.

4.9.2 Tiling array design

The "BaSysBio *Bacillus subtilis* T1 385K" array was designed by Hanne Jarmer (Center for Biological Sequence Analysis, Department of Systems Biology, Technical University of Denmark, Lyngby, Denmark) using the OligoWiz software and parameters which have recently been published (Rasmussen *et al.*. 2009 [93]). The sequences were synthesized on quartz wafers by NimbleGen (Roche NimbleGen, Madison, WI, USA) in a custom, high-density DNA array format.

4.9.2.1 Tiling array hybridization

The tiling array hybridization was performed at NimbleGen (Roche NimbleGen, Madison, WI, USA) according to the company's standard operating protocols. Briefly, 10 µg of high quality RNA samples were reverse transcribed to cDNA in the presence of actinomycin D with subsequent alkaline RNA hydrolysis. Precipitated and resolved cDNA was labeled with Cy3 dye via NHS-Ester Dye Coupling Reaction. After spin-column based purification and quality control, labeled cDNA was hybridized together with appropriate controls to tiling arrays "BaSysBio Bsub T1 array" [93, 116]. Arrays were washed and scanned and raw intensity data of tiling probes were provided to us for the data analysis.

4.9.2.2 Tiling array raw data analysis

The raw data analysis and condensing of probe data to transcripts/genes was performed by Pierre Nicolas, Aurélie Leduc, and Philippe Bessières (INRA, Mathématique Informatique et Génome, Jouy-en-Josas, France). Intensity values for annotated genes were derived from the individual probe data by calculating the median of the probes located within the genomic coordinates of these genes. These intensity values were uploaded to Genedata Analyst for further statistical analysis and functional categorization.

4.9.3 Statistical and functional data analysis in Genedata Analyst

Relative gene expression data (normalized ratio data) obtained from the Agilent microarrays were used for ratio building against the respective control samples in the corresponding experiments. Significantly regulated genes after a statistical cut-off of three fold change (with a p-value of 0.01 after Benjamini-Hochberg correction) were used for performing K-means clustering and Fisher's exact test in Genedata Analyst. Functional gene categorization was obtained from SubtiWiki (http://SubtiWiki.uni-goettingen.de/wiki/index.php/Categories) and Fisher's exact test for the functional class enrichment was performed in Genedata Analyst.

The intensity data obtained from Tiling array was subjected to median normalization and then normalized to the respective control points. Other statistical tests were performed in a similar manner as mentioned earlier.

4.10 PROTEIN ISOLATION AND ESTIMATION

4.10.1 Sample harvesting and preparation of protein lysate by cell disruption

Protein extracts from frozen pellets were prepared and protein concentrations were determined as described earlier [120, 121]. In short, during the experiment an equivalent volume of 10 or 12 optical density units (OD units) of the bacterial culture was harvested by centrifugation at 8000 rpm for 5 min at 4°C. The supernatant was discarded. After washing the pellets with 10 mL of TE-buffer (20 mM Tris, 10 mM EDTA, pH 8) pellets were stored at -70°C or immediately used for cell disruption. Frozen pellets were resuspended in 500 µL of ice cold TE-buffer and added to a 2 mL vial (Sarstedt) prefilled with 500 µL of unwashed glass beads (160 µm, Sigma Life sciences). Cell disruption was performed by ribolysing (Fast prep-120, BIO 101 Thermo Scientific) for 30 s at 6.5 m/sec speed and then on ice for 5 min. This was repeated for two more times (repetition ensured the disruption efficiency to be 99-99.9% complete) followed by centrifugation at 13000 g (10 min, 4°C). Resultant supernatants were transferred to a new 1.5 mL microcentrifuge tube avoiding carryover of glass beads and centrifuged at 13000 g (30 min, 4°C). This process was repeated once again to remove remaining glass beads and cell debris.

4.10.2 Determination of protein concentrations by Ninhydrin assay

Ninhydrin (2,2-Dihydroxyindane-1,3-dione) reagent is commonly used to detect ammonia or primary and secondary amines. Protein estimation using Ninhydrin was performed according to Starcher *et al.*, 2001 [121]. A calibration curve using BSA (10 mg/mL in TE buffer) was prepared with different concentrations ranging from 0.25 µg/µL to 10 µg/µL. Protein concentration was estimated for samples as mentioned below.

Calibration curve BSA* (10 mg/ mL in TE buffer)

0,25 µg/µL	BSA 2,5 µL BSA + 97,5 µL H_20**	100 µL 12 N HCl*
0,5 µg/µL	BSA 5,0 µL BSA + 95,0 µL H_20**	
1,0 µg/µL	BSA 10,0 µL BSA + 90,0 µL H_20**	
1,5 µg/µL	BSA 15,0 µL BSA + 85,0 µL H_20**	
2,0 µg/µL	BSA 20,0 µL BSA + 80,0 µL H_20**	
4,0 µg/µL	BSA 40,0 µL BSA + 60,0 µL H_20**	
6,0 µg/µL	BSA 60,0 µL BSA + 40,0 µL H_20**	
8,0 µg/µL	BSA 80,0 µL BSA + 20,0 µL H_20**	
10,0 µg/µL	BSA 100,0 µL BSA	
Samples	20µL protein extract	20µL 12 N HCl

*Sigma, **Baker HPLC Water, ***Roth

All the tubes were incubated for 24 hours at 100°C for acid hydrolysis. Ninhydrin reagent was freshly prepared, mixed for 1hour and stored in the dark.

Ninhydrin*	**1g in 38.75 mL ethylene glycol***
4 N sodium acetate buffer(pH 5.5)	12,5 mL
Stannous chloride**	50 mg

*Roth, **Sigma,

Hydrolyzed proteins (BSA and samples) were diluted 1:100. 400 µL of H_2O was added to 200 µL of diluted proteins and 600 µL of ninhydrin reagent was added and incubated for 10 min at 100°C (in the dark). Measurement of OD was done at 575 nm on a spectrophotometer (Ultrospec 2100 pro, GE HealthCare) using appropriate blanks.

4.10.3 Determination of protein concentrations by Bradford assay

The concentration of proteins in aqueous solutions was determined according to Bradford [122]. Quantification is based on a shift of the absorption maximum of the dye Coomassie Brilliant Blue from 465 nm to 595 nm when the dye binds to proteins (to the hydrophobic amino acids). For the estimation of protein concentrations the ready-to-use Protein Assay Reagent (Bio-Rad) was used in a ratio of 1:5. Protein concentrations of unknown samples were determined from a calibration curve of BSA in concentrations ranging from 1 to 12 µg/µL.

4.11 PROTEOLYSIS AND PURIFICATION OF PROTEOME SAMPLES

4.11.1 Proteolysis by trypsin

Disulfide bonds in 2 µg of protein from each sample were initially reduced by addition of 25 mM DTT prepared in 20 mM ammonium bicarbonate and incubated at 60ºC for 1 h. Following reduction, the protein samples were carbamidomethylated with 100 mM iodoacetamide in 20 mM ammonium bicarbonate and incubated at 37ºC in dark. After 30 min, protein samples were subjected to proteolysis using trypsin (Promega) overnight (16 h) in a ratio of 1:25 (trypsin:protein). 1% acetic acid was added to stop the proteolysis. Digested peptides were then desalted to remove the impurities that might interfere with MS analysis.

4.11.2 Purification and in-gel digestion of the proteins

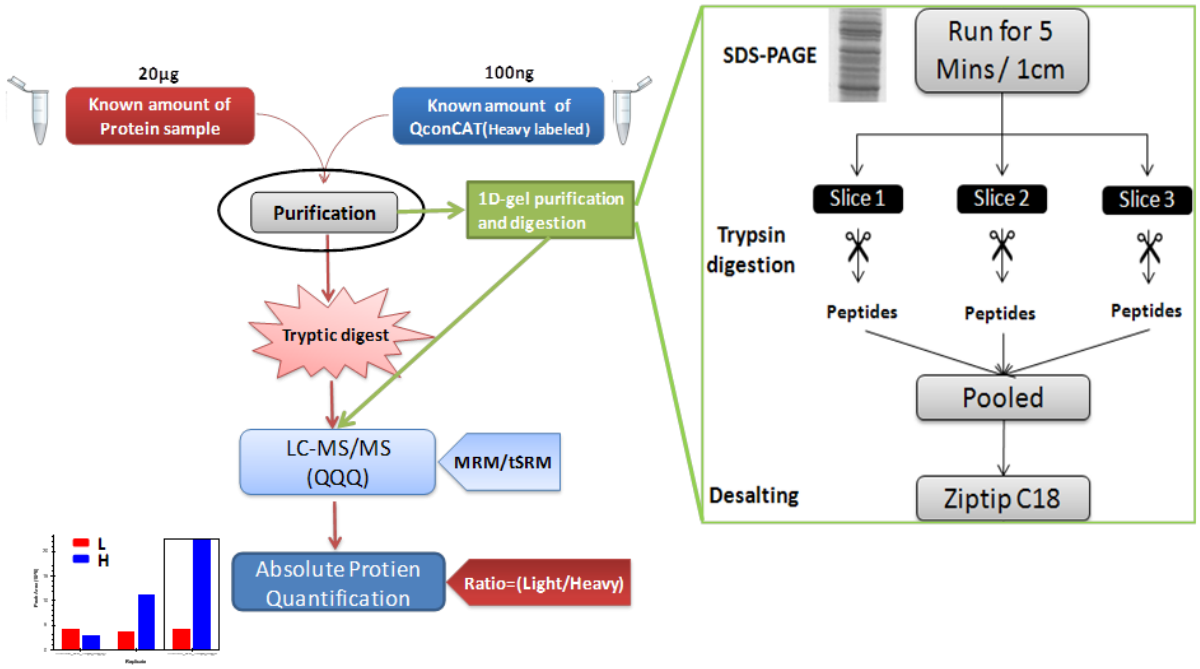

Figure 6: Schematic representation of sample preparation, purification, trypsin digestion and MRM analysis. Inset – 1D-gel based purification of proteins and in-gel trypsin digestion which is required for the samples harvested from fermentation and chemostat cultivations.

Protein samples obtained from different sources like fermentation and Chemostat cultivation tend to contain some impurities that might interfere with trypsin digestion. So, proteins were purified prior to digestion when necessary. In order to purify the protein extracts, 15 µg of protein lysate and a defined amount of QconCAT were applied to a NuPAGE® Bis-Tris Gels 4-12% (Life Technologies Corporation- Carlsbad, California). Separation, staining and destaining were carried out according to the manufacture guidelines except for the run time. The run was stopped exactly after 5 min which allowed the sample to be separated for 1 cm. Each lane was sliced into three pieces which were processed independently (Figure 6). Gel pieces were washed twice with 200 µL of 20 mM ammonium bicarbonate in 50% (v/v) acetonitrile (ACN) for 30 min

at 37 °C. Thereafter the gel pieces were dehydrated by two times washing with 200 µL of ACN for 15 min. Trypsin solution (20 ng/µL trypsin in 20 mM ammonium bicarbonate) was added until the gel pieces stopped swelling. Digestion was allowed to proceed for 16–18 h at 37 °C. Peptides were extracted from the gel pieces with 40 µL of 0.1% (v/v) acetic acid by incubation in an ultrasonic bath for 30 min, followed by a second extraction with 40 µL of 50% ACN in 0.05% acetic acid. The peptide containing supernatants of each band were collected and pooled for each lane; excess liquid was removed by lyophilization. The resulting peptide mixtures were resuspended in 100 µL of buffer A (0.1% acetic acid, 2% ACN) and purified using C18-ZipTip columns (Millipore, Bedford). 300 ng of the purified peptide mixture was used for subsequent MS analysis.

4.11.3 Desalting of peptides by ZipTip®

Peptides derived from tryptic digestions were purified and desalted using C18 resin-ZipTip® pipette tips (Millipore). ZipTip columns were equilibrated by serial pipetting of 100% ACN; 80% ACN in 1% AA; 50% ACN in 1% AA; 30% ACN in 1% AA, and 1% AA. Then the peptides were loaded onto the ZipTip by pipetting 20 times. ZipTip was washed 5 times with 1% AA and peptides were eluted in 50% ACN+1% AA and 80% ACN+1% AA. Eluates were pooled and ACN was removed by vacuum centrifuge concentrator (Eppendorf). Peptides were dissolved in Buffer A (2% ACN, 0.1% AA) to a final concentration of 100 ng/µL and stored at -20°C until MS measurement.

4.12 MASS SPECTROMETRY

4.12.1 MS parameters –LTQ Velos Orbitrap

LC-MS/MS was performed on a Proxeon nano-LC system connected to an LTQ-Velos-Orbitrap-MS (Thermo Scientific) equipped with a nano-ESI source. For liquid chromatography separation an Acclaim PepMap 100 column (C18, 3 ìm, 100 Å) capillary of 15 cm bed length was used. The flow rate used was 300 nL/min for the nano column and the solvent gradient used was from 0% solvent B to 25% solvent B in 60 min). Solvent A was 0.1% AA, whereas aqueous 90% ACN in 0.1% AA was used as solvent B. The MS was operated in the data-dependent mode to automatically switch between Orbitrap-MS and LTQ-MS/MS acquisition. Survey full scan MS spectra (from m/z 300 to 2,000) were acquired in the Orbitrap with resolution R = 60,000 at m/z 400 (after accumulation to a target of 1,000,000 charges in the LTQ) allowed sequential isolation of the most intense ions, up to five, depending on signal intensity, for fragmentation on the linear ion trap using collision induced dissociation at a target value of 100,000 charges. Target ions already selected for MS/MS were dynamically excluded for 60 seconds. General MS conditions were: electrospray voltage, 1.5 kV; no sheath and auxiliary gas flow. Ion selection threshold was 500 counts for MS/MS, and an activation Q-value of 0.25 and activation time of 30 ms were also applied for MS/MS.

4.12.2 MS parameters –TSQ Vantage

Peptide separation was carried out using a Acclaim PepMap 100 column (C18, 5 µm, 100 A˚, 15 cm bed length, Dionex) and applying a binary gradient from 0% to 30% buffer B(100% acetonitrile [v/v], 0.1% acetic acid [v/v]) in 60 min and to 40% buffer B in additional 10 min and to 90% buffer B in additional 10 min at a flow rate of 300 nL min-1 on an online Proxeon nano-LC system (Proxeon, Odense, Denmark).

For MRM, LC-MS/MS experiments were performed on a triple quadrupole mass spectrometer (TSQ Vantage, Thermo Scientific) operated in nano-electrospray mode. For ionization 1600 V-1800 V of spray voltage and 250 °C of capillary temperature were used. The selectivity for both Q1 and Q3 were set to 0.7 Da (FWHM-full width half maximum). The collision gas pressure of Q2 was set at 1.5 mTorr. TSQ Vantage was operated in SRM mode and data acquisition was done in scheduled SRM manner.

4.12.3 Data analysis

Qualitative and relative quantitative (when required) analysis of the MS data was performed with Rosetta Elucidator. The frame and feature annotation was done using the following parameters: retention time minimum cut-off 11 min, retention time maximum cut-off 78 min, m/z minimum cut-off 300 and maximum 1,700 m/z. An intensity threshold of 1,000 counts, an instrument mass accuracy of 10.0 ppm, and an alignment search distance of 4.0 min were applied for binning process. For identification, the *B. subtilis* Uniprot 12.7 forward and reverse FASTA sequence (downloaded from Uniprot) in combination with SEQUEST was used. Oxidation of methionine was set as variable modification and carbamidomethylation of cysteine as static modification. Proteins were considered for further investigation when at least one or more peptides were identified in at least one experiment and p-value less than 0.05.

The relative intensities for the proteins were then imported to Genedata Analyst from Rosetta Elucidator and further data analysis was performed. “Median normalization relative to one” was performed on each of the sample. The final normalized relative intensities were then log transformed and then appropriate controls were chosen for the “control point normalization” used for the further investigation.

Functional gene categorization was obtained from SubtiWiki (http://SubtiWiki.uni-goettingen.de/wiki/index.php/Categories). Fisher’s exact test for the functional class enrichment was performed using the SubtiWiki classification performed in Genedata Analyst.

4.13 ABSOLUTE PROTEIN QUANTIFICATION BY MULTIPLE REACTION MONITORING (MRM)

4.13.1 Design of the QconCATs

Tryptic proteotypic peptides of all the proteins under investigation were selected based on the previous in-house acquired MS data. This peptide list was refined based on the set of rules indicated by Pratt *et al.* (2006) [102]. At least three peptides per protein were finally selected and the list was provided to PolyQuant GmbH, (Bad Abbach Germany) where the synthesis and labeling of QconCATs (concatemers of Q peptides) were performed. In brief, the Q peptides were aligned in a mixed fashion and a complementary gene was synthesized and inserted into a vector, which was later introduced into a heterologous expression system for protein production. The QconCAT proteins were expressed in *Escherichia coli* and were labeled with stable isotopes by growth in the presence of stable isotope–labeled precursors (C13 & N15). The labeled QconCAT proteins were then purified with the help of polyhistidine-tag [123] and quantified. The purified QconCATs were spiked to complex protein mixtures in defined amounts (as described in Figure 6). In general, tryptic digestion of the QconCAT–analyte mix releases each of the QconCAT peptides in a strict stoichiometry of 1:1 unless there is a missed cleavage.

4.13.2 MRM method development

Initially 30 fmol QconCAT protein was digested with trypsin and analyzed using the LTQ-Velos Orbitrap. Proteins were identified via automated SEQUEST[124] search (Sorcerer built 4.04, Sage-N Research Inc., Milpitas, CA, U.S.A.) in integration with TPP (trans proteomic pipeline [125] against a customized databases containing fasta sequences of QconCATs with a mass tolerance of 10 ppm and allowing up to two missed tryptic cleavages as search criteria.

The resultant mzXML and pepXML(peptide sequence assignments of MS/MS scans) files from TPP workflow were used as a spectral library for the software Skyline 1.1 (MacCoss Lab Software)[126]. Appropriate precursor charge state and eight ideal y-type product ions for each peptide were selected for generating an initial test MRM method. With these initial details, a test MS analysis was performed with tryptic digest of 30 fmol of QconCAT and the results were analyzed with the Skyline software. Top four intense transitions for each peptide were then selected for collision energy optimization in accordance with MacLean *et al.* 2010[127]. In the current study optimization of collision energy resulted in 20% signal gain over all peptides tested. The signal gain was more prominent for those peptides that were +3 charged compared to +2 charged peptides. A final method with optimized collision energy and recorded retention time window (five minutes) was generated and this method was used to analyze the complex sample spiked with defined amount of QconCAT. For each peptide three or four product ions were chosen and all the parameters were then applied for both the heavy and light peptides. Complete method used for the targeted analysis was shown in Table 1.

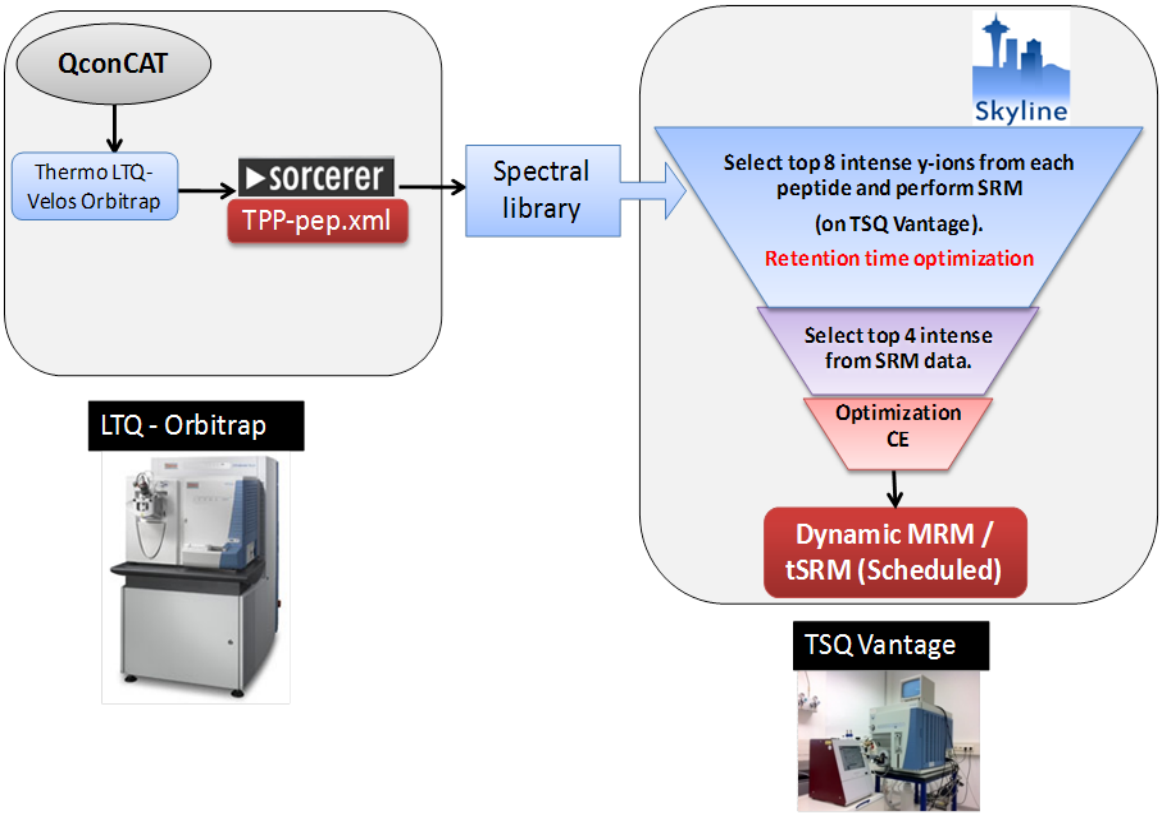

Figure 7 : Workflow representing the method development for MRM based absolute quantification. Transfer of the information from LTQ-Orbitrap measurements to the TSQ Vantage via TPP-pep.xml and subsequent retention time recording and collision energy optimization for the final MRM method.

Table 1: * MRM method summary. Peptides used for the quantification of the proteins: Description of the used peptide information in the following format "Peptide_PeptideCharge_Product ion_Product Charge. Endogenous peptide end with the suffix "L" and heavy peptides as the internal standard for quantification end with suffix "H". CE – optimized collision energy.

Protein	Q1	Q3	Peptide information*	CE
Pgi	1094.513	1066.568	DFATSELEDNPAYQYAVVR_2_y9_1_L	38.9
Pgi	1094.513	735.415	DFATSELEDNPAYQYAVVR_2_y6_1_L	38.9
Pgi	1094.513	607.356	DFATSELEDNPAYQYAVVR_2_y5_1_L	38.9
Pgi	1099.517	1076.576	DFATSELEDNPAYQYAVVR_2_y9_1_H	38.9
Pgi	1099.517	745.423	DFATSELEDNPAYQYAVVR_2_y6_1_H	38.9
Pgi	1099.517	617.364	DFATSELEDNPAYQYAVVR_2_y5_1_H	38.9
Pgi	625.822	904.489	SGTTTEPAIAFR_2_y8_1_L	23.5
Pgi	625.822	803.441	SGTTTEPAIAFR_2_y7_1_L	23.5
Pgi	625.822	674.398	SGTTTEPAIAFR_2_y6_1_L	23.5
Pgi	630.827	914.497	SGTTTEPAIAFR_2_y8_1_H	23.5
Pgi	630.827	813.449	SGTTTEPAIAFR_2_y7_1_H	23.5
Pgi	630.827	684.407	SGTTTEPAIAFR_2_y6_1_H	23.5
Pgi	1084.511	828.421	TLSNEEGFESFVIPDDVGGR_2_y8_1_L	38.6
Pgi	1084.511	715.337	TLSNEEGFESFVIPDDVGGR_2_y7_1_L	38.6
Pgi	1084.511	388.230	TLSNEEGFESFVIPDDVGGR_2_y4_1_L	38.6
Pgi	1089.515	838.429	TLSNEEGFESFVIPDDVGGR_2_y8_1_H	38.6
Pgi	1089.515	725.345	TLSNEEGFESFVIPDDVGGR_2_y7_1_H	38.6
Pgi	1089.515	398.239	TLSNEEGFESFVIPDDVGGR_2_y4_1_H	38.6
PfkA	513.287	732.414	LVDHDIIEILETK_3_y6_1_L	25.2
PfkA	513.287	603.371	LVDHDIIEILETK_3_y5_1_L	25.2
PfkA	513.287	490.287	LVDHDIIEILETK_3_y4_1_L	25.2
PfkA	515.959	740.428	LVDHDIIEILETK_3_y6_1_H	25.2
PfkA	515.959	611.385	LVDHDIIEILETK_3_y5_1_H	25.2
PfkA	515.959	498.301	LVDHDIIEILETK_3_y4_1_H	25.2
PfkA	688.395	971.577	LGAYAVELLLEGK_2_y9_1_L	25.6
PfkA	688.395	900.540	LGAYAVELLLEGK_2_y8_1_L	25.6
PfkA	688.395	801.472	LGAYAVELLLEGK_2_y7_1_L	25.6
PfkA	692.402	979.591	LGAYAVELLLEGK_2_y9_1_H	25.6
PfkA	692.402	908.554	LGAYAVELLLEGK_2_y8_1_H	25.6
PfkA	692.402	809.486	LGAYAVELLLEGK_2_y7_1_H	25.6
PfkA	654.867	1066.600	LELGSVGDIIHR_2_y10_1_L	24.5
PfkA	654.867	953.516	LELGSVGDIIHR_2_y9_1_L	24.5
PfkA	654.867	710.394	LELGSVGDIIHR_2_y6_1_L	24.5
PfkA	659.871	1076.609	LELGSVGDIIHR_2_y10_1_H	24.5
PfkA	659.871	963.525	LELGSVGDIIHR_2_y9_1_H	24.5
PfkA	659.871	720.403	LELGSVGDIIHR_2_y6_1_H	24.5
fbaA	621.346	958.532	SPVILGVSEGAGR_2_y10_1_L	23.4
fbaA	621.346	845.448	SPVILGVSEGAGR_2_y9_1_L	23.4
fbaA	621.346	732.363	SPVILGVSEGAGR_2_y8_1_L	23.4
fbaA	626.350	968.540	SPVILGVSEGAGR_2_y10_1_H	23.4
fbaA	626.350	855.456	SPVILGVSEGAGR_2_y9_1_H	23.4
fbaA	626.350	742.372	SPVILGVSEGAGR_2_y8_1_H	23.4
fbaA	709.368	1091.533	INVNTENQISSAK_2_y10_1_L	26.3
fbaA	709.368	977.490	INVNTENQISSAK_2_y9_1_L	26.3
fbaA	709.368	747.400	INVNTENQISSAK_2_y7_1_L	26.3
fbaA	713.375	1099.547	INVNTENQISSAK_2_y10_1_H	26.3
fbaA	713.375	985.504	INVNTENQISSAK_2_y9_1_H	26.3
fbaA	713.375	755.414	INVNTENQISSAK_2_y7_1_H	26.3
TpiA	910.816	546.325	GLAGLSEEQVAASVIAYEPIWAIGTGK_3_y6_1_L	34.1
TpiA	910.816	475.287	GLAGLSEEQVAASVIAYEPIWAIGTGK_3_y5_1_L	34.1
TpiA	910.816	362.203	GLAGLSEEQVAASVIAYEPIWAIGTGK_3_y4_1_L	34.1
TpiA	913.488	554.339	GLAGLSEEQVAASVIAYEPIWAIGTGK_3_y6_1_H	34.1
TpiA	913.488	483.302	GLAGLSEEQVAASVIAYEPIWAIGTGK_3_y5_1_H	34.1
TpiA	913.488	370.218	GLAGLSEEQVAASVIAYEPIWAIGTGK_3_y4_1_H	34.1
TpiA	704.372	1007.541	TLGEAVSFVEEVK_2_y9_1_L	26.1
TpiA	704.372	936.504	TLGEAVSFVEEVK_2_y8_1_L	26.1
TpiA	704.372	837.435	TLGEAVSFVEEVK_2_y7_1_L	26.1
TpiA	708.379	1015.555	TLGEAVSFVEEVK_2_y9_1_H	26.1
TpiA	708.379	944.518	TLGEAVSFVEEVK_2_y8_1_H	26.1
TpiA	708.379	845.449	TLGEAVSFVEEVK_2_y7_1_H	26.1
GapA	1006.484	1163.569	GILGYSEEPLVSGDYNGNK_2_y11_1_L	36
GapA	1006.484	854.364	GILGYSEEPLVSGDYNGNK_2_y8_1_L	36
GapA	1006.484	767.332	GILGYSEEPLVSGDYNGNK_2_y7_1_L	36
GapA	1010.491	1171.583	GILGYSEEPLVSGDYNGNK_2_y11_1_H	36
GapA	1010.491	862.378	GILGYSEEPLVSGDYNGNK_2_y8_1_H	36
GapA	1010.491	775.346	GILGYSEEPLVSGDYNGNK_2_y7_1_H	36
GapA	845.379	1041.423	VISWYDNESGYSNR_2_y9_1_L	30.7
GapA	845.379	926.396	VISWYDNESGYSNR_2_y8_1_L	30.7
GapA	845.379	376.194	VISWYDNESGYSNR_2_y3_1_L	30.7
GapA	850.383	1051.431	VISWYDNESGYSNR_2_y9_1_H	30.7
GapA	850.383	936.405	VISWYDNESGYSNR_2_y8_1_H	30.7
GapA	850.383	386.202	VISWYDNESGYSNR_2_y3_1_H	30.7
Pgk	679.666	958.449	AFAELADVYVNDAFGAAHR_3_y9_1_L	29
Pgk	679.666	729.379	AFAELADVYVNDAFGAAHR_3_y7_1_L	29
Pgk	683.002	968.457	AFAELADVYVNDAFGAAHR_3_y9_1_H	29
Pgk	683.002	739.387	AFAELADVYVNDAFGAAHR_3_y7_1_H	29
Pgk	670.705	717.414	IVPISEIPSDLEAIDIGTK_3_y7_1_L	28.8
Pgk	670.705	533.293	IVPISEIPSDLEAIDIGTK_3_y5_1_L	28.8
Pgk	670.705	418.266	IVPISEIPSDLEAIDIGTK_3_y4_1_L	28.8
Pgk	673.376	725.428	IVPISEIPSDLEAIDIGTK_3_y7_1_H	28.8
Pgk	673.376	541.307	IVPISEIPSDLEAIDIGTK_3_y5_1_H	28.8
Pgk	673.376	426.280	IVPISEIPSDLEAIDIGTK_3_y4_1_H	28.8
GpmI	644.349	1045.564	EIGVGEIASISGR_2_y11_1_L	24.1
GpmI	644.349	889.474	EIGVGEIASISGR_2_y9_1_L	24.1

Protein	Q1	Q3	Peptide information*	CE
GpmI	644.349	703.410	EIGVGEIASISGR_2_y7_1_L	24.1
GpmI	649.353	1055.572	EIGVGEIASISGR_2_y11_1_H	24.1
GpmI	649.353	899.482	EIGVGEIASISGR_2_y9_1_H	24.1
GpmI	649.353	713.418	EIGVGEIASISGR_2_y7_1_H	24.1
GpmI	661.341	1079.573	NQTFLDAISNAK_2_y10_1_L	24.7
GpmI	661.341	831.457	NQTFLDAISNAK_2_y8_1_L	24.7
GpmI	661.341	718.373	NQTFLDAISNAK_2_y7_1_L	24.7
GpmI	665.348	1087.587	NQTFLDAISNAK_2_y10_1_H	24.7
GpmI	665.348	839.471	NQTFLDAISNAK_2_y8_1_H	24.7
GpmI	665.348	726.387	NQTFLDAISNAK_2_y7_1_H	24.7
Eno	924.971	1065.521	ALVPSGASTGEYEAVELR_2_y9_1_L	33.3
Eno	924.971	879.457	ALVPSGASTGEYEAVELR_2_y7_1_L	33.3
Eno	924.971	587.351	ALVPSGASTGEYEAVELR_2_y5_1_L	33.3
Eno	929.975	1075.529	ALVPSGASTGEYEAVELR_2_y9_1_H	33.3
Eno	929.975	889.465	ALVPSGASTGEYEAVELR_2_y7_1_H	33.3
Eno	929.975	597.359	ALVPSGASTGEYEAVELR_2_y5_1_H	33.3
Pyk	896.988	1109.620	GDLGVEIPAEEVPLVQK_2_y10_1_L	32.4
Pyk	896.988	1012.567	GDLGVEIPAEEVPLVQK_2_y9_1_L	32.4
Pyk	896.988	941.530	GDLGVEIPAEEVPLVQK_2_y8_1_L	32.4
Pyk	900.995	1117.634	GDLGVEIPAEEVPLVQK_2_y10_1_H	32.4
Pyk	900.995	1020.582	GDLGVEIPAEEVPLVQK_2_y9_1_H	32.4
Pyk	900.995	949.544	GDLGVEIPAEEVPLVQK_2_y8_1_H	32.4
Pyk	630.670	826.503	ELLEEHNAQDIQIIPK_3_y7_1_L	27.9
Pyk	630.670	598.392	ELLEEHNAQDIQIIPK_3_y5_1_L	27.9
Pyk	630.670	244.166	ELLEEHNAQDIQIIPK_3_y2_1_L	27.9
Pyk	633.342	834.517	ELLEEHNAQDIQIIPK_3_y7_1_H	27.9
Pyk	633.342	606.406	ELLEEHNAQDIQIIPK_3_y5_1_H	27.9
Pyk	633.342	252.180	ELLEEHNAQDIQIIPK_3_y2_1_H	27.9
Pyc	798.454	1155.637	VIEVAPSVSLSPELR_2_y11_1_L	29.2
Pyc	798.454	1084.600	VIEVAPSVSLSPELR_2_y10_1_L	29.2
Pyc	798.454	801.446	VIEVAPSVSLSPELR_2_y7_1_L	29.2
Pyc	803.458	1165.645	VIEVAPSVSLSPELR_2_y11_1_H	29.2
Pyc	803.458	1094.608	VIEVAPSVSLSPELR_2_y10_1_H	29.2
Pyc	803.458	811.455	VIEVAPSVSLSPELR_2_y7_1_H	29.2
Pyc	623.346	1030.593	TNIPFLENVAK_2_y9_1_L	23.4
Pyc	623.346	820.456	TNIPFLENVAK_2_y7_1_L	23.4
Pyc	623.346	673.388	TNIPFLENVAK_2_y6_1_L	23.4
Pyc	627.353	1038.607	TNIPFLENVAK_2_y9_1_H	23.4
Pyc	627.353	828.471	TNIPFLENVAK_2_y7_1_H	23.4
Pyc	627.353	681.402	TNIPFLENVAK_2_y6_1_H	23.4
PdhA	504.274	844.477	YAISTPVEK_2_y8_1_L	19.5
PdhA	504.274	773.440	YAISTPVEK_2_y7_1_L	19.5
PdhA	504.274	660.356	YAISTPVEK_2_y6_1_L	19.5
PdhA	508.281	852.492	YAISTPVEK_2_y8_1_H	19.5
PdhA	508.281	781.455	YAISTPVEK_2_y7_1_H	19.5
PdhA	508.281	668.370	YAISTPVEK_2_y6_1_H	19.5
PdhA	589.272	1007.432	GLWSEEEEAK_2_y8_1_L	22.3
PdhA	589.272	821.352	GLWSEEEEAK_2_y7_1_L	22.3
PdhA	589.272	734.320	GLWSEEEEAK_2_y6_1_L	22.3

Protein	Q1	Q3	Peptide information*	CE
PdhA	593.279	1015.446	GLWSEEEEAK_2_y8_1_H	22.3
PdhA	593.279	829.367	GLWSEEEEAK_2_y7_1_H	22.3
PdhA	593.279	742.334	GLWSEEEEAK_2_y6_1_H	22.3
PdhB	591.366	997.604	AILSLEAPVLR_2_y9_1_L	22.4
PdhB	591.366	884.520	AILSLEAPVLR_2_y8_1_L	22.4
PdhB	591.366	684.404	AILSLEAPVLR_2_y6_1_L	22.4
PdhB	596.370	1007.612	AILSLEAPVLR_2_y9_1_H	22.4
PdhB	596.370	894.528	AILSLEAPVLR_2_y8_1_H	22.4
PdhB	596.370	694.412	AILSLEAPVLR_2_y6_1_H	22.4
PdhB	595.327	991.509	VVIPSTPYDAK_2_y9_1_L	22.5
PdhB	595.327	878.425	VVIPSTPYDAK_2_y8_1_L	22.5
PdhB	595.327	781.373	VVIPSTPYDAK_2_y7_1_L	22.5
PdhB	599.334	999.524	VVIPSTPYDAK_2_y9_1_H	22.5
PdhB	599.334	886.440	VVIPSTPYDAK_2_y8_1_H	22.5
PdhB	599.334	789.387	VVIPSTPYDAK_2_y7_1_H	22.5
PdhC	670.693	861.421	DGEIVAAPVLALSLSFDHR_3_y7_1_L	28.8
PdhC	670.693	774.389	DGEIVAAPVLALSLSFDHR_3_y6_1_L	28.8
PdhC	674.029	871.430	DGEIVAAPVLALSLSFDHR_3_y7_1_H	28.8
PdhC	674.029	784.398	DGEIVAAPVLALSLSFDHR_3_y6_1_H	28.8
PdhC	811.917	960.500	SVFEISDEINGLATK_2_y9_1_L	29.6
PdhC	811.917	716.430	SVFEISDEINGLATK_2_y7_1_L	29.6
PdhC	811.917	603.346	SVFEISDEINGLATK_2_y6_1_L	29.6
PdhC	815.924	968.514	SVFEISDEINGLATK_2_y9_1_H	29.6
PdhC	815.924	724.444	SVFEISDEINGLATK_2_y7_1_H	29.6
PdhC	815.924	611.360	SVFEISDEINGLATK_2_y6_1_H	29.6
PdhD	744.739	719.420	TNVPNIYAIGDIIEGPPLAHK_3_y7_1_L	30.4
PdhD	744.739	662.398	TNVPNIYAIGDIIEGPPLAHK_3_y6_1_L	30.4
PdhD	744.739	565.346	TNVPNIYAIGDIIEGPPLAHK_3_y5_1_L	30.4
PdhD	747.410	727.434	TNVPNIYAIGDIIEGPPLAHK_3_y7_1_H	30.4
PdhD	747.410	670.413	TNVPNIYAIGDIIEGPPLAHK_3_y6_1_H	30.4
PdhD	747.410	573.360	TNVPNIYAIGDIIEGPPLAHK_3_y5_1_H	30.4
PdhD	543.830	874.499	VLNSTGALALK_2_y9_1_L	20.8
PdhD	543.830	760.456	VLNSTGALALK_2_y8_1_L	20.8
PdhD	543.830	572.377	VLNSTGALALK_2_y6_1_L	20.8
PdhD	547.837	882.513	VLNSTGALALK_2_y9_1_H	20.8
PdhD	547.837	768.471	VLNSTGALALK_2_y8_1_H	20.8
PdhD	547.837	580.391	VLNSTGALALK_2_y6_1_H	20.8
PdhD	672.315	923.458	GEAYFVDSNSVR_2_y8_1_L	25
PdhD	672.315	776.390	GEAYFVDSNSVR_2_y7_1_L	25
PdhD	672.315	677.321	GEAYFVDSNSVR_2_y6_1_L	25
PdhD	677.319	933.466	GEAYFVDSNSVR_2_y8_1_H	25
PdhD	677.319	786.398	GEAYFVDSNSVR_2_y7_1_H	25
PdhD	677.319	687.330	GEAYFVDSNSVR_2_y6_1_H	25
CitZ	508.798	650.362	VPGLVAAFSR_2_y6_1_L	19.7
CitZ	508.798	551.294	VPGLVAAFSR_2_y5_1_L	19.7
CitZ	508.798	459.264	VPGLVAAFSR_2_y9_2_L	19.7
CitZ	513.802	660.370	VPGLVAAFSR_2_y6_1_H	19.7
CitZ	513.802	561.302	VPGLVAAFSR_2_y5_1_H	19.7
CitZ	513.802	464.268	VPGLVAAFSR_2_y9_2_H	19.7

Protein	Q1	Q3	Peptide information*	CE
CitZ	755.899	1140.605	EAAVPQEIIEHFK_2_y9_1_L	27.8
CitZ	755.899	620.340	EAAVPQEIIEHFK_2_y10_2_L	27.8
CitZ	755.899	570.806	EAAVPQEIIEHFK_2_y9_2_L	27.8
CitZ	759.906	1148.619	EAAVPQEIIEHFK_2_y9_1_H	27.8
CitZ	759.906	624.347	EAAVPQEIIEHFK_2_y10_2_H	27.8
CitZ	759.906	574.813	EAAVPQEIIEHFK_2_y9_2_H	27.8
CitB	626.665	884.484	FVEFFGPGIAELPLADR_3_y8_1_L	27.8
CitB	626.665	571.320	FVEFFGPGIAELPLADR_3_y5_1_L	27.8
CitB	626.665	576.325	FVEFFGPGIAELPLADR_3_y11_2_L	27.8
CitB	630.001	894.492	FVEFFGPGIAELPLADR_3_y8_1_H	27.8
CitB	630.001	581.328	FVEFFGPGIAELPLADR_3_y5_1_H	27.8
CitB	630.001	581.329	FVEFFGPGIAELPLADR_3_y11_2_H	27.8
CitB	701.388	946.532	NDLLITSVLSGNR_2_y9_1_L	26
CitB	701.388	833.448	NDLLITSVLSGNR_2_y8_1_L	26
CitB	701.388	732.400	NDLLITSVLSGNR_2_y7_1_L	26
CitB	706.393	956.540	NDLLITSVLSGNR_2_y9_1_H	26
CitB	706.393	843.456	NDLLITSVLSGNR_2_y8_1_H	26
CitB	706.393	742.408	NDLLITSVLSGNR_2_y7_1_H	26
Icd	800.422	1126.647	TGEWLPAETLDVIR_2_y10_1_L	29.2
Icd	800.422	1013.563	TGEWLPAETLDVIR_2_y9_1_L	29.2
Icd	800.422	507.285	TGEWLPAETLDVIR_2_y9_2_L	29.2
Icd	805.427	1136.655	TGEWLPAETLDVIR_2_y10_1_H	29.2
Icd	805.427	1023.571	TGEWLPAETLDVIR_2_y9_1_H	29.2
Icd	805.427	512.289	TGEWLPAETLDVIR_2_y9_2_H	29.2
Icd	808.378	914.462	ENTEDIYAGIEYAK_2_y8_1_L	29.5
Icd	808.378	751.398	ENTEDIYAGIEYAK_2_y7_1_L	29.5
Icd	808.378	680.361	ENTEDIYAGIEYAK_2_y6_1_L	29.5
Icd	812.385	922.476	ENTEDIYAGIEYAK_2_y8_1_H	29.5
Icd	812.385	759.413	ENTEDIYAGIEYAK_2_y7_1_H	29.5
Icd	812.385	688.376	ENTEDIYAGIEYAK_2_y6_1_H	29.5
OdhA	676.820	1036.495	TQSGYPVQDETK_2_y9_1_L	25.2
OdhA	676.820	979.473	TQSGYPVQDETK_2_y8_1_L	25.2
OdhA	676.820	816.410	TQSGYPVQDETK_2_y7_1_L	25.2
OdhA	680.827	1044.509	TQSGYPVQDETK_2_y9_1_H	25.2
OdhA	680.827	987.487	TQSGYPVQDETK_2_y8_1_H	25.2
OdhA	680.827	824.424	TQSGYPVQDETK_2_y7_1_H	25.2
OdhA	844.908	947.479	NPNTVSEVQELSESR_2_y8_1_L	30.7
OdhA	844.908	848.411	NPNTVSEVQELSESR_2_y7_1_L	30.7
OdhA	844.908	478.226	NPNTVSEVQELSESR_2_y4_1_L	30.7
OdhA	849.912	957.488	NPNTVSEVQELSESR_2_y8_1_H	30.7
OdhA	849.912	858.419	NPNTVSEVQELSESR_2_y7_1_H	30.7
OdhA	849.912	488.234	NPNTVSEVQELSESR_2_y4_1_H	30.7
OdhB	634.629	978.437	QAEPAAQEVSEEAQSEAK_3_y9_1_L	28
OdhB	634.629	762.363	QAEPAAQEVSEEAQSEAK_3_y7_1_L	28
OdhB	634.629	434.225	QAEPAAQEVSEEAQSEAK_3_y4_1_L	28
OdhB	637.300	986.452	QAEPAAQEVSEEAQSEAK_3_y9_1_H	28
OdhB	637.300	770.377	QAEPAAQEVSEEAQSEAK_3_y7_1_H	28
OdhB	637.300	442.239	QAEPAAQEVSEEAQSEAK_3_y4_1_H	28
OdhB	657.686	758.456	VPELAESISEGTIAQWLK_3_y6_1_L	28.5

Protein	Q1	Q3	Peptide information*	CE
OdhB	657.686	645.372	VPELAESISEGTIAQWLK_3_y5_1_L	28.5
OdhB	657.686	574.335	VPELAESISEGTIAQWLK_3_y4_1_L	28.5
OdhB	660.357	766.470	VPELAESISEGTIAQWLK_3_y6_1_H	28.5
OdhB	660.357	653.386	VPELAESISEGTIAQWLK_3_y5_1_H	28.5
OdhB	660.357	582.349	VPELAESISEGTIAQWLK_3_y4_1_H	28.5
SucC	676.341	933.452	VAFTAEEAVESAK_2_y9_1_L	25.2
SucC	676.341	862.415	VAFTAEEAVESAK_2_y8_1_L	25.2
SucC	676.341	591.288	VAFTAEEAVESAK_2_y11_2_L	25.2
SucC	680.348	941.467	VAFTAEEAVESAK_2_y9_1_H	25.2
SucC	680.348	870.429	VAFTAEEAVESAK_2_y8_1_H	25.2
SucC	680.348	595.295	VAFTAEEAVESAK_2_y11_2_H	25.2
SucC	558.327	873.519	EIAFAINIPK_2_y8_1_L	21.3
SucC	558.327	655.414	EIAFAINIPK_2_y6_1_L	21.3
SucC	558.327	584.377	EIAFAINIPK_2_y5_1_L	21.3
SucC	562.334	881.533	EIAFAINIPK_2_y8_1_H	21.3
SucC	562.334	663.428	EIAFAINIPK_2_y6_1_H	21.3
SucC	562.334	592.391	EIAFAINIPK_2_y5_1_H	21.3
SucC	597.882	967.630	QVGLTLPLVVR_2_y9_1_L	22.6
SucC	597.882	797.524	QVGLTLPLVVR_2_y7_1_L	22.6
SucC	597.882	583.393	QVGLTLPLVVR_2_y5_1_L	22.6
SucC	602.886	977.638	QVGLTLPLVVR_2_y9_1_H	22.6
SucC	602.886	807.533	QVGLTLPLVVR_2_y7_1_H	22.6
SucC	602.886	593.401	QVGLTLPLVVR_2_y5_1_H	22.6
SucD	437.263	776.467	PVVGFIGGK_2_y8_1_L	17.3
SucD	437.263	677.398	PVVGFIGGK_2_y7_1_L	17.3
SucD	437.263	578.330	PVVGFIGGK_2_y6_1_L	17.3
SucD	441.270	784.481	PVVGFIGGK_2_y8_1_H	17.3
SucD	441.270	685.412	PVVGFIGGK_2_y7_1_H	17.3
SucD	441.270	586.344	PVVGFIGGK_2_y6_1_H	17.3
SdhA	892.910	973.495	YEGWEFLGAVLDDDR_2_y9_1_L	32.3
SdhA	892.910	860.411	YEGWEFLGAVLDDDR_2_y8_1_L	32.3
SdhA	892.910	633.284	YEGWEFLGAVLDDDR_2_y5_1_L	32.3
SdhA	897.914	983.503	YEGWEFLGAVLDDDR_2_y9_1_H	32.3
SdhA	897.914	870.419	YEGWEFLGAVLDDDR_2_y8_1_H	32.3
SdhA	897.914	643.292	YEGWEFLGAVLDDDR_2_y5_1_H	32.3
SdhA	567.824	964.535	LGGIIEIYEK_2_y8_1_L	21.6
SdhA	567.824	794.429	LGGIIEIYEK_2_y6_1_L	21.6
SdhA	567.824	681.345	LGGIIEIYEK_2_y5_1_L	21.6
SdhA	571.831	972.549	LGGIIEIYEK_2_y8_1_H	21.6
SdhA	571.831	802.444	LGGIIEIYEK_2_y6_1_H	21.6
SdhA	571.831	689.360	LGGIIEIYEK_2_y5_1_H	21.6
SdhB	864.441	1032.511	AWIPIDGTYDLGPGPR_2_y10_1_L	31.3
SdhB	864.441	735.883	AWIPIDGTYDLGPGPR_2_y14_2_L	31.3
SdhB	864.441	679.341	AWIPIDGTYDLGPGPR_2_y13_2_L	31.3
SdhB	869.445	1042.519	AWIPIDGTYDLGPGPR_2_y10_1_H	31.3
SdhB	869.445	740.887	AWIPIDGTYDLGPGPR_2_y14_2_H	31.3
SdhB	869.445	684.345	AWIPIDGTYDLGPGPR_2_y13_2_H	31.3
SdhB	482.746	748.410	DTNLQAFR_2_y6_1_L	18.8
SdhB	482.746	521.283	DTNLQAFR_2_y4_1_L	18.8

Protein	Q1	Q3	Peptide information*	CE
SdhB	482.746	393.224	DTNLQAFR_2_y3_1_L	18.8
SdhB	487.750	758.418	DTNLQAFR_2_y6_1_H	18.8
SdhB	487.750	531.291	DTNLQAFR_2_y4_1_H	18.8
SdhB	487.750	403.233	DTNLQAFR_2_y3_1_H	18.8
SdhB	663.891	946.532	GIPLTTSIAALNR_2_y9_1_L	24.8
SdhB	663.891	544.320	GIPLTTSIAALNR_2_y5_1_L	24.8
SdhB	663.891	578.838	GIPLTTSIAALNR_2_y11_2_L	24.8
SdhB	668.895	956.540	GIPLTTSIAALNR_2_y9_1_H	24.8
SdhB	668.895	554.328	GIPLTTSIAALNR_2_y5_1_H	24.8
SdhB	668.895	583.842	GIPLTTSIAALNR_2_y11_2_H	24.8
SdhC	538.306	775.482	NWLFVLQR_2_y6_1_L	20.6
SdhC	538.306	662.398	NWLFVLQR_2_y5_1_L	20.6
SdhC	538.306	515.330	NWLFVLQR_2_y4_1_L	20.6
SdhC	543.310	785.491	NWLFVLQR_2_y6_1_H	20.6
SdhC	543.310	672.407	NWLFVLQR_2_y5_1_H	20.6
SdhC	543.310	525.338	NWLFVLQR_2_y4_1_H	20.6
FumC	633.820	1052.501	LTGQTFSSSPNK_2_y10_1_L	23.8
FumC	633.820	867.421	LTGQTFSSSPNK_2_y8_1_L	23.8
FumC	633.820	766.373	LTGQTFSSSPNK_2_y7_1_L	23.8
FumC	637.827	1060.515	LTGQTFSSSPNK_2_y10_1_H	23.8
FumC	637.827	875.435	LTGQTFSSSPNK_2_y8_1_H	23.8
FumC	637.827	774.387	LTGQTFSSSPNK_2_y7_1_H	23.8
FumC	542.249	829.380	NSDQTIHPNDDVNR_3_y7_1_L	25.9
FumC	542.249	503.257	NSDQTIHPNDDVNR_3_y4_1_L	25.9
FumC	542.249	388.230	NSDQTIHPNDDVNR_3_y3_1_L	25.9
FumC	545.585	839.388	NSDQTIHPNDDVNR_3_y7_1_H	25.9
FumC	545.585	513.266	NSDQTIHPNDDVNR_3_y4_1_H	25.9
FumC	545.585	398.239	NSDQTIHPNDDVNR_3_y3_1_H	25.9
mdh	665.033	926.494	ELADVVLVDIPQLENPTK_3_y8_1_L	28.6
Mdh	665.033	701.383	ELADVVLVDIPQLENPTK_3_y6_1_L	28.6
Mdh	665.033	463.751	ELADVVLVDIPQLENPTK_3_y8_2_L	28.6
Mdh	667.705	934.508	ELADVVLVDIPQLENPTK_3_y8_1_H	28.6
Mdh	667.705	709.397	ELADVVLVDIPQLENPTK_3_y6_1_H	28.6
Mdh	667.705	467.758	ELADVVLVDIPQLENPTK_3_y8_2_H	28.6
Mdh	811.445	1137.688	YSYAGGIPLETLIPK_2_y11_1_L	29.6
Mdh	811.445	1023.645	YSYAGGIPLETLIPK_2_y9_1_L	29.6
Mdh	811.445	910.561	YSYAGGIPLETLIPK_2_y8_1_L	29.6
Mdh	815.453	1145.702	YSYAGGIPLETLIPK_2_y11_1_H	29.6
Mdh	815.453	1031.659	YSYAGGIPLETLIPK_2_y9_1_H	29.6
Mdh	815.453	918.575	YSYAGGIPLETLIPK_2_y8_1_H	29.6
MaeA	676.815	861.421	AYEQFQAQPDR_2_y7_1_L	25.2
MaeA	676.815	714.353	AYEQFQAQPDR_2_y6_1_L	25.2
MaeA	676.815	586.294	AYEQFQAQPDR_2_y5_1_L	25.2
MaeA	681.819	871.430	AYEQFQAQPDR_2_y7_1_H	25.2
MaeA	681.819	724.361	AYEQFQAQPDR_2_y6_1_H	25.2
MaeA	681.819	596.303	AYEQFQAQPDR_2_y5_1_H	25.2
MaeA	504.261	851.426	GVAFSLEER_2_y7_1_L	19.5
MaeA	504.261	780.389	GVAFSLEER_2_y6_1_L	19.5
MaeA	504.261	633.320	GVAFSLEER_2_y5_1_L	19.5

Protein	Q1	Q3	Peptide information*	CE
MaeA	509.266	861.434	GVAFSLEER_2_y7_1_H	19.5
MaeA	509.266	790.397	GVAFSLEER_2_y6_1_H	19.5
MaeA	509.266	643.328	GVAFSLEER_2_y5_1_H	19.5
YtsJ	679.018	920.535	SDFPNQVNNVLAFPGIFR_3_y8_1_L	29
YtsJ	679.018	807.451	SDFPNQVNNVLAFPGIFR_3_y7_1_L	29
YtsJ	679.018	589.346	SDFPNQVNNVLAFPGIFR_3_y5_1_L	29
YtsJ	682.354	930.544	SDFPNQVNNVLAFPGIFR_3_y8_1_H	29
YtsJ	682.354	817.459	SDFPNQVNNVLAFPGIFR_3_y7_1_H	29
YtsJ	682.354	599.354	SDFPNQVNNVLAFPGIFR_3_y5_1_H	29
YtsJ	615.317	1015.494	ITVDPEEVAEK_2_y9_1_L	23.2
YtsJ	615.317	916.426	ITVDPEEVAEK_2_y8_1_L	23.2
YtsJ	615.317	801.399	ITVDPEEVAEK_2_y7_1_L	23.2
YtsJ	619.324	1023.508	ITVDPEEVAEK_2_y9_1_H	23.2
YtsJ	619.324	924.440	ITVDPEEVAEK_2_y8_1_H	23.2
YtsJ	619.324	809.413	ITVDPEEVAEK_2_y7_1_H	23.2
PckA	662.990	980.468	IDWGPVNQPISEEAFER_3_y8_1_L	28.6
PckA	662.990	867.384	IDWGPVNQPISEEAFER_3_y7_1_L	28.6
PckA	662.990	780.352	IDWGPVNQPISEEAFER_3_y6_1_L	28.6
PckA	666.326	990.477	IDWGPVNQPISEEAFER_3_y8_1_H	28.6
PckA	666.326	877.393	IDWGPVNQPISEEAFER_3_y7_1_H	28.6
PckA	666.326	790.361	IDWGPVNQPISEEAFER_3_y6_1_H	28.6
PckA	862.855	930.432	EANYDDSFYTENTR_2_y7_1_L	31.3
PckA	862.855	783.363	EANYDDSFYTENTR_2_y6_1_L	31.3
PckA	862.855	620.300	EANYDDSFYTENTR_2_y5_1_L	31.3
PckA	867.859	940.440	EANYDDSFYTENTR_2_y7_1_H	31.3
PckA	867.859	793.371	EANYDDSFYTENTR_2_y6_1_H	31.3
PckA	867.859	630.308	EANYDDSFYTENTR_2_y5_1_H	31.3
GapB	545.853	906.577	ALSLVLPHLK_2_y8_1_L	20.9
GapB	545.853	706.461	ALSLVLPHLK_2_y6_1_L	20.9
GapB	545.853	494.309	ALSLVLPHLK_2_y4_1_L	20.9
GapB	549.860	914.591	ALSLVLPHLK_2_y8_1_H	20.9
GapB	549.860	714.475	ALSLVLPHLK_2_y6_1_H	20.9
GapB	549.860	502.323	ALSLVLPHLK_2_y4_1_H	20.9
GapB	726.367	931.509	EYDIDIVVEATGK_2_y9_1_L	26.8
GapB	726.367	703.398	EYDIDIVVEATGK_2_y7_1_L	26.8
GapB	726.367	604.330	EYDIDIVVEATGK_2_y6_1_L	26.8
GapB	730.374	939.524	EYDIDIVVEATGK_2_y9_1_H	26.8
GapB	730.374	711.413	EYDIDIVVEATGK_2_y7_1_H	26.8
GapB	730.374	612.344	EYDIDIVVEATGK_2_y6_1_H	26.8
YYdE	714.714	900.551	ETNVGEELLQEVAILESLR_3_y8_1_L	29.8
YYdE	714.714	730.446	ETNVGEELLQEVAILESLR_3_y6_1_L	29.8
YYdE	714.714	617.362	ETNVGEELLQEVAILESLR_3_y5_1_L	29.8
YYdE	718.051	910.560	ETNVGEELLQEVAILESLR_3_y8_1_H	29.8
YYdE	718.051	740.454	ETNVGEELLQEVAILESLR_3_y6_1_H	29.8
YYdE	718.051	627.370	ETNVGEELLQEVAILESLR_3_y5_1_H	29.8
YYdE	510.772	665.325	ELLDVFER_2_y5_1_L	19.7
YYdE	510.772	550.298	ELLDVFER_2_y4_1_L	19.7
YYdE	510.772	451.230	ELLDVFER_2_y3_1_L	19.7
YYdE	515.776	675.334	ELLDVFER_2_y5_1_H	19.7

Protein	Q1	Q3	Peptide information*	CE
YYdE	515.776	560.307	ELLDVFER_2_y4_1_H	19.7
YYdE	515.776	461.238	ELLDVFER_2_y3_1_H	19.7
GlnA	624.864	1007.577	LQFTDILGTIK_2_y9_1_L	23.5
GlnA	624.864	860.509	LQFTDILGTIK_2_y8_1_L	23.5
GlnA	624.864	759.461	LQFTDILGTIK_2_y7_1_L	23.5
GlnA	628.871	1015.591	LQFTDILGTIK_2_y9_1_H	23.5
GlnA	628.871	868.523	LQFTDILGTIK_2_y8_1_H	23.5
GlnA	628.871	767.475	LQFTDILGTIK_2_y7_1_H	23.5
GlnA	592.338	970.557	NVEIPVSQLGK_2_y9_1_L	22.4
GlnA	592.338	841.514	NVEIPVSQLGK_2_y8_1_L	22.4
GlnA	592.338	728.430	NVEIPVSQLGK_2_y7_1_L	22.4
GlnA	596.345	978.571	NVEIPVSQLGK_2_y9_1_H	22.4
GlnA	596.345	849.528	NVEIPVSQLGK_2_y8_1_H	22.4
GlnA	596.345	736.444	NVEIPVSQLGK_2_y7_1_H	22.4
GltA	945.502	961.510	ASQLDLSTLLYQPEGVR_2_y8_1_L	34
GltA	945.502	848.426	ASQLDLSTLLYQPEGVR_2_y7_1_L	34
GltA	945.502	557.304	ASQLDLSTLLYQPEGVR_2_y5_1_L	34
GltA	950.506	971.518	ASQLDLSTLLYQPEGVR_2_y8_1_H	34
GltA	950.506	858.434	ASQLDLSTLLYQPEGVR_2_y7_1_H	34
GltA	950.506	567.312	ASQLDLSTLLYQPEGVR_2_y5_1_H	34
GltA	668.320	992.458	TLEPGSDFQWR_2_y8_1_L	24.9
GltA	668.320	636.325	TLEPGSDFQWR_2_y4_1_L	24.9
GltA	668.320	496.733	TLEPGSDFQWR_2_y8_2_L	24.9
GltA	673.324	1002.467	TLEPGSDFQWR_2_y8_1_H	24.9
GltA	673.324	646.334	TLEPGSDFQWR_2_y4_1_H	24.9
GltA	673.324	501.737	TLEPGSDFQWR_2_y8_2_H	24.9
GltB	591.781	853.420	TNNFPEFTGR_2_y7_1_L	22.4
GltB	591.781	706.352	TNNFPEFTGR_2_y6_1_L	22.4
GltB	591.781	333.188	TNNFPEFTGR_2_y3_1_L	22.4
GltB	596.785	863.429	TNNFPEFTGR_2_y7_1_H	22.4
GltB	596.785	716.360	TNNFPEFTGR_2_y6_1_H	22.4
GltB	596.785	343.196	TNNFPEFTGR_2_y3_1_H	22.4
GltB	721.891	944.495	GQSLIVWAINEGR_2_y8_1_L	26.7
GltB	721.891	845.426	GQSLIVWAINEGR_2_y7_1_L	26.7
GltB	721.891	659.347	GQSLIVWAINEGR_2_y6_1_L	26.7
GltB	726.895	954.503	GQSLIVWAINEGR_2_y8_1_H	26.7
GltB	726.895	855.435	GQSLIVWAINEGR_2_y7_1_H	26.7
GltB	726.895	669.355	GQSLIVWAINEGR_2_y6_1_H	26.7
YerD	577.290	604.366	EYEQTVISGK_2_y6_1_L	21.9
YerD	577.290	404.250	EYEQTVISGK_2_y4_1_L	21.9
YerD	577.290	291.166	EYEQTVISGK_2_y3_1_L	21.9
YerD	581.298	612.381	EYEQTVISGK_2_y6_1_H	21.9
YerD	581.298	412.265	EYEQTVISGK_2_y4_1_H	21.9
YerD	581.298	299.180	EYEQTVISGK_2_y3_1_H	21.9
YerD	509.264	831.421	VSEEVADIR_2_y7_1_L	19.7
YerD	509.264	702.378	VSEEVADIR_2_y6_1_L	19.7
YerD	509.264	288.203	VSEEVADIR_2_y2_1_L	19.7
YerD	514.268	841.429	VSEEVADIR_2_y7_1_H	19.7
YerD	514.268	712.386	VSEEVADIR_2_y6_1_H	19.7

Protein	Q1	Q3	Peptide information*	CE
YerD	514.268	298.211	VSEEVADIR_2_y2_1_H	19.7
ProA	558.798	916.473	TVENVQEAVK_2_y8_1_L	21.3
ProA	558.798	787.431	TVENVQEAVK_2_y7_1_L	21.3
ProA	558.798	574.320	TVENVQEAVK_2_y5_1_L	21.3
ProA	562.806	924.488	TVENVQEAVK_2_y8_1_H	21.3
ProA	562.806	795.445	TVENVQEAVK_2_y7_1_H	21.3
ProA	562.806	582.334	TVENVQEAVK_2_y5_1_H	21.3
ProA	799.923	887.458	ELLDQLENAGVEIR_2_y8_1_L	29.2
ProA	799.923	758.416	ELLDQLENAGVEIR_2_y7_1_L	29.2
ProA	799.923	573.335	ELLDQLENAGVEIR_2_y5_1_L	29.2
ProA	804.927	897.466	ELLDQLENAGVEIR_2_y8_1_H	29.2
ProA	804.927	768.424	ELLDQLENAGVEIR_2_y7_1_H	29.2
ProA	804.927	583.344	ELLDQLENAGVEIR_2_y5_1_H	29.2
ProB	561.793	876.442	VFIGTGSGEQK_2_y9_1_L	21.4
ProB	561.793	763.358	VFIGTGSGEQK_2_y8_1_L	21.4
ProB	561.793	438.725	VFIGTGSGEQK_2_y9_2_L	21.4
ProB	565.800	884.456	VFIGTGSGEQK_2_y9_1_H	21.4
ProB	565.800	771.372	VFIGTGSGEQK_2_y8_1_H	21.4
ProB	565.800	442.732	VFIGTGSGEQK_2_y9_2_H	21.4
ProB	745.422	998.599	QYSLTPGQILLTR_2_y9_1_L	27.4
ProB	745.422	897.552	QYSLTPGQILLTR_2_y8_1_L	27.4
ProB	745.422	502.335	QYSLTPGQILLTR_2_y4_1_L	27.4
ProB	750.426	1008.608	QYSLTPGQILLTR_2_y9_1_H	27.4
ProB	750.426	907.560	QYSLTPGQILLTR_2_y8_1_H	27.4
ProB	750.426	512.343	QYSLTPGQILLTR_2_y4_1_H	27.4
ProJ	884.484	489.278	GIIPIINENDTVTVNR_2_y4_1_L	32
ProJ	884.484	799.431	GIIPIINENDTVTVNR_2_y14_2_L	32
ProJ	884.484	742.889	GIIPIINENDTVTVNR_2_y13_2_L	32
ProJ	889.488	499.286	GIIPIINENDTVTVNR_2_y4_1_H	32
ProJ	889.488	804.435	GIIPIINENDTVTVNR_2_y14_2_H	32
ProJ	889.488	747.893	GIIPIINENDTVTVNR_2_y13_2_H	32
ProJ	557.329	871.525	LEALVDQVVK_2_y8_1_L	21.3
ProJ	557.329	687.404	LEALVDQVVK_2_y6_1_L	21.3
ProJ	557.329	588.335	LEALVDQVVK_2_y5_1_L	21.3
ProJ	561.336	879.539	LEALVDQVVK_2_y8_1_H	21.3
ProJ	561.336	695.418	LEALVDQVVK_2_y6_1_H	21.3
ProJ	561.336	596.349	LEALVDQVVK_2_y5_1_H	21.3
ProG	644.841	933.464	LLEAETEAGISR_2_y9_1_L	24.1
ProG	644.841	862.426	LLEAETEAGISR_2_y8_1_L	24.1
ProG	644.841	733.384	LLEAETEAGISR_2_y7_1_L	24.1
ProG	649.845	943.472	LLEAETEAGISR_2_y9_1_H	24.1
ProG	649.845	872.435	LLEAETEAGISR_2_y8_1_H	24.1
ProG	649.845	743.392	LLEAETEAGISR_2_y7_1_H	24.1
ProG	589.332	950.531	LNELLSVFSR_2_y8_1_L	22.3
ProG	589.332	708.404	LNELLSVFSR_2_y6_1_L	22.3
ProG	589.332	595.320	LNELLSVFSR_2_y5_1_L	22.3
ProG	594.337	960.539	LNELLSVFSR_2_y8_1_H	22.3
ProG	594.337	718.412	LNELLSVFSR_2_y6_1_H	22.3
ProG	594.337	605.328	LNELLSVFSR_2_y5_1_H	22.3

Protein	Q1	Q3	Peptide information*	CE
ProI	815.438	1102.574	ALLETIGDATLVEER_2_y10_1_L	29.7
ProI	815.438	989.490	ALLETIGDATLVEER_2_y9_1_L	29.7
ProI	815.438	817.441	ALLETIGDATLVEER_2_y7_1_L	29.7
ProI	820.442	1112.582	ALLETIGDATLVEER_2_y10_1_H	29.7
ProI	820.442	999.498	ALLETIGDATLVEER_2_y9_1_H	29.7
ProI	820.442	827.450	ALLETIGDATLVEER_2_y7_1_H	29.7
ProI	694.854	958.495	EITSPGGTTEAGLR_2_y10_1_L	25.8
ProI	694.854	861.442	EITSPGGTTEAGLR_2_y9_1_L	25.8
ProI	694.854	479.751	EITSPGGTTEAGLR_2_y10_2_L	25.8
ProI	699.859	968.504	EITSPGGTTEAGLR_2_y10_1_H	25.8
ProI	699.859	871.451	EITSPGGTTEAGLR_2_y9_1_H	25.8
ProI	699.859	484.755	EITSPGGTTEAGLR_2_y10_2_H	25.8
ProH	565.332	929.541	SIGAQTLLGAAK_2_y10_1_L	21.5
ProH	565.332	801.483	SIGAQTLLGAAK_2_y8_1_L	21.5
ProH	565.332	673.424	SIGAQTLLGAAK_2_y7_1_L	21.5
ProH	569.340	937.556	SIGAQTLLGAAK_2_y10_1_H	21.5
ProH	569.340	809.497	SIGAQTLLGAAK_2_y8_1_H	21.5
ProH	569.340	681.439	SIGAQTLLGAAK_2_y7_1_H	21.5
ProH	524.269	732.425	DAENALSSLK_2_y7_1_L	20.2
ProH	524.269	547.345	DAENALSSLK_2_y5_1_L	20.2
ProH	524.269	434.261	DAENALSSLK_2_y4_1_L	20.2
ProH	528.277	740.439	DAENALSSLK_2_y7_1_H	20.2
ProH	528.277	555.359	DAENALSSLK_2_y5_1_H	20.2
ProH	528.277	442.275	DAENALSSLK_2_y4_1_H	20.2
ProH	653.866	963.551	LTELELQYGIK_2_y8_1_L	24.4
ProH	653.866	850.467	LTELELQYGIK_2_y7_1_L	24.4
ProH	653.866	721.424	LTELELQYGIK_2_y6_1_L	24.4
ProH	657.873	971.565	LTELELQYGIK_2_y8_1_H	24.4
ProH	657.873	858.481	LTELELQYGIK_2_y7_1_H	24.4
ProH	657.873	729.439	LTELELQYGIK_2_y6_1_H	24.4

.

4.14 ENZYME ACTIVITY ASSAYS (PERFORMED BY MICHAEL KOHLSTEDT, BRAUNSCHWEIG)

For determination of phosphoglucoisomerase activity, cells were disrupted in a bench top homogenizer (MP Biomedicals, Santa Anna, USA) in 100 mM Tris/HCl (pH 7.8) containing 10 mM $MgCl_2$. Activity was quantified using glucose 6-phosphate dehydrogenase (G6PDH) as coupling enzyme and online monitoring of NADPH formation at 340 nm. The assay was performed at pH 7.8 with 100 mM Tris/HCl, 10 mM $MgCl_2$, 0.5 mM NADP, 1.25 U G6PDH, 4 mM fructose 6-phosphate and 20 µL crude cell extract. Cell disruption and activity measurement for isocitrate dehydrogenase were also carried out in 100 mM Tris/HCl (pH 7.8) containing 10 mM $MgCl_2$. The reaction mix for determination of enzyme activity additionally contained 1 mM isocitrate, 0.5 mM NADP and 25 µL of crude cell extract.

4.15 METABOLOME ANALYSIS (PERFORMED BY HANNA MEYER, GREIFSWALD)

Samples for intracellular metabolome analysis were obtained by fast vacuum dependent filtration [128]. A pre-cooled (-20°C) upper part of the filtration system (funnel, filter base) was used for sampling. For sampling, 10-20 OD units of the main culture were poured into a 50 mL falcon tube and cooled with liquid nitrogen for 30 s (sample temperature after cooling 9±2°C), by dipping falcon tube periodically in and out of the N_2 and shaken carefully in between (freezing should be avoided). The cooled culture was filtered (0.45 µm pore size, 47 mm, MilliPore, Schwalbach, Germany) and then quenched with 60% ethanol (w/v) (pre-cooled) and liquid nitrogen and were stored at -80°C until further treatment. For metabolite extraction and cell disruption, samples were thawed on ice (≤ 6°C) and the internal standards were added (20 nmol ribitol and norvaline for GC-MS and 2.5 nmol for LC-MS analysis). Afterwards samples were vortexed and shaken 10 times alternately and centrifuged for 5 min at 4°C at 15,500 g. The supernatant was transferred to a new falcon tube, while the pellet was once more extracted using cold water. The supernatants were combined and restocked with deionized water to a final organic solution concentration of 10% and stored at -80°C prior to lyophilization. Ion pairing-LC-MS measurement was performed using an Agilent HPLC System (1100 series, Agilent Technologies, Waldbronn, Germany) coupled to a Bruker micrOTOF mass spectrometer (Bruker Daltonics, Bremen, Germany) was operated in ESI negative mode using a mass range from 50 to 3000 m/z at a dry. Completely lyophilized samples were dissolved in 100 µL deionized water and centrifuged for 2 min (15,500 g, 4°C). The supernatants were transferred into glass vials with micro inserts for small volume injections (injection volume 25 µL). Chromatographic separation was performed using a RP-C18 AppliChrom OTU LipoMare column (3.5 µm, 150x4.6 mm, AppliChrom, Oranienburg, Germany) equipped with a C18 pre-column (Phenomenex, Aschaffenburg, Germany). The gradient flow rate was 0.4 mL min^{-1} and the total data acquisition runtime was 40 min. The mobile phase was A: 5% methanol and 95% water, containing 10 mM tributylamine as ion-pairing reagent and 15 mM acetic acid for pH adjustment to pH 4.9 and B: (100% methanol. The gradient elution started with 100% A for 2 min, 0-31% B in 2 min, 31-50% B in 18.5 min, 50-60% B in 2.5 min, 60-100% B in 1 min, hold 100% B for 7 min, 100%-0% B in 1 min, and hold 10 min at 0% B. As MS source parameters a dry gas (N_2)

flow rate of 8.0 L min^{-1}, a dry temperature of 180°C, a nebulizer pressure of 1.6 bar, a capillary voltage of 4,000 V and a capillary exit voltage of -150 V were used. Furthermore, the skimmer 1 was set to -50 V, the hexapole 1 to -25 V and the hexapole 2 to -24 V. The transfer time was 50 µs and pre-pulse storage was 8.0 µs. Reference masses of the Agilent "ESI-tune mix" for electro spray applications in negative mode were used for automated m/z calibration in each chromatographic run. Metabolite quantification was done by QuantAnalysis® (Bruker Daltonik, Bremen, Germany). Peak areas of extracted ions were normalized to the internal standard area of camphor sulfonic acid. For determination of the calibration equation, different concentrations of pure standards were measured and analyzed in the same manner. A polynomial regression of degree 2 with a 1/x weighting was used as calibration equation. The computed metabolite concentrations were further normalized to the sample volume and related to the respective cell dry weight. GC-MS (quadrupole) analysis was performed using an Agilent DB-5ms column as described previously [129]. Completely lyophilized samples were derivatized for 90 min at 37°C with MeOX and 30 min at 37°C with MSTFA. After centrifugation for 2 min at room temperature the supernatant was transferred into GC-Vials prior to measurement. Metabolite quantification was done by the ChomaTOF® (LECO) software. Peak areas of extracted ions were normalized to the area of the internal standard ribitol. For determination of the calibration equation, different concentrations of pure standards were measured and analyzed in the same manner. Dependent on the precision of the calibration equation, calibration was done via a polynomial regression of degree 1 or 2 and a 1/x weighting. The computed metabolite concentrations were further normalized to the sample volume and related to the respective cell dry weight. A volume of 4 mL of cell suspension was harvested via fast filtration (cellulose-nitrate, 0.2 µm pore size, 47 mm, Sartorius, Göttingen, Germany) and washed as described previously [130]. Cell-containing filters were incubated (15 min, 100°C) in caps containing 2 mL of 200 µM α-aminobutyric acid as internal standard. Extracts were cooled on ice, transferred into 2 mL tubes and centrifuged (5 min, 16,100 xg, 4°C) to eliminate disrupted cells. Intracellular amino acids were then quantified via HPLC (Agilent Technologies, Waldbronn, Germany) applying OPA pre-column derivatization [131]. In order to quantify proline and cysteine, FMOC derivatization reagent, mercaptoethanol as reducing agent and iodoacetic acid to block sulfhydryl groups were also added to the sample. For extracellular metabolite measurement by ^{1}H-NMR, a volume of 2 mL cell culture was rapidly filtrated through a syringe filter (0.2 µm, Sarstedt, Nümbrecht, Germany). The obtained supernatant was stored at -20°C. Partial volume of the extracellular sample was buffered to pH 7.0 by addition of 200 µL of a 0.2 M sodium hydrogen phosphate buffer (including 1 mM trimethylsilyl propanoic acid, pH 7.0) made up with 50% D_2O to provide a nuclear magnetic resonance (NMR)-lock signal [132]. Spectral referencing was done relative to 1 mM sodium trimethylsilyl-[2,2,3,3-D4]-1-propionic acid (TSP) in phosphate buffer. All NMR spectra were obtained at 600.27 MHz at a nominal temperature of 310 K using a Bruker AVANCE-II 600 NMR (Bruker Biospin GmbH, Rheinstetten, Germany). A modified 1D-NOESY pulse sequence was used with pre-saturation on the residual HDO signal during both the relaxation delay and the mixing time. A total of 64 free induction decays (FID scans) were collected using a spectral width of 30 ppm for a one-dimensional spectrum. Data analysis was implemented by AMIX (Bruker Biospin, Rheinstetten, Germany). The signal area of the internal standard TSP was used for direct quantification. A bicinchoninic acid-based protein assay kit (Thermo Fisher Scientific, Rockford, USA) was used for the determination of total extracellular protein in culture supernatant.

4.16 13C METABOLIC FLUX ANALYSIS (PERFORMED BY MICHAEL KOHLSTEDT, BRAUNSCHWEIG)

Cell pellets were washed and hydrolyzed with 6M HCl for 24 h at 105°C. Obtained hydrolysates were transferred in centrifugal filter tubes (0.22 µm pore size, Ultrafree-MC, MilliPore, Schwalbach, Germany) and centrifuged (1 min, 12.000 g) to filter off cell debris. Clear hydrolysates where dried under a constant nitrogen stream for 30 min at room temperature. Afterwards, derivatization of amino acids was carried out at 80°C in 50 µL dimethylformamide containing 0.1% pyridine and 50 µL N-methyl-N-t-butyldimethylsilyl-trifluoroacetamide (MBDSTFA, Macherey-Nagel, Düren, Germany) for 30 min. Derivatized amino acids were separated by a 5975C GC and analyzed on a single-quadrupole 7890A MS with electron impact ionization (both Agilent Technologies, Waldbronn, Deutschland). In a first scan peaks were checked for quality (retention time, peak symmetry, no isobaric overlays, etc.). In a second more sensitive run only desired fragment ions (selected ion monitoring), containing the complete carbon backbone of the amino acid, were measured. Labeling information can be extracted from mass spectra and is corrected for naturally occurring isotopes. Macromolecular cell composition was reconstructed from previous biomass models of *B. subtilis* (Dauner & Sauer, 2001; Oh *et al.*, 2007), yielding building block requirements of anabolic precursor metabolites (G6P, F6P, R5P, E4P, GAP, 3PG, PEP, PYR, AcCoA, AKG, OAA). The cell composition further considered the potential influence of salt adaptation of *Bacillus* to high salinity, particularly cellular changes in protein and ion content, intracellular amino acid pools quantified in this study, as well as variations in cell wall fraction and composition under osmotic stress. López *et al.* observed an increase in cardiolipin content, an altered ratio of glyco- to phospholipids, as well as differences in fatty acid composition under salt stress. [133]. Metabolic fluxes were estimated using the open source software OpenFLUX [134]. The user-defined metabolic model is parsed into a MATLAB-readable model (Mathworks, Natick, USA). MATLAB subsequently estimates flux parameters using its non-linear constraint-based optimization algorithm FMINCON, an iterative least-square algorithm. Starting with a random initial set of fluxes, the algorithm computed the remaining dependent fluxes via stoichiometric mass balances, estimated the resulting labeling patterns of all compounds in the metabolic network for the given fluxes and compared them with the experimental labeling information until an optimal fit was reached [135]. The used network comprised 75 stoichiometric balance equations for pathways of central carbon metabolism including fluxes into biomass formation and metabolite export (Supplement Table 2). After flux parameter estimation, confidence intervals were determined in 50 iterations by a Monte-Carlo sensitivity analysis. For flux visualization the open source tool VANTED [136] including the FluxMap add-on [137] was used.

4.16.1 Visualization of multi-omics data sets and pathway mapping.

The primary pathways for central carbon metabolism were manually created and annotated using xml editor of the open source software Inkscape (http://inkscape.org/). The primary pathway maps were then used to map the data (to visualize) obtained from the multi-omics experiments with a free web based application ProMeTra [7].

5. RESULTS

5.1 TRYPSIN DIGESTION OPTIMIZATION FOR THE SAMPLES OBTAINED FROM SPORULATING *B. SUBTILIS*

For precise controlled and reproducible growth behavior of bacteria it is often preferred to cultivate bacteria in well-defined fermenter or chemostat based cultivations. During controlled growth at low growth rates a sub-population of *B. subtilis* tends to sporulate – a process known as bet-hedging [138]. The ability of the *B. subtilis* to exhibit population heterogeneity poses a technical challenge when the protein lysates of these cells were subjected to trypsin digestion in-solution for current bottom-up proteomics approaches. In the past, Kuwana et al. [139] were able to identify 165 proteins in a bottom-up proteomics approach from a single sample of *B. subtilis* spores after extensive prefractionation. In addition, the expression patterns of 26 selected proteins were characterized with LacZ reporter gene fusion assays. This approach required increased sample handling and several genetic constructs for the selected proteins. In an another study Wishwas *et al.* [140] identified 55 spore coat proteins via gel-free proteomics approach after isolating the insoluble spore coat fraction. Here, a potential pitfall for the gel-free proteomics approaches for characterizing spores was addressed and a simple method was established to overcome the problem and to reliably monitor the expression levels of several hundred proteins in sporulating *B. subtilis*.

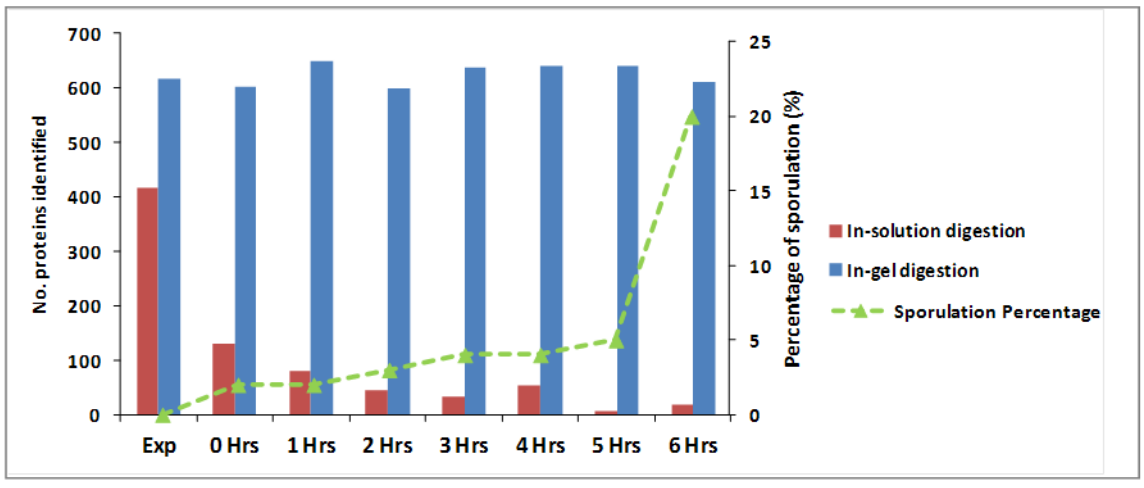

Figure 8: Effect of sporulation on protein identifications via in-solution digestion and in-gel digestion procedure. The *B. subtilis* strain 168 Trp^+ was grown in DSM media and the samples for protein preparation were harvested in exponential phase (Exp), early stationary phase (0 Hrs) and followed by sampling for every hour (see section 4.5.1). Percentage of heat resistant endospores was calculated by heat kill assay (see section 4.5.2). Percentage of heat resistant endospore (▲) of *B. subtilis* grown in DSM and number of proteins identified by LC-MS/MS by in-solution (■) and in-gel (■) digestion methods.

A shotgun proteomics strategy involves digesting proteins into peptides using an endoprotease (preferably trypsin) either in a solution (in-solution) or in a gel (in-gel). The first strategy (in-solution digestion) is much preferred over the second (in-gel digestion) due to its ease of handling and the benefit of handling smaller sample numbers [141]. However, we observed that samples that exhibit even partial sporulation, when subjected to in-solution digestion, yielded a significantly lower number of identified proteins compared to non-sporulating cells rendering the data unusable (Figure 8). The reason behind the low number of identifications was an increase of innate non-

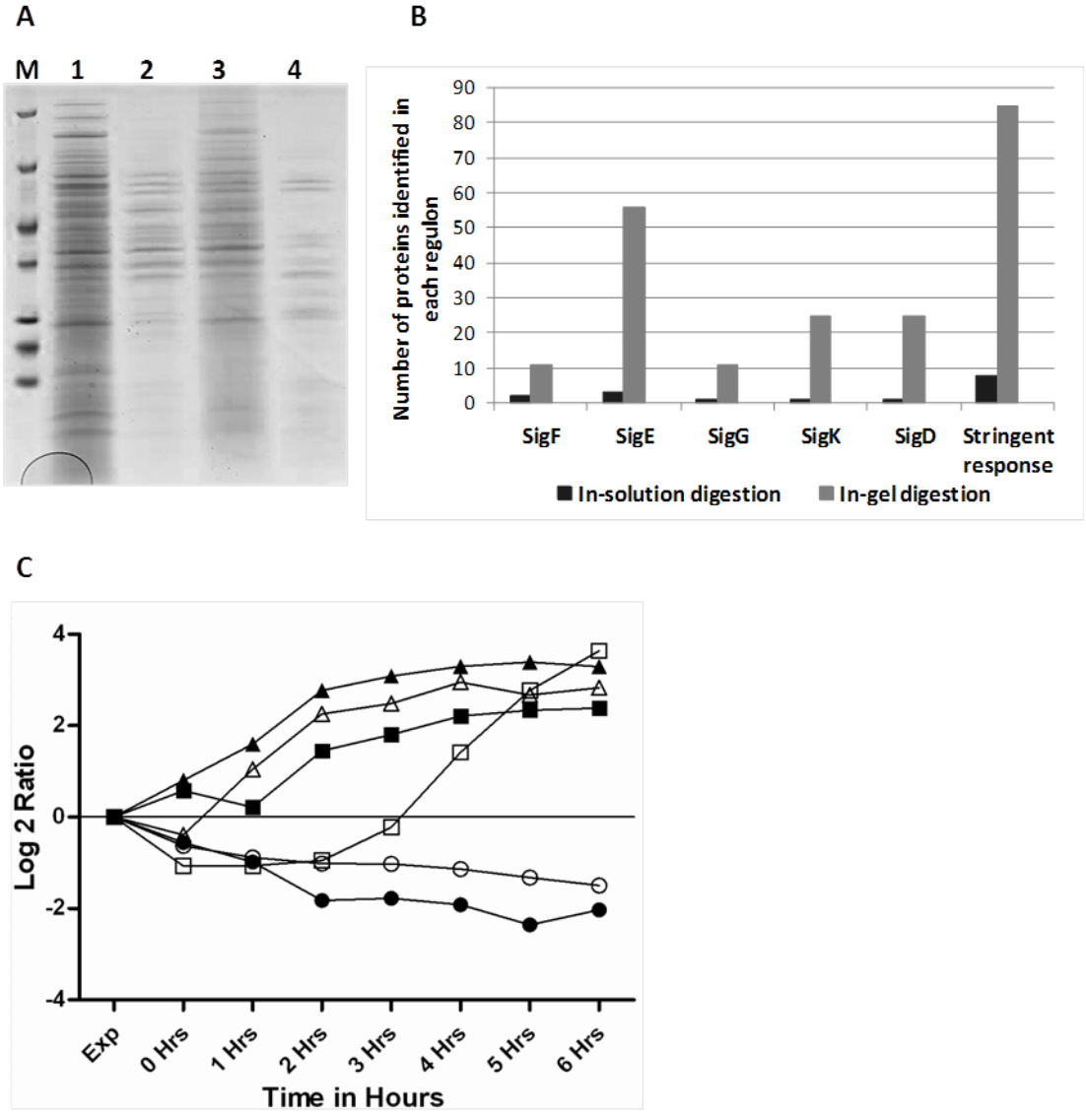

Figure 9: Identification of non-specific proteolytic activity in proteins samples obtianed from sporulating B. subtilis (A) SDS-PAGE: Lane1 – 15µg of fresh protein lysate of the sample 6 Hrs into stationary phase cultivated in DSM media, Lane2 – protein lysate incubated over night, Lane3 – protein lysate incubated overnight along with protein inhibitor cocktail, Lane4 – protein lysate with trypsin incubated overnight. (B) Number of proteins identified from each regulon via in-solution (■) and in-gel (■) digestion methods. (C) Quantification of proteins identified via in-gel digestion method - mean expression of the proteins regulated by the regulators over the time course. All time points were normalized to the exponential (Exp) condition. (▲) SigF (11 proteins), (△) SigE (56 proteins), (■) SigG (11 proteins), (□) SigK (25 proteins), (●) SigD (25 proteins), (○) Stringent response (85 proteins)

specific protease activity when *B. subtilis* started to sporulate. This is a common problem encountered in proteomic studies when *B. subtilis* is grown in chemostats at a very low growth rate, where partial sporulation is unavoidable.

To test our hypothesis *B. subtilis* was grown in Difco Sporulation Medium (DSM) [142] and samples for protein isolation were harvested every hour after the cells had entered stationary phase. The percentage of spores was determined using a heat killing assay. The sample with the highest percentage of spores (at 6 hrs) was used for the subsequent analysis. Overnight incubation (16-18 hours) of the protein lysate with or without trypsin had shown a similar pattern (Figure 9A) in a denaturing SDS-PAGE, where both lanes (lanes 2 & 4) were almost clear; indicating a strong innate non-specific proteolysis. Hence, adding a specific protease like trypsin into the samples that already had non-specific protease activity yielded non-tryptic peptides. This was evident in the subsequent LC-MS/MS analysis, which yielded substantially lower numbers of protein identifications (Figure 8). This innate protease activity was partially inhibited by adding broad spectrum protease inhibitor cocktail (Roche Applied Science) (Figure 9A Lane3); however usage of the protease inhibitors also inhibits trypsin activity.

An alternative approach to avoid non-specific protease activity is to fix/denature the proteins in a SDS-PAGE gel and then digest the gel trapped proteins. It has been reported in the past that separation of proteins by SDS-PAGE is mainly used for pre-fractionation and removal of any contaminants (detergents and other impurities etc,). Conventional in-gel digestion involves running a gel for 10 cm and then cutting the whole lane into a minimum of 10-15 bands and analysing them individually via LC-MS/MS in combination with MudPit [143, 144]. In order to keep sample numbers to a minimum and minimize technical variance we limited the gel run to 1 cm and sliced each lane into 2-3 bands. Each band was individually digested with trypsin and the resultant peptide solution was pooled and then desalted with C18 columns (Millipore, Bedford) and analysed via LC-MS/MS (Figure 6) (details in section 4.11.2).

This strategy improved the protein identifications of the regulon members (Figure 9B) and ensured consistent data quality across multiple samples in a time course (Figure 9C). As indicated in Figure 9C, groups of proteins involved in sporulation that are controlled by the sigma factors SigE, SigF, SigG and SigK [145] were up-regulated when the cells started to sporulate. SigK is the last sigma

factor activated during endospore formation that is responsible for the production of the late sporulation proteins [146], in the current study proteins controlled by SigK were up-regulated at later stage of sporulation as expected. On the other hand proteins controlled by SigD responsible for chemotaxis and several of the ribosomal proteins subject to negative regulation by the stringent response [28] were down regulated as expected for cells entering the stationary phase and initiating sporulation. This implies that the above described method can be reliably used for label free proteomics analysis and permits relative expression profiling of hundreds of proteins in sporulating *B. subtilis* (as shown in the Figure 8).

In conclusion the above proposed method simultaneously solves the problem of the non-specific protease activity encountered in sporulating *B. subtilis* and ensures high data quality for relative quantification via shotgun proteomics approach. This method was used in the subsequent sample processing for all the samples obtained from chemostats.

5.2 MULTI-OMICS PROFILING OF *B. SUBTILIS* DURING THE TRANSITION FROM GROWING TO NON-GROWING STATE

5.2.1 Transcriptome profiling of *B. subtilis* in tri-phase fed-batch fermentation

B. subtilis often encounters conditions of energy limitation depending on the availability of glucose and other carbohydrates in its environment. As glucose is the preferred carbon source, it is important to understand the global physiological adaptation to changes in environmental glucose concentration. Earlier studies had reported global transcriptome [147, 148] and proteome analyses [1, 50, 108] of glucose limitation and glucose starvation experiments performed in shake flask. However, none of the previous studies addressed the dynamic changes of *B. subtilis* physiology in response to the transition from growing to non-growing state in high cell density fermentation under precisely controlled conditions. Therefore, in the current study *B. subtilis* was investigated in a fermenter where the transition from growing to non-growing state (glucose limitation and/or starvation) of *B. subtilis* could be precisely adjusted and monitored.

The *sigK* mutant strain BSG112 was used in this study, which is unable to form mature endospores in order to avoid handling of spores with the 30 L fermenter used in this experiment. The sporulation sigma factor SigK, the last sigma factor activated during endospore formation, is responsible for the production of the late sporulation proteins [146]. So, deletion of *sigK* gene is not supposed to influence the early sporulation response and other adaptational changes associated with the transition of *B. subtilis* from growing to glucose limitation or starvation conditions. To understand the physiological adaptation of *B. subtilis* growing under different glucose concentrations, a three-phase fed-batch fermentation was performed (Figure 10). Briefly, *B. subtilis* was grown exponentially until the glucose was utilized to sub-optimal level and the glucose feed was maintained at low levels for 8 hours, this phase represents the glucose limitation phase. After 8 hours of glucose limitation, the glucose feed was stopped exposing *B. subtilis* to glucose starvation. A drop in the OD_{600} was observed in this phase as the cells started to lyse due to glucose starvation. Samples for transcriptome analysis (Figure 10 blue dots) were harvested and microarray analyses were performed to elucidate the global physiological adaptation at the transcriptional level.

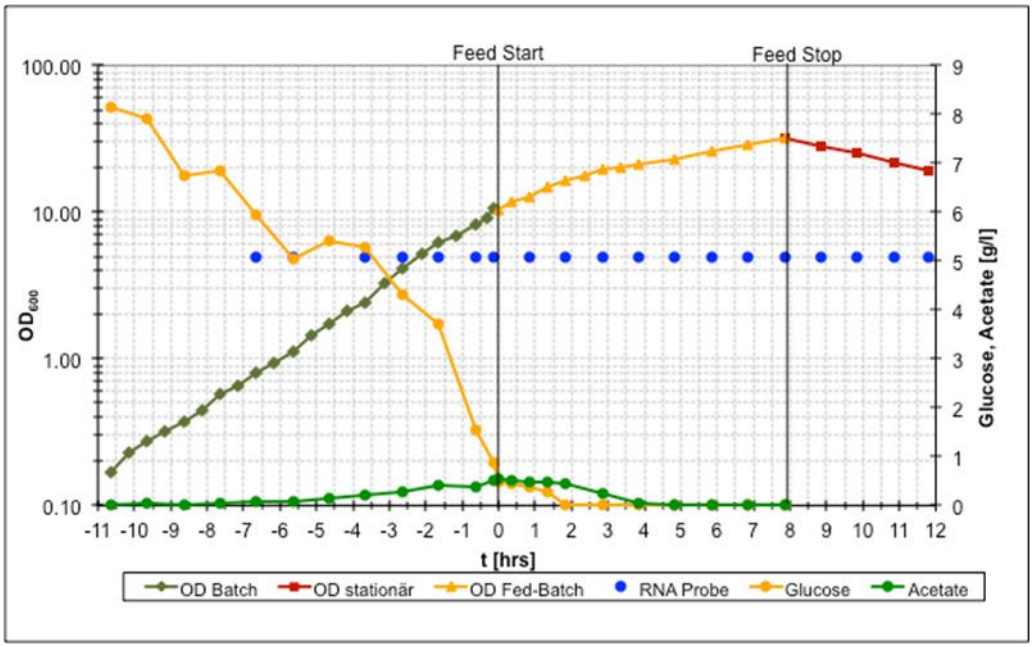

Figure 10: Tri-phase fed-batch fermentation of the *B. subtilis* strain BSG112 (*sigK* mutant) in M9 media (see section 4.3). The figure depicts the growth curve of the fermentation at OD_{600}, glucose concentration (yellow lines) and sampling time points for transcriptome analysis were indicated as blue dots. Glucose feed was started at 0 hrs marking the start of glucose limitation phase and the glucose feed was stopped at 8 hrs marking the start of glucose starvation phase. (Cultivation performed by Dr. Beate Knoke, IBVT Stuttgart).

For the transcriptome data analysis, relative gene expression values obtained from the normalized ratio data were imported into Genedata Analyst for subsequent analysis. The activity of transcriptional regulators during exponential growth, glucose limitation and starvation was analyzed by representing the mean expression of respective target genes throughout the time course of the experiment (genes used for this analysis and their transcriptional regulators are mentioned in the supplementary table S1). Genes involved in the response to glucose limitation and starvation that are controlled by CcpA and the genes regulated by the alternative sigma factors SigB, SigD, SigE, SigF and SigG were considered for the analysis. As depicted in Figure 11, glucose limitation resulted in the induction of genes negatively controlled by CcpA. This induction was much stronger upon entry into glucose starvation phase. The observed regulatory pattern of the genes negatively controlled by CcpA was expected in view of the role of CcpA in mediating carbon catabolite repression (CCR) in the presence of glucose. The major function of CCR is to repress genes necessary for alternate carbon source utilization in the presence of glucose. The general stress regulon SigB exhibited a gradual increase during glucose limitation and further increased upon glucose starvation. Prolonged glucose limitation (after three hours into glucose limitation) in the second phase of the fermentation lead *B. subtilis* to initiate sporulation as reflected by the induction

of the SigF, SigE and SigG regulons. As the cells started to initiate sporulation response even before the entry into glucose starvation phase and deletion of *sigK* gene rendered an artificial situation for *B. subtilis* during the transition from glucose limitation to glucose starvation phase. To avoid this, a different experiment was performed where the cells transition directly from growth to glucose starvation (see next section)

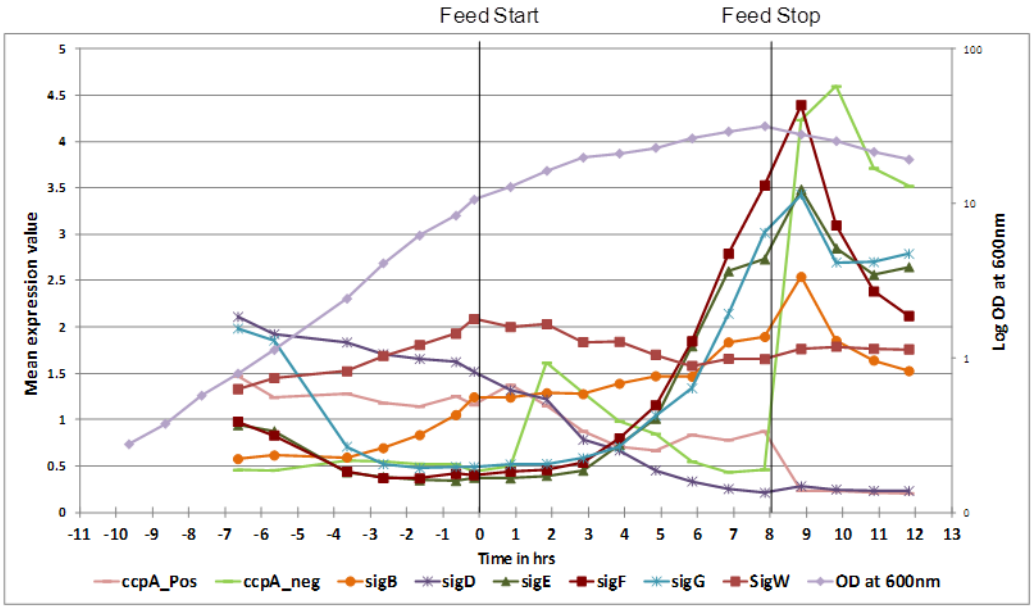

Figure 11 : Average (mean) expression profiles (y-axix) of the regulons controlled by the transcriptional regulators CcpA, SigB, SigD, SigE, SigF and SigG in a tri-phase fed-batch fermentation was represented above. Genes that belong to above mentioned regulons are mentioned in supplementary table 1.

5.2.2 Multi-omics analysis of *B. subtilis* in bi-phase batch fermentation

5.2.2.1 Transcriptome profiling

To prevent the interfering induction of sporulation response, which occurred during the prolonged glucose limitation in the tri-phase batch fermentation, *B. subtilis* was grown in a bi-phase batch fermenter. Within the first phase of this fermentation the cells were grown exponentially. After glucose was exhausted, the cells entered the glucose starvation phase. Samples were harvested for intra-and extra cellular metabolome analysis, intra-and extra cellular proteome analysis and transcriptome analysis. The sampling time points for all the omics analyses are marked as blue dots in Figure 12.

For the transcriptome data analysis, relative gene expression values obtained from the normalized ratio data were used for the subsequent analysis. To get an overview of the data, a Principal Component Analysis (PCA) of the transcriptome data was performed. This method involves a mathematical procedure that transforms a number of possibly correlated variables into a smaller number of uncorrelated variables called principal components (two components for two

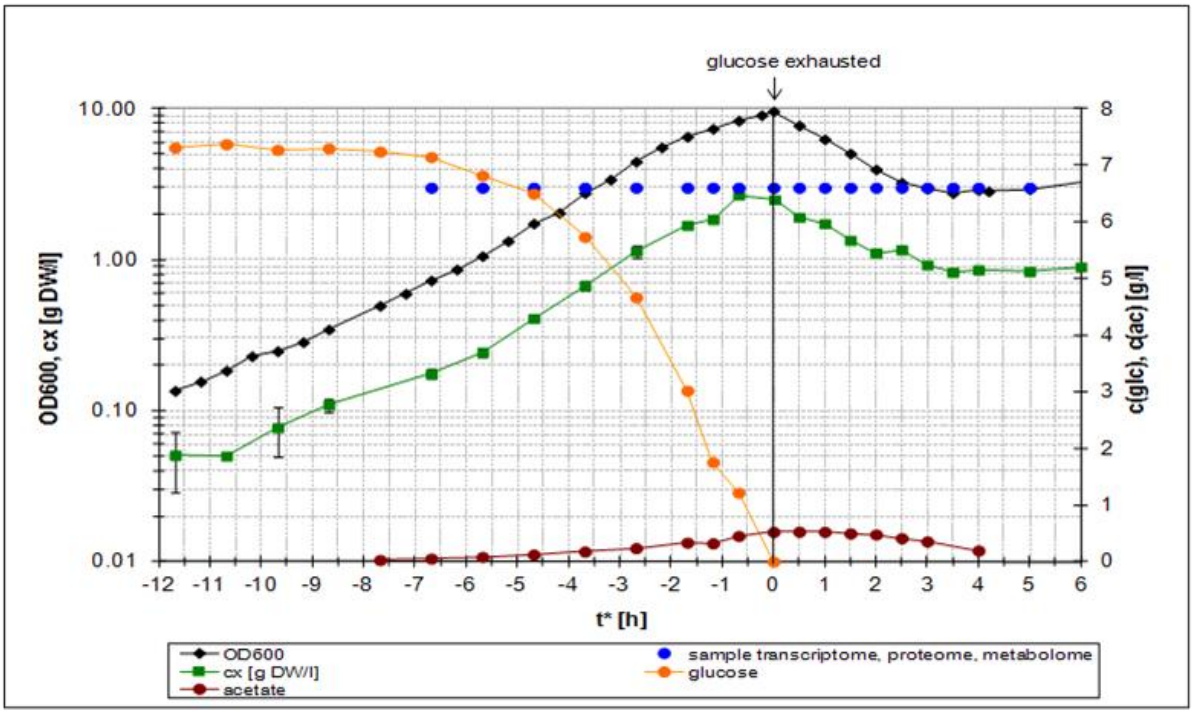

Figure 12: Bi-phase batch fermentation where cells transition from exponential growth phase to glucose starvation phase. The *B. subtilis* strain BSG112 (*sigK* mutant) was grown in M9 media (see section 4.3), growth curve at OD_{600} (green line) was depicted in the figure. At time point "0 hrs" glucose was exhausted from the growth medium (yellow line). Blue circles denote the sampling for the transcriptome, proteome and metabolome analysis. (Cultivation performed by Dr. Beate Knoke, IBVT Stuttgart).

dimensional PCA and three components for three dimensional PCA). The first principal component accounts for the highest variability within the data, and each subsequent component accounts for remaining variability in a decreasing trend.

The ratio data for each of the time point against the common reference pool was considered for the PCA. In the PCA (Figure 13) the conditions segregated into two distinct groups, before (green) and after (red) glucose exhaustion. These two distinguished groups in PCA represent the extent of changes caused by the glucose exhaustion in the medium.

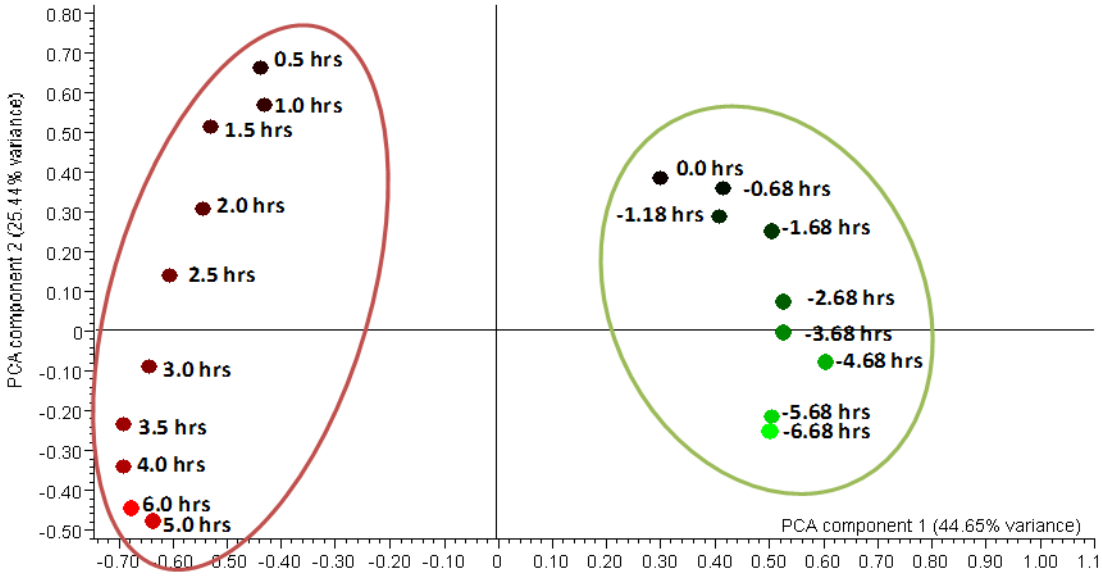

Figure 13:2D-Principal component analysis derived from the transcriptome data of all the time points. A clear clustering was observed for all the samples from exponentially growing *B. subtilis* (green circle) and glucose starved *B. subtilis* (red circle).

Further comprehensive data analysis provided some insight into the temporal coordination of the sigma factors (Figure 14) in response to glucose starvation. Expression profiles from all the genes (regulon) that were controlled by their corresponding sigma factor or transcription factor were averaged and plotted along with the growth curve (Figure 14) (genes used for this analysis and their transcriptional regulators are mentioned in supplementary table S1). Genes regulated by CcpA showed a swift response to glucose exhaustion as anticipated. Most of the members of the SigB regulon containing 157 (SubtiWiki classification) genes were strongly up-regulated immediately upon glucose exhaustion. However, the up regulation of the SigB dependent general stress response was transient [4]. The SigW regulon was less responsive to glucose starvation compared to the SigB regulon. Reduced motility of *B. subtilis* under nutrient limiting conditions has been reported earlier

[1, 149]. In this study, the SigD regulon that is responsible for motility and chemotaxis was also down regulated upon glucose exhaustion.

In the course of prolonged glucose starvation, major sporulation regulons (controlled by SigE, SigF, and SigE) were highly induced. This analysis revealed that in response to glucose deprivation the general stress response and the sporulation response were temporally coordinated and separated. This coordination was achieved by the involvement of the corresponding sigma factors and various transcription factors for each of the process involved in the adaptational responses.

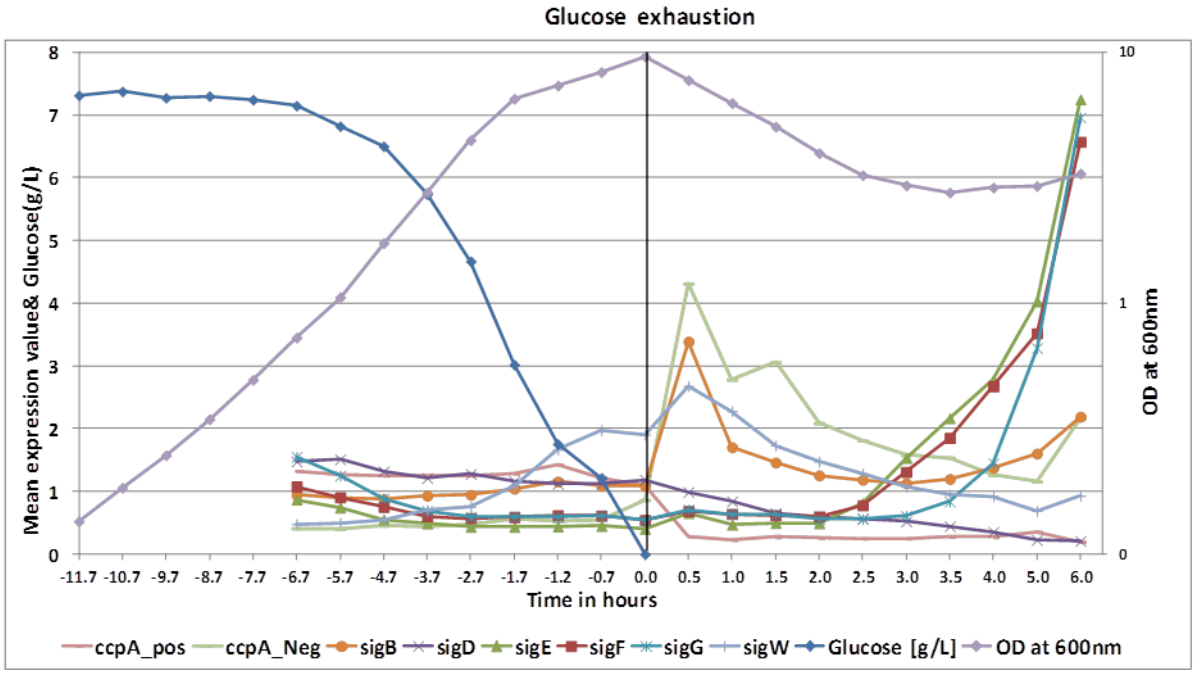

Figure 14: Average (mean) expression profiles of the regulons controlled by CcpA, SigB, SigD, SigE, SigF, SigG and SigW corresponding sigma factors was represented for the bi-phase batch fermentation. Genes that belong to above mentioned regulons are enclosed in the supplementary S1.

According to the SubtiWiki classification, there are 172 transcription factors that are responsible for controlling approximately 50% of the genes (2000 genes) in *B. subtilis*. Most of the regulators have at least two or more genes as their target, highest being 231 genes for the AbrB transcription factor. These transcription factors regulate their target gene expression by either repression or induction via various mechanisms. A detailed analysis of the regulons controlled by the various transcription factors had shown dynamic regulatory patterns. In Figure 15, the average expression profiles of significantly regulated regulons were depicted in two distinct clusters (A & B). Out of 172 regulons, 81 regulons were represented in the clusters (A and B) that were filtered after a statistical cut-off of three fold change and p-Value (ANOVA) of 0.01. Cluster A represents those regulons that were up-regulated at least in one of the time point when compared to the first time point. Cluster B

represents the regulons that were down regulated at least in one of the time point compared to that of the first time point. Two major kinds of regulatory patterns were observed in both clusters; first pattern: the majority of the regulons displayed a swift response to glucose concentration in the medium (e.g., stringent response, PurR, CcpA, LacR, CcpN etc.). The second regulatory pattern, instead of exhibiting a swift response to glucose exhaustion, is characterized by an initial induction (e.g., MdtR, FruR, GlpR) or repression (GerR, SpoVT, FrlR) before glucose exhaustion and later the regulons were gradually repressed or induced. This signifies the magnitudes of dynamic adaptation required by *B. subtilis* upon glucose exhaustion.

Cluster A contains several regulons that correlate with glucose concentration in the medium. Regulons that are related to sporulation like GerR, GerE, SpoVT were either not expressed or down regulated in the presence of glucose and were only up-regulated after prolonged glucose starvation. Nutritional stress stimulated the ribosomal associated protein (RelA) to synthesize (p)ppGpp and thereby modulate the transcription of several genes that mainly code for components of the translational apparatus, this is also known as stringent response [28, 29]. The genes that are controlled by ppGpp exhibited a sharp decline upon glucose exhaustion. A similar pattern was observed for the glucose uptake operon *ptsGHI* controlled by GlcT and the *gapA* operon that encodes the major glycolytic enzymes (GapA, Pgk, TpiA, Pgm, Eno). The purine biosynthesis (PurR) and pyrimidine biosynthesis (PyrR) regulons were strongly down regulated as the cells cease to replicate in the absence of glucose.

Cluster B represents the majority of the genes that were up-regulated upon exhaustion of glucose. This group notably includes the regulons of the pleiotropic transcription factor CcpA (mediates carbon catabolite repression) and of CcpN, the repressor of the gluconeogenic enzymes PckA and GapB. Furthermore, several other regulons were induced upon glucose exhaustion that are responsible for secondary carbon source utilization such as LacR (lactose utilization), ManR (mannose utilization), TreR (trehalose utilization), GmuR (glucomannan utilization), AraR (arabinose utilization), LicT (β-glucan and β -glucoside utilization), LicR (lichenan utilization) and IolR (myo inositol catabolism). Regulons responsible for amino acid utilization and fatty acid degradation were also induced such as the HutP (histidine utilization), RocR (arginine utilization) and FadR (fatty acid degradation). Most of these changes in cluster B indicate the need for energy generation through various compounds in the absence of glucose.

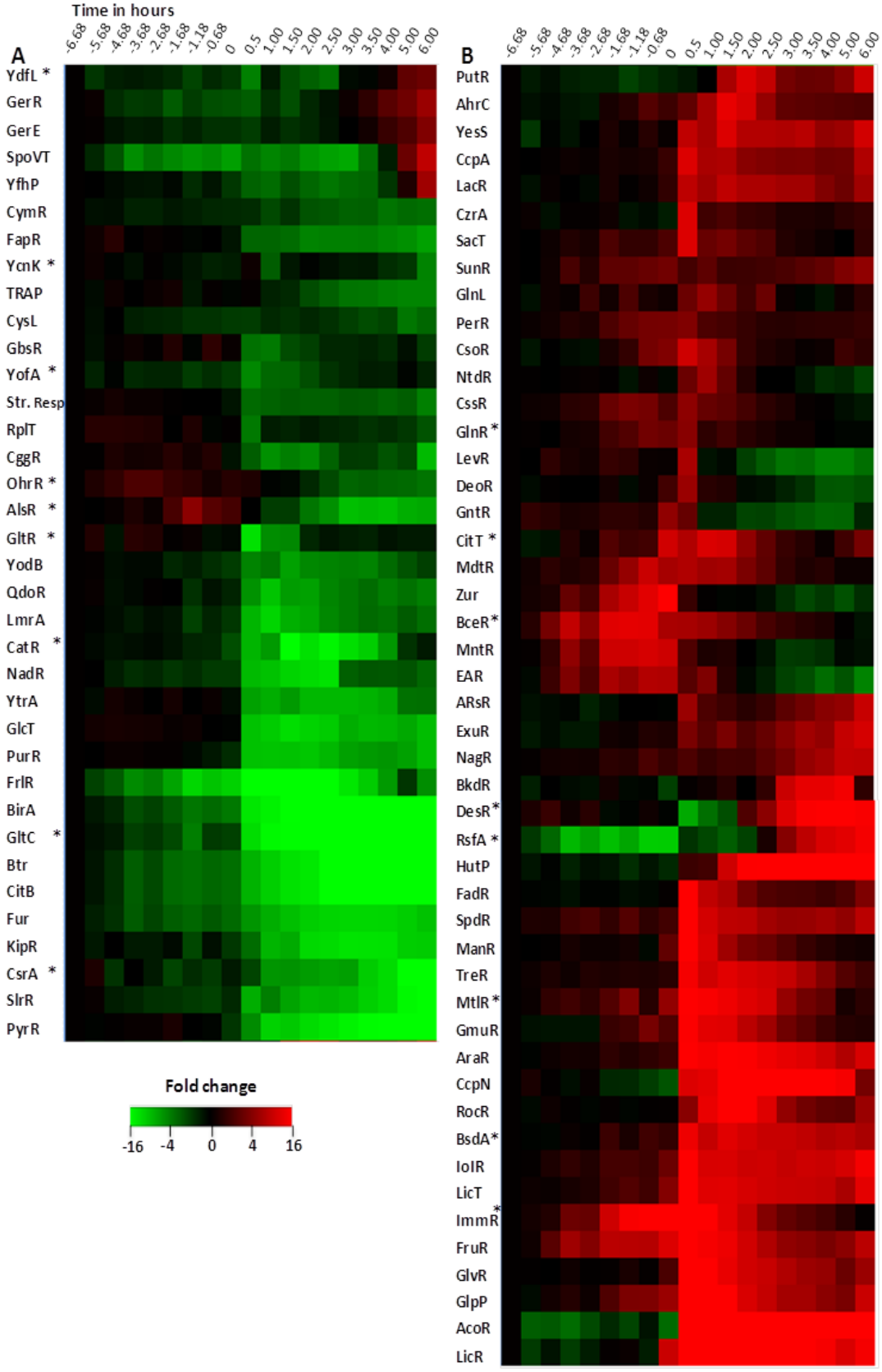

Figure 15: Mean expression profiles of the genes controlled by their corresponding transcription factors. All the time points were normalized to the first time point (-6.68 hrs) and log transformed. Cluster (A) represents the regulons that were up-regulated in at least one of the time points, whereas cluster (B) represents those regulons that were downregulated in at least one time point. An effect size of three fold and p-value (ANOVA) of 0.01 was applied as a cut off. Regulon classification was obtained from SubtiWiki (Version 2012/1). * Regulons with only one or two genes under their control.

5.2.2.2 Changes in the central carbon metabolism as revealed by multi-omics investigation

CCM specific protein abundance data were obtained by analyzing the samples via Multiple Reaction Monitoring (MRM) using QconCAT as an internal standard and measured on a triple quadrupole mass spectrometer (TSQ Vantage - Thermo Scientific). The ratio data against the internal standard (QconCAT) were obtained from the software Skyline and the ratio data was used to calculate the absolute concentration of the individual proteins. The absolute concentration data was used for the normalization with the control time point (time point -6.68 hrs). Transcriptome data for the pathways were obtained from the microarray analysis. The combined data were mapped on to the CCM pathway using the ProMeTra online software.

As glucose is the primary and preferred carbon source, it is valuable to understand the adaptation of the central carbon metabolism to changing glucose levels in a systems perspective. This involves generation and integration of multi-omics data, i.e., mRNA, protein and metabolite abundances. To this regard, the multilevel data was integrated on a custom drawn central carbon metabolism pathway map (Figure 16). Genes involved in the glycolysis showed a significant down regulation after glucose exhaustion; on the contrary genes involved in the TCA cycle were slightly up-regulated after glucose exhaustion. The strongest up regulation was observed with the gluconeogenic genes (*pckA* and *gapB*), whereas *fbp* which is not controlled by CcpN, the transcriptional repressor of gluconeogenesis, was unchanged. Furthermore, the majority of genes involved in the oxidative part of the HMP-shunt pathway (pentose phosphate pathway) were unchanged upon glucose exhaustion with the exception of 6-phosphogluconate dehydrogenase (*gntZ*) for the generation of ribulose-5-phosphate. The HMP shunt pathway plays an important role in generating NADPH for anabolic reactions and generating precursors for tryptophan and nucleotide biosynthesis; therefore the major genes involved in this pathway were not regulated upon the exhaustion of the glucose [148].

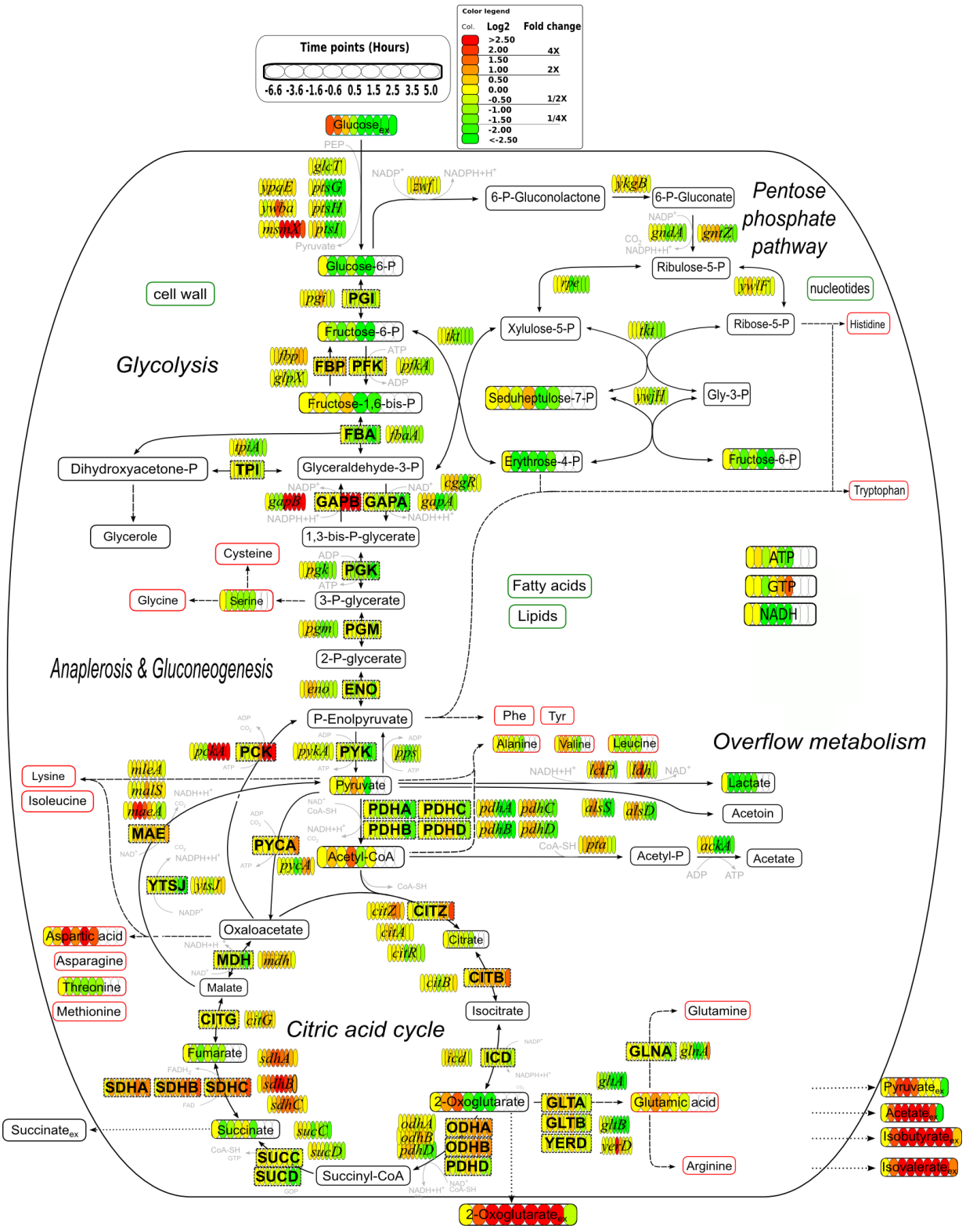

Figure 16 Time course visualization of multi-omics data of central carbon metabolism of bi-phase batch fermentation. To enable multi-omics comparison, data for all the time points were normalized to the first time point (-6.68 hrs) and log transformed. Capital bold letters denote the protein; italics fonts denote the mRNA expression profile and normal fonts represent the metabolites.

Almost for all the encoded proteins, the observed decrease in abundance levels were delayed which can be explained by the difference in the half-lives between mRNAs and proteins. Measurement of intracellular metabolite data was technically not possible for the time points of stationary phase due to increased cell lysis. Overflow metabolism that involves secretion of pyruvate into the extracellular medium was clearly observed as long as excess glucose was present and then the pyruvate was reutilized via TCA cycle to generate energy during stationary phase. Pathway level multi-omics visualization over the time course provided a unique perspective over the complex regulatory patterns involved with each molecule involved in the pathway during stationary phase.

Integration and visualization of multi-omics data sets is often a challenge especially in time course experiments due to the missing values of metabolites and proteins. Regarding the protein measurements, in a conventional shotgun mass spectrometric proteomics approach, it is common to have missing values across the time series due to the high dynamic range of the proteins in the crude protein lysate. In the current study, the missing values were minimized by implementing a targeted approach known as multiple reaction monitoring (MRM) which has the advantage of higher sensitivity and allows to perform the absolute quantification of the proteins. In a similar manner, with respect to the transcriptome data, the intensities obtained by the tiling array [116] hybridizations indicate a robust relative abundance of the mRNAs. In combination of both, relative intensities for mRNA and the absolute abundance of the protein, a correlation plot was generated () for the time point -4.68 hrs. Icd, GlnA and Mdh were the top three abundant in both protein and mRNA levels. The proteins which were involved in the proline biosynthesis and gluconeogenesis displayed lower mRNA and protein abundances. The regression coefficient for the correlation was 0.66 which was close to the value of 0.77 in *Escherichia coli* as measured by Taniguchi *et al.* (2010) [150]. Taniguchi *et al.* measured one protein at a time by fluorescence tagging and mRNA abundance from RNA sequencing (RNAseq). Given the fact that mRNA half-life and protein half-life are dramatically different; the correlation between their abundances was in a good fit. However for the stationary phase sample 5.0 hrs after glucose exhausted (Figure 17B) the correlation coefficient was 0.52 indicating a further mis-match between mRNA abundance and protein abundance.

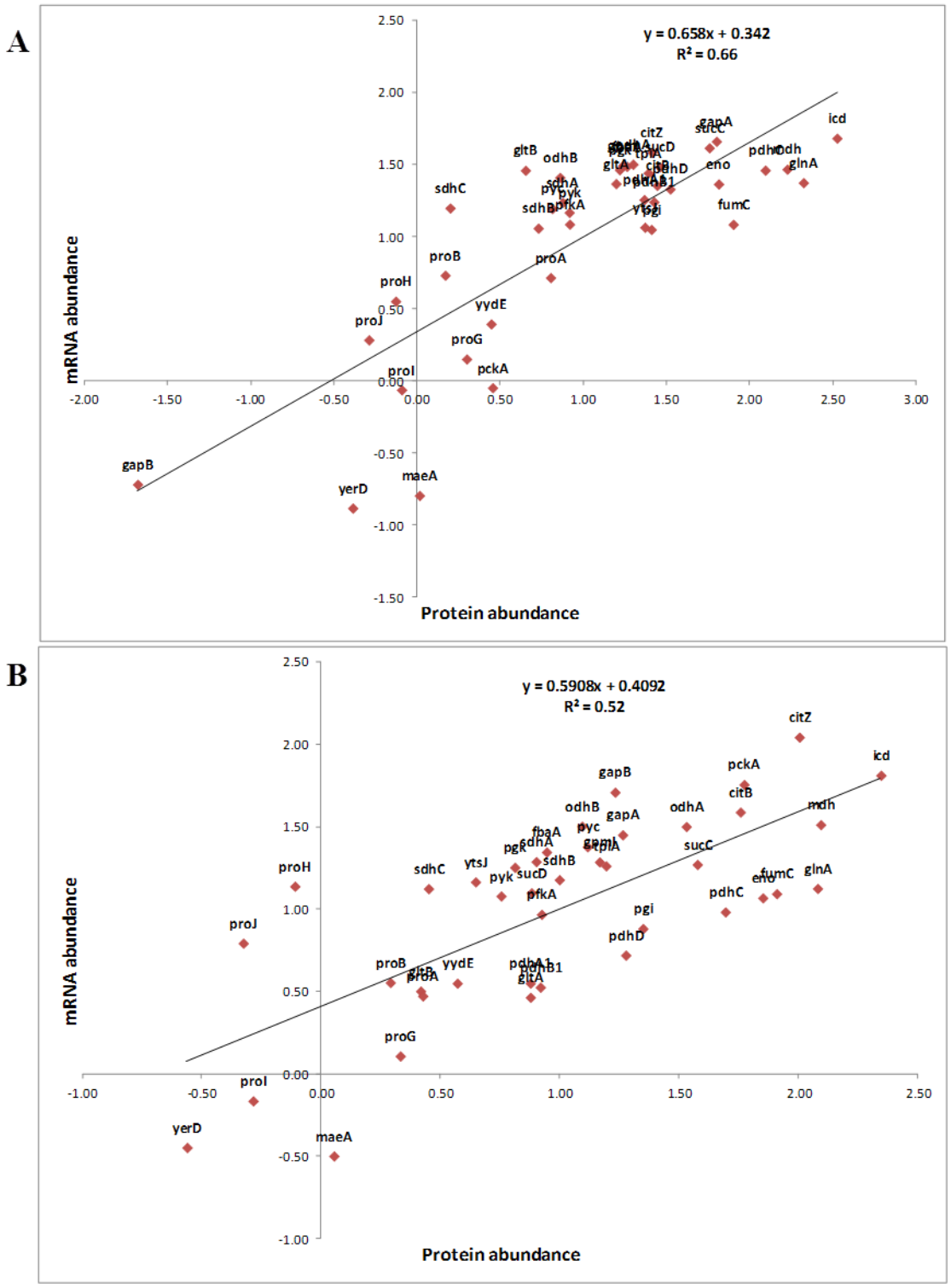

Figure 17: Comparative analysis between mRNA abundance and protein abundance at the time point -3.68 hrs. mRNA (exponentially growing cells) abundance was taken from the intensity data of the tiling array analysis and the protein abundance data was taken from the MRM based absolute quantitation. A correlation coefficient of 0.66 was obtained in this analysis which was close to the known literature value of 0.77[6]. Comparative analysis between mRNA abundance and protein abundance at the time point 5.00 hrs (stationary phase cells). mRNA abundance was taken from the intensity data of the tiling array analysis and the protein abundance data was taken from the MRM based absolute quantitation. A correlation coefficient of 0.52 was obtained in this analysis. In order to compare two different platforms, the data was log transformed and then median normalized relative to 1.

5.3 WHOLE-TRANSCRIPTOME ANALYSIS OF *B. SUBTILIS* AT HIGH TEMPERATURE, LOW TEMPERATURE, HIGH SALT AND DURING GLUCOSE STARVATION

The *B. subtilis* wild type strain 168 Trp^+ was used to comprehensively compare the adaptation of transcription to stress conditions that are encountered by *B. subtilis* in its environmental niches at a global scale in a strand-specific manner to explore the transcriptional plasticity of *B. subtilis*. This comprehensive study was performed within the framework of two European projects BaSysBio and BaCell-SysMO and the stress conditions investigated in this dissertation include growth at high temperature (51°C), low temperature (16°C), high salinity (1.2M NaCl) and glucose starvation (exponential phase, early stationary/transient phase and stationary phase). For the growth at low temperature, high temperature and high salt, bacteria were cultivated in SMM medium. For the glucose starvation experiments M9 medium with glucose and malate were used as the carbon source. All these conditions were performed in shake flasks with three biological replicates for each condition. Transcriptome analysis was performed using the high resolution tiling array technology [93, 116]. The intensity data obtained from the tiling array were median normalized and ratio data were obtained by normalizing to the respective experimental control conditions.

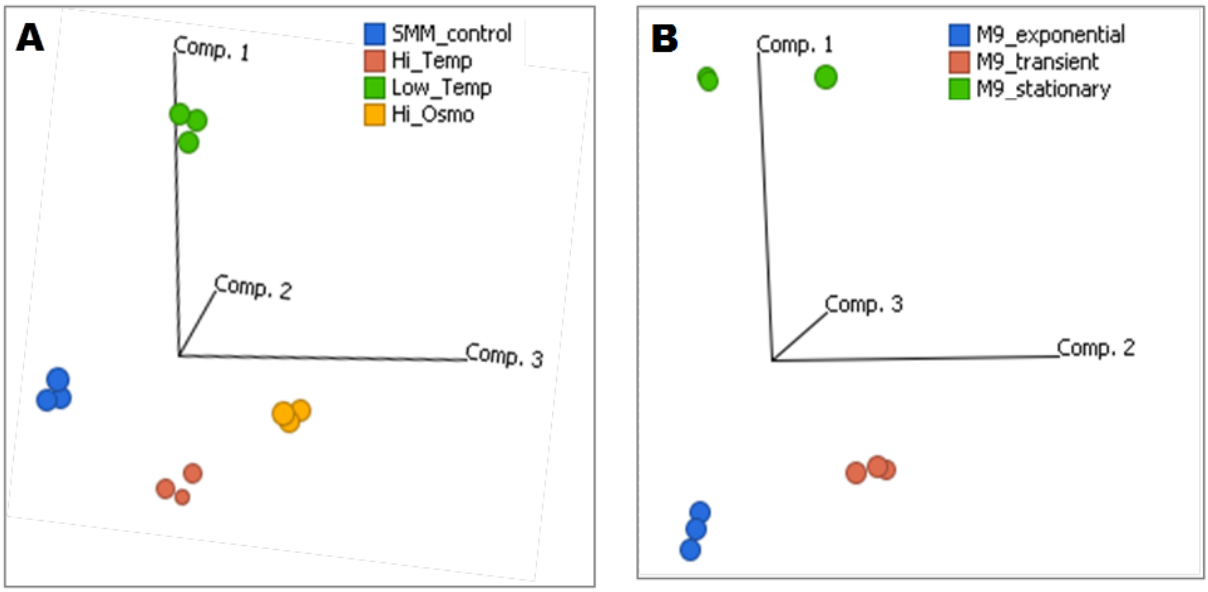

Figure 18 : Principal component analysis of the transcriptome data obtained from the tiling array analysis. The *B. subtilis* wild type strain 168 Trp^+ was grown in SMM media at (A) high temperature (51°C), low temperature (16°C), high salinity (1.2M NaCl) and (B) glucose starvation in M9 media (exponential phase, early stationary/transient phase and stationary phase).

A three dimensional PCA analysis of the median normalized transcriptome data is depicted in Figure 18: The excellent biological and technical reproducibility of the experiments is visualized in the PCA as the samples from the same condition clustered closely together. The distance between the different clusters indicates the changes induced by the different growth conditions.

A bird's eye view comparison between the conditions is visualized in the Figure 19. Distribution of the expression profiles of the complete transcriptome data when compared to the respective controls are shown in Figure 19A. The scattering of the values around the median represents the magnitude of the adaptational response to the corresponding stress condition. Among the stress conditions that were investigated in this context, the M9 stationary phase sample representing glucose starvation had the highest distribution around the median. This indicates that glucose starvation was the most demanding stress condition for *B. subtilis* among the tested stress condition. This observation is also reflected in the number of genes that were regulated upon each stress condition (Figure 19B). Glucose starvation alone accounted for the regulation of more than 1000 genes followed by growth at 16°C, 51°C and continuous growth at high salt, respectively (supplementary table S2).

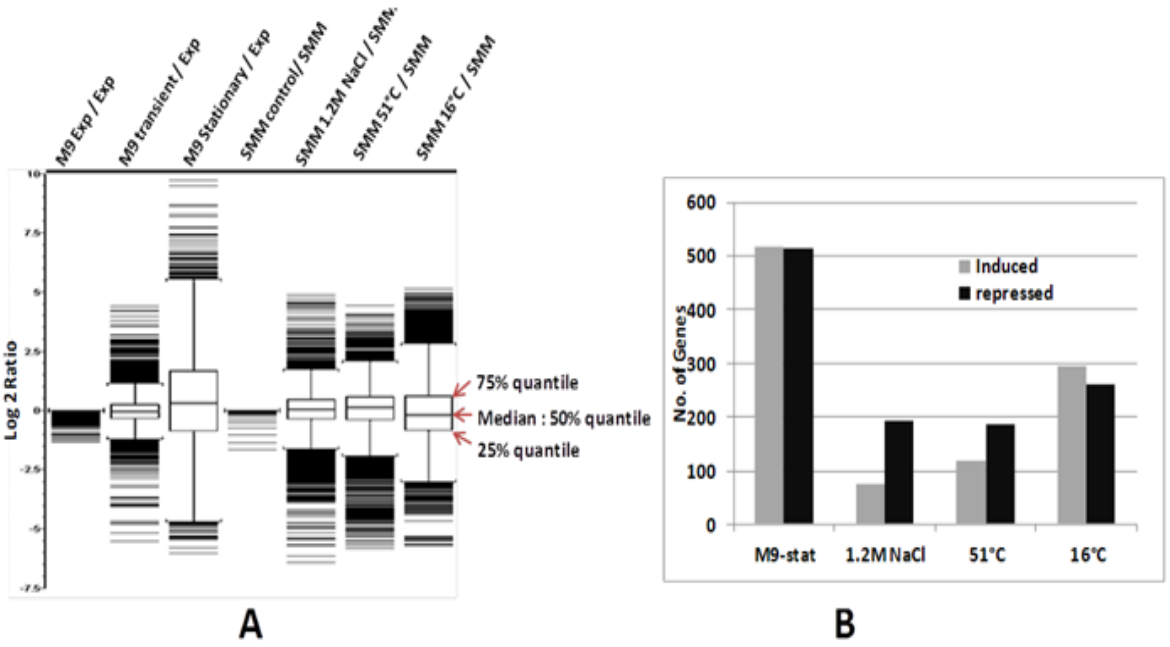

Figure 19: Magnitude of the changes associated with each of the stress conditions. A) Data distribution of the complete transcriptome for each of the conditions when compared to their respective controls (log 2 ratios). The wider the distribution of the expression profiles from the median, the greater is the dynamic physiological response of *B. subtilis* to that of the respective stress condition. B) Number of genes that were regulated in each condition when compared to their respective controls. A statistical cut-off of 3 fold change and p-value of 0.01 was used. Detailed information about the regulated genes was enclosed in supplementary table S2.

A detailed analysis of the genes involved in the functional categories obtained from SubtiWiki database is shown in Figure 20. Figure 20A shows the heat map of the averaged expression profiles of the various categories covered by the main category "Lifestyle". This category represents almost all the major processes required by *B. subtilis* to cope up with environmental stress conditions. The following noticeable changes were observed within the functional categories. Chemotaxis was down regulated in all stress conditions, however, to a lesser extent during growth at high temperature. As expected heat shock proteins were up-regulated at high temperature. Genes of the functional category "Coping with hyper osmotic stress" were up-regulated in cells grown at only high salt as well as high temperature. Genetic competence was down regulated at both high temperature and low temperature growth. Another major response was the up regulation of the general stress response, controlled by SigB, in all the stress conditions, but to a lesser extent during continuous growth at high salt conditions. The largest category containing 348 genes is "sporulation proteins", which was strongly induced during glucose starvation in M9 medium and to a lesser extent during growth at low temperature. The changes associated with sporulation genes partly account for the high biological variation induced by the glucose starvation compared to the remaining stress conditions in Figure 19.

Figure 20B shows the averaged expression profiles of the metabolic processes among the stress conditions. Glucose starvation could affect the highest number of metabolic pathways among the other tested stress condition. Most of the anabolic pathways were down regulated due to glucose starvation, whereas catabolic processes were up-regulated during glucose starvation. These anabolic processes include biosynthesis of cell wall, lipids, cofactors, amino acids etc. The catabolic processes include utilization of amino acids, specific carbon sources, lipids, nucleotides, nitrogen sources etc. As expected iron metabolism was up-regulated only during growth at high salinity [151]. To conclude, metabolic regulation was less pronounced for heat, cold and high salt stressed *B. subtilis* when compared to glucose starvation.

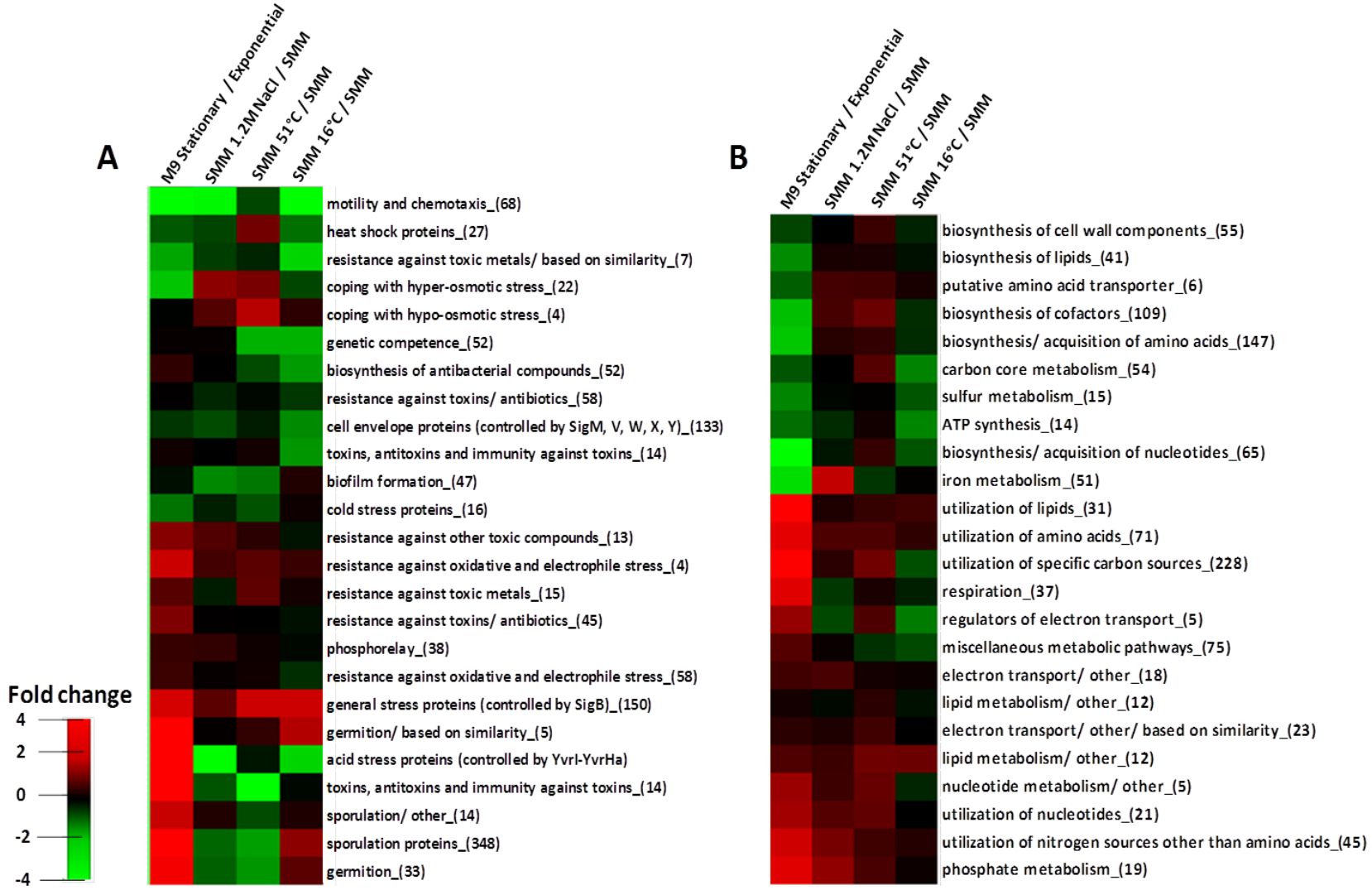

Figure 20 : Heat map overview of expression of the genes involved in metabolic and lifestyle categories. Fold change in comparison to their respective growth controls were obtained from the average expression profiles of the genes categorized by SubtiWiki functional classification A) Lifestyles and B) Metabolism. Number of genes representing each category is represented within the brackets.

5.4 MULTI-OMICS STUDY OF OSMOSTRESSED- AND OSMOPROTECTED *B. SUBTILIS* UNDER GLUCOSE LIMITING CONDITIONS

In its environmental niche *B. subtilis* often encounters a combination of stress conditions. As a result of frequent drying out and scarcity of nutrients, *B. subtilis* might also experience a combination of high osmolar environment and energy starvation. *B. subtilis* has the ability to protect itself from high osmolar environment by either synthesizing proline or by importing osmoprotectants like glycine betaine when available in the environment [85]. However, to endure a combination of stress conditions requires well-orchestrated complex adaptational responses. To understand the intricate adaptational responses a multi-omics level investigation was performed.

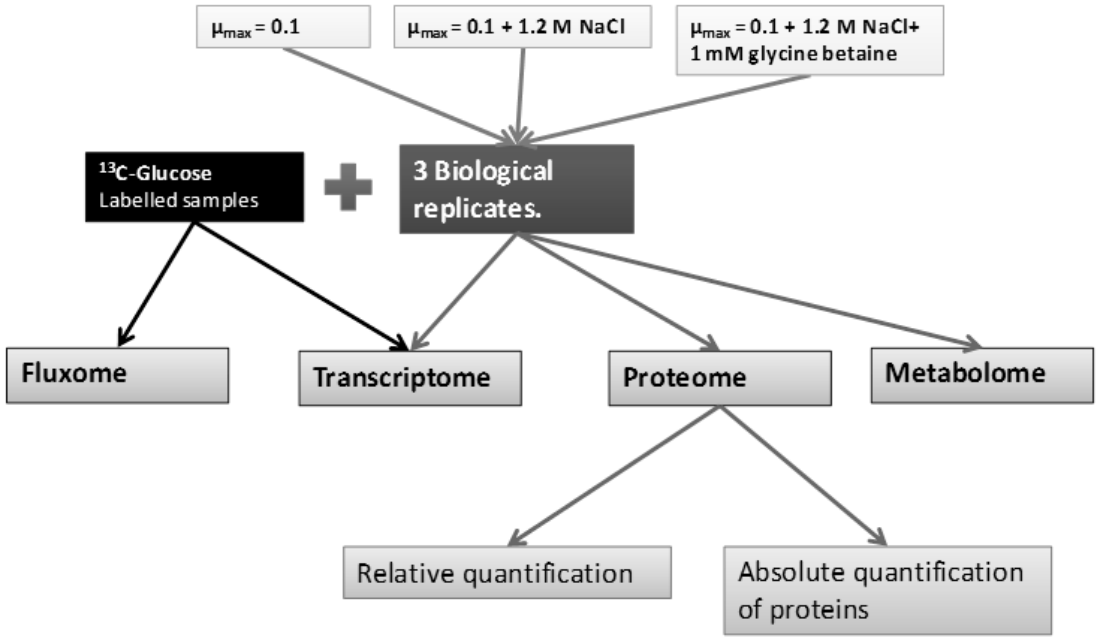

Figure 21 : Experimental overview of the multi-omics investigation of the adaptation of *B. subtilis* to glucose limitation, simultaneous glucose limitation and osmostress, simultaneous glucose limitation and osmoprotection. *B. subtilis* 168 Trp^+ was grown in chemostats under glucose limitation (μ_{max} = 0.1 h^{-1}), osmostress (μ_{max} = 0.1 h^{-1} + 1.2 M NaCl) and osmoprotection (μ_{max} = 0.1 h^{-1} + 1.2 M NaCl + 1 mM glycine betaine). Samples for multi-omics analysis were harvested after the cells reached the metabolic steady state (see Figure 22A).

In this study, the adaptational responses of continuous growth at high salt and the effect of osmoprotection by providing external glycine betaine in combination with glucose starvation were investigated. For this cells were grown at high salt (μ_{max} = 0.1 + 1.2 M NaCl), at high salt in

the presence of glycine betaine (μ_{max} = 0.1 + 1.2 M NaCl + 1 mM glycine betaine; osmo protection) and under glucose limitation as control condition (μ_{max} = 0.1) (Figure 21). Glucose limiting condition devoid of additional stress was considered as control for salt-stress and osmoprotection. Three biological replicates for each condition were investigated and an additional culture with ^{13}C-glucose (label) was used to investigate the flux through the CCM pathway. All the cultivations were performed in collaboration with Prof. Christoph Wittmann group in Braunschweig and I contributed to the study by performing the transcriptome and proteome analysis.

All cultures were grown in chemostats at a constant growth rate of 0.1 h^{-1} (Figure 22A). Samples for the multi-omics investigation were harvested after steady state was reached i.e. after five volume changes. Samples were harvested for transcriptome, intracellular proteome, intracellular metabolome, extracellular metabolome and fluxome analysis (Figure 21). Analyses of the proteome and transcriptome were part of this dissertation, thus they will be discussed in more detail.

For the transcriptome data analysis, relative gene expression values obtained from the normalized ratio data were used for the statistical analysis and functional categorization. For whole proteome analysis, after brief protein purification via SDS-PAGE (see section 5.1) in-gel trypsin digestion was performed and the resultant peptides were analyzed on a LTQvelos-

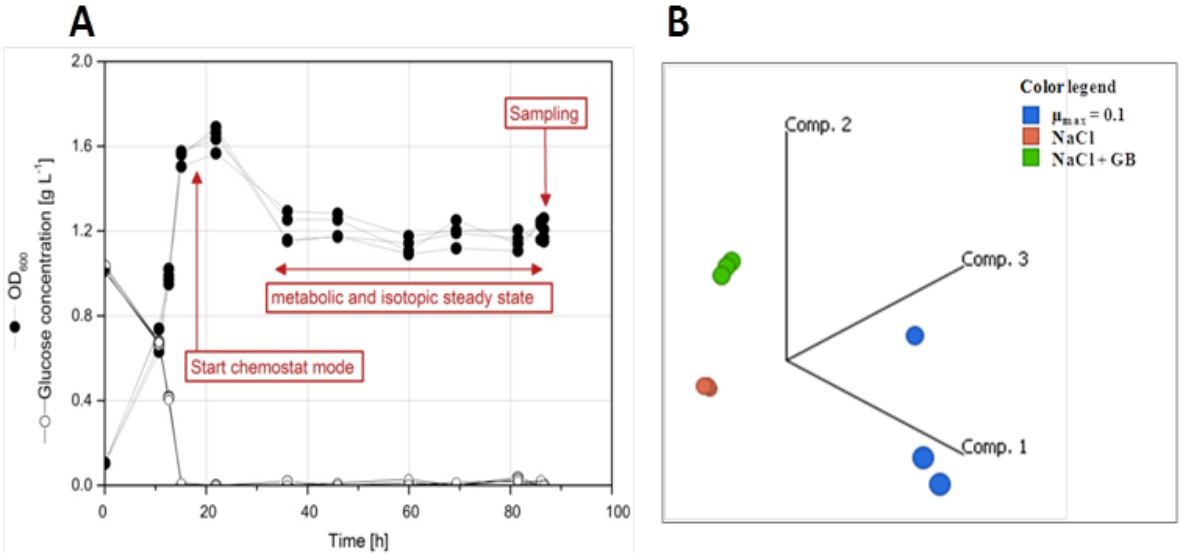

Figure 22 : A) Cultivation profile of four biological replicates of salt-stressed *B. subtilis* 168 Trp^+ grown at 0.1 h^{-1} in M9 minimal medium. Metabolic steady state was obtained after 35 hrs of cultivation and sampling for multi-omics analysis was done approximately after 85 hrs. B) Principal component analysis of combined data from proteome and transcriptome analysis of the samples μ_{max}=0.1 h^{-1} (control – blue cluster), μmax=0.1 h-1+1.2 M NaCl (osmostress – red cluster), μmax=0.1 h-1+1.2 M NaCl+ 1 mM GB (osmoprotection –green cluster).

Orbitrap mass spectrometer (Thermo Scientific). The raw data were processed in the Rosetta Elucidator software and normalized intensities for each protein were imported into Genedata Analyst for further statistical and functional analysis.

A combined PCA analysis (Figure 22B) for transcriptome and proteome data indicated a close clustering of the conditions representing the high reproducibility between the biological replicates. The osmoprotected samples clustered independently to that of the salt-stressed and the control samples, indicating the physiological differences between all three conditions.

5.4.1 Analysis of transcriptional changes

To understand the global changes in the transcriptome data compared to the reference condition (μ_{max}=0.1), the whole transcriptome data was normalized to the reference condition. 1150 genes were significantly regulated in either the high salt grown samples (osmostress) or those grown in the presence of high salt and glycine betaine (osmoprotection) compared to the reference condition with fold change value greater than three and p-value below 0.01 (after Benjamini-Hochberg correction). The regulated genes across all three conditions were subjected to a K-means clustering to reveal six distinct clusters (Figure 23, left box, details enclosed in supplementary table S3). To find enriched functional categories within each of the clusters, a Fisher`s exact test was performed comparing the proportion of genes associated with a given functional category in a cluster to the proportion of genes with the respective function within all genes (SubtiWiki classification, third level). This test provided the enrichment of the functional categories within each cluster and a –log 10 p-value indicating the extent of enrichment.

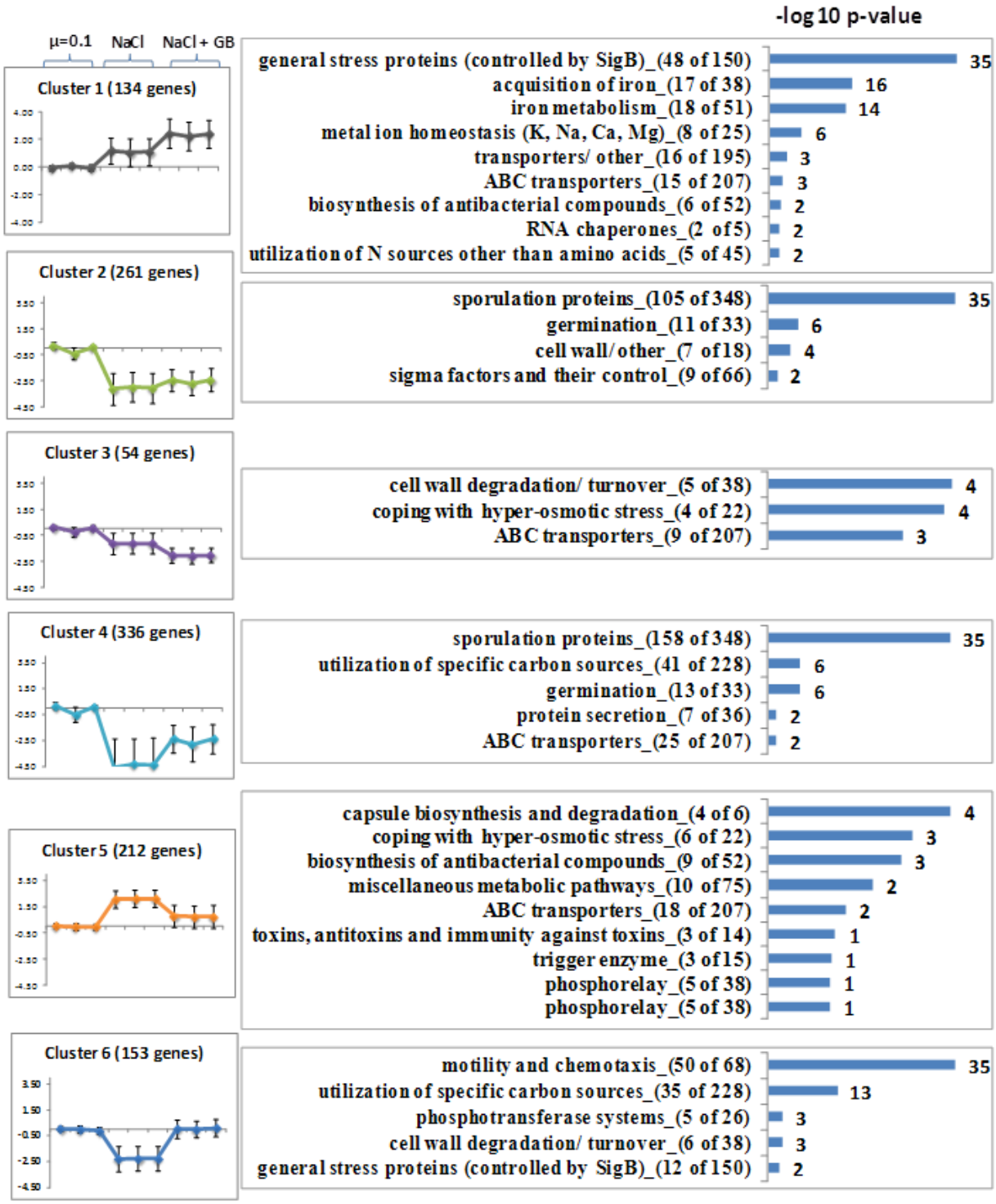

Figure 23 : K-means clustering and functional enrichment of transcriptome data. Graphs showing the average expression profile of each cluster with standard deviation (left) and enriched functional categories using the Fisher's exact test (right). All samples were normalized to the control condition (μ=0.1). The functional categories were adopted from "SubtiWiki". Number of genes in the enriched functional categories in the cluster (X) and the total genes in the parent category(Y) were represented as (X of Y). Detailed information about the regulated genes was enclosed in supplementary table S3.

Cluster 1 represented the genes that were induced by growth in high salt and even further up-regulated under conditions of osmoprotection. The most enriched genes in this cluster belong to the SigB dependent general stress response, iron metabolism (*yukNOP, feuABC, yuiI*) and metal ion homeostasis. Cluster 2 represented the strongly down regulated genes in both growth at high salt and osmoprotection. This cluster represented majorly sporulation proteins (members of SigE, SigF, SigG, SigK regulons). Cluster 3 had the smallest number of genes (54 genes) among all the clusters. The four genes that were included under the functional category of "coping with hyper-osmotic stress" represent the genes of the *opuC* operon. The OpuC transporter system has transporting abilities for various osmoprotectants like glycine betaine, choline or carnitine and is induced by a sudden salt stress, but not in response to continuous growth at high osmolarity [116]. The cluster 4 includes the genes that were strongly down regulated during the growth at high salt and slightly recovered during osmoprotection. The majority of the genes in this cluster encode for sporulation proteins and enzymes involved in the utilization of specific carbon sources and amino acids. Most of the genes enriched in the category belong to "ABC transporters" which were involved in utilization of specific carbon sources and amino acids.

Cluster 5 represented the genes that were strongly up-regulated during growth at high salt and down regulated under conditions of osmoprotection. This cluster contains the most relevant class with respect to the experimental condition, i.e., "coping with hyper osmotic stress" including the *proH* and *proJ* genes. The other genes that belong to this class were *opuAA, opuE, gbsA* and *gbsB.* This cluster also contains genes involved in cell wall degradation and lipid metabolism (*yqiIHK, slp, yxaA, yflE, lip, ywpB, tagC, psd, yocH*), osmoprotectant uptake (*opuA, opuE*). The last cluster 6 represented the genes that were strongly down regulated by growth at high salt and then fully restored during osmoprotection. The majority of genes in this cluster belong to the categories chemotaxis and motility. The genes involved in chemotaxis were strongly down regulated in the high salt adapted samples and this was completely restored during osmoprotection.

5.4.2 Multi-omics investigation of the central carbon metabolism

Apart from the global stress responses involved in the adaptation to growth under high salt conditions, *B. subtilis* possesses a very specific response mechanism in hypertonic medium. This response includes an initial influx of potassium ions that is followed by biosynthesis of high amount of proline as an osmoprotectant. This high amount of proline is synthesized from glutamate which is replenished from the TCA cycle. Glucose is the primary substrate that drives glycolysis and TCA cycle; however, in the current study only limited glucose was available for *B. subtilis* to maintain homeostasis between cell proliferation and production of high proline amount as an osmoprotectant. Hence, it is crucial to understand the adaptational strategy deployed with in the central carbon metabolism to endure at high salinity with limited energy source.

CCM specific protein abundance data were obtained by analyzing the samples via Multiple Reaction Monitoring (MRM) using QconCAT proteins as an internal standard. Measurements were done on a triple quadrupole mass spectrometer (TSQ Vantage - Thermo Scientific). The ratio data against the internal standard (QconCAT) were obtained from the software Skyline and these ratio data were used to calculate the absolute concentration of the individual proteins. The absolute concentration data was used for the normalization with the respective control sample (in this case μ=0.1 reference sample). Transcriptome data for the genes involved in the CCM pathway was obtained from the microarray analysis. The combined data from different omics platforms were mapped on the CCM pathway using ProMeTra online software [7].

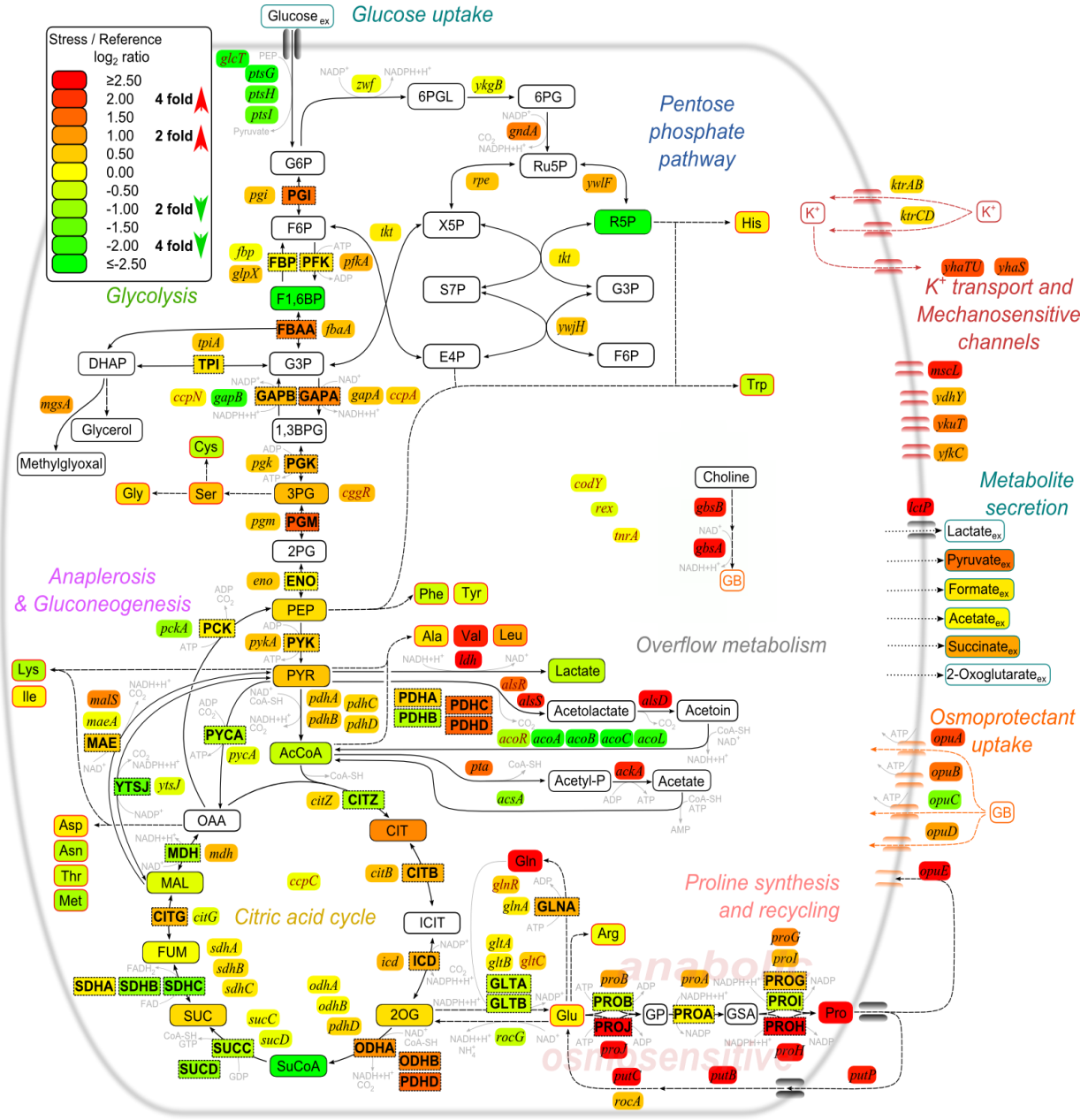

Figure 24 : Integrated view of relative transcript, protein and metabolite concentrations. Data from salt-stressed cells (in the presence of 1.2M NaCl) is compared to control (μ_{max}=0.1 h^{-1}) condition without salt. Log2 ratios of absolute protein abundances from MRM analysis, relative mRNA abundances from microarray analysis from section 5.4.1 and relative abundance of the metabolites were mapped onto the pathway using the ProMeTra online software [7]. Gene expression is represented in italics, protein expression in bold and surrounded by dashed rectangles and metabolite level by rounded rectangles.

The integrated results of the multi-omics data are presented in Figure 24 for the growth at high salt compared to the non-stressed cells (reference). The data mapped onto the pathway diagram indicate a minor overall up regulation of glycolytic enzymes and TCA cycle enzymes until 2-oxoglutarate (2OG) at both transcriptional and translational level with some exceptions like CitZ and PdhB. The proteins Pgi, FbaA, Pgm, PdhC and PdhD showed the strongest expression

among the glycolytic proteins. The rest of TCA cycle was relatively unchanged after the OdhAB and PdhD complex. However, the branched pathway from 2-oxoglutarate to proline was significantly up-regulated to meet the demand of the osmotically induced proline biosynthesis. Namely the co-transcribed genes for *proH* and *proJ* were significantly up-regulated at high salt concentrations, thus increase in the proline biosynthesis could be observed as well. It is known that proline leaks into the medium and has to be re-imported via OpuE. Interestingly the transcription of the genes that were responsible for proline degradation *putC* and *putB* in conjunction with the transporters *putP* and *opuE* were strongly up-regulated. Genes for the osmoprotectant uptake systems *opuA*, *opuB* and *opuD* were also up-regulated; on the other hand the broad spectrum osmoprotectant transport system *opuC* was down regulated by at least two fold. Among the osmoprotectant uptake systems *opuE* exhibited the strongest up regulation. Even though no precursor for glycine betaine biosynthesis was supplied, the transcription of the glycine betaine biosynthetic genes *gbsA* and *gbsB* were strongly up-regulated. The mRNA of mechanosensitive channel *mscL* was also up-regulated to maintain the intracellular homeostasis amid the accumulation of several compounds. Several genes involved in the overflow metabolism were up-regulated that include lactate biosynthesis and export, acetoin biosynthesis and acetate biosynthesis.

Multi-omics data mapped onto the pathway diagram for the CCM pathway during osmoprotection compared to osmostress is represented in Figure 25. Osmoprotection was accomplished by the supplementation of 1 mM glycine betaine to the growth medium already containing 1.2 M NaCl. When compared to the osmostressed cells, little transcriptional regulation in the central carbon metabolism was observed during osmoprotection except for few genes. Genes involved in glucose transport system (*ptsS, ptsH, ptsI*) were significantly up-regulated during osmoprotection. Interestingly the genes involved in gluconeogenesis (*pckA* and *gapB*) were up-regulated. In contrast to the osmostress the genes involved in the utilization of acetoin (product of over flow metabolism): the operon *acoA, acoB, acoC* and *acoL* were significantly up-regulated. The genes that were involved in uptake of proline and other osmoprotectants were strongly down regulated in the presence of glycine betaine. During osmoprotection most of the changes were observed at proteins level.

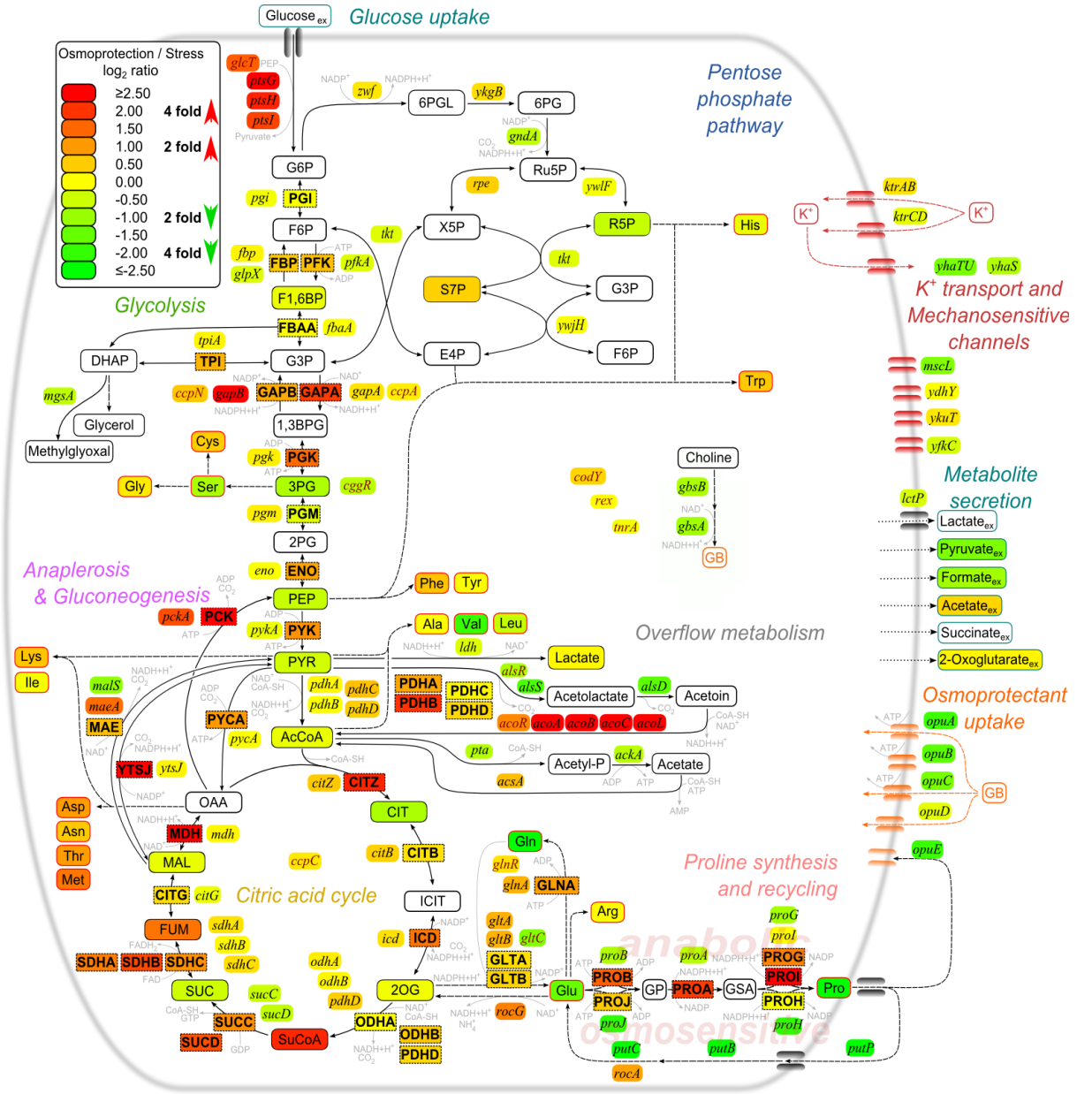

Figure 25: Data from protected salt-stressed cells (in the presence of 1.2M NaCl and 1mM glycine betaine) is compared to salt-stressed cells (with 1.2 M NaCl). Log2 ratios of absolute protein abundances from MRM analysis, relative mRNA abundances from microarray analysis from section 5.4.1 and relative abundance of the metabolites were mapped onto the pathway using the ProMeTra online software [7].Gene expression is written in italics, protein expression in bold and surrounded by dashed rectangles and metabolite level by rounded rectangles.

Almost all the proteins investigated during osmoprotection were either unchanged or significantly up-regulated in comparison to the osmostressed cells; though in some cases the transcriptional regulation was in contradiction. To start with GapA, there was strong increase of GapA protein though the mRNA of *gapA* was unaltered. This observation was also noted for several other proteins notably for Pgk, Eno, Pyk, PdhA and PdhB in glycolysis. In the TCA cycle

CitZ, Icd, Mdh, YtsJ and PckA, which were known to interact [59] with each other, were significantly up-regulated during osmoprotection in comparison to osmostressed cells. Other complexes like succinyl-CoA synthase (SucC, SucD) and succinate dehydrogenase (SdhA, SdhB, SdhC) were up-regulated as well. The most striking observation was that ProJ and ProH levels which were known to rise upon salt stress did not dramatically decrease if glycine betaine was present (osmoprotection) compared to osmostressed cells grown in the presence of 1.2 M NaCl. Furthermore, levels of ProA increased during osmoprotection, while transcription of the encoding gene *proA* even decreased if cells grown in the presence of 1mM glycine beatine were compared to those grown in the presence of 1.2 M NaCl only. The rest of the proline biosynthetic enzymes were present at increased level if cells grown under conditions of osmoprotection with those exposed to 1.2 M NaCl only. As mentioned earlier, these observations for the proline biosynthetic enzymes at protein level were not reflected at the transcriptional level suggesting a strong role of glycine betaine at translational or post translational level.

The flux calculations from the ^{13}C-labelled glucose cultures (experiments performed by M. Kohlstedt, Braunschweig) are represented in the Figure 26. During the reference condition ($\mu_{max} = 0.1$), the flux of the metabolized glucose was distributed across pentose phosphate pathway and glycolysis (Figure 26A). The central skeleton (glycolysis and TCA cycle) of the central carbon metabolism conceded the majority of the flux in this condition. Due to the lack of overflow metabolism a large extent of the flux from glucose was diverted to TCA cycle. Figure 26 B represents the flux distribution during growth at high salt. Remarkably, the cells were able to maintain the overall fluxes through the central skeleton network compared to the reference condition; only differing at two points. The first change includes the increase in the production of over flow metabolites from pyruvate, which was also observed at the transcriptome level. The second major and crucial increase in flux was observed for the production of proline and glutamine. This increase in flux towards proline signifies the role of proline in osmoprotection.

In the presence of glycine betaine, the overall flux distribution throughout the energy generating flux backbone of pentose phosphate and TCA cycle was maintained (Figure 26 C). On the contrary, the flux through overflow metabolism and the proline biosynthesis significantly dropped compared to growth at high salt concentrations. Furthermore, there was an increase in the flux through amino acid biosynthesis from oxalo-acetate and the flux through malate to

pyruvate. The decrease in the flux towards proline biosynthesis signifies the impact of osmoprotection via glycine betaine.

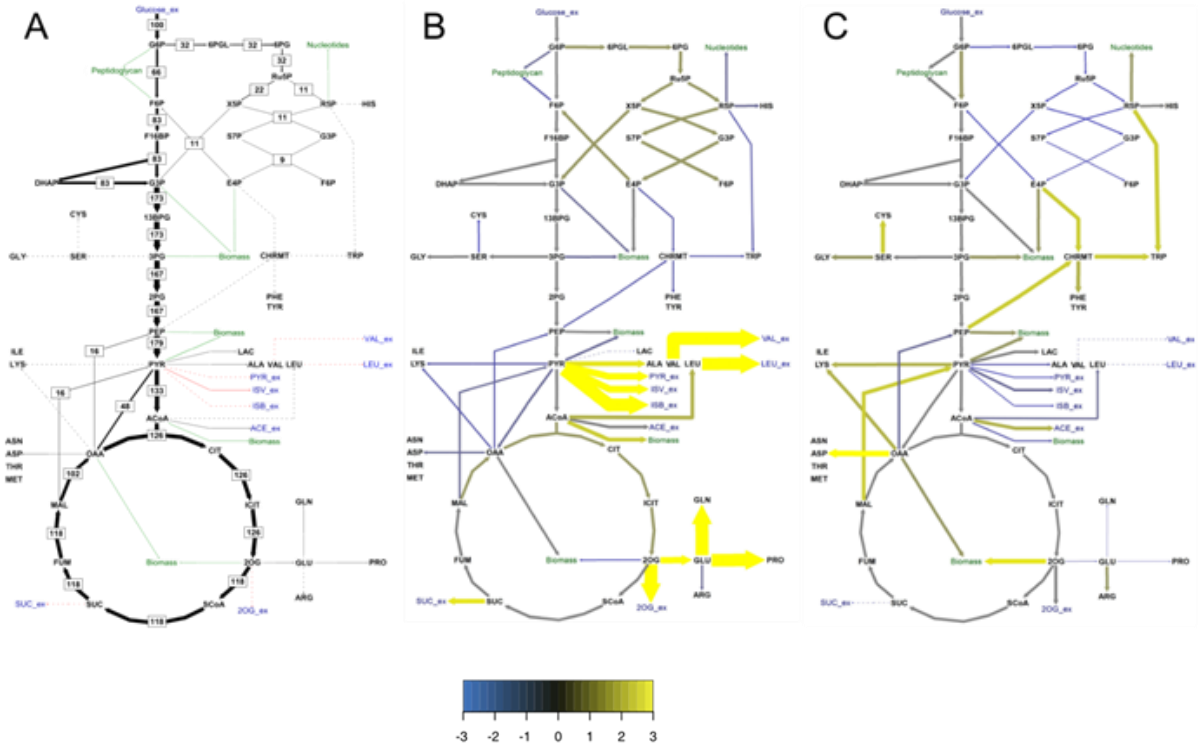

Figure 26 : Relative changes in metabolic flux distribution. Note – width of the arrows signify the magnitude of the flux. A) Relative flux distribution under reference conditions normalized to glucose uptake rate, B) Absolute fluxes in salt-stressed cells compared to non-stressed cells, C) Absolute fluxes in glycine betaine-protected cells compared to salt-stressed (figure courtesy by Michael Kohlstedt, Braunschweig).

On first view, the obviously homeostatic flux state of many of the biochemical conversions in carbon core metabolism (Figure 26 B and C) seemed to be in contradiction to the strongly increased expression level of many proteins (Figure 24, Figure 25). To understand the underlying mechanisms, the impact of salt ions on protein activity was investigated for selected proteins by *in vitro* enzyme kinetics measurements, since *B. subtilis* growing at high salt exhibit an elevated intracellular potassium content of 600 mM [76] (Experiments performed by Michael Kohlstedt, Braunschweig). Two of the most relevant candidates, phosphoglucoisomerase and isocitrate dehydrogenase, were selected. Indeed, the presence of 600 mM K^+ reduced the catalytic activity of the two enzymes by 56% and by 41% (Figure 27). It was interesting to note that proline itself, added in stress induced amounts, could not rescue the catalytic efficiency of the proteins. However, addition of 650 mM glycine betaine, reflecting the intracellular state at 1.2 M NaCl

and 1 mM glycine betaine in the medium could partially restore the original enzyme activity (Figure 27–yellow line). The ability to increase the protein amounts to compensate for lower catalytic activity due to increased salt concentration seems to be a fundamental strategy of *B. subtilis* to cope with the high osmolar conditions. The stabilizing and activating effect of glycine betaine on protein activity at high osmolarity might explain its efficient osmoprotection compared to proline.

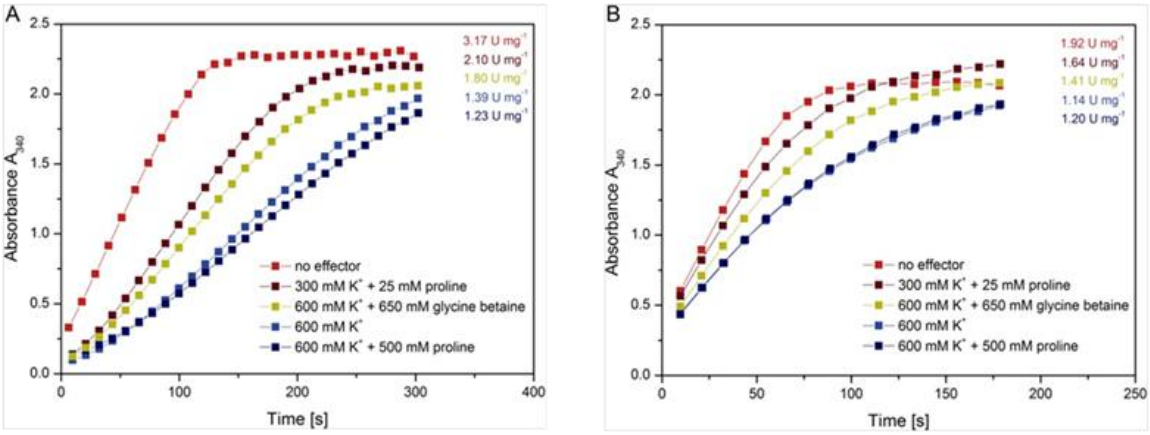

Figure 27 : Influence of NaCl, proline and glycine betaine on specific enzyme activity of A) Phosphoglucoisomerase Pgi and B) Isocitrate dehydrogenase Icd. Effector concentrations were chosen according to metabolomics data obtained in this study and literature data. (Experiments were performed by Michael Kohlstedt, Braunschweig)

Absolute protein abundances of the proline biosynthetic enzymes (pmol per gram dry weight) are depicted in Figure 28. ProB, ProA, ProI and ProG enzymes are required for anabolic proline biosynthesis, whereas the ProJ and ProH enzymes synthesize the high amounts of proline required during osmoprotection. In both pathways ProA is a common enzyme. We now observed that ProA was present at higher levels compared to the rest of the proline biosynthetic enzymes already during exponential growth with growth limiting amounts of glucose. During growth at high salt, ProJ and ProH levels were up-regulated approximately five and eight fold, respectively. On the other hand ProA levels were only marginally increased (less than 1.5 fold). Surprisingly, during osmoprotection, all proteins involved in proline biosynthesis showed higher abundances compared to the reference condition. Despite the observed changes at protein levels, such an effect of glycine betaine on the transcript level of proline biosynthetic genes could not be observed (Figure 25). All the proteins involved in the proline biosynthesis were present in higher abundance in the presence of glycine betaine during osmostress.

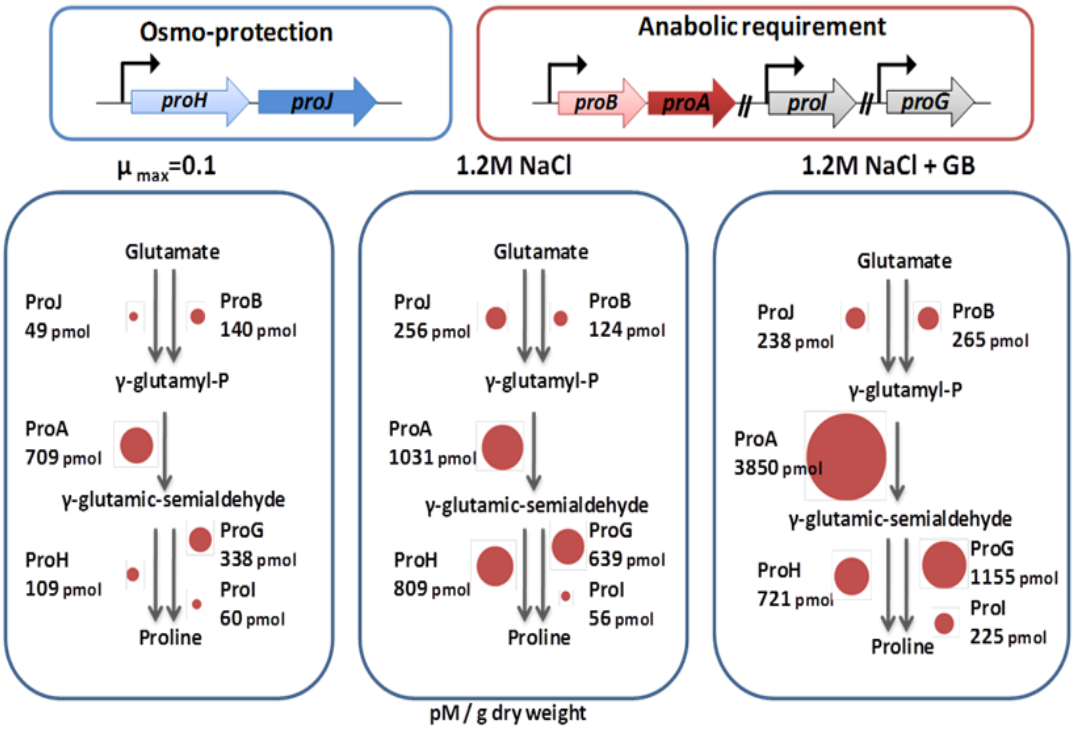

Figure 28 : Absolute amount of proteins involved in proline biosynthesis in the three different conditions μ_{max}=0.1 h^{-1} (control), 1.2 M NaCl (osmostress), 1.2 M NaCl+ 1 mM GB (osmoprotection). Absolute protein concentrations (pico mole/gram dry weight of the sample) were obtained from the MRM analysis. The size of the circle represents the relative abundance of the protein within the pathway.

Though glycine betaine is metabolically inert in *B. subtilis* it was able to influence several other pathways (not related to osmoprotection). Hence, it is crucial to understand the role of glycine betaine during normal growth and during osmoprotection.

5.4.3 Effect of glycine betaine during exponential growth and osmoprotection

The osmoprotection elicited by glycine betaine was already known [85], however, the additional physiological effect of glycine betaine during normal growth and at high salinity was not investigated in detail. Supplementation of glycine betaine at high salinity did not restore the protein abundances of CCM to the reference level); conversely a non-specific increase in the protein abundance was observed. Therefore, to understand the effect exerted by glycine betaine, we investigated the influence of glycine betaine on the growth physiology during normal growth, high salinity and osmoprotection.

To understand the influence of glycine betaine (GB) over the cellular physiology, the wild type strain *B. subtilis* 168 $TrpC^+$ was grown in four different conditions (Figure 29).with high glucose (0.5 % glucose) shake flasks; hence, unlike the chemostat cultivations a constant growth rate could not be maintained. The conditions tested in the experimental setup include growth in SMM, SMM + 1 mM glycine betaine, SMM + 1.2 M NaCl and SMM + 1.2 M NaCl + 1 mM glycine betaine (Figure 29). The growth rate was significantly increased in the presence of glycine betaine either in case of SMM or in SMM + NaCl + GB. To further understand the physiological impact of glycine betaine, samples were harvested for protein preparation at OD_{600} 1 (sample volume equivalent to 15 OD units). All the samples were processed via targeted MRM for the central carbon metabolic proteins and label free LC-MS/MS for whole proteome analysis.

CCM specific protein abundance data were obtained by analyzing the samples via MRM using QconCAT as an internal standard and measured on a triple quadrupole mass spectrometer. The ratio data against the internal standard (QconCAT) were obtained from the software Skyline and the ratio data was used to calculate the absolute concentration of the individual proteins. The absolute concentration data was used for the normalization with the respective control sample (SMM growth control). For whole proteome analysis, after brief protein purification via SDS-PAGE, in-gel trypsin digestion was performed and the resulting peptides were analyzed on a LTQ Velos-Orbitrap mass spectrometer. The raw data were processed in Elucidator software and the normalized intensities for each protein were imported to Genedata for further analysis.

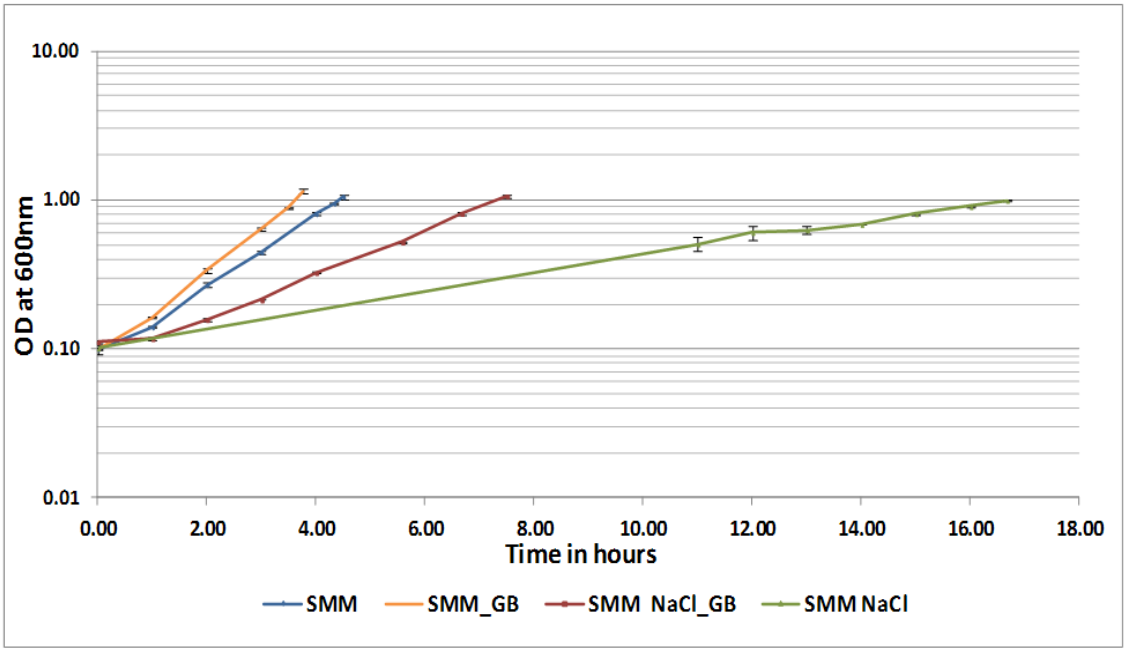

Figure 29 : Growth curve of the *B. subtilis* grown under different conditions. The *B.subtilis* wild type strain 168 Trp^+ was grown in SMM (control), SMM+1mM GB (GB control), SMM+1.2 M NaCl (osmostress), SMM+1.2 M NaCl+1mM GB (osmoprotection) as three biological replicates. Samples for the protein preparations were harvested at OD_{600} 1.0 from all the cultivations.

Principal component analysis of the resulting data sets from the MRM and whole proteome analysis (Figure 30) revealed a separation based on the different conditions. Absolute amounts of the proteins that were targeted with the MRM approach listed in Figure 31 were taken into consideration for the PCA plot in Figure 30A. As a result of whole proteome LC-MS/MS analysis, 1089 proteins (with minimum of 2 peptides) were identified; a PCA plot of the whole proteome analysis is shown in Figure 30B. All the three biological replicates for all the four conditions clustered together for both data sets. The segregation of the clusters denotes the variation induced by the different cultivation conditions. It is evident from the PCA plots that the samples that received glycine betaine during normal growth differed significantly to the other samples.

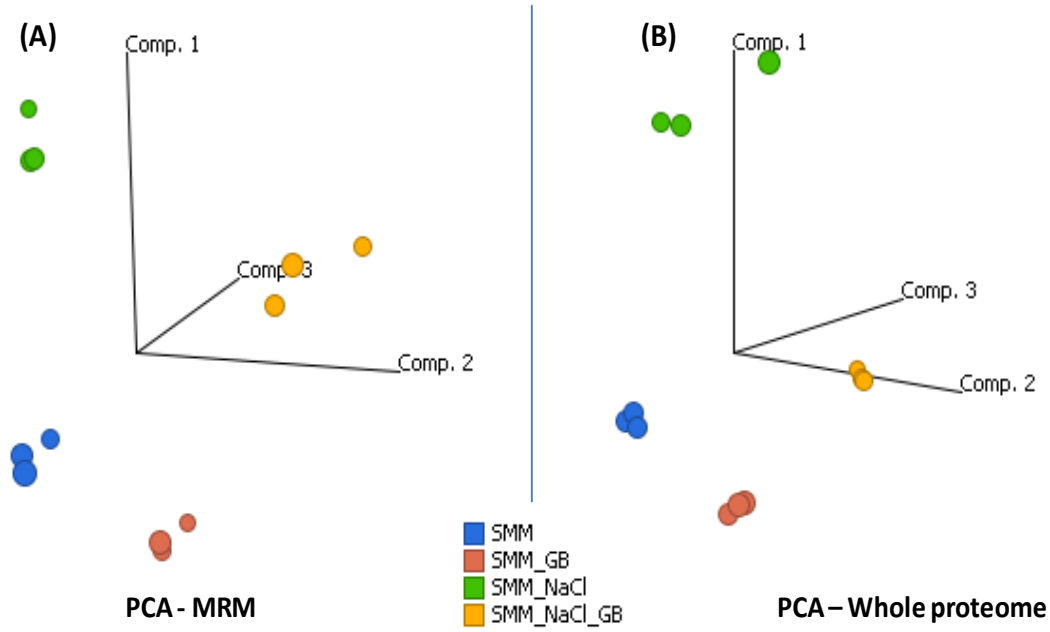

Figure 30 : PCA plots of the A) absolute protein abundances (data obtained from MRM analysis) of the proteins involved in the central carbon metabolism and proline biosynthesis and B) relative protein abundances of the all the identified proteins (data obtained from global proteome analysis). The *B. subtilis* wild type strain 168 Trp^+ was grown in SMM, SMM+1mM GB, SMM+1.2 M NaCl, SMM+1.2 M NaCl+1mM GB. The three biological replicates can be seen as three individual dots within the cluster.

Relative changes of the proteins involved in the central carbon metabolism for the above conditions are represented in the Figure 31. Ratio data was generated by normalizing all samples to the growth reference (SMM) and the ratio data visualization was performed. Subtle changes were observed in the core skeleton of the central carbon metabolism. GB alone did not alter the central carbon metabolism. However, high salt stress influenced levels of some key enzymes like Pgi and Icd, which both were slightly up-regulated. FbaA was also induced at high salt. PckA, which is a major gluconeogenic enzyme, was strongly induced during continuous growth at high salt even in the presence of high glucose concentrations. The glutamate synthase complex was strongly down regulated in the presence of high salt amid the requirement of high glutamate concentrations for the production of proline during osmoprotection. The key enzymes responsible for proline biosynthesis ProJ and ProH were strongly up-regulated. Furthermore, ProA was also slightly up-regulated (1.5 fold) during high salt growth. Interestingly, during osmoprotection (NaCl + GB) ProJ and ProH remained at high levels although the cells do not require proline as an osmoprotectant in the presence of glycine betaine. Apart from proline biosynthesis, FbaA, PdhC, PdhD, OdhA and OdhB were up-regulated upon osmoprotection.

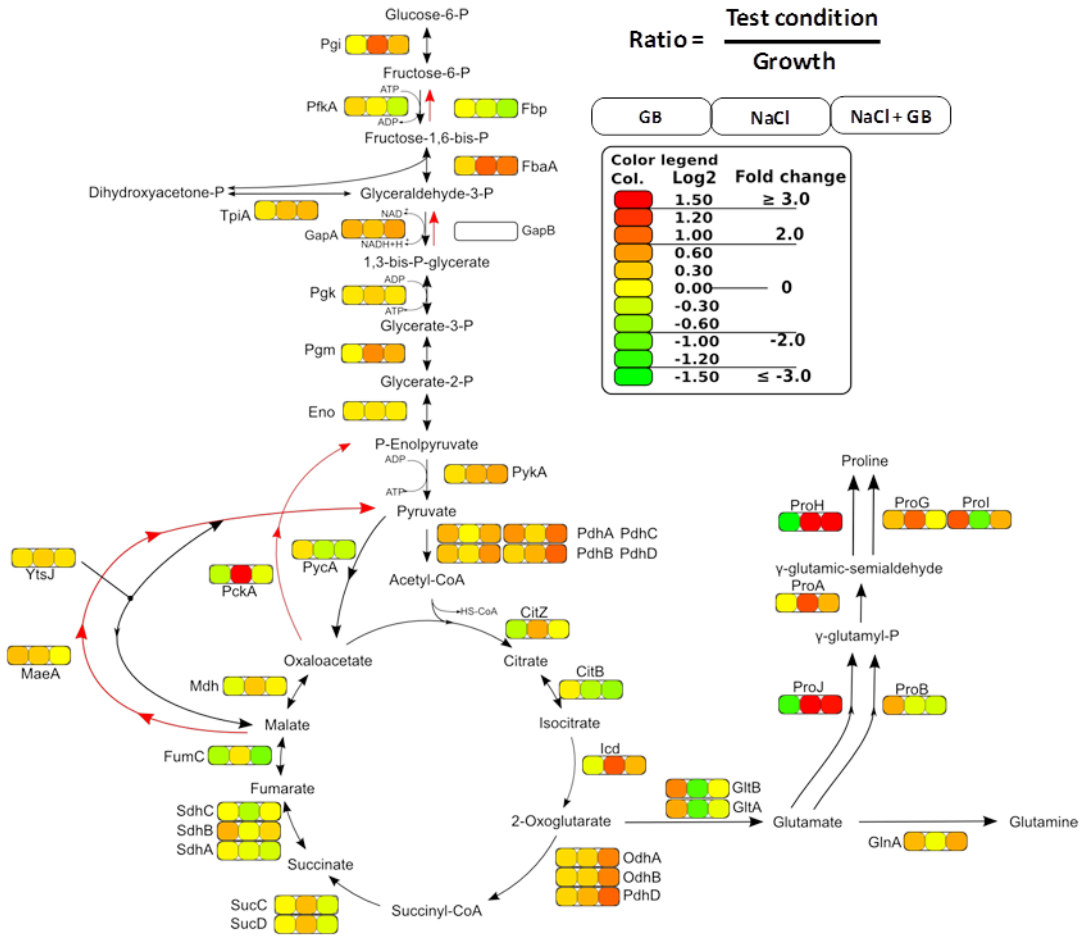

Figure 31 : Relative changes of the proteins in the central carbon metabolism in all conditions compared to the reference condition (SMM). Log2 ratio of protein abundances were obtained from the MRM analysis of the samples cultivated in shake flask with SMM+ 1 mM GB (GB sample), SMM+1.2 M NaCl (NaCl sample), and SMM+1.2 M NaCl+1mM GB (NaCl+GB sample) compared to the growth reference SMM.

Global changes in the proteome as a result of various growth conditions are reported in Figure 32. Relative protein intensities were considered for the data analysis. After normalizing to the respective controls, an effective fold change of 1.5 and a p-value of 0.01 (after Benjamini-Hochberg correction) were applied to filter significantly regulated proteins. The resulting significantly regulated proteins were assigned to functional categories obtained from SubtiWiki. A Fisher's exact test was performed to elucidate the functional class enrichment.

117 proteins were significantly regulated by glycine betaine alone compared to the reference sample grown in SMM. 12 proteins of SigB regulon were down regulated in the presence of glycine betaine. Furthermore, proteins involved in the biosynthesis and acquisition of amino

acids and nucleotides were up-regulated in the presence of the glycine betaine. During continuous growth at high salt 336 proteins were significantly regulated. Of these 26 proteins belonging to the SigB regulon were up-regulated in the presence of high salt. 6 proteins involved in iron uptake and 9 proteins involved in the iron metabolism were up-regulated. This observation supports the earlier (section 5.3 and 5.4.1) transcriptome data analysis the *B. subtilis* grown at high salt experience severe iron limitation. Proteins that belong to translation, biosynthesis and acquisition of amino acids were down regulated during continuous growth at high salt, probably due to lower growth rate compared to the reference condition.

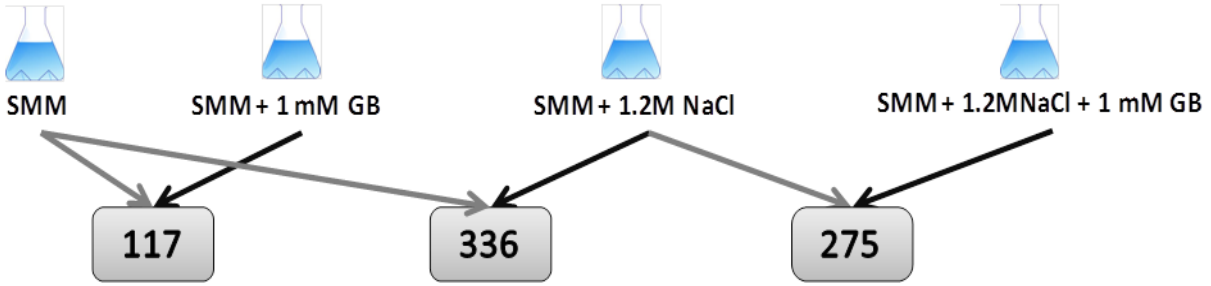

Functional categories classified according to SubtiWiki	Total number of proteins in the category	Regulated proteins that were enriched by Fischer`s Exact test		
		SMM+GB / SMM	SMM +1.2 M NaCl/SMM	SMM +1.2 M NaCl + GB / SMM + 1.2 M NaCl
General stress proteins (controlled by SigB)	150	12 (11↓ 1↑)	27 (1↓ 26↑)	19(18↓ 1↑)
Coping with hyper-osmotic stress	22	5(5↓)	5(1↓ 4↑)	6(6↓)
Biosynthesis/ acquisition of amino acids	147	19(1↓ 18↑)	34(30↓ 4↑)	29(1↓ 28↑)
Biosynthesis/ acquisition of nucleotides	65	6(6↑)	16(16↓)	23(2↓ 21↑)
Electron transport/ other	18	3(3↓ ↑)	5(5↑)	8(6↓ 2↑)
Acquisition of iron	38		7(1↓ 6↑)	
Iron metabolism	51		10(1↓ 9↑)	
Translation	180		25(22↓ 3↑)	21(2↓19 ↑)
Sporulation proteins	348	22(17↓ 5↑)		
Motility and chemotaxis	68		10(10↓)	
Sulfur metabolism	15			4(4↑)
Resistance against oxidative and electrophile stress	58		12(12↑)	
ABC transporters	207	11(6↓ 5↑)		
Utilization of nitrogen sources other than amino acids	45	4(4↑)		

Figure 32 : Comparative analysis of influence of GB on global protein expression pattern. Number of proteins that were significantly regulated with a statistical cut-off of fold change 1.5 and p-value of 0.01 (after Benjamini Hochberg correction) between the conditions tested were represented in the above figure. Proteins that belong to the functional categories (SubtiWiki) for each set of the regulated proteins were shown in the brackets. The green numbers indicate the number of down regulated proteins and the red numbers indicate the number of up-regulated proteins.

Presence of glycine betaine during continuous growth at high salt provides better osmoprotection compared to the internally synthesized proline. This was phenotypically evident from the drastically improved growth rate during osmoprotection (NaCl + GB) and the changes observed in the proteome compared to continuous growth at high salt. The major changes observed in the proteome correlate with the increased growth rate with increased levels of proteins involved in the biosynthesis of amino acids, nucleotides and translation. Some of the proteomic changes observed in the presence of glycine betaine during osmoprotection (SMM+ NaCl + GB) could be also observed in the presence of glycine betaine during normal growth (SMM + GB) with a difference in the number of proteins regulated in each functional category. During osmoprotection the number of proteins regulated in each functional category was higher compared to the presence of glycine betaine during normal growth. This difference could be due to the fact that the influence of glycine betaine was higher or more effective when the cells were growing at high salt compared to the presence of glycine betaine during normal growth.

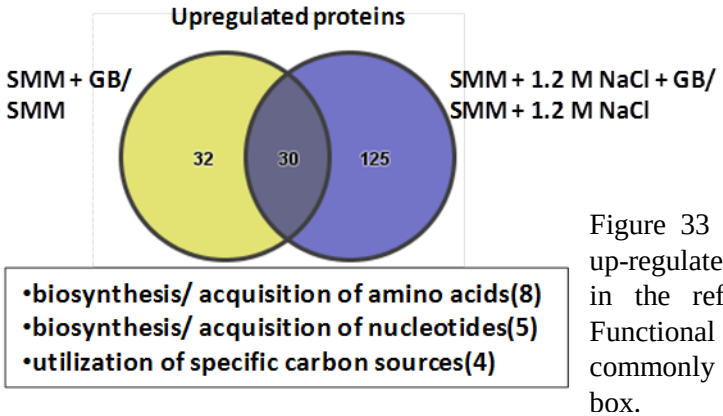

Figure 33 : Venn diagram representing proteins up-regulated in the presence of the glycine betaine in the reference condition and at high salt. Functional classes for the 30 proteins that were commonly influenced by GB are provided in the box.

The proteins that increase in level in the presence of glycine betaine either during normal growth or during osmoprotection are represented in the Venn diagram of Figure 33. 30 proteins were commonly up-regulated under both conditions. These proteins include those involved in the biosynthesis acquisition of amino acids, nucleotides and utilization of specific carbon sources. A group of 5 proteins (GudB, LysS, PurF, GSP13 (*yugL*), CarB) were previously described as unstable during glucose starvation in *B: subtilis* by Gerth *et al.* 2009 [1]. In this study Gerth *et al.* reported around 200 unstable proteins of which 80 proteins were targets of the ClpP/ClpC and ClpP/X proteases. Out of 200 of the unstable proteins, 45 proteins were covered in the current proteome study.

Levels of these unstable proteins under the different conditions analyzed in the current study are represented in Figure 34. All samples were normalized to the reference (SMM). For the osmoprotection sample the osmostress sample was taken as a reference to compensate for effects of high salt independent of glycine betaine. Log2 transformed ratios are visualized in Figure 34. This analysis indicates the increase in level of most of the previously known unstable proteins in the presence of glycine betaine either during growth or during osmoprotection. Furthermore, during osmostress there was a strong decrease in level/ apparently degradation of these proteins when compared to that of the other conditions. For several of those proteins that were decreased in level during osmostress the level was either restored or even further up-regulated during osmoprotection.

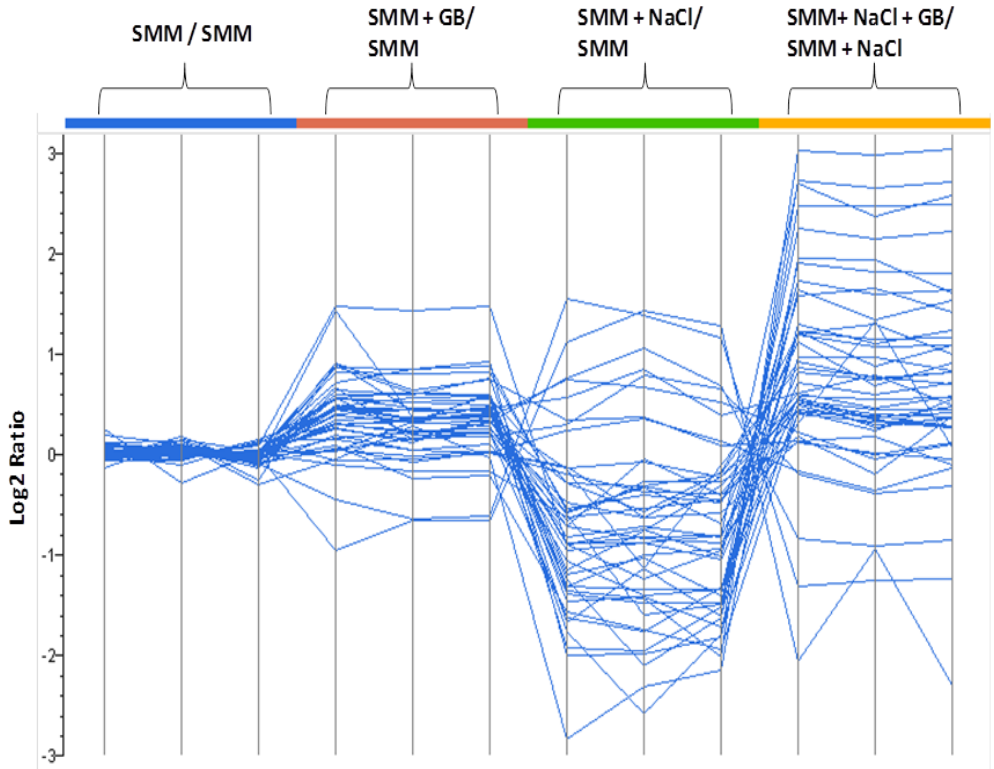

Figure 34 : Regulation of the unstable proteins [1, 2] in the presence of glycine betaine (SMM+ 1 mM GB), osmostress (SMM+1 M NaCl) and osmoprotection (SMM+1 M NaCl+10 mM GB) in comparison with their respective growth controls. Log2 ratios were derived by normalizing the relative protein quantities (from global proteome) compared to their respective controls.

Annotation			Fold change[a]		
Protein Name	**Uniprot ID**	**Gene description**	**GB**	**NaCl**	**NaCl+GB**
ArgB	P68729	Acetylglutamate kinase	**1.60**	**-2.79**	**2.30**
AroA	P39912	Protein aroA(G)	**1.26**	**-1.74**	**1.72**
BioB	P53557	Biotin synthase	**1.18**	**-1.39**	**1.71**
CarB	P18185	Carbamoyl-phosphate synthase arginine-specific large chain	**1.74**	**-1.40**	**1.86**
CheW	P39802	Chemotaxis protein	**1.24**	**-2.43**	**1.25**
ClpC	P37571	Negative regulator of genetic competence	**-1.11**	**-1.47**	**1.30**
CspB	P32081	Cold shock protein	**1.04**	**-5.44**	**3.52**
CspD	P51777	Cold shock protein	**1.51**	**1.50**	**1.53**
Ctc	P14194	General stress protein	**-1.49**	**2.55**	**-2.43**
Efp	P49778	Elongation factor P	**1.23**	**-1.68**	**1.30**
GlmS	P39754	Glucosamine--fructose-6-phosphate aminotransferase [isomerizing]	**1.68**	**1.20**	**1.04**
GltA	P39812	Glutamate synthase [NADPH] large chain	**1.49**	**-2.55**	**2.23**
GudB	P50735	NAD-specific glutamate dehydrogenase	**2.72**	**-1.81**	**5.78**
GyrA	P05653	DNA gyrase subunit A	**1.06**	**-1.32**	**1.08**
IleS	Q45477	Isoleucyl-tRNA synthetase	**1.05**	**-1.26**	**1.38**
IlvA	P37946	Threonine dehydratase biosynthetic	**1.01**	**-1.26**	**1.45**
IlvB	P37251	Acetolactate synthase large subunit	**1.27**	**-1.93**	**1.58**
LeuA	P94565	2-isopropylmalate synthase	**1.44**	**-3.52**	**2.06**
LeuC	P80858	3-isopropylmalate dehydratase large subunit	**1.45**	**-2.92**	**1.33**
LeuD	P94568	3-isopropylmalate dehydratase small subunit	**1.15**	**-2.98**	**1.47**
LysC	P08495	Aspartokinase 2	**1.82**	**-3.85**	**6.42**
MetE	P80877	methyltetrahydropteroyltriglutamate--homocysteine methyltransferase	**1.31**	**-2.06**	**3.12**
MtnK	O31663	Methylthioribose kinase	**1.49**	**-1.28**	**2.15**
MurAA	P70965	UDP-N-acetylglucosamine 1-carboxyvinyltransferase 1	**1.35**	**-4.15**	**1.88**
NrdE	P50620	Ribonucleoside-diphosphate reductase subunit alpha	**1.27**	**-1.21**	**1.77**
PurB	P12047	Adenylosuccinate lyase	**1.39**	**-1.87**	**2.89**
PurF	P00497	Amidophosphoribosyltransferase precursor	**1.57**	**-3.05**	**8.00**
PurL	P12042	Phosphoribosylformylglycinamidine synthase II	**1.43**	**-2.33**	**4.57**
PurQ	P12041	Phosphoribosylformylglycinamidine synthase 1	**1.29**	**-3.18**	**5.52**
Pyc	Q9KWU4	Pyruvate carboxylase	**1.19**	**-1.49**	**1.05**
pyrB	P05654	Aspartate carbamoyltransferase	**1.29**	**-2.36**	**2.81**
RpoB	P37870	DNA-directed RNA polymerase subunit beta	**1.22**	**-1.86**	**1.36**
SecA	P28366	Preprotein translocase subunit	**1.33**	**-1.38**	**1.31**
SpoVG	P28015	Putative septation protein	**-1.10**	**-3.39**	**1.27**
ThiC	P45740	Thiamine biosynthesis protein	**1.31**	**1.55**	**1.06**
ThrRS	P18255	Threonyl-tRNA synthetase 1	**1.34**	**-2.14**	**1.29**
Tig	P80698	Trigger factor	**-1.00**	**-1.12**	**1.31**
Tuf	P33166	Elongation factor Tu	**1.14**	**-1.33**	**1.01**
xpt	P42085	Xanthine phosphoribosyltransferase	**1.36**	**-2.75**	**3.54**
YfhM	O31581	YfhM protein	**-1.71**	**2.40**	**-3.42**
YhaM	O07521	3'-5' exoribonuclease	**-1.03**	**1.17**	**-1.18**
YhxA	P33189	Uncharacterized aminotransferase	**1.64**	**-1.78**	**1.47**
YjbV	O31620	YjbV protein	**1.20**	**1.76**	**-1.83**
YloV	O34751	YloV protein	**1.09**	**1.48**	**-1.24**

Annotation			Fold change[a]		
Protein Name	**Uniprot ID**	**Gene description**	**GB**	**NaCl**	**NaCl+GB**
YugI	P80870	General stress protein 13	**1.74**	**-1.46**	**2.23**

Table 2: Quantification of the impact of high salt and glycine betaine on presumably unstable proteins that were reported in Gerth *et al.* [1] and covered in the current study. ([a])- Fold change was calculated for the GB and NaCl sample compared to the reference growth sample SMM, whereas fold change for NaCl+GB was compared to NaCl sample as a reference.

The increase in level of these unstable proteins in the presence of glycine betaine could be due to two different reasons. The first reason could be that the level of these proteins could be regulated in a growth rate dependent manner. Since the growth rate was higher in the presence of glycine betaine the unstable proteins could have been maintained at higher abundance under this condition. The second reason could be a biophysical stabilization of the unstable proteins directly by glycine betaine. To conclude, in the presence of glycine betaine regardless of growth condition could indirectly affect many physiological processes by either improved growth rate or by biophysical protein stabilization.

5.4.4 Comparative analysis of the central carbon metabolism during osmostress and osmoprotection at high and low glucose

During osmoprotection, *B. subtilis* requires additional resources to cope with growth at high salt concentrations. To investigate the adaptational responses towards osmostress and osmoprotection in the presence of high and low glucose a comparative analysis was performed. In Figure 35 a comparative analysis of the abundance of proteins involved in the CCM and proline biosynthesis was visualized. The ratio of the protein abundances for the high glucose condition (shake flask) compared to the low glucose condition (chemostat) was used for visualization. There was a significant effect of glucose concentration on the protein abundances within the CCM imposed by different glucose concentration. A major difference was observed for the glycolytic proteins; almost all of the glycolytic proteins were present at fivefold higher level in the shake flask samples compared to the chemostat samples. The proteins with the lowest difference in abundance within the glycolytic enzymes were the Pgi and PdhD. The pattern was different for proteins of the glycolysis and the TCA cycle. Many of the TCA cycle enzymes were present at lower level in the presence of high versus low glucose as expected. However, a few highly abundant proteins like Icd, FumC and Mdh displayed higher levels in the presence of excess glucose. Furthermore, the proline biosynthetic enzymes were present in lower amounts during high versus low glucose. Increased glycolysis in the presence of high glucose and decreased TCA cycle indicate an increase in over flow metabolism in the shake flask experimental setup due to the high glucose concentration.

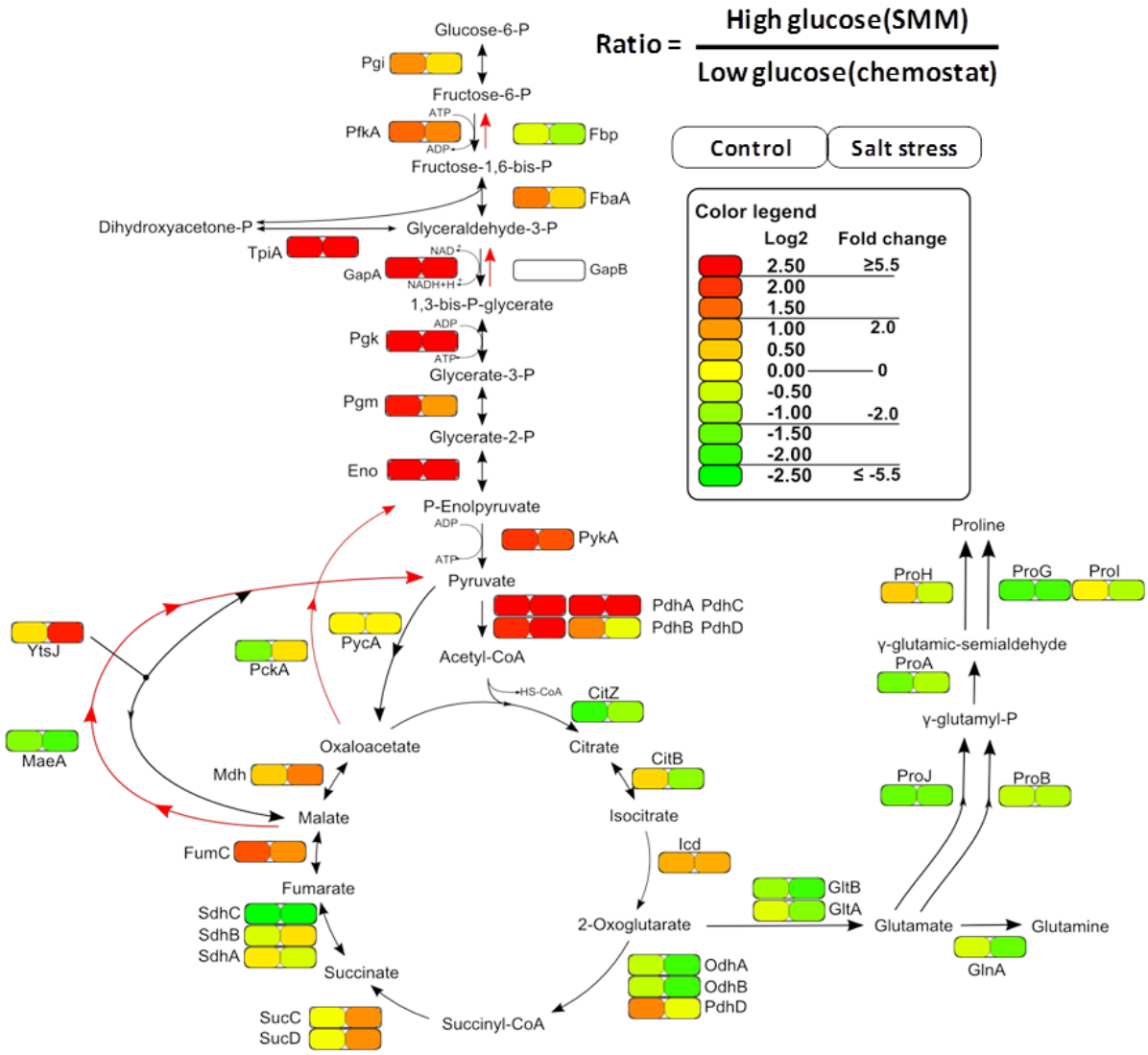

Figure 35: Influence of glucose concentration during normal growth (none-stressed cells) and osmostress (1.2 M NaCl) onto the level of enzymes of the CCM and proline biosynthesis. Log2 ratio of protein abundances were obtained from the MRM analysis of high glucose samples cultivated in shake flasks (results from section 5.4.3) and low glucose samples cultivated in chemostat (results from section 5.4.2).

Comparisons of the effect of osmostress during high and low glucose on CCM and proline biosynthetic enzymes normalized to the respective non-stressed control are shown in Figure 36. This comparison was performed to analyze the adaptational differences of *B. subtilis* to osmostress in the presence of high glucose and low glucose. In the presence of high glucose, the central carbon metabolic enzymes were not significantly regulated when compared to its growth control (SMM). The only significant change was found for PckA which is a major gluconeogenic

enzyme and was strongly up-regulated in the presence of high glucose. Osmostress during low glucose significantly influenced the central carbon metabolism. Many proteins in the central core carbon metabolism were increased in level during osmostress compared to the none-stressed control cells; namely Pgi, FbaA, Pgm, PdhC, PdhD of glycolysis and CitB, OdhA, OdhB, FumC of TCA cycle were up-regulated. The switch point from 2-oxoglutarate to glutamate (glutamate synthase complex - GltA and GltB) was unchanged in the presence of low glucose but strongly down regulated in high glucose grown cells. Furthermore, the crucial proteins that are responsible for osmoprotection cells by producing high amounts of proline, ProJ and ProH, were induced to a similar extent regardless of the glucose concentration.

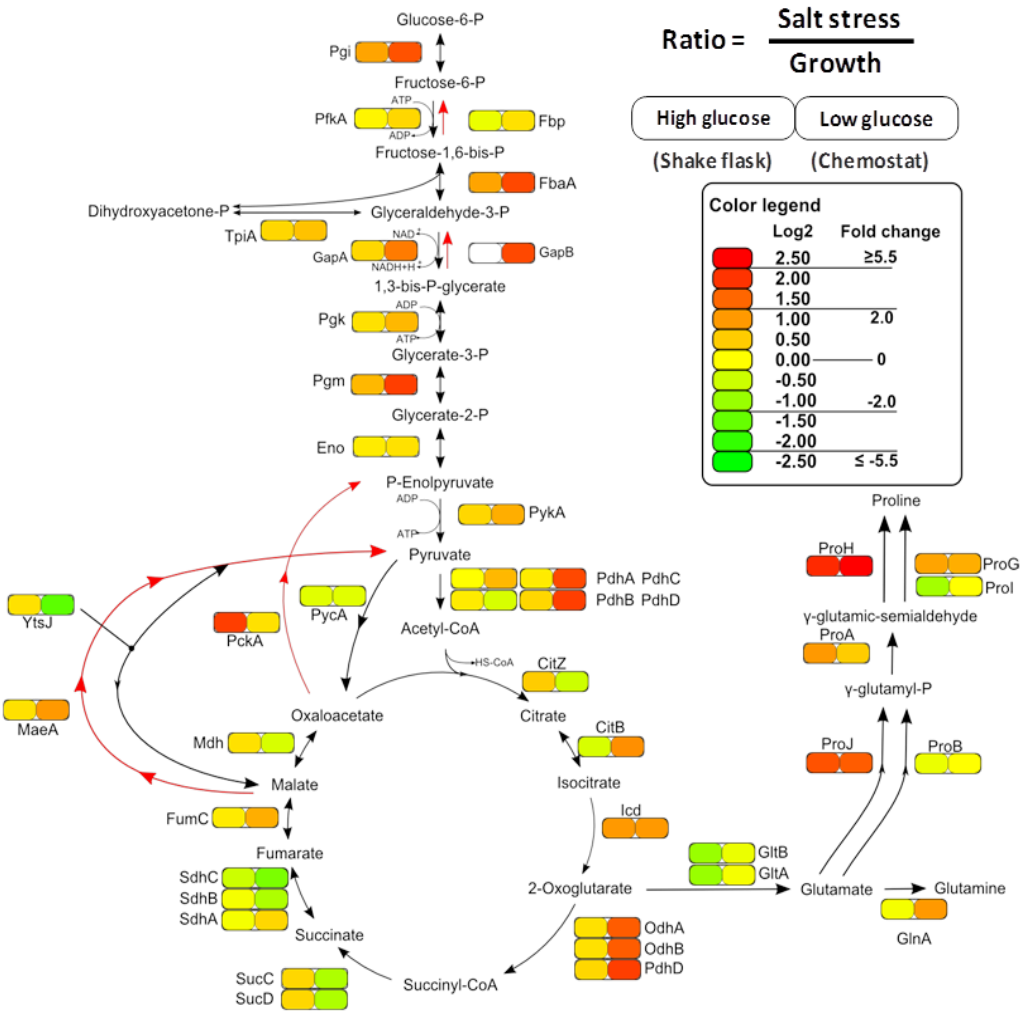

Figure 36: Comparative analysis of protein changes during salt stress (1.2 M NaCl) at high glucose (shake flask) and at low glucose (chemostat); both compared to their respective growth controls (none-stressed cells). Log2 ratio of protein abundances were obtained from the MRM analysis of shake flask samples (results from section 5.4.3) and chemostat samples (results from section 5.4.2).

A similar comparison for the osmoprotected samples with glycine betaine at high and low glucose was performed (Figure 37). Again, there was not much difference observed during osmoprotection at high glucose (left rectangle) in either central carbon metabolic enzymes or the proline biosynthetic enzymes. Major changes in protein level were observed during osmoprotection at low glucose (right rectangle). As seen in the osmoprotected samples grown in the chemostat (see section 5.4.2, Figure 25) most of the effects of glycine betaine were not represented at transcriptional level, so the effects of glycine betaine were probably post-transcriptional or translational. For some unknown reasons the stabilization effects imposed by glycine betaine were not significantly observed for the proteins involved in CCM unlike the unstable proteins at high glucose.

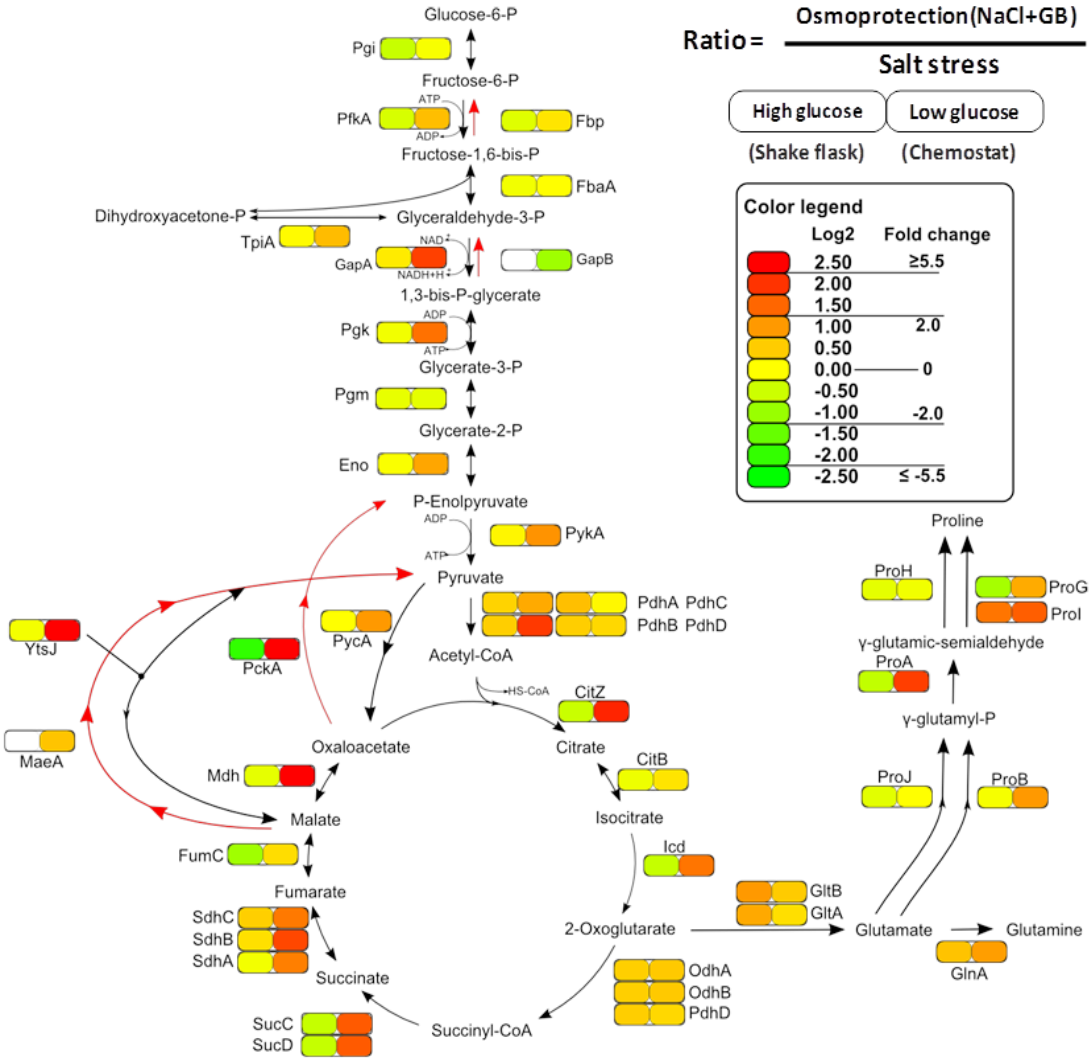

Figure 37: Comparative analysis of protein changes during osmoprotection (1.2 M NaCl + 1 mM GB) at high glucose (shake flask) and at low glucose concentrations (chemostat); both conditions are compared to their respective osmostressed samples (1.2 M NaCl). Log2 ratio of protein abundances were obtained from the MRM analysis of shake flask samples (results from section 5.4.3) and chemostat samples (results from section 5.4.2).

5.4.5 Effect of ProH and ProJ over-expression and glutamate supplementation onto the osmo-adaptation of *B. subtilis*

Improving the osmoprotection capabilities of *B. subtilis* with its existing machinery would contribute to a better biotechnological application and might also provide new insights into the physiological regulation and its kinetics. To this regard, two questions were asked: 1) would higher levels of ProJ and ProH enzymes provide better osmoprotection? 2) would the supplementation with external glutamate omit a potential bottleneck and result in higher proline levels and hence a better osmoprotection?

In a different set of experiments we wanted to explore if the enzymes ProH and ProJ or glutamate levels constitute bottlenecks for the osmoadaptation of *B. subtilis*. These experiments were done in collaboration with the group of Prof. Erhard Bremer in Marburg and I contributed to this study with the proteome analyses described below. Three different strains were used in this experiment and each strain was grown in four different conditions in triplicate Figure 38. The conditions include growth in SMM (reference), SMM + NaCl, SMM + glutamate and SMM + glutamate + NaCl. The strains include JH642 (wild type), MDB22 (*amyE* control) and MDB28 (*proHJ* overexpression from the *amyE* locus). Overexpression of ProJ and ProH was achieved by replacing the original promoter by a perfect osmotically inducible SigA promoter (M10). The M10 promoter (Figure 39B) was a result of a series of mutations of its original promoter. The resultant promoter activity was assayed with TreA activity [152] and the results were shown in Figure 39C. All the mutant constructs were tested for the promoter activity during normal growth and the osmostress. Among the tested mutants, M10 was the strongest expressed

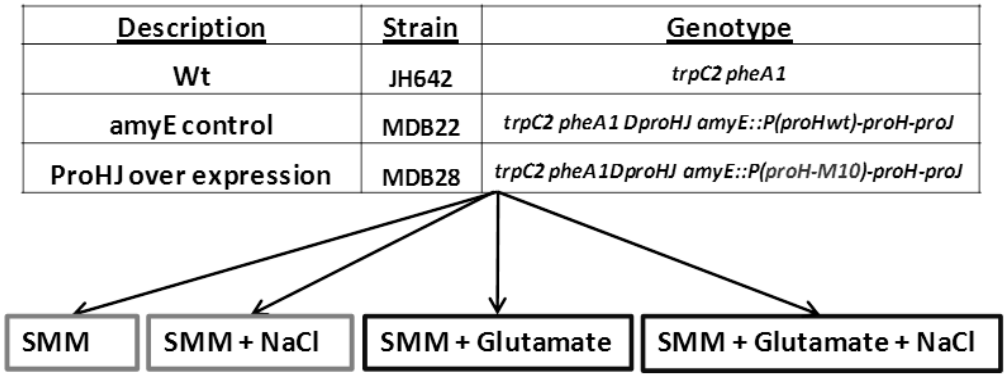

Figure 38 : Experimental setup and strain description for testing the effect of the *proHJ* over expression and supplement of glutamate during osmostress. The *B. subtilis* wild type strain (JH642), the *amyE* control strain (MDB22) and *proHJ* over expressing mutant (MDB28) were grown in four different conditions (SMM, SMM + 1.2 M NaCl, SMM + 10 mM glutamate and SMM +10 mM glutamate + 1.2 M NaCl). Strains construction and all cultivations were performed in the laboratory of Prof. Erhard Bremer in Marburg.

promoter which was a combination of three different mutations (M4, M5 and M7).

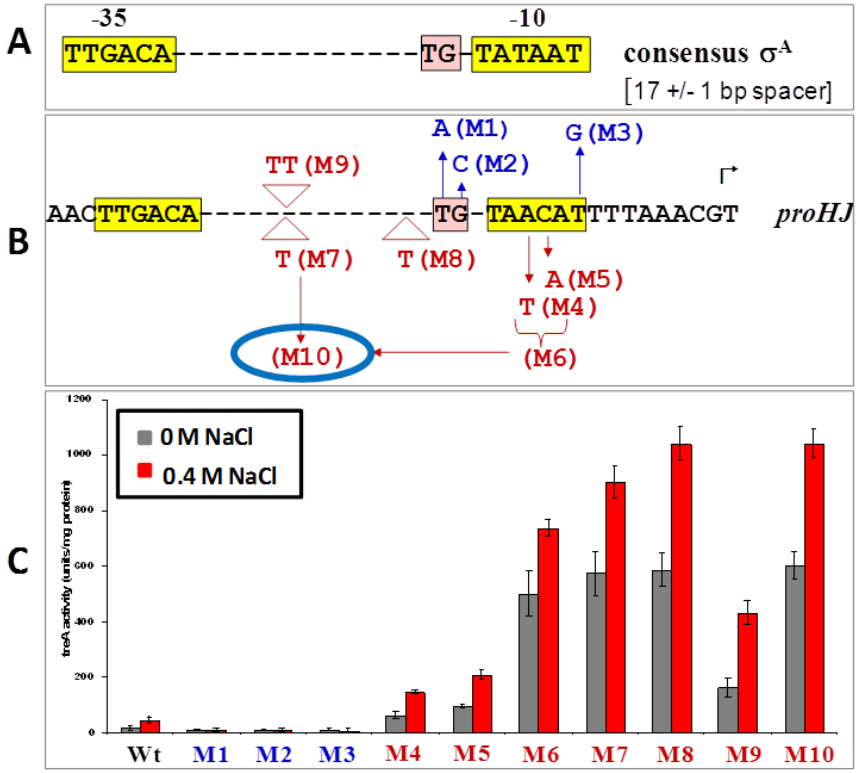

Figure 39 : Construction of the strain MDB28 for the overexpression of ProJ and ProH. A) Conventional SigA promoter. (B) Combination of several point mutations led to the final M10 (blue circle) mutant which was a combination of M6 and M7 mutations (C) TreA enzyme activity assays were performed for each of the tested mutant during normal growth and salt stress (0.4 M NaCl). The promoter with M10 mutation shows highest expression during normal growth and osmostress conditions (Experiments performed and data generated in the laboratory of Prof. Erhard Bremer in Marburg).

All samples mentioned above (Figure 38) were processed for MRM analysis of the central carbon metabolic enzymes and the proline biosynthetic enzymes. The results for the absolute protein abundance for ProJ and ProH proteins are shown in Figure 40. The amount of the proteins ProJ and ProH were at the same basal level in both wild type and *amyE* control strain. However, in strain MDB28 the basal level of none-stressed cells was strongly increased because of the M10 promoter mutation. During continuous growth at high salt, all strains exhibited an increase of ProJ and ProH compared to their basal levels. The uninduced levels of ProJ and ProH in MDB28 were equivalent to the induced levels of wild type and *amyE* control. Osmotically induced levels of ProJ and ProH in MDB28 were 5 - 6 fold higher compared to those of the control samples.

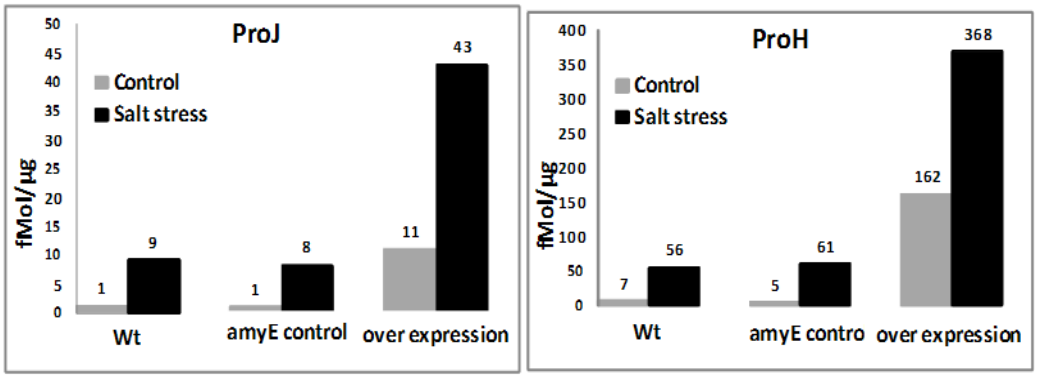

Figure 40 : Absolute protein concentration of the ProJ and ProH enzymes for wild type (JH642), *amyE* control (MDB22) and *proHJ* over expression mutant (MDB28) strains grown in SMM medium (control –in grey) and SMM + 1.2 M NaCl (salt stress –in black). Absolute concentration (fmol/ µg) of the proteins were obtained from MRM analysis.

A principal component analysis of the proteins of CCM and proline biosynthetic pathway of all the strains grown under various conditions is shown in Figure 41. The influence of both ProJ and ProH over expression and glutamate addition is represented in the PCA plot. A clustering of the samples corresponding rather to the cultivation conditions than the type of strain was observed. This dependency of the clustering on the cultivation conditions signifies the more prominent impact of the physiological variation rather than the strains genotype. Glutamate significantly affected the central carbon metabolism under both normal growth and osmostress.

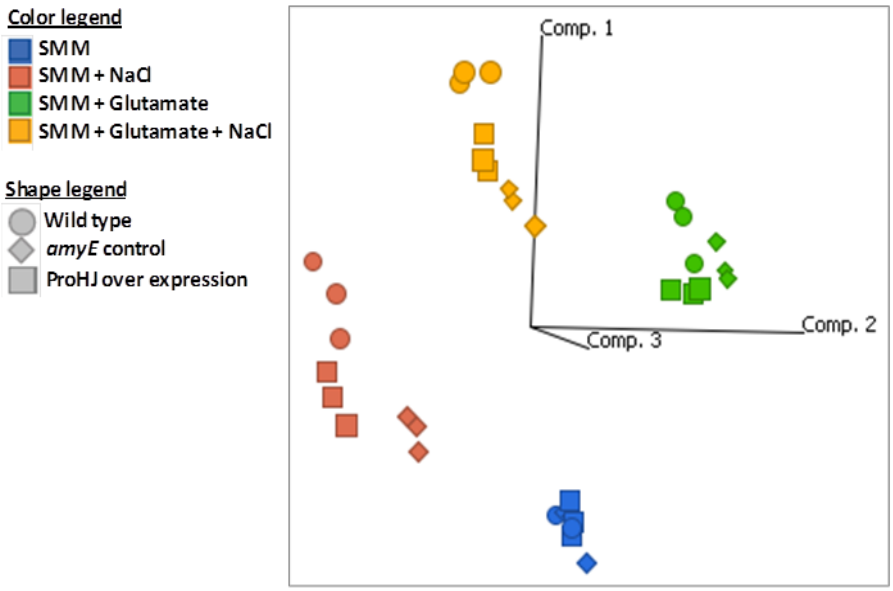

Figure 41 : Principal component analysis based on the protein abundances involved in the central carbon metabolism and proline biosynthesis for the wild type strain (JH642), the *amyE* control strain (MDB22) and *proHJ* over expressing mutant (MDB28) grown in four different conditions (SMM, SMM + 1.2 M NaCl, SMM + 10 mM glutamate and SMM +10 mM glutamate + 1.2 M NaCl). Absolute protein concentrations obtained from MRM analysis was used for the PCA plot.

Absolute amounts of the complete set of proline metabolic enzymes under the tested conditions are comparatively shown in Figure 42. Apart from MDB28, in the normal growing cells, ProA was the protein with highest abundance among all the proline metabolic enzymes. This once again suggests that uninduced levels of the ProA are in excess to the other proline biosynthetic enzymes. During growth at high salinity, unlike ProJ and ProH, ProA was not significantly induced even though it was required for proline biosynthesis. This was also supported by the transcription data displayed in Figure 43 (from a different sample with similar experimental setup – data obtained from the section 3 of the results).

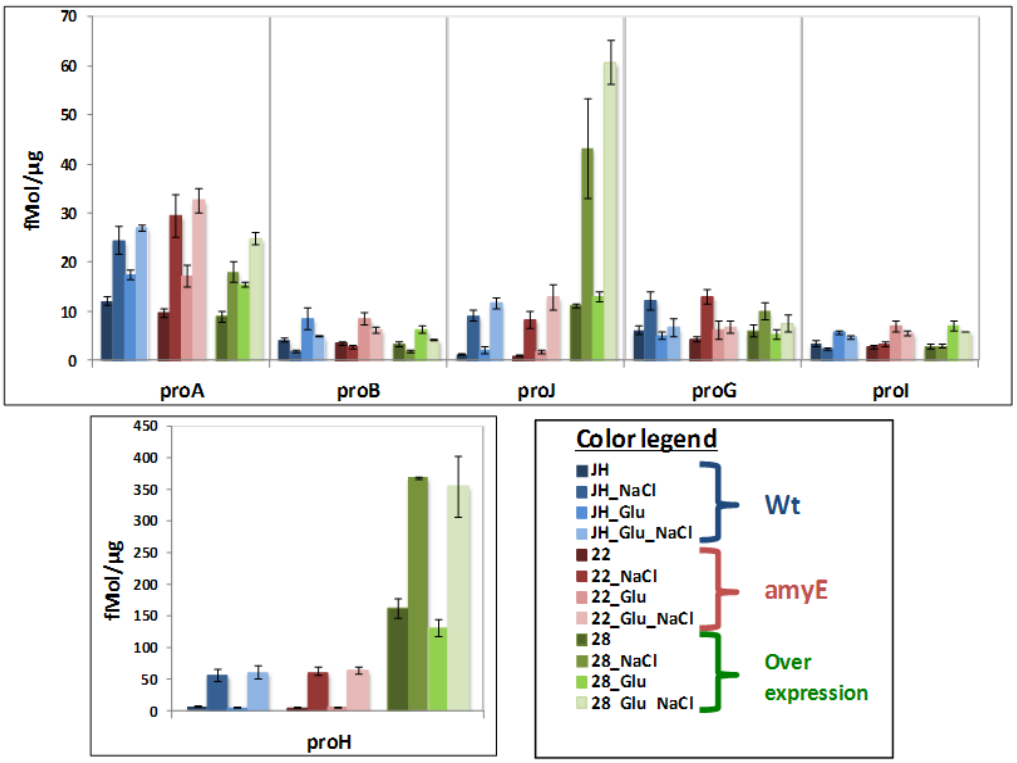

Figure 42 : Influence of ProHJ over expression and supplementation of glutamate on the level of the other proline biosynthetic enzymes during normal growth and salt stress. The strains used in the analysis were the JH642 (Wt- blue), MDB22 (*amyE* control -red) and MDB28 (*proHJ* overexpression - green). The concentration was reported in fmol/µg of protein extract. The standard deviation was calculated from the three biological replicates.

Though the *proA* gene was not osmotically regulated, its protein level increased during growth at high salinity in comparison to none-stressed control cells (Figure 42). Furthermore *proA* and *proB* are co-transcribed from a *sigA* promoter. But the protein of *proB* was down regulated during continuous growth at high salt in comparison to none-stressed control cells (Figure 42). This contrasting regulation of the proteins ProA and ProB translated from the same operon was also observed in the presence of glutamate only samples (SMM + 10 mM glutamate) and

osmostressed glutamate samples (SMM + 10 mM glutamate + 1.2 M NaCl). The transcriptional regulation of *proA* and *proB* under osmostress is represented in Figure 43. The contrasting regulation between transcription and translation might suggest an additional post-translational regulatory mechanism.

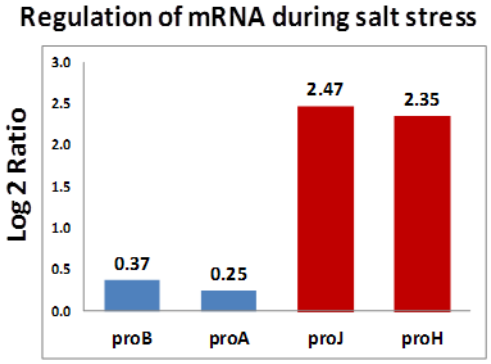

Figure 43 : Gene expression regulation of *proA*, *proB* *proJ* and *proH* genes during osmotic stress compared to the normal growth control (Log2 ratio of osmostressed *vs* control sample). The *B. subtilis* 168 Trp^+ was grown in SMM (control) and SMM with 1.2 M NaCl (salt stress). Data obtained from the tiling array analysis mentioned in the section 5.3.

5.4.6 The effect of glutamate supplementation on osmoadaptation of *B. subtilis*

Glutamate is the precursor for proline that is required in high amounts for osmoprotection. Along with glutamate, osmoprotectants like proline and glycine betaine were supplemented to the cells growing in SMM in the presence of 1.2 M NaCl. These experiments were performed to compare the osmoprotective effects of the glutamate, aspartate, proline and glycine betaine. These experiments were done in collaboration with the group of Erhard Bremer in Marburg and I contributed to this study with the proteome analyses described below.

Dolezeal *et al.* 2006 had shown that addition of glutamate and proline to the osmostressed *B. subtilis* had shown similar growth improvement capabilities (data from doctoral dissertation of Monika Dolezal, Marburg/Lahn, 2006). As the supplementation of the medium with glutamate and proline had similar effect on growth, it is important to explore if the supplementation with glutamate could affect the expression of enzymes that are involved in synthesis of proline. In this regard, addition of glutamate did not affect the levels of ProJ and ProH proteins neither during normal growth nor during osmostress. However, marginal effects of glutamate addition onto the proteins involved in the anabolic proline biosynthetic like ProA, ProB and ProI were noted (Figure 44).

Inclusion of extra glutamate in the medium could also significantly influence several proteins of central carbon metabolism. Strong effects of glutamate were observed for FbaA, PykA, PdhB and PdhD in glycolysis, which were up-regulated in the presence of glutamate during both normal growth and osmostress (Figure 44). In TCA cycle Cit B and FumC was strongly down regulated by the addition of glutamate. On the contrary the main enzyme responsible for the utilization of malate the malic enzyme (YtsJ) was strongly up-regulated in the presence of glutamate indicating a probable increase in the pyruvate concentration. The other observation during osmostress without glutamate was that the gluconeogenic protein PckA was up-regulated. Upregulation of PckA during osmostress was also observed in earlier experiments in SMM media in the presence of high glucose (refer section 5.4.3, Figure 31). Hence, expression of PckA amid the presence of high glucose concentration under osmostress was reproducible again in this experiment. However upon the supplementation of additional glutamate during osmostress PckA was not up-regulated. A significant decrease in CitZ enzyme was observed in the presence of glutamate indicating a probable rerouting of pyruvate to overflow metabolism to produce more amount of lactate or acetate.

In summary, excess glutamate besides triggering partial improvement of osmoprotection also affected the levels of several proteins in the central carbon metabolism.

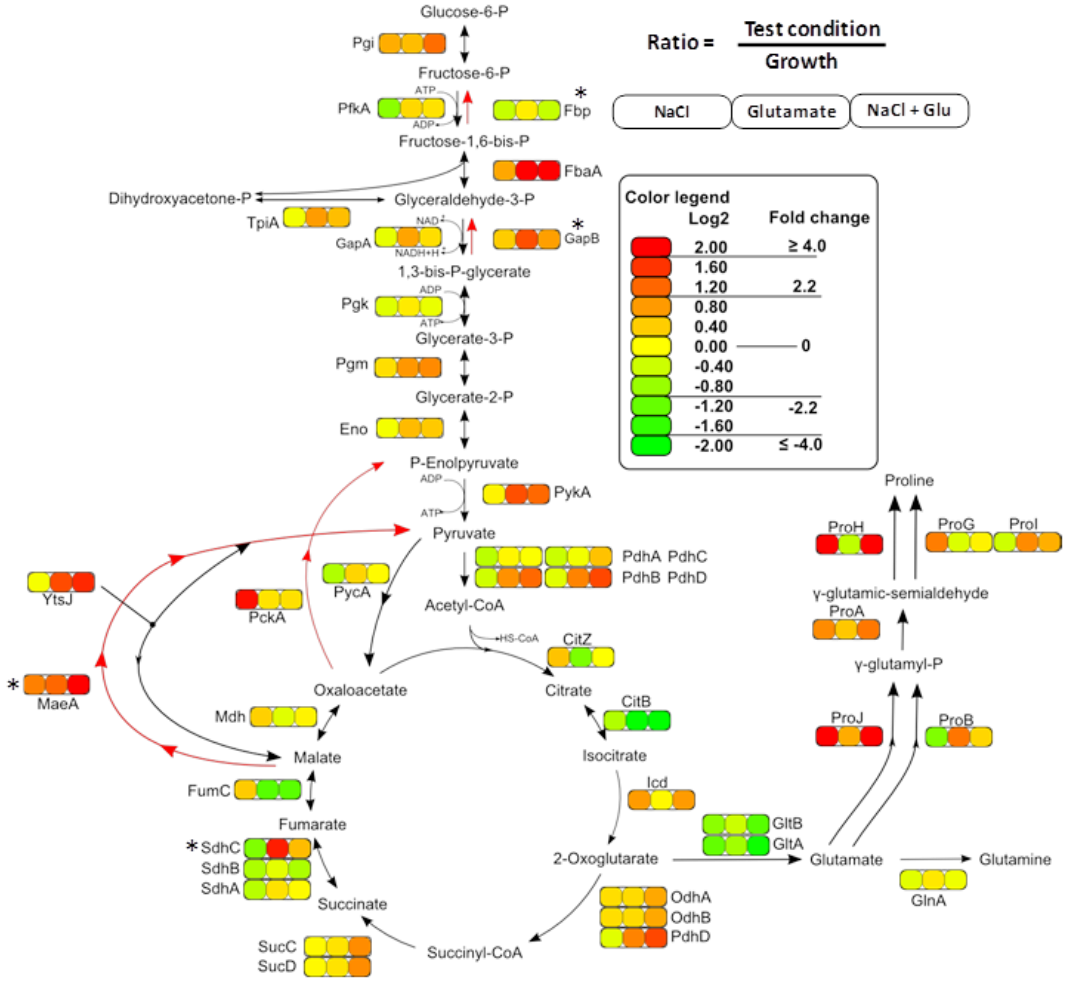

Figure 44 : Effect of supplementation of additional glutamate on proteins of central carbon metabolism during normal growth and osmostress. Samples for protein preparation for the MRM analysis were obtained from the *B. subtilis* wildtype strain JH642 grown in SMM (growth reference), SMM + 1.2 M NaCl (NaCl sample), SMM + 10 mM glutamate (glutamate sample) and SMM +10 mM glutamate + 1.2 M NaCl (NaCl+Glu sample). All samples were normalized to the growth reference (SMM) and Log 2 transformed. *- data not significant for very low abundant proteins.

6. DISCUSSION

In its natural habitat, the soil, *B. subtilis* encounters several different stress and starvation conditions [4]. These stresses could be due to abrupt environmental changes or due to prolonged environmental stress conditions. The ability of bacteria to survive under these conditions is governed by extremely complex and sophisticated regulatory mechanisms that in turn respond to several of the environmental cues consisting of a wide range of internal and external signals. Sporulation is a long and energy consuming process that confers a state of dormancy to *B. subtilis* and is the last resort available for *B. subtilis* if all the survival strategies fail [145]. Therefore, understanding the adaptational mechanisms that enable survival of *B. subtilis* is of great importance for understanding its physiology.

The most common forms of stress conditions encountered by *B. subtilis* in its habitat are energy limitation, temperature fluctuation and osmotic stress. In this study, a similar set of environmental challenges was addressed in a laboratory setup. In the past, several studies [2, 80, 81, 119, 149] have extensively characterized each of those conditions with limited data coverage of the different cellular components mediating adaptational responses (e.g.: transcriptomics, proteomics, metabolomics). These omics data sets help to understand the regulation at different regulatory layers during adaptational responses to environmental conditions [153] and are a prerequisite for valid systems biology studies. In the present work, multi-omics and systems-wide approaches were used to understand complex adaptational responses.

6.1 MULTI-OMICS PROFILING OF *B. SUBTILIS* DURING THE TRANSITION FROM GROWING TO NON-GROWING STATE

B. subtilis was investigated in a chemically defined medium under glucose limited and glucose depleted conditions. A non-sporulating *B. subtilis* strain with a mutation in the gene *spoIVCB* encoding the sigma factor K that is responsible for the formation of mature endospores [154] was used. The non-sporulating strain had to be used in this experiment in order to avoid the necessity of removing mature endospores from the fermentation apparatus.

An initial experiment of a tri-phase fed-batch fermentation was performed to understand the genome-wide transcriptional responses to glucose limitation, followed by glucose depletion (see section 5.2.1, Figure 10). The mean expression profiles of the major regulons controlled by alternative sigma factors were not immediately up or down regulated upon glucose limitation (see Figure 11) indicating that glucose limitation alone is not sufficient to significantly perturb the system. Presence of glucose in the medium leads to carbon catabolite repression (CCR) by CcpA which is dependent on presence of the protein HPr and glycolytic intermediates G6P and FBP (see introduction) [35, 58, 155]. Binding of the CcpA-Hpr complex to the *cre* sites on the DNA involves repression of genes involved in metabolism of various secondary carbon sources. Under conditions of glucose limitation a derepression of genes responsible for secondary carbon metabolism was observed. However, the derepression of CcpA regulated genes during glucose limitation was not as strong (mean fold change of 3) as when the cells experienced glucose starvation (mean fold change of 9). This fine tuning of the CcpA regulation with varying glucose concentration is accomplished by a mechanism in which the glycolytic intermediates G6P and FBP increase the affinity of HPr-Ser46-P towards CcpA and thus enhance binding of the complex to *cre* sites [156].

The expression of the general stress response regulon controlled by SigB was gradually up-regulated upon glucose limitation. Energy stress (low ATP level) is sensed by RsbP (PP2C serine phosphatase) which is then conveyed to the RsbV regulator of SigB [157] (Figure 45). Low ATP levels likely limit the kinase activity of RsbW for RsbV thereby allowing SigB to be free [5]. During glucose limitation the extent of ATP depletion was obviously not sufficient to significantly increase SigB activity. But also during glucose starvation the expected strong expression of SigB regulon was not observed, which could be due to ongoing sporulation due to prolonged glucose limitation.

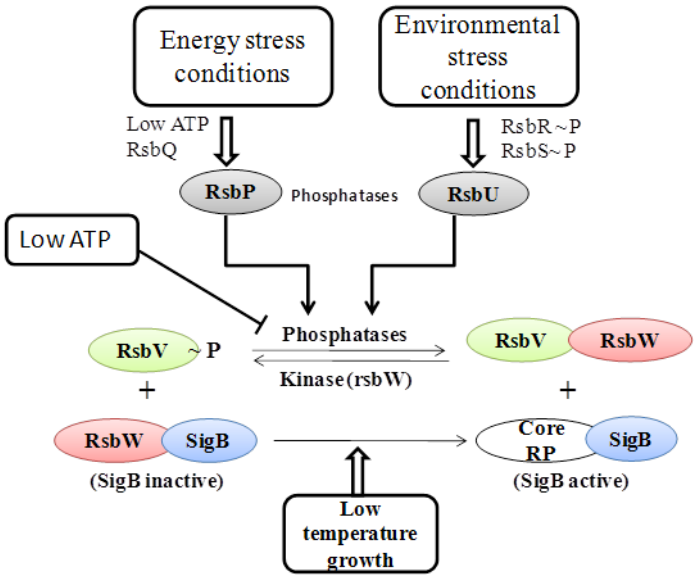

Figure 45: Regulation of the signal transduction pathway for the activation of SigB. Energy and environmental stress conditions affect SigB activity via the activation of the phosphatases RsbP and RsbU. The phosphatases then dephosphorylate RsbV, which leads to a partner switching of RsbW leaving SigB free to bind to the core RNA polymerase and thus transcribing SigB-dependent genes. [4, 5]. (Figure obtained from Hecker *et al.* 2007 [4]

Prolonged glucose limitation induced the sporulation response with the induction of the regulons SigE, SigF and SigG, consistent with the fact that both high cell density and energy starvation (glucose and amino acid limitation) are major stimuli for the initiation of sporulation [50, 145]. In the third phase of the fermentation upon entry into glucose starvation, the adaptational responses were overlapping and not separable from the ongoing sporulation response of the *sigK* mutant strain. Hence, a different experimental setup, a bi-phase batch fermentation was designed where the cells directly shifted from exponential growth to glucose starvation (section 5.2.2, Figure 12).

6.2 MULTI-OMICS ANALYSIS OF *B. SUBTILIS* CULTIVATED IN BI-PHASE BATCH FERMENTATION

In its habitat, while growing on various carbon sources, *B. subtilis* first utilizes the available glucose completely and if available malate is co-metabolized along with glucose [113]. While scavenging for alternative energy sources it concomitantly adapts to the starvation phase as long as possible and finally initiates sporulation. A previous study by Otto *et al.* (2010) [2] analyzed the transcriptome, metabolome and proteome of *B. subtilis* during exponential growth and stationary phase in shake flasks. Compared to the present study the samples were harvested at lower optical densities, due to growth in the shake flask, and the authors studied fewer (five) time points during the transition from exponential growth to stationary phase. A different study by Blom *et al.* 2011 was performed using a batch fermentation strategy, but rich medium (TY medium) to reflect regular laboratory conditions. The authors analyzed the transcriptome of *B. subtilis* in a time-resolved manner with 40 time points at 10 minutes intervals. The present study utilized a combination of chemically defined medium and high cell density batch fermentation with sampling time intervals of 30 to 60 min for a multi-omics characterization.

Unlike glucose limitation, the shift from exponential growth to strict glucose starvation was able to significantly influence the general stress regulon controlled by SigB and genes negatively controlled by CcpA. In the bi-phase fermentation both regulons showed a similar expression pattern but the SigB regulon was characterized by a more transient induction as expected. The main mechanism responsible for the transient response is the auto regulation of the *sigB* gene and the genes encoding the regulators RsbV, RsbW and RsbX, of which the anti-sigma factor RsbW exerts negative feedback regulation under most SigB activating conditions (Figure 46) [25].

Figure 46: Promoter organization of the genes involved in the regulation of SigB activity and auto regulation of the *sigB* gene. The genes for the protein that positively (*rsbV* and *sigB*) and negatively regulate (*rsbW* and *rsbX*) the SigB activity are under the control of SigB itself. (Figure obtained from Hecker *et al.* 2007 [4].

Transcriptional plasticity during various stress conditions in *B. subtilis* is primarily due to the functioning of various alternate sigma factors [116]. The SigD regulon responsible for flagella synthesis and chemotaxis was significantly and gradually down regulated with the decline of glucose availability. The regulon of the extra cytoplasmic sigma factor SigW which is responsible for protection against antimicrobial compounds and cell wall stress [26] did not show a strong regulation when glucose was exhausted. However, in the study of Blom *et al.* (2011) [149] the SigW regulon was highly induced when cells entered late stationary phase in a nutrient rich medium. Availability of different types of nutrients between the two studies and other fermentation parameters might be responsible for this difference in the expression pattern of the SigW regulon.

As part of the adaptational response, glucose exhaustion led to significant changes in the major metabolic pathways both in the search of new energy sources and optimal use of existing resources. This was evident from the changes observed in the expression pattern for several regulons which contain genes for major metabolic pathways (see Figure 15) (81 out of 172 regulons were regulated more than threefold at least at one time point). A strong down regulation of biosynthetic pathways like purine biosynthesis (PurR regulon) and pyrimidine biosynthesis (PyrR regulon) was observed upon glucose starvation as the cells stopped to proliferate, hence, the need for nucleotides was diminished. This regulation is mediated by the purine repressor PurR. PurR represses its target genes upon binding to the Pur Box sequence of the target genes [158]. This binding is inhibited by the presence of PRPP (5-phosphoribosyl1-pyrophosphate) a product obtained from ribose-5-phophate from HMP shunt pathway, which operates efficiently in the presence of glucose [159, 160]. On the other hand the PyrR regulates the genes involved in pyrimidine biosynthesis by binding to the anti-terminator region of the nascent mRNA in the operon and reducing the translation rate. This binding of PyrR is promoted by the presence of UMP/UDP/UTP [161, 162], which are in turn dependent on PRPP and ATP for their synthesis. Glucose starvation also led to amino acid starvation, which caused the stringent response via the ribosome associated protein RelA. RelA is also known to be involved in the activation of SigB during nutritional stress [163].

Glucose starved *B. subtilis* cells screen for the availability for new carbon source or other energy sources. This was apparent from the up regulation of several secondary carbon source-metabolizing genes during glucose starvation [50, 147]. This also includes amino acid and fatty

acid utilization genes in order to redirect the resources to pentose phosphate pathway via gluconeogenesis [148]. The pentose phosphate pathway provides the cell with NADPH and precursors for nucleotide biosynthesis in order to proliferate. All these pathways together play an instrumental role to regulate the cell proliferation before switching to sporulation response during famine.

Central carbon metabolism reacted swiftly to the glucose exhaustion as expected during glucose starvation. The upper part (glycolysis) and lower part (TCA cycle) of the central carbon metabolism showed two distinct patterns of regulation. Expression of the genes involved in the glycolysis was down regulated upon glucose exhaustion. This was partly achieved by the repressive effect of CggR on its own operon (*cggR-gapA-pgk-tpi-pgm-eno*), which hosts the major part of the glycolytic genes. CggR repression is antagonized in the presence of FBP, which is a product of glucose catabolism. On the other hand the TCA cycle was up-regulated after the glucose exhaustion. This is due to the two regulators CcpA (via carbon catabolite repression - CCR) and CcpC, which regulate *citZ, icd*, *mdh* and *citZ, citB* genes respectively. The activity of the regulators CcpA and CcpC is in turn dependent on the availability of the metabolites FBP and citrate which are the products of the glucose catabolism. Gluconeogenesis (*pckA* and *gapB*) was strongly up-regulated as soon as the glucose starvation began, as both genes are under control by CcpN, which actively senses the ATP and ADP levels. The dependency of these regulatory proteins (CcpA, CcpC, CcpN) on the intermediary metabolites is decisive for the regulation of the enzymes in the metabolic pathways. This is one of the main mechanisms that connect gene expression with environmental cues.

Overflow metabolism during excess glucose was observed in terms of pyruvate and acetate excretion into the medium and then re-utilizing both metabolites during the stationary phase. In the presence of excess glucose the depleted NAD^+ pools can be regenerated by the synthesis of lactate as a part of overflow metabolism. However, the measurement of extracellular lactate was not possible with the methods used in this study.

When comparing the changes observed in the proteome with the changes of the transcriptome analysis, a sudden decline in the mRNA of the glycolytic enzymes was observed at transcriptional level, owing to short half-life of mRNA. Whereas these proteins were only

gradually down regulated as the half-life of proteins is much longer compared to mRNA; some proteins have lifetime even longer than the life cycle of the growing cells [164]. However, the gluconeogenic proteins (GapB and PckA) were immediately up-regulated after glucose exhaustion due to the fact that transcription and translation are coupled in prokaryotes, leading to an immediate increase in protein abundance following the spontaneous increase of the mRNA.

It was shown by Taniguchi *et al.* (2010) that correlation between mRNA abundance and protein abundance is often subjected to stochastic regulation [150]. The authors showed that at multicellular level the mean correlation (regression coefficient - r) for the abundances of transcripts and proteins for several genes was $r = 0.77$. This correlation was obtained by using RNA-seq (for mRNA) and single molecule fluorescent microscopy (for protein) [6, 165]. Jong *et al.* (2012) showed in *B. subtilis* that at single cell level glucose starvation introduced large phenotypic heterogeneity across the culture leading to survival of only a sub population at the end. However, at single cell level in *E. coli* there was no correlation between the transcription and translation from the same gene [150]. This is due to the short half-life of mRNA and much longer half-life of the protein, as mRNA measurement only reflects recent (few minutes) history whereas protein measurement reflects history over a longer period of time. A similar correlation analysis between mRNA abundance and protein abundance was performed in the current study for the whole population. Relative mRNA abundances were obtained from the intensity values of tiling array experiments and compared to the absolute protein abundance obtained from the MRM analysis. The correlation *r* between mRNA abundance and protein abundance was 0.66 in an exponentially growing sample. The data obtained using the current methods reflect a mixture of cells and do not consider population heterogeneity effects as discussed above. However during the stationary phase the correlation coefficient of 0.52 was observed. In stationary phase it is expected that most of the mRNA associated to glycolysis are down regulated and the existing mRNA are immediately degraded, but in the case of proteins, though the translation is reduced, the existing proteins are not degraded immediately. Hence it is expected to have a mismatch between abundances of mRNA and proteins. On the contrary mRNA and proteins involved in TCA cycle start to increase in abundance in stationary phase, which shows an opposite regulatory pattern in comparison to glycolysis. Therefore the correlation coefficient as anticipated in stationary phase did not dramatically decrease in comparison to the exponentially growing cells. Absolute protein quantification calculated by MRM has a limitation; this method cannot be used to directly measure stochastic regulation. Nevertheless, a virtual stochastic simulation [166, 167] can be performed using the MRM data sets and microarray data sets to

understand the stochastic regulation. In a similar approach using MRM data Maeir *et al.* (2011) [166] had shown that in *M. pneumoniae* post-transcriptional regulatory mechanisms, in particular translation efficiency, rather than post-translational (protein turn-over) mechanisms predominantly contribute to protein abundances which are largely decoupled from overall mRNA abundances.

To conclude, an extensive time course investigation of high cell density fermentation was performed. The differences between prolonged glucose limitation and prolonged glucose starvation responses were investigated at transcriptome level. Central carbon metabolism pathway based multi-omics experiments were performed and the data were successfully integrated. A correlation analysis of relative transcript abundance and absolute protein abundance was performed. The correlation analysis gave an approximate estimate which was on par with much complex methodologies reported earlier.

6.3 WHOLE-TRANSCRIPTOME ANALYSIS OF *B. SUBTILIS* AT HIGH TEMPERATURE, LOW TEMPERATURE, HIGH SALT AND DURING GLUCOSE STARVATION

Analyses of the transcriptional changes associated with various stress conditions that are commonly encountered by *B. subtilis* help us to understand the adaptational responses necessary for its survival. In this study the main environmental stress conditions that are encountered by *B. subtilis* in its habitat were investigated: growth at high or low temperature, high osmolarity, and glucose limitation. Several studies in the past had reported transcriptional and proteomics changes associated with these stress conditions individually [2, 37, 50, 81, 93, 147, 148, 168]. In this thesis, as part of a structural re-annotation study of the transcriptome of *B. subtilis*, the transcriptome wide adaptational responses for the above mentioned stress conditions was investigated in detail with strand-specific tiling-arrays. The study, published by Nicolas *et al.* (2012) [116], was performed in two large consortia where the samples from the bi-phase batch fermentation (section 5.2.2) and the samples discussed here were part of 104 different conditions investigated. Altogether, 1583 new RNA features were reported and 2935 promoters were classified to the various sigma factors. These sigma factors accounted for 66 % of the variance in transcriptional activity. In the scope of the current thesis the physiological adaptation responses among the conditions mentioned above were analyzed.

Among the conditions tested in this study, glucose starvation influenced the largest number of genes. The magnitude of changes imposed are in the following decreasing order: 1) glucose starvation, 2) growth at 16°C, 3) growth at 51°C and 4) growth at 1.2 M NaCl. The physiological changes imposed by glucose starvation could be distinguished into two different categories: nutrient exploitation and the effects resulting from slow or no growth. In other stress conditions, the cells were analyzed during exponential growth in the presence of high glucose and varying growth rates due to the physiological stresses imposed.

Every different environmental stress demands a specific adaptational response from *B. subtilis*; this was evident from the distinct number of genes regulated and with minimal overlap of genes regulated in each of the stress conditions (Figure 47). Only 8 genes were commonly regulated among all four stress conditions tested.

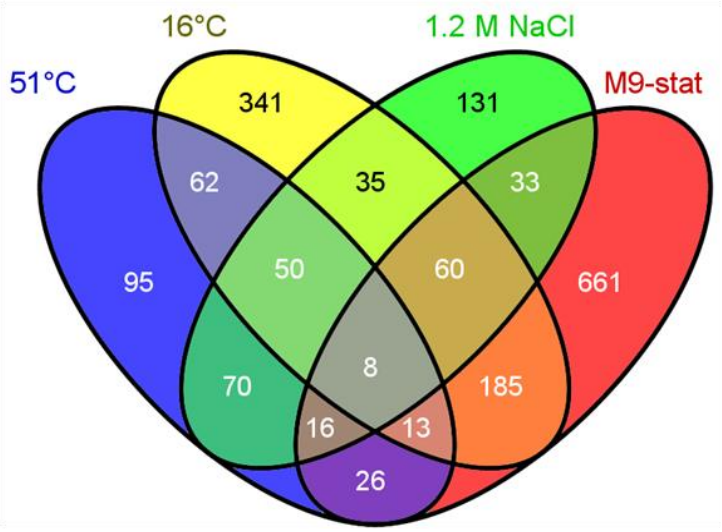

Figure 47: Venn diagram representing the overlap of the significantly regulated genes during growth at high temperature (51°C) vs SMM, low temperature (16°C) vs SMM, high salinity (1.2M NaCl) vs SMM, glucose starvation (M9-stat) vs exponentially growing in M9 media (fold change cut-off of three, p-valve 0.01 Welch t-test). List of the significantly regulated genes enclosed in supplementary table S2.

The genes involved in chemotaxis and motility were down regulated in all the stress conditions tested in this study suggesting that cells cease active swimming during prolonged stress conditions. Reduced expression of genes involved in chemotaxis was also reported earlier during sudden osmotic upshift (sudden osmotic shock) [81] and continuous growth at high salt (adaptation) [80] or growth at low temperature [118]. Of the proteins classified as heat shock proteins, the majority of which are molecular chaperones, the major heat shock proteins (GroEL, GroES, DnaK and GrpE controlled by the HrcA repressor), ClpC and HtpG were up-regulated more than two fold in cells grown at high temperature (51°C). These chaperones prevent proteins from misfolding and promote the refolding during growth at high temperature [169].

Sporulation was induced during glucose starvation [50] and growth at low temperature [118] making these stress conditions more demanding with respect to the number of genes required for adaptation than the heat and salt stresses. Sporulation-specific responses at low temperature involved the up regulation of genes that are associated to the SigF, SigE and SigG regulons [118, 170]. General stress response proteins controlled by SigB were up-regulated during starvation (as discussed earlier) [50, 171], at high temperature [70, 171], continuous growth at high salt [80, 171] and growth at low temperature [118]. Koburger *et al*. 2005 [147] had reported that SigB mediated general stress response as one of the major class of genes to be upregulated upon glucose starvation, the other major class being the genes under the control of stringent response which were down regulated upon glucose starvation. The SigB mediated stress response is also crucial for *B. subtilis* to survive in other conditions such as ethanol stress (9%), acid stress (pH

4.3) and desiccation as indicated by Völker *et al.* (1999) [171]. Other conditions that induce the SigB regulon include growth on plates, growth with glycerol as carbon source, biofilm formation, phosphate starvation, oxidative stress, and oxygen limitation [116, 172]. Several genes of the SigB regulon are also under the control of one or more other transcriptional regulators leading to an overlap between regulons within the transcriptional regulatory network. Nannapaneni *et al.* (2012) [172] performed a targeted microarray analysis examining 350 genes and defined the SigB regulon to contain 203 genes out of which 37 genes are also regulated by other regulators. Nannepaneni *et al.* have performed the study based on three previous [173-175] studies that described the SigB regulon. Based on the tiling array data, Nicolas *et al.* (2012) [116] classified 287 annotated genes and 133 previously un-annotated RNA features to be members of the SigB regulon. Of the 287 annotated genes, 214 were assigned to regulation by more than one sigma factor. This classification was performed based on the DNA sequences near the transcription start sites as well as the condition-dependent promoter activities as inferred from the expression levels downstream of the transcription start sites. Among the two latest studies that described the SigB regulon, the later study by Nicolas *et al.* is unbiased as the complete genome of *B. subtilis* was examined by microarray hybridizations, whereas the former study (Nannapaneni *et al*.) was based on annotated genes and in particular analyzed 350 genes previously reported to be controlled by SigB. To summarize, the ability of SigB to connect different regulons and indirectly co-ordinate various adaptational responses results in a higher order SigB modulon [4].

Major expression changes of genes involved in metabolism were observed in glucose starved *B. subtilis* cells. Glucose being the primary carbon and energy source for *B. subtilis*, glucose deprivation drives major alterations in the metabolic pathways. These changes include up regulation of the genes involved in exploring alternate energy sources and utilization of existing resources. The other metabolic responses correspond to growth rate effects where biosynthesis of various compounds was down regulated in glucose starved *B. subtilis*. The other stress conditions investigated in this study when compared to glucose starvation did not trigger the same magnitude of changes in genes associated to cellular metabolism. *B. subtilis* grown at high salt suffers from iron limitation thus inducing genes involved in iron metabolism [80, 151]. Several members of the Fur regulon which were associated to iron acquisition such as the genes involved in biosynthesis of the siderophore bacillibactin and other iron uptake systems were up-regulated [176]. As excess intracellular concentration of iron is deleterious to cellular physiology as it forms toxic hydroxyl radicals [177], iron homeostasis is achieved by the activity of the Fur repressor in the presence of excess iron and the release of the repressor causes the derepression

of the genes involved in iron acquisition and uptake during iron limitation [178]. Two previous studies analyzed the effect of high salinity on iron limitation in *B. subtilis* (Steil *et al.* 2003 [80] and Hoffmann *et al.* 2002 [151]) but used a different strain (JH642) [179] containing a mutation (sfp^0) which prevents or strongly reduces the phosphopantetheinylation of DhbB and DhbF leading to highly reduced production of bacillibactin. The bacillibactin precursor 2,3-dihydroxybenzoate is a much less efficient iron scavenging compound, making this strain susceptible for iron limitation [176]. In the present study the *B. subtilis* strain 168 Trp^+ was used which is a Sfp^+ strain. However, even in the presence of a proper siderophore synthesis apparatus producing normal amounts of bacillibactin, a strong iron limitation could be observed under high salt conditions. Hoffmann *et al*. (2002) analyzed the DHB production in strains with sfp^+ (KE10) and sfp^- (JH642) at 0.7 M NaCl; unlike JH642, in the KE10 strain DHB production was not increased during high salinity indicating no iron limitation in the cells containing sfp^+. In contrast to the previous finding, in the present study using 1.2 M NaCl the genes of the *dhb* operon (Figure 48) were strongly up-regulated during continuous growth at high salt, indicating that the cells indeed experienced iron limitation at high salinity. This may indicate that at higher osmolarity - 1.2 M NaCl –in this study, compared to 0.7 M NaCl used in the previous study, even *B. subtilis* cells containing the sfp^+ gene experience iron limitation. Interestingly, in case of the halophilic bacterium *Chromohalobacter salexigens*, the requirement for iron is reduced at high salt, and the Fur regulator was shown to mediate iron homeostasis at high salinity [180]. Thus, the regulatory connection between iron homeostasis and high osmolarity might depend on the type of bacteria and their corresponding habitats, linked with distinct adaptational strategies to cope with changing osmotic conditions.

6.4 MULTI-OMICS STUDY OF OSMOSTRESSED AND OSMOPROTECTED

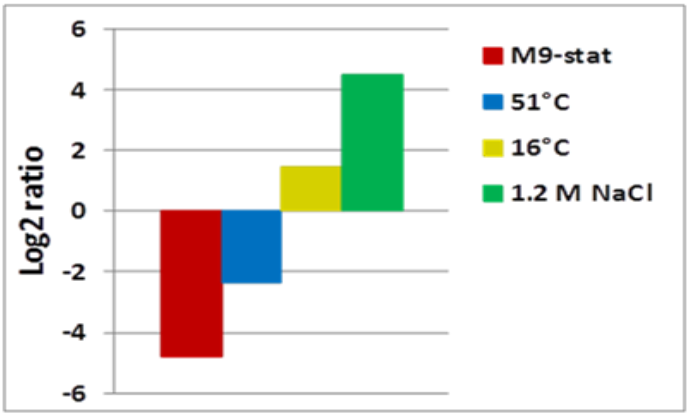

Figure 48: Average Log2 ratio (compared to the growth controls) of the expression of the *dhb* operon controlled by the iron sensing regulator Fur. The Log2 ratios were obtained by comparing high temperature (51°C) vs SMM, low temperature (16°C) vs SMM, high salinity (1.2M NaCl) vs SMM, glucose starvation (M9-stat) vs exponentially growing in M9 media stress conditions. Data obtained from the tiling array analysis mentioned in the section 4.3.

B. SUBTILIS IN GLUCOSE LIMITING CONDITIONS

In its natural environmental niche, *B. subtilis* often encounters multiple stress conditions that include nutrient starvation or limitation, temperature fluctuation, flooding or desiccation. In this study a combination of nutrient limitation and desiccation that are comparable to glucose limitation and growth at high salinity were simulated in chemostat cultivations. The usage of chemostats ensured a constant growth rate at any given condition by altering (via dilution) the concentration of the growth limiting factor (e.g. glucose) [181]. In addition to glucose limitation (μ_{max}=0.1) and glucose limitation with 1.2 M NaCl, a third condition combining glucose limitation and osmoprotection (1.2 M NaCl + 1 mM glycine betaine) was investigated in a multi-omics approach. In the past, several studies had reported the flux data through central carbon metabolism (CCM) in *B. subtilis* cultivated in chemostat [182-185]. In the current study, for the first time, a multi-omics approach was implemented to analyze the molecules (mRNAs, proteins and metabolites) involved in the central carbon metabolism. As a part of the multi-omics analysis, a complete transcriptome analysis was also performed to understand the overall physiology under the tested conditions.

Several earlier studies addressed changes in gene expression associated with growth at high salinity in *B. subtilis* [80, 81, 151, 186], but had to cope with varying growth rates because the experiments had been performed using shake flask cultures. In the current study chemostat cultivations were performed at a unified growth rate, so the changes observed were arguably associated to the exclusive stress conditions imposed. This in combination with multi-omics investigation gave a comprehensive understanding of the adaptational responses in *B. subtilis*.

Major changes associated with growth at high salinity were discussed in the section 6.3; like induction of the genes in the general stress response (SigB regulon), induction of genes associated to iron metabolism, suppression of sporulation etc.. High osmotic strength in the medium prevented sporulation likely via multiple ways; e.g. by reduced expression and phosphorylation of Spo0A, reduced or no synthesis of SigE and SigF [187]. Changes in membrane composition (increased fluidity with saturated straight chain fatty acids) in hypertonic medium [133] that could inhibit KinA (two-component sensor kinase requires for sporulation initiation) leading to lowered Spo0A-P thereby impeding sporulation. Changes in phospholipid composition cold also effect the correct folding of membrane proteins (e.g. SpoIIGA, FtsH, etc.) that process the pro-sigma factors (SigE and SigF) required for sporulation [187]. In conclusion, regardless of presence or absence of osmoprotectant like glycine betaine in high osmolarity

medium, expression of sporulation genes was dramatically reduced compared to the control sample.

Down regulation of genes involved in chemotaxis during glucose starvation (section 6.2) and during multiple stress conditions including continuous growth at high salt (section 6.3) were discussed earlier. In the particular experiment discussed here *B. subtilis* was exposed to a combination of both glucose limitation and high salt, which resulted in down regulation of majority of the genes involved in chemotaxis. However, we cannot distinguish to which both entities contributed to the total reduction of genes involved in chemotaxis. Furthermore, expression of chemotaxis genes was restored in the presence of glycine betaine.

Genes responsible for utilization of alternate carbon sources are usually up-regulated under glucose starvation or limitation. In the current study, there was a strong down regulation of the genes associated to the utilization of alternate carbon sources during continuous growth at high salt in comparison to the reference and osmoprotection conditions. This might reflect the fact that under all conditions cells were already experiencing glucose/ energy limitation and thus the extra strain for producing more proline and the respective enzymes, this required further down-regulation of other genes. However, there was no indication of starvation from the adenylate energy charge (AEC) of the cell (Table 3, measurements performed by Hanna Meyer, Greifswald) during growth at high salinity. This might indicate that the *B. subtilis* prioritizes the protection from high salinity rather than seeking for an alternative carbon source during simultaneous glucose limitation and high salt adaptation growth. Producing large amounts of proline consequently from the utilization of limited available glucose fulfilled this priority. Surprisingly for unknown reasons during osmoprotection the ATP level was approximately three folds less compared to the reference and salt stress conditions.

Table 3: Intracellular levels of adenylates and adenylate energy charge (AEC) for non-stressed, salt-stressed and osmoprotected *B. subtilis*. (Measurements performed by Hanna Meyer, Greifswald)

	Unit	Reference*	Salt stress*	Osmoprotection*
AMP	mmol g_{DCW}^{-1}	1.86 ± 0.49	1.53 ± 1.42	1.85 ± 0.64
ADP	mmol g_{DCW}^{-1}	4.08 ± 0.62	5.79 ± 3.25	3.18 ± 0.51
ATP	mmol g_{DCW}^{-1}	19.20 + 2.29	17.40 ± 6.77	6.67 ± 0.85
AEC	-	0.84 ± 0.03	0.83 ± 0.04	0.71 ± 0.06

*Values refer to standard deviations from three biological replicates chemostat experiments

6.4.1 Multi-omics investigation of central carbon metabolism

Both glucose limitation and growth at high salt are interconnected as the osmoprotectant proline is synthesized from glucose. To this regard, comprehensive understanding of the central carbon metabolism and biosynthesis of proline is important. Comprehensive understanding of a pathway is possible when all the molecules associated to the pathway were measured, so in the current study a multi-omics investigation was performed and this provided unique insights into the adaptational response at a systems level.

The key prerequisite for the growth at high salt was to amass high amount of intracellular proline which was achieved by the strong up-regulation of both *proHJ* transcription and ProHJ protein levels more than fivefold (see Figure 24) [68, 78]. Though both the enzymes were transcribed from the same promoter controlled by SigA and mRNA levels should thus be equal, but the abundances of proteins were quite different with ProH being three fold higher in abundance compared to ProJ. This apparent difference could arise from the position of ProJ being at the distal end of the operon or due to translation or stability of the proteins. The main outcome from the stoichiometry measurement of the proteins was that ProA present in excess in any given condition over the rest of the proline biosynthetic enzymes (Figure 28). This observation solves the riddle how *B. subtilis* can satisfy its need for ProA during high salt growth even if its gene is not subject to osmotic regulation in contrast to those of encoding ProH and ProJ. High abundance of ProA complies with the demands of the anabolic proline biosynthesis and the high amounts of proline required for osmoprotection. It is clear from the data that key enzymes show a high abundance within their specific pathway. This could be shown for ProA, which is required for the anabolic and osmotically induced proline biosynthesis in *B. subtilis*, and was always present in higher abundance compared to the rest of the proline biosynthetic enzymes. This strategy might give an added advantage to *B. subtilis* to adapt quickly to sudden osmotic up shift in the environment.

In the presence of the both osmoprotectant glycine betaine and 1.2 M NaCl the proline levels were close to those in control cells in the absence of high salt. Moreover mRNA levels of *proJ* and *proH* were also low as in control cells, but protein levels remained well above those observed in non-stressed control cells. Moreover in the presence of glycine betaine, ProA was

present in significantly higher amounts (three fold) although its expression is not osmotically regulated. This discrepancy of mRNA and proline pools at the one side and protein levels on the other side could be explained by the ability of GB to stabilize proteins that were produced basal level expression of the the *proHJ* operon by the major sigma factor SigA [9]. However, the low levels of proline observed in the presence of large amounts of ProH and ProJ would also imply an impact of GB on activity of both proteins. A potential effect of GB on protein stabilization was discussed in detail in section 6.4.2. Though regulation of activity of ProJ and ProH has not been explored in detail in *B. subtilis* yet, presence of protein and absence of proline suggests a possibility for activity regulation.

It was shown that the intracellular concentration of proline can reach 400mM [188] during growth at 1 M NaCl and this amount is even higher during sudden osmotic up shift to 0.4 M NaCl [76]. Amassing high amount of intracellular proline also creates a concentration gradient which facilitates the leakage of proline to extracellular environment which is also observed in *E. coli* [189]. Proline leakage has also been shown to occur in *B. subtilis* and the excreted proline is sequestered mainly by the OpuE transporter to ensure effective osmoprotection [72, 188]. In the current study, OpuE was also strongly up-regulated at high salinity to sequester extracellular proline. The process of proline leakage and the re-import via the OpuE transporter might also offer fine-tuning the intracellular turgor pressure for *B. subtilis* at high salinity [188]. *B. subtilis* can also take up proline and use it as a nutrient, which is then catabolized to glutamate by the PutBCP proteins with PutP constituting the second importer of the extracellular proline besides OpuE. In the presence of external proline, PutR promotes the expression of the *putBCP* gene cluster [8]. The *putBCP* gene cluster is repressed in the presence of other amino acids by CodY (by replacing PutR) which is in turn dependent on the metabolite GTP [190]. In the current study, simultaneous glucose limitation and growth at high salinity induced the expression of the *putBCP* genes to tenfold or higher to intermediate levels. However, this is in contrast to Moses *et al.* 2012 [83] who described for shake flask cultures that the high amount proline produced as an osmoprotectant at high salinity did not induce the *putBCP* gene cluster since such a induction would be futile. This apparent difference could be the result by the very low amounts of intracellular GTP (measurements performed by Hanna Meyer, Greifswald) levels during high salinity in chemostat cultures (Figure 49) that could lead to release of CodY from the *putBCP* gene cluster and thereby causing the derepression and intermediate expression of the *putBCP* operon; on the other hand excess extracellular proline present due to leakage might also contribute to the PutR mediated intermediate expression of the *putBCP* gene cluster. To

conclude, the co-occurrence of low GTP amount and high intracellular proline levels might facilitate the intermediary activation of the proline catabolic pathway.

In the presence of glycine betaine (GB), the gene cluster *putBCP* was strongly down regulated (see Figure 24) compared to the growth at high salinity. This could be explained by the greatly reduced intracellular proline levels in the presence of glycine betaine, which would diminish leakage thereby preventing activation of the PutR protein. During osmoprotection, enhanced repression by CodY was unlikely because the amount of GTP decreased even further in the presence of GB.

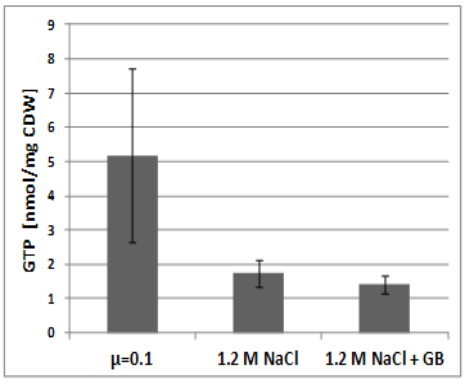

Figure 49: GTP concentration obtained from LC-MS measurements of the intracellular metabolome analysis form the samples involved in the current study. GTP concentrations were significantly reduced in the presence of high salt (1.2 M NaCl) and during osmoprotection (1.2 M NaCl + GB). (Measurements performed by Hanna Meyer, Greifswald)

Regardless of the condition analyzed in this study; the reference, growth at high salinity and during the osmoprotection: the flux through central skeleton of CCM was relatively stable (see Figure 26). But the mRNA and proteins that are involved in CCM differed strongly between these conditions. This implies that molecules necessary to run the system itself were dynamically regulated to maintain a homeostatic flux under the conditions tested.

With few exceptions, both transcriptome and proteome were in good agreement across the conditions tested. The majority of the glycolytic enzymes showed a slight increase in the abundance during growth at high salt compared to the reference sample (see Figure 24). This observation was also made partially in the TCA cycle for the components of the CitB, Icd and Odh complex. All these changes likely occur to provide enough 2-oxogluterate to produce high amounts of proline to provide osmoprotection to the cell. However, the slight increase in the enzyme abundance in the CCM did not result in increase in the flux of CCM during growth at

high salt. All these changes occur amid maintaining a constant flux through the CCM in the presence of high salt (see fig Figure 26). The advantage of higher abundance of enzymes during high salt was compensated by the loss in enzyme activity (see Figure 27) of the enzymes due to high K^+ intracellular concentration [76] at high salinity. This hypothesis was tested on two key enzymes of the CCM such as Pgi, Icd, Pyk (data not shown) and Mdh (data not shown), where both the enzymes exhibited 56% (for Pgi) and 41% (for Icd) loss of enzyme activity at 600 mM K+ ion concentration. Out of these enzymes, Pgi and Icd were proven to be required for altered flux rerouting [191] providing an alternate path for carbon flux in various conditions. The increase in protein abundance to compensate the loss of enzyme activity could be an adaptational strategy to achieve a constant flux adopted by *B. subtilis* when there is a combination of glucose limitation and high salinity. However it is not clear how this flux balancing is achieved, it could be due to the dependency of the pleiotropic regulators (CcpA, CodY etc.,) on the intracellular metabolites (ATP, GTP, FBP etc) to regulate their target genes. Key metabolites for global control of metabolism such as ATP, GTP and fructose-1,6-bisphosphate (F1,6BP) were strongly decreased in the presence of salt stress. This suggested that metabolic control is crucial to maintain steady state of flux.

Concurrent presence of proline with elevated K+ concentration was not able to restore the loss in enzyme activity. However, 650 mM of glycine betaine was able to restore the enzyme activity partially. This advantage of glycine betaine over proline might be the reason behind the better osmoprotection offered by glycine betaine. Addition of glycine betaine prevented the accumulation of proline as an osmoprotectant, as accumulation of *de novo* synthesized substrates (like proline [76, 192]) are slow due to transcription and translation of the components involved and more cost intensive than uptake of a substrate present in the environment. Thus, the naturally available osmoprotectants like glycine betaine are readily taken up by existing or newly synthesized transporters [193].

Though glycine betaine is metabolically inert in *B. subtilis*, it could affect several proteins in central carbon metabolism. Interestingly, most of the significantly affected proteins in the presence of GB were known to form complexes. In this case the metabolon (CitZ-Icd-Mdh-PckA-YtsJ) formed within the TCA cycle [59] were present in higher abundance which were in non-correlation with their respective gene expression. This was also observed in the SdhABC complex as well. Pertaining to the idea of protein complex stabilization in the presence of GB, it is worth discussing about a probable protein complex between ProJ, ProA and ProH; a similar pattern was observed for these proteins as well, where the mRNA levels remain unchanged but

the protein levels were up-regulated. Moreover the intermediates produced by the pathway are known to be lethal to the cellular metabolism in *B. subtilis* [78] and other organisms[194, 195]; unless these intermediates are channeled with in a complex, the cellular physiology might not endure the high amount of proline generated as an osmoprotectant. A further investigation involving the co-purification of these proteins is necessary to prove the existence of this potential complex.

In *E. coli*, increase in osmolality causes the loss of intracellular water thereby decreasing the space between the biomolecules, this leads to crowding and increase in biomolecular (proteins and nucleic acid) concentration *in vivo* [196]. Testing such a hypothesis *in vitro* also resulted in crowding of biomolecules which subsequently reduced the biomolecular diffusion rates and had thermodynamically driven biomolecular assembly and aggregation [197, 198]. In the overcrowded circumstances *in vivo* proline is more effective than GB in preventing aggregations [199, 200] probably due to the ability of proline to interact with proteins [199] whereas GB cannot interact with proteins as it is devoid of hydrogen bond donor [201]. Due to the overcrowding at high osmolality in conjunction with inability of GB to interact with proteins, protein aggregation (via preferential interactions) might be favored. These physiochemical properties of GB could be the major reason behind the novel changes including the increased protein content and the protein complex stabilization phenomenon.

To conclude, protein stoichiometry measurements in conjunction with other omics technologies provided unique and unbiased insights into the regulatory mechanisms adopted by *B. subtilis* under varying growth conditions. Though glycine betaine provided osmoprotection, the molecular phenotype of these osmoprotected cells differed from that of the reference condition and the growth at high salinity. These observations raised further questions about the physiological changes induced by glycine betaine apart from being an osmoprotectant.

6.4.2 Effect of glycine betaine during exponential growth and osmoprotection

To understand the effect of the GB on a global proteome scale and its impact on the protein stoichiometry (possible aggregations), shake flask experiments were performed in SMM media where glucose was present in excess. Unlike the chemostat experiments, in shake flask experiments the growth rates were variable and dependent on the media composition. Several earlier studies addressed the biophysical characteristics of proline [202] and GB *in vivo* and *in vitro* and their impact on biomolecular interactions [196] and protein stabilization [199, 200, 203]. Extending these findings, in the current study effects of GB during normal growth and as an osmoprotectant and proline at high salinity were investigated to decipher the role of GB and proline on the cellular physiology at the protein level.

Significant differences in the growth rate were observed in all the conditions tested (see Figure 29). The growth rates were in the decreasing order of SMM + GB > SMM > SMM + 1 mM GB + 1.2 M NaCl > SMM + 1.2 M NaCl. Though GB itself is metabolically inert in *B. subtilis*, the difference in the growth rate in the presence GB over the *de novo* synthesized proline could be mainly explained by the biophysical characteristic of GB. In *E. coli*, accumulation of osmoprotectants like GB or proline extends the growth rate of the osmotically stressed cells by fundamentally altering the cellular water distribution via the free cytoplasmic water (unbound water to macromolecules) and the water bound to the macromolecules [196, 204, 205]. Higher amounts of free cytoplasmic water promote higher growth rate and vice versa as observed in yeast [206] and *E. coli* [196]. Glycine betaine can be accumulated up to intracellular concentrations of ≥500 mM by *B. subtilis* during high salinity [70, 76]. Osmoprotectants like GB are known to increase free cytoplasmic water more than other osmolytes at similar concentrations [196]. This specific effect of GB is achieved by its ability to remain in the free cytoplasmic water as it cannot bind to the macromolecules [201] thereby increasing osmolality of the free cytoplasmic water and offering better osmoprotection compared to other osmolytes like proline or trehalose.

Pertaining to the differences in the growth rate, significant changes in the global proteome were observed (see fig Figure 30). Most of the observed changes correlate to the improved growth rate in the presence of GB; the changes include up regulation of proteins involved in translation, biosynthesis and acquisition of nucleic acids and amino acids. The changes that are not directly correlated to the growth rate affect proteins of the SigB regulon. In the presence of GB during

normal growth or at high salinity, a down regulation of members of SigB regulon compared to the respective exponential growing reference conditions could be observed. During the exponential growth the cells might not experience any stress, so the expression of SigB regulon could be at basal level through promoter leakage (for some proteins), and for some unknown reason this minimal effect is even abolished in the presence of GB. The proteins that were commonly up-regulated in the presence of GB during normal growth and during osmoprotection (Figure 33) were mainly involved in anabolic processes such as biosynthesis/acquisition of amino acids and nucleotides. This increase in anabolic proteins is related to increase in growth rate that is in turn increased in the presence of GB due to its biophysical properties.

Protein complexes in CCM were not stabilized in the presence of GB in the shake flask samples unlike in the chemostat (see Figure 37). The stabilization effect by GB can thus possibly depend on any of the three reasons. 1) the effect of GB on protein complex stabilization could be more prominent when GB is present in the media for longer period (in chemostat which is greater than 48 hours) compared to shake flask (less than 10 hours), 2) influence of GB over protein stabilization could be higher in slow growing cells (samples cultivated in chemostats) in comparison to fast growing cells (samples cultivated in shake flasks), 3) finally protein stabilization by GB could be pronounced during energy limitation (chemostat) in comparison to excess energy (shake flask). However it is not clear with the current data what could be the potential reason for GB to stabilize the proteins. Many of the unstable proteins (see Table 2 and Figure 34) that were thought to be the targets of ClpCP protease upon entry into starvation phase in *B. subtilis* [1] were present in higher amount in the presence of GB. Most of these target proteins of the protease ClpCP are the first-committed-step enzymes for biosynthesis of aromatic and branched chain amino acids, cell wall precursors, purines, and pyrimidines [1]. Association of these unstable proteins to the anabolic pathways renders the *B. subtilis* a growth advantage in the presence of GB. As GB is metabolically inert in *B. subtilis* the global changes induced by GB could be primarily due to biophysical properties of GB that indirectly led to the changes associated with the metabolism.

Absolute quantification of CCM proteins in the shake flask cultivated samples (high glucose) had revealed only minor changes either in the presence of GB or high salinity or osmoprotection; this is in contrast to the glucose limited chemostat cultivated samples where major changes were observed in the CCM proteins. The fundamental differences between both the conditions (shake flask and chemostat) are glucose concentrations and growth rates. Expression of the glycolytic enzymes primarily depends on the availability of glucose. Presence of excess amount of glucose

allowed the higher expression of glycolytic enzymes in shake flask compared to that of chemostat cultivated samples (see Figure 35); this effect was observed both in the reference condition and at high salinity. The existing high amount of glucose and glycolytic proteins were sufficient to synthesize large amounts of proline required for osmoprotection at high salinity rendering the CCM proteins majorly unaffected. Higher abundance of glycolytic enzymes due to excess glucose could have abrogated the process of flux balancing (loss of enzyme activity compensated by the increase in enzyme concentration) that is observed in glucose limited chemostat at high salinity (see section 6.4.1).

Though the rest of the protein complexes were not stabilized in CCM during osmoprotection in the shake flask, the presumed protein complex between ProA-ProJ-ProH was stabilized in shake flasks reproducing the result from the chemostat cultivations (see Figure 37). In a similar experimental set up Hoffmann *et al.* 2012 [207] it was shown that addition of 1 mM GB at high salinity completely abolished the synthesis of proline, this result suggested that there might not be any expression (mRNA and protein) of *proHJ* in the presence of GB. However, the current results suggest that indeed the proteins are available in both shake flask and chemostat experimental setup even in the presence of GB, but they might be enzymatically inactive to produce proline. These results also imply there might a potential regulation of ProH/J activity involved that could respond to high salinity and osmoprotectants like GB.

6.4.3 The effect of ProH, ProJ over-expression and glutamate supplementation

The proteins ProH and ProJ play a key role in providing osmoprotection to the *B. subtilis* by producing high amounts of proline (intracellular concentration of 400 mM [188]) as an osmoprotectant [9]. Glutamate is the precursor required for the synthesis of proline for both anabolic and osmoprotective purposes. Glutamate was decreased (approximately 450 mM to 100 mM) approximately four fold with increasing salinity (up to 1 M NaCl) in the medium to synthesize proline [9]. Despite the production of high amounts of proline and utilization of glutamate, the cells grow at least four times slower than the reference condition. The above result raised two questions: 1) whether the ProJ and ProH proteins are the limiting factors that hinder the growth?; 2) whether the available glutamate is sufficient for the synthesis of the optimal amount of proline? To address these two questions over expression of ProJ and ProH and supplementation of glutamate during high salinity were performed for the better understanding of the dynamics of osmoprotection in *B. subtilis* that involves proline as an osmoprotectant. These experiments were performed in a joint effort with the group of Erhard Bremer in Marburg and I was responsible for the proteome analysis in these studies.

Over expression of *proHJ* was achieved by introducing a combination of point mutations into a wild type SigA promoter of *proHJ* to generate the M10 promoter (consensus SigA promoter) in the strain MDB28 (see Figure 39). On par with the TreA activity assay of *proHJ* fusions in the strain M10, absolute protein quantification also showed over expression of ProJ and ProH. Over expression of both these proteins did not provide better osmoprotection. This lack of improved osmoprotection of *B. subtilis* amid the over expression of ProJ and ProH could be due to several reasons. Even though the concentration of these proteins increased significantly in the MDB28 compared to that of wild type JH642 strain the proline concentrations did not increase proportionally with the increase in the enzyme concentration as indicated in Table 4 (Data obtained from the doctoral dissertation of Monika Dolezal, Marburg/Lahn, 2006). This could be explained by two possible reasons; 1) a possible activity regulation of ProJ and ProH that was already discussed in the section 6.4.1, 2) the other possibility is leakage of proline to the extracellular environment via an unknown system because the mechanosensitive channels (MscL and MscS) were proven to be not involved in the leakage of proline [188]. The unknown system could be a passive carrier/transporter as the washing of cells with conventional buffers like TE buffer resulted in loss of total intracellular proline as the cell are osmotically down shocked (data not shown). All these possible explanations point out to the fact that higher concentrations of proline could lead to endo-osmosis due to higher intracellular turgor pressure that is also

deleterious to the cellular physiology. Hence, *B. subtilis* keeps the proline concentration at optimal levels required for its protection and the rest synthesis is either enzymatically inhibited or leaked to extracellular environment, which could be re-imported via PutP or OpuE transporter system. This re-import mechanism of proline could also play a crucial role in fine-tuning the turgor pressure of *B. subtilis*.

Table 4: TreA activity of *proHJ* fusion strain and their corresponding intracellular proline concentrations in the strains JH642 (wild type) and M10 (*proHJ* over expression) under normal growth (0 M NaCl) and at moderate salinity (0.4 M NaCl). *Data obtained from the doctoral dissertation of Monika Dolezal, Marburg/Lahn, 2006.

	ProJ and ProH expression (TreA activity nmol min^{-1} mg $Protein^{-1}$)		**Proline amount(µmol g TG^{-1})**	
	0 M NaCl	**0.4 M NaCl**	**0 M NaCl**	**0.4 M NaCl**
JH642	14	42	1.6	37
MDB28	602	1043	24	122

We also assessed the effect of ProHJ overexpression on the levels of the other proline biosynthetic enzymes during low and high osmolarity. ProA which has a dual role in both anabolic and osmoprotective synthesis of proline was increased by two fold whereas the co-expressed protein ProB was unchanged or slightly decreased during high salinity in comparison to none-stressed cells (see Figure 42), this was observed in both normal strain (JH642) and ProHJ over expression strain (MDB28). However, in a similar experimental setup the *B. subtilis* wild type strain 168 Trp^+, the mRNA levels of *proA* and *proB* (see Figure 43) were not significantly increased in the presence of high salinity in comparison to the none-stressed cells. Unchanged mRNA expression and increase in amount of only the protein ProA might once again indicate a potential complex formation between ProJ-ProA-ProH that might be stabilized when required (in this case during high salinity). The amount of ProA was concomitantly elevated along with the increased expression of ProJ and ProH indicating the protection of ProA in the complex. Interestingly the secondary analogue of the ProH enzyme, ProG was up-regulated by approximately two fold during high salinity, although the exact regulatory mechanism of ProG is unknown. As expected the anabolic route of the proline biosynthesis involving ProB and ProI proteins was unchanged during high salinity. Over expression of ProJ and ProH did not affect the levels of proteins involved in the CCM.

Addition of external glutamate only partially improved the osmoprotection capabilities owing to the fact that further increase in the amount of proline (which is already at 400 mM of

intracellular proline at 1 M NaCl [83, 188]) could also be deleterious due to increase in turgor pressure. ProJ and ProH were unaffected upon addition of glutamate; however the anabolic route of proline biosynthesis (ProA, ProB and ProI) was up-regulated in the presence of glutamate which indicates a feed forward activation of this pathway in the presence of the substrate glutamate. Furthermore, supplementation with glutamate induced some changes to the proteins in the CCM, some of which were not reported earlier. To our knowledge there were two independent studies that investigated the effect of glutamate on the global transcriptome [208, 209]. Schilling *et al.* (2007) employed the CGSE medium (glucose, succinate and glutamate) and reported the transcriptional profiles and the flux associated with the proteins involved in the CCM. The authors indicated several changes in CCM that are subjected to metabolic regulation mediated by post-translational changes. Bang-Ce C *et al.* 2009 performed a glucose limited chemostat supplemented with glutamate, valine and glutamine independently and performed global transcriptome analysis. Due to glucose limiting conditions, the gluconeogenic pathway was activated much stronger in the presence of glutamate indicating the entry of glutamate into the TCA and thereby expressing gluconeogenic enzymes. In the case of experiments performed by Schilling *et al.* (2007) a high glucose concentration of 0.5% was used comparable with the current study. The major difference was the presence of succinate along with glutamate in the medium. The data from Schilling *et al.* 2007 showed an increase in the overflow metabolism especially the acetate production was increased in the presence of glutamate.

In the current study a significant increase in YtsJ (malic enzyme) indicates a possible increase of pyruvate that might lead to the production overflow metabolites like acetate and lactate. This observation is also supported by the significant decrease in the CitZ and CitB, which marks the entry of acetyl Co-A into TCA cycle. Measurement of metabolome and flux of the CCM under these conditions would provide more information. Increase in the overflow metabolism and decreased channeling of pyruvate to TCA cycle implies that presence of high glucose favors overflow metabolism which is aggravated further in the presence of glutamate, which also takes care of replenishing TCA cycle intermediates. Simultaneous use of multiples energy sources (in this case glucose via glycolysis and glutamate via TCA and glycolysis) demonstrates the versatile and unique regulatory mechanisms associated to the CCM proteins to efficiently utilize the available energy sources which are often limited in the natural habitat for *B. subtilis*.

In the presence of glucose the GltA and GltB enzymes (both subunits of GOGAT) are responsible for converting 2-oxogluterate to glutamate. Expression of *gltAB* genes is controlled by the LysR-type transcription activator GltC in the presence of glucose [46]. GOGAT is an

iron-containing enzyme which is regulated upon the availability of iron [210]. Iron mediated expression of GOGAT is brought about by the non-coding RNA FsrA which blocks the translation of GltAB by binding to the mRNA of *gltAB* upon iron limitation [211]. Due to high salt mediated iron limitation (discussed in the section 6.4) a strong repression of *gltAB* was observed in the current experiment and also in the section 6.4.2. This repression of *gltAB* also continued in the presence of glutamate probably due to the binding and subsequent inactivation of GltC by RocG in the presence of glutamate [212].

Entry of glutamate into TCA cycle is catalyzed by the functional glutamate dehydrogenase (RocG) which is activated by transcription factors RocR and AhrC in the presence of nitrogen source like arginine and repressed in the presence of glucose by CcpA [3]. Therefore, in the presence of both glucose and glutamate can repress and express *rocG* respectively. Under similar experimental conditions a basal level expression of *rocG* gene was observed by Schilling *et al.* 2007, which was sufficient to convert excess glutamate to 2-oxogluterate that can replenish the reduced intermediates of the TCA cycle. Some of the changes observed in the CCM upon addition of glutamate however raised further questions; changes such as upregulation of most of the glycolytic enzymes (PfkA, all the proteins from the *cggR* operon) in the presence of glutamate – suggesting a possible increase in flux through glycolysis. In order to comprehensively understand the concomitant effect of glucose and glutamate on the metabolic pathways a detailed global transcriptome and proteome analysis would be necessary.

To summarize, overexpression of ProH and ProJ enzymes did not improve the osmoprotection efficiency and this lack of improvement could be due to possible activity regulation of ProH and PorJ or proline leakage to extra cellular environment via unknown mechanism. Proline alone is not the best osmoprotectant compared to glycine betaine (as GB improves growth rate due to its biophysical properties, see section 6.4.1), so supplementation of additional glutamate or proline could not dramatically increase the osmoprotection efficiency or improve the growth rate.

7. REFERENCES

1. Gerth, U., et al., *Clp-dependent proteolysis down-regulates central metabolic pathways in glucose-starved Bacillus subtilis.* J Bacteriol, 2008. **190**(1): p. 321-31.
2. Otto, A., et al., *Systems-wide temporal proteomic profiling in glucose-starved Bacillus subtilis.* Nat Commun, 2010. **1**: p. 137.
3. Gunka, K. and F.M. Commichau, *Control of glutamate homeostasis in Bacillus subtilis: a complex interplay between ammonium assimilation, glutamate biosynthesis and degradation.* Mol Microbiol, 2012. **85**(2): p. 213-24.
4. Hecker, M., J. Pane-Farre, and U. Volker, *SigB-dependent general stress response in Bacillus subtilis and related gram-positive bacteria.* Annu Rev Microbiol, 2007. **61**: p. 215-36.
5. Alper, S., et al., *Role of adenosine nucleotides in the regulation of a stress-response transcription factor in Bacillus subtilis.* J Mol Biol, 1996. **260**(2): p. 165-77.
6. Yu, J., et al., *Probing gene expression in live cells, one protein molecule at a time.* Science, 2006. **311**(5767): p. 1600-3.
7. Neuweger, H., et al., *Visualizing post genomics data-sets on customized pathway maps by ProMeTra-aeration-dependent gene expression and metabolism of Corynebacterium glutamicum as an example.* BMC Syst Biol, 2009. **3**(25d1be63-110d-eace-5a84-5b7166bfedfe): p. 82.
8. Bremer, E., *Adaptation to changing osmolarity. In" Bacillus subtilis and its closest relatives: from genes to cells.* ASM press, Washington, 2002: p. 385-391. Edited by A. L. Sonnenshein, J. A. Hoch, R. Losick & American Society for Microbiology.
9. Brill, J., et al., *Osmotically controlled synthesis of the compatible solute proline is critical for cellular defense of Bacillus subtilis against high osmolarity.* J Bacteriol, 2011. **193**(19): p. 5335-46.
10. Lehnik-Habrink, M., et al., *RNA degradation in Bacillus subtilis: an interplay of essential endo- and exoribonucleases.* Mol Microbiol, 2012. **84**(6): p. 1005-17.
11. Liu, W.T., et al., *Imaging mass spectrometry of intraspecies metabolic exchange revealed the cannibalistic factors of Bacillus subtilis.* Proc Natl Acad Sci U S A, 2010. **107**(37): p. 16286-90.
12. Burkholder, P.R. and N.H. Giles, Jr., *Induced biochemical mutations in Bacillus subtilis.* Am J Bot, 1947. **34**(6): p. 345-8.
13. Anagnostopoulos, C. and J. Spizizen, *Requirements for Transformation in Bacillus Subtilis.* J Bacteriol, 1961. **81**(5): p. 741-6.
14. Kunst, F., et al., *The complete genome sequence of the gram-positive bacterium Bacillus subtilis.* Nature, 1997. **390**(6657): p. 249-56.
15. Barbe, V., et al., *From a consortium sequence to a unified sequence: the Bacillus subtilis 168 reference genome a decade later.* Microbiology, 2009. **155**(Pt 6): p. 1758-75.
16. Belda, E., et al., *An updated metabolic view of the Bacillus subtilis 168 genome.* Microbiology, 2013. **159**(Pt 4): p. 757-70.
17. Kobayashi, K., et al., *Essential Bacillus subtilis genes.* Proc Natl Acad Sci U S A, 2003. **100**(8): p. 4678-83.
18. Harwood, C.R., *Bacillus subtilis and its relatives: molecular biological and industrial workhorses.* Trends Biotechnol, 1992. **10**(7): p. 247-56.
19. Manachini, P.L., M.G. Fortina, and C. Parini, *Enzymic Modification of Vegetable Protein by a Crude Preparation from a Strain of Bacillus-Licheniformis.* Journal of the Science of Food and Agriculture, 1988. **45**(3): p. 263-266.

20. Guglielmetti, S., D. Mora, and C. Parini, *Small rolling circle plasmids in Bacillus subtilis and related species: organization, distribution, and their possible role in host physiology.* Plasmid, 2007. **57**(3): p. 245-64.
21. Pandey, A., C.R. Soccol, and D. Mitchell, *New developments in solid state fermentation: I-bioprocesses and products.* Process Biochemistry, 2000. **35**(10): p. 1153-1169.
22. Klier, A.F. and G. Rapoport, *Genetics and regulation of carbohydrate catabolism in Bacillus.* Annu Rev Microbiol, 1988. **42**: p. 65-95.
23. Dubnau, D., *Genetic competence in Bacillus subtilis.* Microbiological reviews, 1991. **55**(3): p. 395-819.
24. Driks, A., *Bacillus subtilis spore coat.* Microbiol Mol Biol Rev, 1999. **63**(1): p. 1-20.
25. Haldenwang, W.G., *The sigma factors of Bacillus subtilis.* Microbiol Rev, 1995. **59**(1): p. 1-30.
26. Butcher, B.G. and J.D. Helmann, *Identification of Bacillus subtilis sigma-dependent genes that provide intrinsic resistance to antimicrobial compounds produced by Bacilli.* Mol Microbiol, 2006. **60**(3): p. 765-82.
27. Molle, V., et al., *Additional targets of the Bacillus subtilis global regulator CodY identified by chromatin immunoprecipitation and genome-wide transcript analysis.* J Bacteriol, 2003. **185**(6): p. 1911-22.
28. Wendrich, T.M., et al., *Dissection of the mechanism for the stringent factor RelA.* Mol Cell, 2002. **10**(4): p. 779-88.
29. Eymann, C., et al., *Bacillus subtilis functional genomics: global characterization of the stringent response by proteome and transcriptome analysis.* J Bacteriol, 2002. **184**(9): p. 2500-20.
30. Krebs, H.A. and W.A. Johnson, *The role of citric acid in intermediate metabolism in animal tissues.* FEBS Lett, 1980. **117 Suppl**: p. K1-10.
31. Fisher, S.H. and A.L. Sonenshein, *Control of carbon and nitrogen metabolism in Bacillus subtilis.* Annu Rev Microbiol, 1991. **45**: p. 107-35.
32. Stulke, J. and W. Hillen, *Regulation of carbon catabolism in Bacillus species.* Annu Rev Microbiol, 2000. **54**: p. 849-80.
33. Skarlatos, P. and M.K. Dahl, *The glucose kinase of Bacillus subtilis.* J Bacteriol, 1998. **180**(12): p. 3222-6.
34. Fillinger, S., et al., *Two glyceraldehyde-3-phosphate dehydrogenases with opposite physiological roles in a nonphotosynthetic bacterium.* J Biol Chem, 2000. **275**(19): p. 14031-7.
35. Fujita, Y., *Carbon catabolite control of the metabolic network in Bacillus subtilis.* Biosci Biotechnol Biochem, 2009. **73**(2): p. 245-59.
36. Durand, S., et al., *Three essential ribonucleases-RNase Y, J1, and III-control the abundance of a majority of Bacillus subtilis mRNAs.* PLoS Genet, 2012. **8**(3): p. e1002520.
37. Yoshida, K., et al., *Combined transcriptome and proteome analysis as a powerful approach to study genes under glucose repression in Bacillus subtilis.* Nucleic Acids Research, 2001. **29**(3): p. 683-692.
38. Servant, P., D. Le Coq, and S. Aymerich, *CcpN (YqzB), a novel regulator for CcpA-independent catabolite repression of Bacillus subtilis gluconeogenic genes.* Mol Microbiol, 2005. **55**(5): p. 1435-51.
39. Doan, T., et al., *The Bacillus subtilis ywkA gene encodes a malic enzyme and its transcription is activated by the YufL/YufM two-component system in response to malate.* Microbiology-Sgm, 2003. **149**(8e2dec97-84f3-1186-536a-c99093901b62): p. 2331-2343.
40. Lerondel, G., et al., *YtsJ has the major physiological role of the four paralogous malic enzyme isoforms in Bacillus subtilis.* J Bacteriol, 2006. **188**(13): p. 4727-36.

41. Doan, T. and S. Aymerich, *Regulation of the central glycolytic genes in Bacillus subtilis: binding of the repressor CggR to its single DNA target sequence is modulated by fructose-1,6-bisphosphate.* Molecular Microbiology, 2003. **47**(6): p. 1709-1721.
42. Fujita, Y., et al., *Identification and expression of the Bacillus subtilis fructose-1, 6-bisphosphatase gene (fbp).* J Bacteriol, 1998. **180**(16): p. 4309-13.
43. Cruz Ramos, H., et al., *Fermentative metabolism of Bacillus subtilis: physiology and regulation of gene expression.* J Bacteriol, 2000. **182**(11): p. 3072-80.
44. Alén, C. and A. Sonenshein, *Bacillus subtilis aconitase is an RNA-binding protein.* Proceedings of the National Academy of Sciences of the United States of America, 1999. **96**(f3351a19-aa68-f3c2-2084-85df091d2cd6): p. 10412-10419.
45. Deshpande, K.L. and J.F. Kane, *Glutamate synthase from Bacillus subtilis: in vitro reconstitution of an active amidotransferase.* Biochem Biophys Res Commun, 1980. **93**(1): p. 308-14.
46. Wacker, I., et al., *The regulatory link between carbon and nitrogen metabolism in Bacillus subtilis: regulation of the gltAB operon by the catabolite control protein CcpA.* Microbiology-Sgm, 2003. **149**(dd2ee540-dea2-368e-1367-19d688c4edc9): p. 3001-3009.
47. Belitsky, B.R., et al., *Role of TnrA in nitrogen source-dependent repression of Bacillus subtilis glutamate synthase gene expression.* J Bacteriol, 2000. **182**(21): p. 5939-47.
48. Belitsky, B. and A. Sonenshein, *Role and regulation of Bacillus subtilis glutamate dehydrogenase genes.* Journal of bacteriology, 1998. **180**(9c6e73f6-4e9f-f5d6-43f9-6d96f9d82a6e): p. 6298-6603.
49. Gunka, K., et al., *A high-frequency mutation in Bacillus subtilis: requirements for the decryptification of the gudB glutamate dehydrogenase gene.* J Bacteriol, 2012. **194**(5): p. 1036-44.
50. Bernhardt, J., et al., *Bacillus subtilis during feast and famine: visualization of the overall regulation of protein synthesis during glucose starvation by proteome analysis.* Genome Res, 2003. **13**(2): p. 224-37.
51. Deutscher, J., et al., *Protein kinase-dependent HPr/CcpA interaction links glycolytic activity to carbon catabolite repression in gram-positive bacteria.* Mol Microbiol, 1995. **15**(6): p. 1049-53.
52. Lavergne, J.-P., J.-M. Jault, and A. Galinier, *Insights into the functioning of Bacillus subtilis HPr kinase/phosphatase: affinity for its protein substrates and role of cations and phosphate.* Biochemistry, 2002. **41**(3e2bb96f-b832-57c6-0bca-9bb5f0a5a267): p. 6218-6243.
53. Weber, J., A. Kayser, and U. Rinas, *Metabolic flux analysis of Escherichia coli in glucose-limited continuous culture. II. Dynamic response to famine and feast, activation of the methylglyoxal pathway and oscillatory behaviour.* Microbiology, 2005. **151**(Pt 3): p. 707-16.
54. Jin, S. and A.L. Sonenshein, *Identification of two distinct Bacillus subtilis citrate synthase genes.* J Bacteriol, 1994. **176**(15): p. 4669-79.
55. Dingman, D.W. and A.L. Sonenshein, *Purification of aconitase from Bacillus subtilis and correlation of its N-terminal amino acid sequence with the sequence of the citB gene.* J Bacteriol, 1987. **169**(7): p. 3062-7.
56. Jourlin-Castelli, C., et al., *CcpC, a novel regulator of the LysR family required for glucose repression of the citB gene in Bacillus subtilis.* J Mol Biol, 2000. **295**(4): p. 865-78.
57. Kim, H.J., et al., *Complex regulation of the Bacillus subtilis aconitase gene.* J Bacteriol, 2003. **185**(5): p. 1672-80.
58. Sonenshein, A.L., *Control of key metabolic intersections in Bacillus subtilis.* Nat Rev Microbiol, 2007. **5**(12): p. 917-27.

59. Meyer, F.M., et al., *Physical interactions between tricarboxylic acid cycle enzymes in Bacillus subtilis: evidence for a metabolon.* Metab Eng, 2011. **13**(1): p. 18-27.
60. Srere, P.A., *Complexes of sequential metabolic enzymes.* Annu Rev Biochem, 1987. **56**(8463f0bb-6da5-76af-4e2f-cf4dd65e14ac): p. 89-124.
61. Commichau, F.M., et al., *Novel activities of glycolytic enzymes in Bacillus subtilis: interactions with essential proteins involved in mRNA processing.* Mol Cell Proteomics, 2009. **8**(6): p. 1350-60.
62. Huynen, M.A., T. Dandekar, and P. Bork, *Variation and evolution of the citric-acid cycle: a genomic perspective.* Trends Microbiol, 1999. **7**(7): p. 281-91.
63. Shivers, R.P., S.S. Dineen, and A.L. Sonenshein, *Positive regulation of Bacillus subtilis ackA by CodY and CcpA: establishing a potential hierarchy in carbon flow.* Mol Microbiol, 2006. **62**(3): p. 811-22.
64. Freese, E.B. and C.L. Marks, *Developmental block in citric acid cycle mutants of Bacillus subtilis.* J Bacteriol, 1973. **116**(3): p. 1466-8.
65. Ireton, K., et al., *Krebs cycle function is required for activation of the Spo0A transcription factor in Bacillus subtilis.* Proceedings of the National Academy of Sciences of the United States of America, 1995. **92**(7): p. 2845-2854.
66. Licht, A., R. Golbik, and S. Brantl, *Identification of ligands affecting the activity of the transcriptional repressor CcpN from Bacillus subtilis.* J Mol Biol, 2008. **380**(1): p. 17-30.
67. Wood, J.M., *Bacterial osmosensing transporters.* Methods Enzymol, 2007. **428**(0a95e8df-f001-0d6f-38d3-9fe52bdabb1c): p. 77-107.
68. Kempf, B. and E. Bremer, *Uptake and synthesis of compatible solutes as microbial stress responses to high-osmolality environments.* Archives of Microbiology, 1998. **170**(5): p. 319-330.
69. Wood, J.M., et al., *Osmosensing and osmoregulatory compatible solute accumulation by bacteria.* Comp Biochem Physiol A Mol Integr Physiol, 2001. **130**(3): p. 437-60.
70. Holtmann, G. and E. Bremer, *Thermoprotection of Bacillus subtilis by exogenously provided glycine betaine and structurally related compatible solutes: involvement of Opu transporters.* J Bacteriol, 2004. **186**(6): p. 1683-93.
71. Du, Y., et al., *Structures of the substrate-binding protein provide insights into the multiple compatible solute binding specificities of the Bacillus subtilis ABC transporter OpuC.* Biochem J, 2011. **436**(2): p. 283-9.
72. von Blohn, C., et al., *Osmostress response in Bacillus subtilis: characterization of a proline uptake system (OpuE) regulated by high osmolarity and the alternative transcription factor sigma B.* Mol Microbiol, 1997. **25**(1): p. 175-87.
73. Holtmann, G., et al., *KtrAB and KtrCD: Two K+ uptake systems in Bacillus subtilis and their role in adaptation to hypertonicity.* Journal of Bacteriology, 2003. **185**(4): p. 1289-1298.
74. Sutherland, L., et al., *Osmotic Regulation of Transcription - Induction of the Prou Betaine Transport Gene Is Dependent on Accumulation of Intracellular Potassium.* Journal of Bacteriology, 1986. **168**(2): p. 805-814.
75. Booth, I.R., et al., *Enteric bacteria and osmotic stress: an integrated homeostatic system.* Soc Appl Bacteriol Symp Ser, 1988. **17**(3c17856a-dc1d-f858-be59-b95f0c112412): p. 35S-49S.
76. Whatmore, A.M., J.A. Chudek, and R.H. Reed, *The effects of osmotic upshock on the intracellular solute pools of Bacillus subtilis.* J Gen Microbiol, 1990. **136**(12): p. 2527-35.
77. Brill, J., et al., *T-box-mediated control of the anabolic proline biosynthetic genes of Bacillus subtilis.* Microbiology, 2011. **157**(Pt 4): p. 977-87.
78. Belitsky, B.R., et al., *Multiple genes for the last step of proline biosynthesis in Bacillus subtilis.* J Bacteriol, 2001. **183**(14): p. 4389-92.

79. Sonenshein, A.L., J.A. Hoch, and R. Losick, *Adaptation to changing osmolarity. In Bacillus subtilis and its closest relatives.* Amer Society for Microbiology, 2002(84f5af48-2711-cf1b-b4ff-a14ae3a8ec32).
80. Steil, L., et al., *Genome-wide transcriptional profiling analysis of adaptation of Bacillus subtilis to high salinity.* J Bacteriol, 2003. **185**(21): p. 6358-70.
81. Hahne, H., et al., *A comprehensive proteomics and transcriptomics analysis of Bacillus subtilis salt stress adaptation.* J Bacteriol, 2010. **192**(3): p. 870-82.
82. Zhou, Y., et al., *Direct linking of metabolism and gene expression in the proline utilization A protein from Escherichia coli.* Amino Acids, 2008. **35**(4): p. 711-8.
83. Moses, S., et al., *Proline utilization by Bacillus subtilis: uptake and catabolism.* J Bacteriol, 2012. **194**(4): p. 745-58.
84. Olkhova, E., et al., *Homology model of the Na+/proline transporter PutP of Escherichia coli and its functional implications.* J Mol Biol, 2011. **406**(1): p. 59-74.
85. Boch, J., et al., *Synthesis of the osmoprotectant glycine betaine in Bacillus subtilis: characterization of the gbsAB genes.* J Bacteriol, 1996. **178**(17): p. 5121-9.
86. Kappes, R.M., B. Kempf, and E. Bremer, *Three transport systems for the osmoprotectant glycine betaine operate in Bacillus subtilis: characterization of OpuD.* J Bacteriol, 1996. **178**(17): p. 5071-9.
87. Boch, J., B. Kempf, and E. Bremer, *Osmoregulation in Bacillus subtilis: synthesis of the osmoprotectant glycine betaine from exogenously provided choline.* J Bacteriol, 1994. **176**(17): p. 5364-71.
88. Hoffmann, T. and E. Bremer, *Protection of Bacillus subtilis against cold stress via compatible-solute acquisition.* J Bacteriol, 2011. **193**(7): p. 1552-62.
89. Hoffmann, T., et al., *Responses of Bacillus subtilis to hypotonic challenges: physiological contributions of mechanosensitive channels to cellular survival.* Appl Environ Microbiol, 2008. **74**(8): p. 2454-60.
90. Wang, Z., M. Gerstein, and M. Snyder, *RNA-Seq: a revolutionary tool for transcriptomics.* Nat Rev Genet, 2009. **10**(1): p. 57-63.
91. Stoughton, R.B., *Applications of DNA microarrays in biology.* Annu Rev Biochem, 2005. **74**: p. 53-82.
92. Yazaki, J., B.D. Gregory, and J.R. Ecker, *Mapping the genome landscape using tiling array technology.* Curr Opin Plant Biol, 2007. **10**(5): p. 534-42.
93. Rasmussen, S., H.B. Nielsen, and H. Jarmer, *The transcriptionally active regions in the genome of Bacillus subtilis.* Mol Microbiol, 2009. **73**(6): p. 1043-57.
94. McLafferty, F.W., *Mass spectrometry across the sciences.* Proc Natl Acad Sci U S A, 2008. **105**(47): p. 18088-9.
95. Karas, M. and F. Hillenkamp, *Laser desorption ionization of proteins with molecular masses exceeding 10,000 daltons.* Anal Chem, 1988. **60**(20): p. 2299-301.
96. Fenn, J.B., et al., *Electrospray ionization for mass spectrometry of large biomolecules.* Science, 1989. **246**(4926): p. 64-71.
97. Kellie, J.F., et al., *The emerging process of Top Down mass spectrometry for protein analysis: biomarkers, protein-therapeutics, and achieving high throughput.* Mol Biosyst, 2010. **6**(9): p. 1532-9.
98. Cox, J. and M. Mann, *Quantitative, high-resolution proteomics for data-driven systems biology.* Annu Rev Biochem, 2011. **80**(1): p. 273-99.
99. Liu, H., R.G. Sadygov, and J.R. Yates, 3rd, *A model for random sampling and estimation of relative protein abundance in shotgun proteomics.* Anal Chem, 2004. **76**(14): p. 4193-201.
100. Gerber, S.A., et al., *Absolute quantification of proteins and phosphoproteins from cell lysates by tandem MS.* Proc Natl Acad Sci U S A, 2003. **100**(12): p. 6940-5.

101. Hanke, S., et al., *Absolute SILAC for accurate quantitation of proteins in complex mixtures down to the attomole level.* J Proteome Res, 2008. **7**(3): p. 1118-30.
102. Pratt, J.M., et al., *Multiplexed absolute quantification for proteomics using concatenated signature peptides encoded by QconCAT genes.* Nature Protocols, 2006. **1**(2): p. 1029-1043.
103. Abbatiello, S.E., et al., *Automated detection of inaccurate and imprecise transitions in peptide quantification by multiple reaction monitoring mass spectrometry.* Clin Chem, 2010. **56**(2): p. 291-305.
104. Beynon, R.J., et al., *Multiplexed absolute quantification in proteomics using artificial QCAT proteins of concatenated signature peptides.* Nat Methods, 2005. **2**(8): p. 587-9.
105. Wolf-Yadlin, A., et al., *Multiple reaction monitoring for robust quantitative proteomic analysis of cellular signaling networks.* Proc Natl Acad Sci U S A, 2007. **104**(14): p. 5860-5.
106. Picotti, P., et al., *Full dynamic range proteome analysis of S. cerevisiae by targeted proteomics.* Cell, 2009. **138**(4): p. 795-806.
107. Costenoble, R., et al., *Comprehensive quantitative analysis of central carbon and amino-acid metabolism in Saccharomyces cerevisiae under multiple conditions by targeted proteomics.* Mol Syst Biol, 2011. **7**: p. 464.
108. Eymann, C., et al., *A comprehensive proteome map of growing Bacillus subtilis cells.* Proteomics, 2004. **4**(10): p. 2849-76.
109. Hahne, H., et al., *From complementarity to comprehensiveness--targeting the membrane proteome of growing Bacillus subtilis by divergent approaches.* Proteomics, 2008. **8**(19): p. 4123-36.
110. Macek, B., et al., *The serine/threonine/tyrosine phosphoproteome of the model bacterium Bacillus subtilis.* Mol Cell Proteomics, 2007. **6**(4): p. 697-707.
111. Elsholz, A.K., et al., *Global impact of protein arginine phosphorylation on the physiology of Bacillus subtilis.* Proc Natl Acad Sci U S A, 2012. **109**(19): p. 7451-6.
112. Cho, K.H. and O. Wolkenhauer, *Systems biology: Discovering the dynamic behavior of biochemical networks.* BioSystems Rev, 2005. **1**(1).
113. Kleijn, R.J., et al., *Metabolic fluxes during strong carbon catabolite repression by malate in Bacillus subtilis.* J Biol Chem, 2010. **285**(3): p. 1587-96.
114. Buescher, J.M., et al., *Global network reorganization during dynamic adaptations of Bacillus subtilis metabolism.* Science, 2012. **335**(6072): p. 1099-103.
115. Ferguson, M.L., et al., *Reconciling molecular regulatory mechanisms with noise patterns of bacterial metabolic promoters in induced and repressed states.* Proc Natl Acad Sci U S A, 2012. **109**(1): p. 155-60.
116. Nicolas, P., et al., *Condition-dependent transcriptome reveals high-level regulatory architecture in Bacillus subtilis.* Science, 2012. **335**(6072): p. 1103-6.
117. Hardiman, T., et al., *Topology of the global regulatory network of carbon limitation in Escherichia coli.* J Biotechnol, 2007. **132**(4): p. 359-74.
118. Budde, I., et al., *Adaptation of Bacillus subtilis to growth at low temperature: a combined transcriptomic and proteomic appraisal.* Microbiology, 2006. **152**(Pt 3): p. 831-53.
119. Holtmann, G., et al., *RsbV-independent induction of the SigB-dependent general stress regulon of Bacillus subtilis during growth at high temperature.* J Bacteriol, 2004. **186**(18): p. 6150-8.
120. Maass, S., et al., *Efficient, global-scale quantification of absolute protein amounts by integration of targeted mass spectrometry and two-dimensional gel-based proteomics.* Anal Chem, 2011. **83**(7): p. 2677-84.
121. Starcher, B., *A ninhydrin-based assay to quantitate the total protein content of tissue samples.* Anal Biochem, 2001. **292**(1): p. 125-9.

122. Bradford, M.M., *A rapid and sensitive method for the quantitation of microgram quantities of protein utilizing the principle of protein-dye binding.* Anal Biochem, 1976. **72**: p. 248-54.
123. Hochuli, E., et al., *Genetic Approach to Facilitate Purification of Recombinant Proteins with a Novel Metal Chelate Adsorbent.* Bio-Technology, 1988. **6**(11): p. 1321-1325.
124. Eng, J.K., A.L. McCormack, and J.R. Yates, *An approach to correlate tandem mass spectral data of peptides with amino acid sequences in a protein database.* J Am Soc Mass Spectrom, 1994. **5**(11): p. 976-89.
125. Keller, A., et al., *A uniform proteomics MS/MS analysis platform utilizing open XML file formats.* Mol Syst Biol, 2005. **1**: p. 2005 0017.
126. MacLean, B., et al., *Skyline: an open source document editor for creating and analyzing targeted proteomics experiments.* Bioinformatics, 2010. **26**(7): p. 966-8.
127. Maclean, B., et al., *Effect of collision energy optimization on the measurement of peptides by selected reaction monitoring (SRM) mass spectrometry.* Anal Chem, 2010. **82**(24): p. 10116-24.
128. Meyer, H., M. Liebeke, and M. Lalk, *A protocol for the investigation of the intracellular Staphylococcus aureus metabolome.* Anal Biochem, 2010. **401**(2): p. 250-9.
129. Liebeke, M., et al., *Depletion of thiol-containing proteins in response to quinones in Bacillus subtilis.* Mol Microbiol, 2008. **69**(6): p. 1513-29.
130. Bolten, C.J., et al., *Sampling for metabolome analysis of microorganisms.* Anal Chem, 2007. **79**(10): p. 3843-9.
131. Kromer, J.O., et al., *In vivo quantification of intracellular amino acids and intermediates of the methionine pathway in Corynebacterium glutamicum.* Anal Biochem, 2005. **340**(1): p. 171-3.
132. Liebeke, M., et al., *A metabolomics and proteomics study of the adaptation of Staphylococcus aureus to glucose starvation.* Mol Biosyst, 2011. **7**(4): p. 1241-53.
133. Lopez, C.S., et al., *Variations of the envelope composition of Bacillus subtilis during growth in hyperosmotic medium.* Curr Microbiol, 1998. **36**(1): p. 55-61.
134. Quek, L.E., et al., *OpenFLUX: efficient modelling software for 13C-based metabolic flux analysis.* Microb Cell Fact, 2009. **8**: p. 25.
135. Wittmann, C., *Fluxome analysis using GC-MS.* Microb Cell Fact, 2007. **6**: p. 6.
136. Junker, B.H., C. Klukas, and F. Schreiber, *VANTED: a system for advanced data analysis and visualization in the context of biological networks.* BMC Bioinformatics, 2006. **7**: p. 109.
137. Rohn, H., et al., *FluxMap: a VANTED add-on for the visual exploration of flux distributions in biological networks.* BMC Syst Biol, 2012. **6**: p. 33.
138. Veening, J.W., et al., *Bet-hedging and epigenetic inheritance in bacterial cell development.* Proc Natl Acad Sci U S A, 2008. **105**(11): p. 4393-8.
139. Kuwana, R., et al., *Proteomics characterization of novel spore proteins of Bacillus subtilis.* Microbiology, 2002. **148**(Pt 12): p. 3971-82.
140. Abhyankar, W., et al., *Gel-free proteomic identification of the Bacillus subtilis insoluble spore coat protein fraction.* Proteomics, 2011. **11**(23): p. 4541-50.
141. Wisniewski, J.R., et al., *Universal sample preparation method for proteome analysis.* Nat Methods, 2009. **6**(5): p. 359-62.
142. Schaeffer, P., J. Millet, and J.P. Aubert, *Catabolic repression of bacterial sporulation.* Proc Natl Acad Sci U S A, 1965. **54**(3): p. 704-11.
143. Washburn, M.P., D. Wolters, and J.R. Yates, 3rd, *Large-scale analysis of the yeast proteome by multidimensional protein identification technology.* Nat Biotechnol, 2001. **19**(3): p. 242-7.
144. Shevchenko, A., et al., *Mass spectrometric sequencing of proteins silver-stained polyacrylamide gels.* Anal Chem, 1996. **68**(5): p. 850-8.

145. Errington, J., *Regulation of endospore formation in Bacillus subtilis.* Nat Rev Microbiol, 2003. **1**(2): p. 117-26.
146. Kodama, T., et al., *A novel small protein of Bacillus subtilis involved in spore germination and spore coat assembly.* Biosci Biotechnol Biochem, 2011. **75**(6): p. 1119-28.
147. Koburger, T., et al., *Genome-wide mRNA profiling in glucose starved Bacillus subtilis cells.* Mol Genet Genomics, 2005. **274**(1): p. 1-12.
148. Blencke, H.M., et al., *Transcriptional profiling of gene expression in response to glucose in Bacillus subtilis: regulation of the central metabolic pathways.* Metab Eng, 2003. **5**(2): p. 133-49.
149. Blom, E.J., et al., *Time-resolved transcriptomics and bioinformatic analyses reveal intrinsic stress responses during batch culture of Bacillus subtilis.* PLoS One, 2011. **6**(11): p. e27160.
150. Taniguchi, Y., et al., *Quantifying E. coli proteome and transcriptome with single-molecule sensitivity in single cells.* Science, 2010. **329**(5991): p. 533-8.
151. Hoffmann, T., et al., *High-salinity-induced iron limitation in Bacillus subtilis.* J Bacteriol, 2002. **184**(3): p. 718-27.
152. Gotsche, S. and M.K. Dahl, *Purification and characterization of the phospho-alpha(1,1)glucosidase (TreA) of Bacillus subtilis 168.* J Bacteriol, 1995. **177**(10): p. 2721-6.
153. Bruggeman, F.J. and H.V. Westerhoff, *The nature of systems biology.* Trends Microbiol, 2007. **15**(1): p. 45-50.
154. Kroos, L., B. Kunkel, and R. Losick, *Switch protein alters specificity of RNA polymerase containing a compartment-specific sigma factor.* Science, 1989. **243**(4890): p. 526-9.
155. Schumacher, M.A., et al., *Structural mechanism for the fine-tuning of CcpA function by the small molecule effectors glucose 6-phosphate and fructose 1,6-bisphosphate.* J Mol Biol, 2007. **368**(4): p. 1042-50.
156. Seidel, G., et al., *Quantitative interdependence of coeffectors, CcpA and cre in carbon catabolite regulation of Bacillus subtilis.* FEBS J, 2005. **272**(10): p. 2566-77.
157. Vijay, K., et al., *A PP2C phosphatase containing a PAS domain is required to convey signals of energy stress to the sigmaB transcription factor of Bacillus subtilis.* Molecular Microbiology, 2000. **35**(1): p. 180-188.
158. Weng, M., P.L. Nagy, and H. Zalkin, *Identification of the Bacillus subtilis pur operon repressor.* Proc Natl Acad Sci U S A, 1995. **92**(16): p. 7455-9.
159. Ebbole, D.J. and H. Zalkin, *Interaction of a putative repressor protein with an extended control region of the Bacillus subtilis pur operon.* J Biol Chem, 1989. **264**(6): p. 3553-61.
160. Rappu, P., et al., *A role for a highly conserved protein of unknown function in regulation of Bacillus subtilis purA by the purine repressor.* J Bacteriol, 1999. **181**(12): p. 3810-5.
161. Lu, Y., R.J. Turner, and R.L. Switzer, *Function of RNA secondary structures in transcriptional attenuation of the Bacillus subtilis pyr operon.* Proc Natl Acad Sci U S A, 1996. **93**(25): p. 14462-7.
162. Hobl, B. and M. Mack, *The regulator protein PyrR of Bacillus subtilis specifically interacts in vivo with three untranslated regions within pyr mRNA of pyrimidine biosynthesis.* Microbiology, 2007. **153**(Pt 3): p. 693-700.
163. Zhang, S.Y. and W.G. Haldenwang, *RelA is a component of the nutritional stress activation pathway of the Bacillus subtilis transcription factor sigma(B).* Journal of Bacteriology, 2003. **185**(19): p. 5714-5721.
164. Koch, A.L. and H.R. Levy, *Protein turnover in growing cultures of Escherichia coli.* J Biol Chem, 1955. **217**(2): p. 947-57.
165. Cai, L., N. Friedman, and X.S. Xie, *Stochastic protein expression in individual cells at the single molecule level.* Nature, 2006. **440**(7082): p. 358-62.

166. Maier, T., et al., *Quantification of mRNA and protein and integration with protein turnover in a bacterium.* Mol Syst Biol, 2011. **7**: p. 511.
167. Ander, M., et al., *SmartCell, a framework to simulate cellular processes that combines stochastic approximation with diffusion and localisation: analysis of simple networks.* Systems biology, 2004. **1**(1): p. 129-138.
168. Kaan, T., et al., *Genome-wide transcriptional profiling of the Bacillus subtilis cold-shock response.* Microbiology, 2002. **148**(Pt 11): p. 3441-55.
169. Sherman, M. and A.L. Goldberg, *Heat shock in Escherichia coli alters the protein-binding properties of the chaperonin groEL by inducing its phosphorylation.* Nature, 1992. **357**(6374): p. 167-9.
170. Steil, L., et al., *Genome-wide analysis of temporally regulated and compartment-specific gene expression in sporulating cells of Bacillus subtilis.* Microbiology, 2005. **151**(Pt 2): p. 399-420.
171. Volker, U., B. Maul, and M. Hecker, *Expression of the sigmaB-dependent general stress regulon confers multiple stress resistance in Bacillus subtilis.* J Bacteriol, 1999. **181**(13): p. 3942-8.
172. Nannapaneni, P., et al., *Defining the structure of the general stress regulon of Bacillus subtilis using targeted microarray analysis and random forest classification.* Microbiology, 2012. **158**(Pt 3): p. 696-707.
173. Helmann, J.D., et al., *Global transcriptional response of Bacillus subtilis to heat shock.* J Bacteriol, 2001. **183**(24): p. 7318-28.
174. Price, C.W., et al., *Genome-wide analysis of the general stress response in Bacillus subtilis.* Mol Microbiol, 2001. **41**(4): p. 757-74.
175. Petersohn, A., et al., *Global analysis of the general stress response of Bacillus subtilis.* J Bacteriol, 2001. **183**(19): p. 5617-31.
176. May, J.J., T.M. Wendrich, and M.A. Marahiel, *The dhb operon of Bacillus subtilis encodes the biosynthetic template for the catecholic siderophore 2,3-dihydroxybenzoate-glycine-threonine trimeric ester bacillibactin.* J Biol Chem, 2001. **276**(10): p. 7209-17.
177. Zheng, M. and G. Storz, *Oxidative stress.* Bacterial Stress Responses, 2000: p. 47-59.
178. Bsat, N. and J.D. Helmann, *Interaction of Bacillus subtilis Fur (ferric uptake repressor) with the dhb operator in vitro and in vivo.* J Bacteriol, 1999. **181**(14): p. 4299-307.
179. Grossman, T., et al., *Isolation and characterization of Bacillus subtilis genes involved in siderophore biosynthesis: relationship between B. subtilis sfpo and Escherichia coli entD genes.* Journal of bacteriology, 1993. **175**(19): p. 6203-6211.
180. Argandona, M., et al., *Interplay between iron homeostasis and the osmotic stress response in the halophilic bacterium Chromohalobacter salexigens.* Appl Environ Microbiol, 2010. **76**(11): p. 3575-89.
181. Novick, A. and L. Szilard, *Experiments with the Chemostat on spontaneous mutations of bacteria.* Proc Natl Acad Sci U S A, 1950. **36**(12): p. 708-19.
182. Tannler, S., S. Decasper, and U. Sauer, *Maintenance metabolism and carbon fluxes in Bacillus species.* Microb Cell Fact, 2008. **7**: p. 19.
183. Dauner, M., et al., *Intracellular carbon fluxes in riboflavin-producing Bacillus subtilis during growth on two-carbon substrate mixtures.* Appl Environ Microbiol, 2002. **68**(4): p. 1760-71.
184. Dauner, M., T. Storni, and U. Sauer, *Bacillus subtilis metabolism and energetics in carbon-limited and excess-carbon chemostat culture.* J Bacteriol, 2001. **183**(24): p. 7308-17.
185. Sauer, U., et al., *Physiology and metabolic fluxes of wild-type and riboflavin-producing Bacillus subtilis.* Appl Environ Microbiol, 1996. **62**(10): p. 3687-96.
186. Hoper, D., J. Bernhardt, and M. Hecker, *Salt stress adaptation of Bacillus subtilis: a physiological proteomics approach.* Proteomics, 2006. **6**(5): p. 1550-62.

187. Ruzal, S.M., et al., *Osmotic strength blocks sporulation at stage II by impeding activation of early sigma factors in Bacillus subtilis.* Current Microbiology, 1998. **36**(2): p. 75-79.
188. Hoffmann, T., et al., *Synthesis, release, and recapture of compatible solute proline by osmotically stressed Bacillus subtilis cells.* Appl Environ Microbiol, 2012. **78**(16): p. 5753-62.
189. Rancourt, D.E., et al., *Proline excretion by Escherichia coli K12.* Biotechnol Bioeng, 1984. **26**(1): p. 74-80.
190. Belitsky, B.R., *Indirect repression by Bacillus subtilis CodY via displacement of the activator of the proline utilization operon.* J Mol Biol, 2011. **413**(2): p. 321-36.
191. Fischer, E. and U. Sauer, *Large-scale in vivo flux analysis shows rigidity and suboptimal performance of Bacillus subtilis metabolism.* Nat Genet, 2005. **37**(6): p. 636-40.
192. Kuhlmann, A.U. and E. Bremer, *Osmotically regulated synthesis of the compatible solute ectoine in Bacillus pasteurii and related Bacillus spp.* Appl Environ Microbiol, 2002. **68**(2): p. 772-83.
193. Wood, J.M., *Bacterial osmoregulation: a paradigm for the study of cellular homeostasis.* Annu Rev Microbiol, 2011. **65**: p. 215-38.
194. Arst, H.N., Jr., S.A. Jones, and C.R. Bailey, *A method for the selection of deletion mutations in the L-proline catabolism gene cluster of Aspergillus nidulans.* Genet Res, 1981. **38**(2): p. 171-95.
195. Maxwell, S.A. and G.E. Davis, *Differential gene expression in p53-mediated apoptosis-resistant vs. apoptosis-sensitive tumor cell lines.* Proc Natl Acad Sci U S A, 2000. **97**(24): p. 13009-14.
196. Cayley, S. and M.T. Record, Jr., *Roles of cytoplasmic osmolytes, water, and crowding in the response of Escherichia coli to osmotic stress: biophysical basis of osmoprotection by glycine betaine.* Biochemistry, 2003. **42**(43): p. 12596-609.
197. Minton, A.P., *The influence of macromolecular crowding and macromolecular confinement on biochemical reactions in physiological media.* J Biol Chem, 2001. **276**(14): p. 10577-80.
198. Zimmerman, S.B. and A.P. Minton, *Macromolecular crowding: biochemical, biophysical, and physiological consequences.* Annu Rev Biophys Biomol Struct, 1993. **22**: p. 27-65.
199. Ignatova, Z. and L.M. Gierasch, *Inhibition of protein aggregation in vitro and in vivo by a natural osmoprotectant.* Proc Natl Acad Sci U S A, 2006. **103**(36): p. 13357-61.
200. Ignatova, Z. and L.M. Gierasch, *Effects of osmolytes on protein folding and aggregation in cells.* Methods Enzymol, 2007. **428**: p. 355-72.
201. Capp, M.W., et al., *Interactions of the osmolyte glycine betaine with molecular surfaces in water: thermodynamics, structural interpretation, and prediction of m-values.* Biochemistry, 2009. **48**(43): p. 10372-9.
202. Cayley, S., B.A. Lewis, and M.T. Record, Jr., *Origins of the osmoprotective properties of betaine and proline in Escherichia coli K-12.* J Bacteriol, 1992. **174**(5): p. 1586-95.
203. Guinn, E.J., et al., *Quantifying why urea is a protein denaturant, whereas glycine betaine is a protein stabilizer.* Proc Natl Acad Sci U S A, 2011. **108**(41): p. 16932-7.
204. Dinnbier, U., et al., *Transient accumulation of potassium glutamate and its replacement by trehalose during adaptation of growing cells of Escherichia coli K-12 to elevated sodium chloride concentrations.* Arch Microbiol, 1988. **150**(4): p. 348-57.
205. Konopka, M.C., J.C. Weisshaar, and M.T. Record, Jr., *Methods of changing biopolymer volume fraction and cytoplasmic solute concentrations for in vivo biophysical studies.* Methods Enzymol, 2007. **428**: p. 487-504.
206. Albertyn, J., S. Hohmann, and B.A. Prior, *Characterization of the osmotic-stress response in Saccharomyces cerevisiae: osmotic stress and glucose repression regulate glycerol-3-phosphate dehydrogenase independently.* Curr Genet, 1994. **25**(1): p. 12-8.

207. Hoffmann, T., et al., *Osmotic control of opuA expression in Bacillus subtilis and its modulation in response to intracellular glycine betaine and proline pools.* J Bacteriol, 2013. **195**(3): p. 510-22.
208. Ye, B.C., et al., *Time-resolved transcriptome analysis of Bacillus subtilis responding to valine, glutamate, and glutamine.* PLoS One, 2009. **4**(9): p. e7073.
209. Schilling, O., et al., *Transcriptional and metabolic responses of Bacillus subtilis to the availability of organic acids: transcription regulation is important but not sufficient to account for metabolic adaptation.* Applied and environmental microbiology, 2007. **73**(2): p. 499-507.
210. Miethke, M., et al., *Iron starvation triggers the stringent response and induces amino acid biosynthesis for bacillibactin production in Bacillus subtilis.* J Bacteriol, 2006. **188**(24): p. 8655-7.
211. Smaldone, G.T., et al., *A global investigation of the Bacillus subtilis iron-sparing response identifies major changes in metabolism.* J Bacteriol, 2012. **194**(10): p. 2594-605.
212. Commichau, F.M., et al., *A regulatory protein-protein interaction governs glutamate biosynthesis in Bacillus subtilis: the glutamate dehydrogenase RocG moonlights in controlling the transcription factor GltC.* Mol Microbiol, 2007. **65**(3): p. 642-54.

8. SUPPLEMENTARY TABLES

Table S5: List of genes belonging to the corresponding regulons used for the transcriptome analysis of bi-phase batch and tri-phase fed-batch fermentations.

Gene name	BSU number	Regulon	Regulator	Mode of action	Description
leuD	BSU28250	CcpA regulon	CcpA_pos	activation	3-isopropylmalate dehydratase small subunit
leuC	BSU28260	CcpA regulon	CcpA_pos	activation	3-isopropylmalate dehydratase large subunit
leuB	BSU28270	CcpA regulon	CcpA_pos	activation	3-isopropylmalate dehydrogenase
leuA	BSU28280	CcpA regulon	CcpA_pos	activation	2-isopropylmalate synthase
ilvC	BSU28290	CcpA regulon	CcpA_pos	activation	Ketol-acid reductoisomerase
ilvH	BSU28300	CcpA regulon	CcpA_pos	activation	Acetolactate synthase small subunit
ilvB	BSU28310	CcpA regulon	CcpA_pos	activation	Acetolactate synthase large subunit
ackA	BSU29470	CcpA regulon	CcpA_pos	activation	Acetate kinase
pta	BSU37660	CcpA regulon	CcpA_pos	activation	Phosphate acetyltransferase
glpQ	BSU02130	CcpA regulon	CcpA_neg	repression	Glycerophosphoryl diester phosphodiesterase
glpT	BSU02140	CcpA regulon	CcpA_neg	repression	Glycerol-3-phosphate transporter
amyE	BSU03040	CcpA regulon	CcpA_neg	repression	Alpha-amylase
phrC	BSU03780	CcpA regulon	CcpA_neg	repression	Phosphatase rapC inhibitor
dctP	BSU04470	CcpA regulon	CcpA_neg	repression	C4-dicarboxylate transport protein
rsbV	BSU04710	CcpA regulon	CcpA_neg	repression	Anti-sigma-B factor antagonist
rsbW	BSU04720	CcpA regulon	CcpA_neg	repression	Serine-protein kinase rsbW
sigB	BSU04730	CcpA regulon	CcpA_neg	repression	RNA polymerase sigma-B factor
rsbX	BSU04740	CcpA regulon	CcpA_neg	repression	Phosphoserine phosphatase rsbX
gmuB	BSU05810	CcpA regulon	CcpA_neg	repression	Oligo-beta-mannoside-specific phosphotransferase
gmuA	BSU05820	CcpA regulon	CcpA_neg	repression	Oligo-beta-mannoside-specific phosphotransferase
gmuC	BSU05830	CcpA regulon	CcpA_neg	repression	Oligo-beta-mannoside permease IIC component
gmuD	BSU05840	CcpA regulon	CcpA_neg	repression	6-phospho-beta-glucosidase gmuD
gmuR	BSU05850	CcpA regulon	CcpA_neg	repression	HTH-type transcriptional regulator GmuR
gmuE	BSU05860	CcpA regulon	CcpA_neg	repression	Putative fructokinase
gmuF	BSU05870	CcpA regulon	CcpA_neg	repression	Probable mannose-6-phosphate isomerase gmuF
gmuG	BSU05880	CcpA regulon	CcpA_neg	repression	Mannan endo-1,4-beta-mannosidase
yesM	BSU06950	CcpA regulon	CcpA_neg	repression	Sensor histidine kinase yesM
pel	BSU07560	CcpA regulon	CcpA_neg	repression	Pectate lyase
citM	BSU07610	CcpA regulon	CcpA_neg	repression	Mg (2+)/citrate complex secondary transporter
yflN	BSU07620	CcpA regulon	CcpA_neg	repression	Uncharacterized protein yflN
treP	BSU07800	CcpA regulon	CcpA_neg	repression	PTS system trehalose-specific EIIBC component
treA	BSU07810	CcpA regulon	CcpA_neg	repression	Trehalose-6-phosphate hydrolase
treR	BSU07820	CcpA regulon	CcpA_neg	repression	Trehalose operon transcriptional repressor
yfkN	BSU07840	CcpA regulon	CcpA_neg	repression	Trifunctional nucleotide phosphoesterase protein YfkN
acoA	BSU08060	CcpA regulon	CcpA_neg	repression	Acetoin:2,6-dichlorophenolindophenol oxidoreductase
acoB	BSU08070	CcpA regulon	CcpA_neg	repression	Acetoin:2,6-dichlorophenolindophenol oxidoreductase
acoC	BSU08080	CcpA regulon	CcpA_neg	repression	Dihydrolipoyllysine-residue acetyltransferase component
acoL	BSU08090	CcpA regulon	CcpA_neg	repression	Dihydrolipoyl dehydrogenase
acoR	BSU08100	CcpA regulon	CcpA_neg	repression	Acetoin dehydrogenase operon transcriptional activator
sspH	BSU08110	CcpA regulon	CcpA_neg	repression	Small, acid-soluble spore protein H
malA	BSU08180	CcpA regulon	CcpA_neg	repression	Maltose-6'-phosphate glucosidase
glvR	BSU08190	CcpA regulon	CcpA_neg	repression	HTH-type transcriptional regulator GlvR
malP	BSU08200	CcpA regulon	CcpA_neg	repression	PTS system maltose-specific EIICB component [Includes:
glpF	BSU09280	CcpA regulon	CcpA_neg	repression	Glycerol uptake facilitator protein
glpK	BSU09290	CcpA regulon	CcpA_neg	repression	Glycerol kinase
glpD	BSU09300	CcpA regulon	CcpA_neg	repression	Aerobic glycerol-3-phosphate dehydrogenase
yhaR	BSU09880	CcpA regulon	CcpA_neg	repression	Putative enoyl-CoA hydratase/isomerase yhaR
lcfB	BSU10270	CcpA regulon	CcpA_neg	repression	Long-chain-fatty-acid--CoA ligase
uxaC	BSU12300	CcpA regulon	CcpA_neg	repression	Uronate isomerase
yjmB	BSU12310	CcpA regulon	CcpA_neg	repression	Uncharacterized symporter yjmB
yjmC	BSU12320	CcpA regulon	CcpA_neg	repression	Uncharacterized oxidoreductase yjmC

Gene name	BSU number	Regulon	Regulator	Mode of action	Description
yjmD	BSU12330	CcpA regulon	CcpA_neg	repression	Uncharacterized zinc-type alcohol dehydrogenase-like
uxuA	BSU12340	CcpA regulon	CcpA_neg	repression	Mannonate dehydratase
yjmF	BSU12350	CcpA regulon	CcpA_neg	repression	Uncharacterized oxidoreductase uxuB
exuT	BSU12360	CcpA regulon	CcpA_neg	repression	Hexuronate transporter
exuR	BSU12370	CcpA regulon	CcpA_neg	repression	Probable HTH-type transcriptional repressor ExuR
uxaB	BSU12380	CcpA regulon	CcpA_neg	repression	Altronate oxidoreductase
uxaA	BSU12390	CcpA regulon	CcpA_neg	repression	Altronate hydrolase
ldt	BSU14040	CcpA regulon	CcpA_neg	repression	Putative L,D-transpeptidase YkuD
abbA	BSU14120	CcpA regulon	CcpA_neg	repression	Uncharacterized protein ykzF
ykuL	BSU14130	CcpA regulon	CcpA_neg	repression	CBS domain-containing protein ykuL
ccpC	BSU14140	CcpA regulon	CcpA_neg	repression	Uncharacterized HTH-type transcriptional regulator
ctaC	BSU14890	CcpA regulon	CcpA_neg	repression	Cytochrome c oxidase subunit 2
ylbP	BSU15100	CcpA regulon	CcpA_neg	repression	Uncharacterized N-acetyltransferase ylbP
sucC	BSU16090	CcpA regulon	CcpA_neg	repression	Succinyl-CoA ligase [ADP-forming] subunit beta
sucD	BSU16100	CcpA regulon	CcpA_neg	repression	Succinyl-CoA ligase [ADP-forming] subunit alpha
xynP	BSU17570	CcpA regulon	CcpA_neg	repression	Uncharacterized symporter ynaJ
xynB	BSU17580	CcpA regulon	CcpA_neg	repression	Beta-xylosidase
xylA	BSU17600	CcpA regulon	CcpA_neg	repression	Xylose isomerase
xylB	BSU17610	CcpA regulon	CcpA_neg	repression	Xylulose kinase
yozM	BSU18960	CcpA regulon	CcpA_neg	repression	Prophage-derived-like uncharacterized protein yozM
yobO	BSU19030	CcpA regulon	CcpA_neg	repression	Putative phage-related protein yobO
odhB	BSU19360	CcpA regulon	CcpA_neg	repression	Dihydrolipoyllysine-residue succinyltransferase
odhA	BSU19370	CcpA regulon	CcpA_neg	repression	2-oxoglutarate dehydrogenase E1 component
cwlS	BSU19410	CcpA regulon	CcpA_neg	repression	D-gamma-glutamyl-meso-diaminopimelic acid
yopL	BSU20850	CcpA regulon	CcpA_neg	repression	SPBc2 prophage-derived uncharacterized protein yopL
kdgT	BSU22090	CcpA regulon	CcpA_neg	repression	2-keto-3-deoxygluconate permease
kdgA	BSU22100	CcpA regulon	CcpA_neg	repression	KHG/KDPG aldolase [Includes: 4-hydroxy-2-
kdgK	BSU22110	CcpA regulon	CcpA_neg	repression	2-dehydro-3-deoxygluconokinase
kdgR	BSU22120	CcpA regulon	CcpA_neg	repression	HTH-type transcriptional regulator KdgR
kduI	BSU22130	CcpA regulon	CcpA_neg	repression	4-deoxy-L-threo-5-hexosulose-uronate ketol-isomerase
kduD	BSU22140	CcpA regulon	CcpA_neg	repression	2-dehydro-3-deoxy-D-gluconate 5-dehydrogenase
qcrA	BSU22560	CcpA regulon	CcpA_neg	repression	Menaquinol-cytochrome c reductase iron-sulfur subunit
ypiF	BSU22570	CcpA regulon	CcpA_neg	repression	Uncharacterized protein ypiF
resE	BSU23110	CcpA regulon	CcpA_neg	repression	Sensor histidine kinase resE
resD	BSU23120	CcpA regulon	CcpA_neg	repression	Transcriptional regulatory protein resD
resC	BSU23130	CcpA regulon	CcpA_neg	repression	Cytochrome c biogenesis protein ResC
resB	BSU23140	CcpA regulon	CcpA_neg	repression	Cytochrome c biogenesis protein resB
resA	BSU23150	CcpA regulon	CcpA_neg	repression	Thiol-disulfide oxidoreductase resA
yqiQ	BSU24120	CcpA regulon	CcpA_neg	repression	Methylisocitrate lyase
mmgE	BSU24130	CcpA regulon	CcpA_neg	repression	2-methylcitrate dehydratase
mmgD	BSU24140	CcpA regulon	CcpA_neg	repression	2-methylcitrate synthase
mmgC	BSU24150	CcpA regulon	CcpA_neg	repression	Acyl-CoA dehydrogenase
mmgB	BSU24160	CcpA regulon	CcpA_neg	repression	Probable 3-hydroxybutyryl-CoA dehydrogenase
mmgA	BSU24170	CcpA regulon	CcpA_neg	repression	Acetyl-CoA acetyltransferase
cccA	BSU25190	CcpA regulon	CcpA_neg	repression	Cytochrome c-550
phrE	BSU25840	CcpA regulon	CcpA_neg	repression	Phosphatase rapE inhibitor
yqxI	BSU25890	CcpA regulon	CcpA_neg	repression	Uncharacterized protein yqxI
sacC	BSU27030	CcpA regulon	CcpA_neg	repression	Levanase
levG	BSU27040	CcpA regulon	CcpA_neg	repression	Fructose permease IID component
levF	BSU27050	CcpA regulon	CcpA_neg	repression	Fructose permease IIC component
levE	BSU27060	CcpA regulon	CcpA_neg	repression	Fructose-specific phosphotransferase enzyme IIB
levD	BSU27070	CcpA regulon	CcpA_neg	repression	Fructose-specific phosphotransferase enzyme IIA
etfA	BSU28520	CcpA regulon	CcpA_neg	repression	Electron transfer flavoprotein subunit alpha
etfB	BSU28530	CcpA regulon	CcpA_neg	repression	Electron transfer flavoprotein subunit beta
fadB	BSU28540	CcpA regulon	CcpA_neg	repression	Probable enoyl-CoA hydratase
fadB	BSU28540	CcpA regulon	CcpA_neg	repression	Probable enoyl-CoA hydratase
fadR	BSU28550	CcpA regulon	CcpA_neg	repression	Fatty acid metabolism regulator protein
lcfA	BSU28560	CcpA regulon	CcpA_neg	repression	Long-chain-fatty-acid--CoA ligase
cstA	BSU28710	CcpA regulon	CcpA_neg	repression	Carbon starvation protein A homolog
abfA	BSU28720	CcpA regulon	CcpA_neg	repression	Alpha-N-arabinofuranosidase 1

Gene name	BSU number	Regulon	Regulator	Mode of action	Description
araQ	BSU28730	CcpA regulon	CcpA_neg	repression	L-arabinose transport system permease protein AraQ
araP	BSU28740	CcpA regulon	CcpA_neg	repression	L-arabinose transport system permease protein AraP
araN	BSU28750	CcpA regulon	CcpA_neg	repression	Probable arabinose-binding protein
araM	BSU28760	CcpA regulon	CcpA_neg	repression	Glycerol-1-phosphate dehydrogenase [NADP)+]
araL	BSU28770	CcpA regulon	CcpA_neg	repression	Arabinose operon protein AraL
araD	BSU28780	CcpA regulon	CcpA_neg	repression	L-ribulose-5-phosphate 4-epimerase
araB	BSU28790	CcpA regulon	CcpA_neg	repression	Ribulokinase
araA	BSU28800	CcpA regulon	CcpA_neg	repression	L-arabinose isomerase
phoR	BSU29100	CcpA regulon	CcpA_neg	repression	Alkaline phosphatase synthesis sensor protein phoR
phoP	BSU29110	CcpA regulon	CcpA_neg	repression	Alkaline phosphatase synthesis transcriptional regulatory
mdh	BSU29120	CcpA regulon	CcpA_neg	repression	Malate dehydrogenase
icd	BSU29130	CcpA regulon	CcpA_neg	repression	Isocitrate dehydrogenase [NADP]
citZ	BSU29140	CcpA regulon	CcpA_neg	repression	Citrate synthase 2
yttP	BSU29630	CcpA regulon	CcpA_neg	repression	Probable HTH-type transcriptional regulator YttP
acsA	BSU29680	CcpA regulon	CcpA_neg	repression	Acetyl-coenzyme A synthetase
acuA	BSU29690	CcpA regulon	CcpA_neg	repression	Acetoin utilization protein AcuA
acuB	BSU29700	CcpA regulon	CcpA_neg	repression	Acetoin utilization protein AcuB
acuC	BSU29710	CcpA regulon	CcpA_neg	repression	Acetoin utilization protein AcuC
fadE	BSU32820	CcpA regulon	CcpA_neg	repression	Probable acyl-CoA dehydrogenase
fadA	BSU32830	CcpA regulon	CcpA_neg	repression	3-ketoacyl-CoA thiolase
fadN	BSU32840	CcpA regulon	CcpA_neg	repression	Probable 3-hydroxyacyl-CoA dehydrogenase
araE	BSU33960	CcpA regulon	CcpA_neg	repression	Arabinose-proton symporter
sigL	BSU34200	CcpA regulon	CcpA_neg	repression	RNA polymerase sigma-54 factor
yvcI	BSU34780	CcpA regulon	CcpA_neg	repression	Uncharacterized Nudix hydrolase yvcI
nagA	BSU35010	CcpA regulon	CcpA_neg	repression	N-acetylglucosamine-6-phosphate deacetylase
yvnA	BSU35050	CcpA regulon	CcpA_neg	repression	Uncharacterized HTH-type transcriptional regulator
yvmB	BSU35080	CcpA regulon	CcpA_neg	repression	Uncharacterized HTH-type transcriptional regulator
rbsR	BSU35910	CcpA regulon	CcpA_neg	repression	Ribose operon repressor
rbsK	BSU35920	CcpA regulon	CcpA_neg	repression	Ribokinase
rbsD	BSU35930	CcpA regulon	CcpA_neg	repression	D-ribose pyranase
rbsA	BSU35940	CcpA regulon	CcpA_neg	repression	Ribose import ATP-binding protein RbsA
rbsC	BSU35950	CcpA regulon	CcpA_neg	repression	Ribose transport system permease protein rbsC
rbsB	BSU35960	CcpA regulon	CcpA_neg	repression	D-ribose-binding protein
rapF	BSU37460	CcpA regulon	CcpA_neg	repression	Response regulator aspartate phosphatase F
rocG	BSU37790	CcpA regulon	CcpA_neg	repression	Catabolic NAD-specific glutamate dehydrogenase RocG
ywdA	BSU38030	CcpA regulon	CcpA_neg	repression	Uncharacterized protein ywdA
sacA	BSU38040	CcpA regulon	CcpA_neg	repression	Sucrose-6-phosphate hydrolase
sacP	BSU38050	CcpA regulon	CcpA_neg	repression	PTS system sucrose-specific EIIBC component
galT	BSU38190	CcpA regulon	CcpA_neg	repression	Galactose-1-phosphate uridylyltransferase
galK	BSU38200	CcpA regulon	CcpA_neg	repression	Galactokinase
licH	BSU38560	CcpA regulon	CcpA_neg	repression	Probable 6-phospho-beta-glucosidase
licA	BSU38570	CcpA regulon	CcpA_neg	repression	Lichenan-specific phosphotransferase enzyme IIA
licC	BSU38580	CcpA regulon	CcpA_neg	repression	Lichenan permease IIC component
licB	BSU38590	CcpA regulon	CcpA_neg	repression	Lichenan-specific phosphotransferase enzyme IIB
cydD	BSU38730	CcpA regulon	CcpA_neg	repression	ATP-binding/permease protein CydD
cydC	BSU38740	CcpA regulon	CcpA_neg	repression	ATP-binding/permease protein CydC
cydB	BSU38750	CcpA regulon	CcpA_neg	repression	Cytochrome d ubiquinol oxidase subunit 2
cydA	BSU38760	CcpA regulon	CcpA_neg	repression	Cytochrome d ubiquinol oxidase subunit 1
cimH	BSU38770	CcpA regulon	CcpA_neg	repression	Citrate/malate transporter
msmX	BSU38810	CcpA regulon	CcpA_neg	repression	Maltodextrin import ATP-binding protein MsmX
yxkF	BSU38820	CcpA regulon	CcpA_neg	repression	Uncharacterized protein yxkF
yxjF	BSU38970	CcpA regulon	CcpA_neg	repression	Uncharacterized oxidoreductase yxjF
scoB	BSU38980	CcpA regulon	CcpA_neg	repression	Probable succinyl-CoA:3-ketoacid coenzyme A
scoA	BSU38990	CcpA regulon	CcpA_neg	repression	Probable succinyl-CoA:3-ketoacid coenzyme A
yxjC	BSU39000	CcpA regulon	CcpA_neg	repression	Uncharacterized transporter YxjC
bglS	BSU39070	CcpA regulon	CcpA_neg	repression	Beta-glucanase
yxiE	BSU39250	CcpA regulon	CcpA_neg	repression	Universal stress protein YxiE
bglH	BSU39260	CcpA regulon	CcpA_neg	repression	Aryl-phospho-beta-D-glucosidase BglH
bglP	BSU39270	CcpA regulon	CcpA_neg	repression	PTS system beta-glucoside-specific EIIBCA component
abn2	BSU39330	CcpA regulon	CcpA_neg	repression	Uncharacterized protein yxiA

Gene name	BSU number	Regulon	Regulator	Mode of action	Description
hutP	BSU39340	CcpA regulon	CcpA_neg	repression	Hut operon positive regulatory protein
hutH	BSU39350	CcpA regulon	CcpA_neg	repression	Histidine ammonia-lyase
hutU	BSU39360	CcpA regulon	CcpA_neg	repression	Urocanate hydratase
hutI	BSU39370	CcpA regulon	CcpA_neg	repression	Imidazolonepropionase
hutG	BSU39380	CcpA regulon	CcpA_neg	repression	Formimidoylglutamase
hutM	BSU39390	CcpA regulon	CcpA_neg	repression	Putative histidine permease
pdp	BSU39400	CcpA regulon	CcpA_neg	repression	Pyrimidine-nucleoside phosphorylase
nupC	BSU39410	CcpA regulon	CcpA_neg	repression	Pyrimidine nucleoside transport protein
dra	BSU39420	CcpA regulon	CcpA_neg	repression	Deoxyribose-phosphate aldolase
iolJ	BSU39670	CcpA regulon	CcpA_neg	repression	6-phospho-5-dehydro-2-deoxy-D-gluconate aldolase
iolI	BSU39680	CcpA regulon	CcpA_neg	repression	Inosose isomerase
iolH	BSU39690	CcpA regulon	CcpA_neg	repression	Protein iolH
iolG	BSU39700	CcpA regulon	CcpA_neg	repression	Inositol 2-dehydrogenase/D-chiro-inositol 3-
iolF	BSU39710	CcpA regulon	CcpA_neg	repression	Minor myo-inositol transporter iolF
iolE	BSU39720	CcpA regulon	CcpA_neg	repression	Inosose dehydratase
iolD	BSU39730	CcpA regulon	CcpA_neg	repression	3D-(3,5/4)-trihydroxycyclohexane-1,2-dione hydrolase
iolC	BSU39740	CcpA regulon	CcpA_neg	repression	5-dehydro-2-deoxygluconokinase
iolB	BSU39750	CcpA regulon	CcpA_neg	repression	5-deoxy-glucuronate isomerase
iolA	BSU39760	CcpA regulon	CcpA_neg	repression	Methylmalonate semialdehyde dehydrogenase [acylating]
gntR	BSU40050	CcpA regulon	CcpA_neg	repression	Gluconate operon transcriptional repressor
gntK	BSU40060	CcpA regulon	CcpA_neg	repression	Gluconokinase
gntP	BSU40070	CcpA regulon	CcpA_neg	repression	Gluconate permease
gntZ	BSU40080	CcpA regulon	CcpA_neg	repression	6-phosphogluconate dehydrogenase, decarboxylating
phrG	BSU40310	CcpA regulon	CcpA_neg	repression	Phosphatase rapG inhibitor
yaaH	BSU00160	SigB regulon	SigB		Spore germination protein yaaH
yaaI	BSU00170	SigB regulon	SigB		Uncharacterized isochorismatase family protein yaaI
ctc	BSU00520	SigB regulon	SigB		General stress protein CTC
spoVC	BSU00530	SigB regulon	SigB		Peptidyl-tRNA hydrolase
ctsR	BSU00830	SigB regulon	SigB		Transcriptional regulator CtsR
mcsA	BSU00840	SigB regulon	SigB		Uncharacterized protein yacH
mcsB	BSU00850	SigB regulon	SigB		Putative ATP:guanido phosphotransferase yacI
clpC	BSU00860	SigB regulon	SigB		Negative regulator of genetic competence ClpC/MecB
radA	BSU00870	SigB regulon	SigB		DNA repair protein RadA homolog
disA	BSU00880	SigB regulon	SigB		DNA integrity scanning protein DisA
yacL	BSU00890	SigB regulon	SigB		Uncharacterized PIN and TRAM-domain containing
ispD	BSU00900	SigB regulon	SigB		2-C-methyl-D-erythritol 4-phosphate cytidylyltransferase
ispF	BSU00910	SigB regulon	SigB		2-C-methyl-D-erythritol 2,4-cyclodiphosphate synthase
cypC	BSU02100	SigB regulon	SigB		Fatty-acid peroxygenase
ybyB	BSU02110	SigB regulon	SigB		Uncharacterized protein ybyB
ycbP	BSU02590	SigB regulon	SigB		Uncharacterized protein ycbP
ycdF	BSU02830	SigB regulon	SigB		Glucose 1-dehydrogenase 2
ycdG	BSU02840	SigB regulon	SigB		Probable oligo-1,6-glucosidase 2
yceC	BSU02890	SigB regulon	SigB		Stress response protein SCP2
yceD	BSU02900	SigB regulon	SigB		General stress protein 16U
yceE	BSU02910	SigB regulon	SigB		Uncharacterized protein YceE
yceF	BSU02920	SigB regulon	SigB		Uncharacterized membrane protein yceF
yceG	BSU02930	SigB regulon	SigB		Uncharacterized protein yceG
yceH	BSU02940	SigB regulon	SigB		Uncharacterized protein yceH
nadE	BSU03130	SigB regulon	SigB		NH(3)-dependent NAD (+) synthetase
gabD	BSU03910	SigB regulon	SigB		Succinate-semialdehyde dehydrogenase [NADP+)]
ydaD	BSU04190	SigB regulon	SigB		General stress protein 39
ydaE	BSU04200	SigB regulon	SigB		Probable D-lyxose ketol-isomerase
ydaF	BSU04210	SigB regulon	SigB		Putative ribosomal N-acetyltransferase YdaF
ydaG	BSU04220	SigB regulon	SigB		General stress protein 26
ydaP	BSU04340	SigB regulon	SigB		Putative thiamine pyrophosphate-containing protein ydaP
ydaS	BSU04370	SigB regulon	SigB		UPF0410 protein ydaS
ydaT	BSU04380	SigB regulon	SigB		Uncharacterized protein ydaT
gsiB	BSU04400	SigB regulon	SigB		Glucose starvation-inducible protein B
ydbD	BSU04430	SigB regulon	SigB		Probable manganese catalase
rsbV	BSU04710	SigB regulon	SigB		Anti-sigma-B factor antagonist

Gene name	BSU number	Regulon	Regulator	Mode of action	Description
rsbW	BSU04720	SigB regulon	SigB		Serine-protein kinase rsbW
sigB	BSU04730	SigB regulon	SigB		RNA polymerase sigma-B factor
rsbX	BSU04740	SigB regulon	SigB		Phosphoserine phosphatase rsbX
ydeC	BSU05150	SigB regulon	SigB		Uncharacterized HTH-type transcriptional regulator YdeC
mhqO	BSU05490	SigB regulon	SigB		Putative ring-cleaving dioxygenase mhqO
mhqP	BSU05500	SigB regulon	SigB		Putative oxidoreductase mhqP
ydhK	BSU05790	SigB regulon	SigB		Uncharacterized protein ydhK
yerD	BSU06590	SigB regulon	SigB		Uncharacterized membrane protein yerD
opuE	BSU06660	SigB regulon	SigB		Osmoregulated proline transporter
yflT	BSU07550	SigB regulon	SigB		General stress protein 17M
yflH	BSU07680	SigB regulon	SigB		Uncharacterized protein yflH
yflA	BSU07750	SigB regulon	SigB		Uncharacterized transporter yflA
yfkT	BSU07760	SigB regulon	SigB		Putative spore germination protein YfkT
yfkS	BSU07770	SigB regulon	SigB		Uncharacterized protein yfkS
yfkM	BSU07850	SigB regulon	SigB		General stress protein 18
yfkJ	BSU07880	SigB regulon	SigB		Low molecular weight protein-tyrosine-phosphatase yfkJ
yfkI	BSU07890	SigB regulon	SigB		Uncharacterized protein yfkI
yfkH	BSU07900	SigB regulon	SigB		Putative ribonuclease-like protein yfkH
chaA	BSU07920	SigB regulon	SigB		Putative cation exchanger yfkE
yfkD	BSU07930	SigB regulon	SigB		Uncharacterized protein yfkD
yfhD	BSU08490	SigB regulon	SigB		Uncharacterized protein yfhD
yfhE	BSU08500	SigB regulon	SigB		Uncharacterized protein yfhE
yfhF	BSU08510	SigB regulon	SigB		Epimerase family protein yfhF
yfhK	BSU08570	SigB regulon	SigB		Uncharacterized protein yfhK
yfhL	BSU08580	SigB regulon	SigB		Uncharacterized protein yfhL
yfhM	BSU08590	SigB regulon	SigB		AB hydrolase superfamily protein yfhM
csbB	BSU08600	SigB regulon	SigB		Putative glycosyltransferase CsbB
yhcM	BSU09140	SigB regulon	SigB		Uncharacterized protein yhcM
ygxB	BSU09390	SigB regulon	SigB		Uncharacterized protein ygxB
yhdF	BSU09450	SigB regulon	SigB		Uncharacterized oxidoreductase yhdF
yhdN	BSU09530	SigB regulon	SigB		General stress protein 69
plsC	BSU09540	SigB regulon	SigB		1-acyl-sn-glycerol-3-phosphate acyltransferase
nhaX	BSU09690	SigB regulon	SigB		Stress response protein nhaX
yhxD	BSU10430	SigB regulon	SigB		Uncharacterized oxidoreductase yhxD
yitT	BSU11120	SigB regulon	SigB		UPF0750 membrane protein yitT
yjbC	BSU11490	SigB regulon	SigB		Putative acetyltransferase YjbC
spx	BSU11500	SigB regulon	SigB		Regulatory protein spx
yjzE	BSU11839	SigB regulon	SigB		Sporulation-specific transcription factor spoVIF
yjgB	BSU12150	SigB regulon	SigB		Uncharacterized protein yjgB
yjgC	BSU12160	SigB regulon	SigB		Probable oxidoreductase yjgC
yjgD	BSU12170	SigB regulon	SigB		Uncharacterized protein yjgD
ykgB	BSU13010	SigB regulon	SigB		Uncharacterized protein YkgB
ykgA	BSU13020	SigB regulon	SigB		Uncharacterized protein ykgA
ohrB	BSU13160	SigB regulon	SigB		Organic hydroperoxide resistance protein ohrB
guaD	BSU13170	SigB regulon	SigB		Guanine deaminase
spo0E	BSU13640	SigB regulon	SigB		Aspartyl-phosphate phosphatase Spo0E
ykuT	BSU14210	SigB regulon	SigB		Uncharacterized MscS family protein YkuT
ykzI	BSU14660	SigB regulon	SigB		Uncharacterized protein ykzI
ylxP	BSU16640	SigB regulon	SigB		Uncharacterized protein ylxP
ymzB	BSU17240	SigB regulon	SigB		Uncharacterized protein ymzB
yoxC	BSU18510	SigB regulon	SigB		Uncharacterized protein yoxC
yoxB	BSU18520	SigB regulon	SigB		Uncharacterized protein yoxB
yoaA	BSU18530	SigB regulon	SigB		Uncharacterized N-acetyltransferase YoaA
yocB	BSU19150	SigB regulon	SigB		Uncharacterized protein yocB
yocK	BSU19240	SigB regulon	SigB		General stress protein 16O
ypuD	BSU23300	SigB regulon	SigB		Uncharacterized protein ypuD
ypuC/1	BSU23329	SigB regulon	SigB		Uncharacterized protein ypuD
ypuC/2	BSU23330	SigB regulon	SigB		Uncharacterized protein ypzJ
ypuB	BSU23340	SigB regulon	SigB		Uncharacterized protein ypuB
yqjL	BSU23830	SigB regulon	SigB		Uncharacterized protein yqjL

Gene name	BSU number	Regulon	Regulator	Mode of action	Description
bmrU	BSU24000	SigB regulon	SigB		Putative lipid kinase BmrU
bmr	BSU24010	SigB regulon	SigB		Multidrug resistance protein 1
bmrR	BSU24020	SigB regulon	SigB		Multidrug-efflux transporter 1 regulator
yqhQ	BSU24490	SigB regulon	SigB		Uncharacterized protein yqhQ
yqhP	BSU24500	SigB regulon	SigB		Uncharacterized protein yqhP
corA	BSU24740	SigB regulon	SigB		Magnesium transport protein CorA
yqhB	BSU24750	SigB regulon	SigB		UPF0053 protein yqhB
rsbRD	BSU24760	SigB regulon	SigB		RsbT co-antagonist protein rsbRD
mgsR	BSU24770	SigB regulon	SigB		Regulatory protein MgsR
sodA	BSU25020	SigB regulon	SigB		Superoxide dismutase [Mn]
era	BSU25290	SigB regulon	SigB		GTPase Era
cdd	BSU25300	SigB regulon	SigB		Cytidine deaminase
yraA	BSU27020	SigB regulon	SigB		Putative cysteine protease yraA
bofC	BSU27750	SigB regulon	SigB		Protein BofC
csbX	BSU27760	SigB regulon	SigB		Alpha-ketoglutarate permease
ysnF	BSU28340	SigB regulon	SigB		Stress response protein ysnF
trxA	BSU28500	SigB regulon	SigB		Thioredoxin
ysdB	BSU28830	SigB regulon	SigB		Sigma-w pathway protein ysdB
phoR	BSU29100	SigB regulon	SigB		Alkaline phosphatase synthesis sensor protein phoR
phoP	BSU29110	SigB regulon	SigB		Alkaline phosphatase synthesis transcriptional regulatory
ytkL	BSU29410	SigB regulon	SigB		UPF0173 metal-dependent hydrolase ytkL
ytxJ	BSU29760	SigB regulon	SigB		Uncharacterized protein ytxJ
ytxH	BSU29770	SigB regulon	SigB		Uncharacterized protein ytxH
ytxG	BSU29780	SigB regulon	SigB		UPF0478 protein ytxG
dps	BSU30650	SigB regulon	SigB		General stress protein 20U
ytiA	BSU30700	SigB regulon	SigB		50S ribosomal protein L31 type B
ytaB	BSU30930	SigB regulon	SigB		Uncharacterized membrane protein ytaB
yugU	BSU31280	SigB regulon	SigB		UPF0047 protein yugU
yuzA	BSU31380	SigB regulon	SigB		Uncharacterized membrane protein yuzA
yvrE	BSU33200	SigB regulon	SigB		Uncharacterized protein yvrE
yvgN	BSU33400	SigB regulon	SigB		Glyoxal reductase
yvgO	BSU33410	SigB regulon	SigB		Stress response protein yvgO
iolW	BSU33530	SigB regulon	SigB		Uncharacterized oxidoreductase YvaA
rnr	BSU33610	SigB regulon	SigB		Ribonuclease R
yvaK	BSU33620	SigB regulon	SigB		Carboxylesterase
clpP	BSU34540	SigB regulon	SigB		ATP-dependent Clp protease proteolytic subunit
csbA	BSU35180	SigB regulon	SigB		Protein CsbA
yvyD	BSU35310	SigB regulon	SigB		Putative sigma-54 modulation protein
gtaB	BSU35670	SigB regulon	SigB		UTP--glucose-1-phosphate uridylyltransferase
ywtG	BSU35830	SigB regulon	SigB		Putative metabolite transport protein ywtG
ywsB	BSU35970	SigB regulon	SigB		Cell wall-binding protein ywsB
csbD	BSU36670	SigB regulon	SigB		Stress response protein CsbD
ywmF	BSU36680	SigB regulon	SigB		Uncharacterized membrane protein ywmF
ywmE	BSU36720	SigB regulon	SigB		Uncharacterized protein ywmE
ywlB	BSU36960	SigB regulon	SigB		Uncharacterized protein ywlB
ywjC	BSU37210	SigB regulon	SigB		Uncharacterized protein ywjC
ywiE	BSU37240	SigB regulon	SigB		Probable cardiolipin synthase YwiE
ywzA	BSU38180	SigB regulon	SigB		UPF0410 protein ywzA
gspA	BSU38430	SigB regulon	SigB		General stress protein A
yxzF	BSU38610	SigB regulon	SigB		Uncharacterized protein yxzF
aag	BSU38620	SigB regulon	SigB		Putative 3-methyladenine DNA glycosylase
katX	BSU38630	SigB regulon	SigB		Catalase X
yxkO	BSU38720	SigB regulon	SigB		ADP-dependent
aldY	BSU38830	SigB regulon	SigB		Uncharacterized aldehyde dehydrogenase AldY
yxjJ	BSU38930	SigB regulon	SigB		Uncharacterized protein yxjJ
yxjI	BSU38940	SigB regulon	SigB		Uncharacterized protein yxjI
yxiS	BSU39040	SigB regulon	SigB		Uncharacterized protein yxiS
katE	BSU39050	SigB regulon	SigB		Catalase-2
csbC	BSU39810	SigB regulon	SigB		Probable metabolite transport protein CsbC
yxbG	BSU39840	SigB regulon	SigB		Uncharacterized oxidoreductase yxbG

Gene name	BSU number	Regulon	Regulator	Mode of action	Description
yxnA	BSU40000	SigB regulon	SigB		Uncharacterized oxidoreductase yxnA
yxaB	BSU40030	SigB regulon	SigB		General stress protein 30
yycD	BSU40450	SigB regulon	SigB		Uncharacterized protein yycD
ybdO	BSU02050	SigD regulon	SigD		Uncharacterized protein ybdO
tlpC	BSU03440	SigD regulon	SigD		Methyl-accepting chemotaxis protein tlpC
yfmT	BSU07350	SigD regulon	SigD		Putative aldehyde dehydrogenase yfmT
yfmS	BSU07360	SigD regulon	SigD		Putative sensory transducer protein yfmS
lytF	BSU09370	SigD regulon	SigD		Peptidoglycan endopeptidase LytF
hemAT	BSU10380	SigD regulon	SigD		Heme-based aerotactic transducer hemAT
cwlQ	BSU11570	SigD regulon	SigD		Putative murein lytic transglycosylase yjbJ
yjcP	BSU11940	SigD regulon	SigD		Uncharacterized protein yjcP
yjcQ	BSU11950	SigD regulon	SigD		Uncharacterized protein yjcQ
yjfB	BSU12120	SigD regulon	SigD		Uncharacterized protein yjfB
motB	BSU13680	SigD regulon	SigD		Motility protein B
motA	BSU13690	SigD regulon	SigD		Motility protein A
mcpC	BSU13950	SigD regulon	SigD		Methyl-accepting chemotaxis protein mcpC
cheV	BSU14010	SigD regulon	SigD		Chemotaxis protein CheV
ylqB	BSU15960	SigD regulon	SigD		Uncharacterized protein ylqB
flgB	BSU16180	SigD regulon	SigD		Flagellar basal body rod protein FlgB
flgC	BSU16190	SigD regulon	SigD		Flagellar basal-body rod protein flgC
fliE	BSU16200	SigD regulon	SigD		Flagellar hook-basal body complex protein FliE
fliF	BSU16210	SigD regulon	SigD		Flagellar M-ring protein
fliG	BSU16220	SigD regulon	SigD		Flagellar motor switch protein FliG
fliH	BSU16230	SigD regulon	SigD		Probable flagellar assembly protein fliH
fliI	BSU16240	SigD regulon	SigD		Flagellum-specific ATP synthase
fliJ	BSU16250	SigD regulon	SigD		Flagellar FliJ protein
ylxF	BSU16260	SigD regulon	SigD		FlaA locus 22.9 kDa protein
fliK	BSU16270	SigD regulon	SigD		Probable flagellar hook-length control protein
ylxG	BSU16280	SigD regulon	SigD		FlaA locus uncharacterized protein ylxG
flgE	BSU16290	SigD regulon	SigD		Flagellar basal-body rod protein flgG
fliL	BSU16300	SigD regulon	SigD		Flagellar protein FliL
fliM	BSU16310	SigD regulon	SigD		Flagellar motor switch protein FliM
fliY	BSU16320	SigD regulon	SigD		Flagellar motor switch phosphatase FliY
cheY	BSU16330	SigD regulon	SigD		Chemotaxis protein CheY
fliZ	BSU16340	SigD regulon	SigD		Flagellar biosynthetic protein fliZ
fliP	BSU16350	SigD regulon	SigD		Flagellar biosynthetic protein fliP
fliQ	BSU16360	SigD regulon	SigD		Flagellar biosynthetic protein FliQ
fliR	BSU16370	SigD regulon	SigD		Flagellar biosynthetic protein fliR
flhB	BSU16380	SigD regulon	SigD		Flagellar biosynthetic protein flhB
flhA	BSU16390	SigD regulon	SigD		Flagellar biosynthesis protein flhA
flhF	BSU16400	SigD regulon	SigD		Flagellar biosynthesis protein flhF
ylxH	BSU16410	SigD regulon	SigD		Uncharacterized protein ylxH
cheB	BSU16420	SigD regulon	SigD		Chemotaxis response regulator protein-glutamate
cheA	BSU16430	SigD regulon	SigD		Chemotaxis protein CheA
cheW	BSU16440	SigD regulon	SigD		Chemotaxis protein CheW
cheC	BSU16450	SigD regulon	SigD		CheY-P phosphatase CheC
cheD	BSU16460	SigD regulon	SigD		Chemoreceptor glutamine deamidase CheD
sigD	BSU16470	SigD regulon	SigD		RNA polymerase sigma-D factor
swrB	BSU16480	SigD regulon	SigD		Swarming motility protein swrB
yoaH	BSU18610	SigD regulon	SigD		Putative methyl-accepting chemotaxis protein yoaH
cwlS	BSU19410	SigD regulon	SigD		D-gamma-glutamyl-meso-diaminopimelic acid
degR	BSU21940	SigD regulon	SigD		Regulatory protein DegR
sigA	BSU25200	SigD regulon	SigD		RNA polymerase sigma factor rpoD
yscB	BSU28890	SigD regulon	SigD		Uncharacterized protein yscB
tlpB	BSU31230	SigD regulon	SigD		Methyl-accepting chemotaxis protein tlpB
mcpA	BSU31240	SigD regulon	SigD		Methyl-accepting chemotaxis protein mcpA
tlpA	BSU31250	SigD regulon	SigD		Methyl-accepting chemotaxis protein tlpA
mcpB	BSU31260	SigD regulon	SigD		Methyl-accepting chemotaxis protein mcpB
fliT	BSU35320	SigD regulon	SigD		Flagellar protein FliT
fliS	BSU35330	SigD regulon	SigD		Flagellar protein fliS

Gene name	BSU number	Regulon	Regulator	Mode of action	Description
fliD	BSU35340	SigD regulon	SigD		Flagellar hook-associated protein 2
yvyC	BSU35350	SigD regulon	SigD		Uncharacterized protein yvyC
hag	BSU35360	SigD regulon	SigD		Flagellin
flgL	BSU35400	SigD regulon	SigD		Flagellar hook-associated protein 3
flgK	BSU35410	SigD regulon	SigD		Flagellar hook-associated protein 1
yvyG	BSU35420	SigD regulon	SigD		Uncharacterized protein yvyG
flgM	BSU35430	SigD regulon	SigD		Negative regulator of flagellin synthesis
yvyF	BSU35440	SigD regulon	SigD		Uncharacterized protein yvyF
lytC	BSU35620	SigD regulon	SigD		N-acetylmuramoyl-L-alanine amidase LytC
lytB	BSU35630	SigD regulon	SigD		Amidase enhancer
lytA	BSU35640	SigD regulon	SigD		Membrane-bound protein lytA
lytD	BSU35780	SigD regulon	SigD		Beta-N-acetylglucosaminidase
pgdS	BSU35860	SigD regulon	SigD		Gamma-DL-glutamyl hydrolase
flhP	BSU36390	SigD regulon	SigD		Flagellar hook-basal body complex protein flhP
flhO	BSU36400	SigD regulon	SigD		Flagellar hook-basal body complex protein flhO
ywcH	BSU38100	SigD regulon	SigD		Uncharacterized protein ywcH
nfrA	BSU38110	SigD regulon	SigD		FMN reductase
epr	BSU38400	SigD regulon	SigD		Minor extracellular protease epr
dltA	BSU38500	SigD regulon	SigD		D-alanine--poly
dltB	BSU38510	SigD regulon	SigD		Protein dltB
dltC	BSU38520	SigD regulon	SigD		D-alanine--poly
dltD	BSU38530	SigD regulon	SigD		Protein dltD
dltE	BSU38540	SigD regulon	SigD		Uncharacterized oxidoreductase dltE
yxkC	BSU38850	SigD regulon	SigD		Uncharacterized protein yxkC
yaaH	BSU00160	SigE regulon	SigE		Spore germination protein yaaH
bofA	BSU00230	SigE regulon	SigE		Sigma-K factor-processing regulatory protein BofA
yabP	BSU00600	SigE regulon	SigE		Spore protein yabP
yabQ	BSU00610	SigE regulon	SigE		Spore protein yabQ
divIC	BSU00620	SigE regulon	SigE		Cell division protein divIC
yabR	BSU00630	SigE regulon	SigE		Uncharacterized protein yabR
cwlD	BSU01530	SigE regulon	SigE		Germination-specific N-acetylmuramoyl-L-alanine
pdaB	BSU01570	SigE regulon	SigE		Probable polysaccharide deacetylase pdaB
cwlJ	BSU02600	SigE regulon	SigE		Cell wall hydrolase CwlJ
ycgF	BSU03090	SigE regulon	SigE		Putative amino acid efflux protein ycgF
ycgG	BSU03100	SigE regulon	SigE		Uncharacterized protein ycgG
yckC	BSU03390	SigE regulon	SigE		Uncharacterized protein yckC
ydcA	BSU04610	SigE regulon	SigE		Putative rhomboid protease ydcA
ydcC	BSU04630	SigE regulon	SigE		Sporulation protein ydcC
ydhD	BSU05710	SigE regulon	SigE		Putative sporulation-specific glycosylase ydhD
ydhF	BSU05730	SigE regulon	SigE		Uncharacterized protein ydhF
phoB	BSU05740	SigE regulon	SigE		Alkaline phosphatase 3
ydjP	BSU06280	SigE regulon	SigE		AB hydrolase superfamily protein ydjP
yeaA	BSU06290	SigE regulon	SigE		Uncharacterized protein yeaA
cotJA	BSU06890	SigE regulon	SigE		Protein CotJA
cotJB	BSU06900	SigE regulon	SigE		Protein CotJB
cotJC	BSU06910	SigE regulon	SigE		Protein CotJC
yesJ	BSU06920	SigE regulon	SigE		Uncharacterized N-acetyltransferase YesJ
yesK	BSU06930	SigE regulon	SigE		Uncharacterized protein yesK
yfnD	BSU07310	SigE regulon	SigE		Uncharacterized protein yfnD
prkA	BSU08970	SigE regulon	SigE		Protein prkA
yhbH	BSU08980	SigE regulon	SigE		Stress response UPF0229 protein yhbH
yhcO	BSU09165	SigE regulon	SigE		Lipoprotein yhcN
spoVR	BSU09400	SigE regulon	SigE		Stage V sporulation protein R
yheD	BSU09770	SigE regulon	SigE		Endospore coat-associated protein yheD
yheC	BSU09780	SigE regulon	SigE		Endospore coat-associated protein yheC
yhaX	BSU09830	SigE regulon	SigE		Stress response protein yhaX
yhaL	BSU09940	SigE regulon	SigE		Sporulation protein yhaL
yhxC	BSU10400	SigE regulon	SigE		Uncharacterized oxidoreductase yhxC
yhjR	BSU10610	SigE regulon	SigE		Uncharacterized protein yhjR
asnO	BSU10790	SigE regulon	SigE		Asparagine synthetase [glutamine-hydrolyzing] 3

Gene name	BSU number	Regulon	Regulator	Mode of action	Description
yitC	BSU10940	SigE regulon	SigE		Probable 2-phosphosulfolactate phosphatase
yitD	BSU10950	SigE regulon	SigE		Phosphosulfolactate synthase
yjaV	BSU11290	SigE regulon	SigE		Uncharacterized protein yjaV
cotO	BSU11730	SigE regulon	SigE		Spore coat protein O
yjcA	BSU11790	SigE regulon	SigE		Sporulation protein yjcA
yjdH	BSU12050	SigE regulon	SigE		Uncharacterized protein yjdH
yjfA	BSU12110	SigE regulon	SigE		Uncharacterized protein yjfA
yjmC	BSU12320	SigE regulon	SigE		Uncharacterized oxidoreductase yjmC
yjmD	BSU12330	SigE regulon	SigE		Uncharacterized zinc-type alcohol dehydrogenase-like
uxuA	BSU12340	SigE regulon	SigE		Mannonate dehydratase
yjmF	BSU12350	SigE regulon	SigE		Uncharacterized oxidoreductase uxuB
exuT	BSU12360	SigE regulon	SigE		Hexuronate transporter
exuR	BSU12370	SigE regulon	SigE		Probable HTH-type transcriptional repressor ExuR
uxaB	BSU12380	SigE regulon	SigE		Altronate oxidoreductase
uxaA	BSU12390	SigE regulon	SigE		Altronate hydrolase
ykvI	BSU13710	SigE regulon	SigE		Uncharacterized membrane protein ykvI
ykvU	BSU13830	SigE regulon	SigE		Sporulation protein ykvU
stoA	BSU13840	SigE regulon	SigE		Sporulation thiol-disulfide oxidoreductase A
yknT	BSU14250	SigE regulon	SigE		Sporulation protein cse15
ctaA	BSU14870	SigE regulon	SigE		Heme A synthase
ylbJ	BSU15030	SigE regulon	SigE		Sporulation integral membrane protein ylbJ
gerR	BSU15090	SigE regulon	SigE		Uncharacterized protein ylbO
spoVD	BSU15170	SigE regulon	SigE		Stage V sporulation protein D
spoVE	BSU15210	SigE regulon	SigE		Stage V sporulation protein E
murG	BSU15220	SigE regulon	SigE		UDP-N-acetylglucosamine--N-acetylmuramyl-
murB	BSU15230	SigE regulon	SigE		UDP-N-acetylenolpyruvoylglucosamine reductase
divIB	BSU15240	SigE regulon	SigE		Cell division protein DivIB
ylxW	BSU15250	SigE regulon	SigE		UPF0749 protein ylxW
ylxX	BSU15260	SigE regulon	SigE		UPF0749 protein ylxX
sbp	BSU15270	SigE regulon	SigE		Small basic protein
spoVM	BSU15810	SigE regulon	SigE		Stage V sporulation protein M
cotE	BSU17030	SigE regulon	SigE		Spore coat protein E
spoVK	BSU17420	SigE regulon	SigE		Stage V sporulation protein K
yncD	BSU17640	SigE regulon	SigE		Alanine racemase 2
yndA	BSU17720	SigE regulon	SigE		Uncharacterized protein yndA
yngE	BSU18210	SigE regulon	SigE		Uncharacterized carboxylase YngE
yngF	BSU18220	SigE regulon	SigE		Putative enoyl-CoA hydratase/isomerase yngF
yngG	BSU18230	SigE regulon	SigE		Hydroxymethylglutaryl-CoA lyase yngG
yngH	BSU18240	SigE regulon	SigE		Biotin carboxylase 2
yngI	BSU18250	SigE regulon	SigE		Putative acyl-CoA synthetase YngI
yngJ	BSU18260	SigE regulon	SigE		Probable acyl-CoA dehydrogenase YngJ
yoaW	BSU18780	SigE regulon	SigE		Uncharacterized protein yoaW
yobW	BSU19110	SigE regulon	SigE		Protein csk22
yocL	BSU19250	SigE regulon	SigE		Uncharacterized protein yocL
sqhC	BSU19320	SigE regulon	SigE		Squalene--hopene cyclase
sodF	BSU19330	SigE regulon	SigE		Probable superoxide dismutase [Fe]
yokU	BSU19689	SigE regulon	SigE		Uncharacterized protein yodI
kamA	BSU19690	SigE regulon	SigE		L-lysine 2,3-aminomutase
yodP	BSU19700	SigE regulon	SigE		Uncharacterized N-acetyltransferase YodP
yodQ	BSU19710	SigE regulon	SigE		Uncharacterized metallohydrolase yodQ
yodR	BSU19720	SigE regulon	SigE		Probable coenzyme A transferase subunit beta
yodS	BSU19730	SigE regulon	SigE		Probable coenzyme A transferase subunit alpha
yodT	BSU19740	SigE regulon	SigE		Uncharacterized aminotransferase YodT
ypqA	BSU22240	SigE regulon	SigE		Uncharacterized protein ypqA
ypjB	BSU22520	SigE regulon	SigE		Uncharacterized protein ypjB
spoIVA	BSU22800	SigE regulon	SigE		Stage IV sporulation protein A
spmB	BSU23170	SigE regulon	SigE		Spore maturation protein B
spmA	BSU23180	SigE regulon	SigE		Spore maturation protein A
dacB	BSU23190	SigE regulon	SigE		D-alanyl-D-alanine carboxypeptidase dacB
spoIIM	BSU23530	SigE regulon	SigE		Stage II sporulation protein M

Gene name	BSU number	Regulon	Regulator	Mode of action	Description
yqiQ	BSU24120	SigE regulon	SigE		Methylisocitrate lyase
mmgE	BSU24130	SigE regulon	SigE		2-methylcitrate dehydratase
mmgD	BSU24140	SigE regulon	SigE		2-methylcitrate synthase
mmgC	BSU24150	SigE regulon	SigE		Acyl-CoA dehydrogenase
mmgB	BSU24160	SigE regulon	SigE		Probable 3-hydroxybutyryl-CoA dehydrogenase
mmgA	BSU24170	SigE regulon	SigE		Acetyl-CoA acetyltransferase
spoIIIA	BSU24360	SigE regulon	SigE		Stage III sporulation protein AH
spoIIIA	BSU24370	SigE regulon	SigE		Stage III sporulation protein AG
spoIIIA	BSU24380	SigE regulon	SigE		Stage III sporulation protein AF
spoIIIA	BSU24390	SigE regulon	SigE		Stage III sporulation protein AE
spoIIIA	BSU24400	SigE regulon	SigE		Stage III sporulation protein AD
spoIIIA	BSU24410	SigE regulon	SigE		Stage III sporulation protein AC
spoIIIA	BSU24420	SigE regulon	SigE		Stage III sporulation protein AB
spoIIIA	BSU24430	SigE regulon	SigE		Stage III sporulation protein AA
yqfZ	BSU25060	SigE regulon	SigE		Uncharacterized protein yqfZ
ispG	BSU25070	SigE regulon	SigE		4-hydroxy-3-methylbut-2-en-1-yl diphosphate synthase
yqfD	BSU25350	SigE regulon	SigE		Uncharacterized protein yqfD
yqfC	BSU25360	SigE regulon	SigE		Uncharacterized protein yqfC
yqxA	BSU25520	SigE regulon	SigE		Uncharacterized protein yqxA
spoIIP	BSU25530	SigE regulon	SigE		Stage II sporulation protein P
nucB	BSU25750	SigE regulon	SigE		Sporulation-specific extracellular nuclease
spoIVC	BSU25760	SigE regulon	SigE		Sporulation-specific extracellular nuclease
spoIVC	BSU25770	SigE regulon	SigE		Putative DNA recombinase
spoIIIC	BSU26390	SigE regulon	SigE		Uncharacterized protein yqaB
yrrS	BSU27300	SigE regulon	SigE		Uncharacterized membrane protein yrrS
pbpI	BSU27310	SigE regulon	SigE		Penicillin-binding protein 4B
glnQ	BSU27430	SigE regulon	SigE		Glutamine transport ATP-binding protein GlnQ
glnH	BSU27440	SigE regulon	SigE		ABC transporter glutamine-binding protein glnH
glnM	BSU27450	SigE regulon	SigE		Probable glutamine ABC transporter permease protein
glnP	BSU27460	SigE regulon	SigE		Probable glutamine ABC transporter permease protein
spoVB	BSU27670	SigE regulon	SigE		Stage V sporulation protein B
coxA	BSU27830	SigE regulon	SigE		Sporulation cortex protein CoxA
safA	BSU27840	SigE regulon	SigE		SpoIVD-associated factor A
spoIVF	BSU27970	SigE regulon	SigE		Stage IV sporulation protein FB
spoIVF	BSU27980	SigE regulon	SigE		Stage IV sporulation protein FA
ysxE	BSU28100	SigE regulon	SigE		Uncharacterized protein ysxE
spoVID	BSU28110	SigE regulon	SigE		Stage VI sporulation protein D
ysnD	BSU28320	SigE regulon	SigE		Uncharacterized protein ysnD
gerM	BSU28380	SigE regulon	SigE		Spore germination protein gerM
ytxC	BSU28960	SigE regulon	SigE		Uncharacterized protein ytxC
phoR	BSU29100	SigE regulon	SigE		Alkaline phosphatase synthesis sensor protein phoR
phoP	BSU29110	SigE regulon	SigE		Alkaline phosphatase synthesis transcriptional regulatory
ytvI	BSU29160	SigE regulon	SigE		UPF0118 membrane protein ytvI
ytrH	BSU29239	SigE regulon	SigE		DNA polymerase III subunit alpha
ytrI	BSU29240	SigE regulon	SigE		Sporulation membrane protein ytrI
yteV	BSU30080	SigE regulon	SigE		Sporulation protein cse60
glgP	BSU30940	SigE regulon	SigE		Glycogen phosphorylase
glgA	BSU30950	SigE regulon	SigE		Glycogen synthase
glgD	BSU30960	SigE regulon	SigE		Glycogen biosynthesis protein glgD
glgC	BSU30970	SigE regulon	SigE		Glucose-1-phosphate adenylyltransferase
glgB	BSU30980	SigE regulon	SigE		1,4-alpha-glucan branching enzyme GlgB
yuzC	BSU31730	SigE regulon	SigE		Uncharacterized protein yuzC
yunB	BSU32350	SigE regulon	SigE		Sporulation protein yunB
yusR	BSU32900	SigE regulon	SigE		Short-chain dehydrogenase/reductase homolog yusR
bdbC	BSU33470	SigE regulon	SigE		Disulfide bond formation protein C
bdbD	BSU33480	SigE regulon	SigE		Disulfide bond formation protein D
ctpB	BSU35240	SigE regulon	SigE		Carboxy-terminal processing protease CtpB
mbl	BSU36410	SigE regulon	SigE		MreB-like protein
spoIIID	BSU36420	SigE regulon	SigE		Stage III sporulation protein D
usd	BSU36430	SigE regulon	SigE		Protein usd

Gene name	BSU number	Regulon	Regulator	Mode of action	Description
spoIID	BSU36750	SigE regulon	SigE		Stage II sporulation protein D
spsK	BSU37820	SigE regulon	SigE		Spore coat polysaccharide biosynthesis protein spsK
spsJ	BSU37830	SigE regulon	SigE		Spore coat polysaccharide biosynthesis protein spsJ
gerQ	BSU37920	SigE regulon	SigE		Spore coat protein gerQ
ywcB	BSU38230	SigE regulon	SigE		Uncharacterized protein ywcB
ywcA	BSU38240	SigE regulon	SigE		Uncharacterized symporter ywcA
yxjF	BSU38970	SigE regulon	SigE		Uncharacterized oxidoreductase yxjF
scoB	BSU38980	SigE regulon	SigE		Probable succinyl-CoA:3-ketoacid coenzyme A
scoA	BSU38990	SigE regulon	SigE		Probable succinyl-CoA:3-ketoacid coenzyme A
yxjC	BSU39000	SigE regulon	SigE		Uncharacterized transporter YxjC
yxeD	BSU39590	SigE regulon	SigE		Uncharacterized protein yxeD
yybI	BSU40630	SigE regulon	SigE		Uncharacterized protein yybI
yyaD	BSU40940	SigE regulon	SigE		Uncharacterized protein yyaD
gin	BSU00240	SigF regulon	SigF		Protein CsfB
ksgA	BSU00420	SigF regulon	SigF		Ribosomal RNA small subunit methyltransferase A
fin	BSU00540	SigF regulon	SigF		Uncharacterized protein yabK
spoVT	BSU00560	SigF regulon	SigF		Stage V sporulation protein T
yabT	BSU00660	SigF regulon	SigF		Probable serine/threonine-protein kinase yabT
mcsA	BSU00840	SigF regulon	SigF		Uncharacterized protein yacH
mcsB	BSU00850	SigF regulon	SigF		Putative ATP:guanido phosphotransferase yacI
clpC	BSU00860	SigF regulon	SigF		Negative regulator of genetic competence ClpC/MecB
gerD	BSU01550	SigF regulon	SigF		Spore germination protein gerD
yckD	BSU03400	SigF regulon	SigF		Uncharacterized protein yckD
yhcM	BSU09140	SigF regulon	SigF		Uncharacterized protein yhcM
yhcN	BSU09150	SigF regulon	SigF		Lipoprotein yhcN
yhfM	BSU10280	SigF regulon	SigF		Uncharacterized protein yhfM
yhfW	BSU10390	SigF regulon	SigF		Putative Rieske 2Fe-2S iron-sulfur protein yhfW
yjbA	BSU11410	SigF regulon	SigF		UPF0736 protein yjbA
ylbB	BSU14950	SigF regulon	SigF		Uncharacterized protein ylbB
ylbC	BSU14960	SigF regulon	SigF		Uncharacterized membrane protein ylbC
sigG	BSU15330	SigF regulon	SigF		RNA polymerase sigma-G factor
sspN	BSU18020	SigF regulon	SigF		Small, acid-soluble spore protein N (SASP N)
tlp	BSU18030	SigF regulon	SigF		Small, acid-soluble spore protein Tlp
seaA	BSU22850	SigF regulon	SigF		Uncharacterized protein yphB
yphA	BSU22860	SigF regulon	SigF		Uncharacterized protein yphA
ypfB	BSU22900	SigF regulon	SigF		Uncharacterized protein ypfB
sigF	BSU23450	SigF regulon	SigF		RNA polymerase sigma-F factor
spoIIAB	BSU23460	SigF regulon	SigF		Anti-sigma F factor
spoIIAA	BSU23470	SigF regulon	SigF		Anti-sigma F factor antagonist
dacF	BSU23480	SigF regulon	SigF		D-alanyl-D-alanine carboxypeptidase dacF
spoIVB	BSU24230	SigF regulon	SigF		SpoIVB peptidase
yqhQ	BSU24490	SigF regulon	SigF		Uncharacterized protein yqhQ
yqhP	BSU24500	SigF regulon	SigF		Uncharacterized protein yqhP
yqhH	BSU24580	SigF regulon	SigF		Uncharacterized ATP-dependent helicase yqhH
yqhG	BSU24590	SigF regulon	SigF		Uncharacterized protein yqhG
yqzG	BSU24650	SigF regulon	SigF		Uncharacterized protein yqzG
spoIIP	BSU25530	SigF regulon	SigF		Stage II sporulation protein P
gpr	BSU25540	SigF regulon	SigF		Germination protease
arsC	BSU25780	SigF regulon	SigF		Protein ArsC
arsB	BSU25790	SigF regulon	SigF		Arsenite resistance protein ArsB
yqcK	BSU25800	SigF regulon	SigF		Uncharacterized protein yqcK
arsR	BSU25810	SigF regulon	SigF		Arsenical resistance operon repressor
yrrS	BSU27300	SigF regulon	SigF		Uncharacterized membrane protein yrrS
pbpI	BSU27310	SigF regulon	SigF		Penicillin-binding protein 4B
bofC	BSU27750	SigF regulon	SigF		Protein BofC
csbX	BSU27760	SigF regulon	SigF		Alpha-ketoglutarate permease
lonB	BSU28210	SigF regulon	SigF		Lon protease 2
ytfJ	BSU29500	SigF regulon	SigF		Uncharacterized spore protein ytfJ
ytfI	BSU29510	SigF regulon	SigF		Uncharacterized protein ytfI
mutTA	BSU30630	SigF regulon	SigF		Putative 8-oxo-dGTP diphosphatase YtkD

Gene name	BSU number	Regulon	Regulator	Mode of action	Description
yuiC	BSU32070	SigF regulon	SigF		Uncharacterized protein yuiC
gerAA	BSU33050	SigF regulon	SigF		Spore germination protein A1
gerAB	BSU33060	SigF regulon	SigF		Spore germination protein A2
gerAC	BSU33070	SigF regulon	SigF		Spore germination protein A3
tuaH	BSU35540	SigF regulon	SigF		Putative teichuronic acid biosynthesis glycosyltransferase
tuaG	BSU35550	SigF regulon	SigF		Putative teichuronic acid biosynthesis glycosyltransferase
tuaF	BSU35560	SigF regulon	SigF		Teichuronic acid biosynthesis protein tuaF
ywnJ	BSU36540	SigF regulon	SigF		Uncharacterized membrane protein ywnJ
spoIIQ	BSU36550	SigF regulon	SigF		Stage II sporulation protein Q
spoIIR	BSU36970	SigF regulon	SigF		Stage II sporulation protein R
pbpG	BSU37510	SigF regulon	SigF		Penicillin-binding protein 2D
rsfA	BSU37620	SigF regulon	SigF		Prespore-specific transcriptional regulator rsfA
katX	BSU38630	SigF regulon	SigF		Catalase X
yyaC	BSU40950	SigF regulon	SigF		Uncharacterized protein yyaC
csfG	BSUNA	SigF regulon	SigF		tRNA modification GTPase MnmE
sspF	BSU00450	SigG regulon	SigG		Protein sspF
fin	BSU00540	SigG regulon	SigG		Uncharacterized protein yabK
spoVT	BSU00560	SigG regulon	SigG		Stage V sporulation protein T
ybaK	BSU01520	SigG regulon	SigG		Uncharacterized protein ybaK
cwlD	BSU01530	SigG regulon	SigG		Germination-specific N-acetylmuramoyl-L-alanine
gerD	BSU01550	SigG regulon	SigG		Spore germination protein gerD
csgA	BSU02070	SigG regulon	SigG		Sigma-G-dependent sporulation-specific SASP protein
ybxH	BSU02080	SigG regulon	SigG		Uncharacterized protein ybxH
yckD	BSU03400	SigG regulon	SigG		Uncharacterized protein yckD
gerKA	BSU03700	SigG regulon	SigG		Spore germination protein KA
gerKC	BSU03710	SigG regulon	SigG		Spore germination protein KC
gerKB	BSU03720	SigG regulon	SigG		Spore germination protein KB
glcU	BSU03920	SigG regulon	SigG		Glucose uptake protein glcU
gdh	BSU03930	SigG regulon	SigG		Glucose 1-dehydrogenase
ydfR	BSU05530	SigG regulon	SigG		UPF0702 transmembrane protein ydfR
ydfS	BSU05540	SigG regulon	SigG		UPF0702 transmembrane protein ydfS
yfkR	BSU07780	SigG regulon	SigG		Putative spore germination protein yfkR
yfkQ	BSU07790	SigG regulon	SigG		Uncharacterized membrane protein yfkQ
chaA	BSU07920	SigG regulon	SigG		Putative cation exchanger yfkE
pdaA	BSU07980	SigG regulon	SigG		Probable polysaccharide deacetylase pdaA
sspH	BSU08110	SigG regulon	SigG		Small, acid-soluble spore protein H
sspK	BSU08550	SigG regulon	SigG		Small, acid-soluble spore protein K
fabL	BSU08650	SigG regulon	SigG		Enoyl-[acyl-carrier-protein] reductase [NADPH]
sspE	BSU08660	SigG regulon	SigG		Small, acid-soluble spore protein gamma-type
yhcM	BSU09140	SigG regulon	SigG		Uncharacterized protein yhcM
yhcN	BSU09150	SigG regulon	SigG		Lipoprotein yhcN
yhcQ	BSU09180	SigG regulon	SigG		Spore coat protein F-like protein YhcQ
yhcV	BSU09230	SigG regulon	SigG		CBS domain-containing protein yhcV
sspB	BSU09750	SigG regulon	SigG		Small, acid-soluble spore protein B
pbpF	BSU10110	SigG regulon	SigG		Penicillin-binding protein 1F
yisY	BSU10900	SigG regulon	SigG		AB hydrolase superfamily protein yisY
yitF	BSU10970	SigG regulon	SigG		Putative isomerase yitF
yitG	BSU10980	SigG regulon	SigG		Uncharacterized MFS-type transporter yitG
ykoU	BSU13400	SigG regulon	SigG		Probable ATP-dependent DNA ligase ykoU
ykoV	BSU13410	SigG regulon	SigG		Probable DNA repair protein ykoV
sspD	BSU13470	SigG regulon	SigG		Small, acid-soluble spore protein D
stoA	BSU13840	SigG regulon	SigG		Sporulation thiol-disulfide oxidoreductase A
splA	BSU13920	SigG regulon	SigG		Transcriptional regulator splA
splB	BSU13930	SigG regulon	SigG		Spore photoproduct lyase
ylaJ	BSU14800	SigG regulon	SigG		Uncharacterized lipoprotein ylaJ
sigG	BSU15330	SigG regulon	SigG		RNA polymerase sigma-G factor
yndD	BSU17750	SigG regulon	SigG		Uncharacterized membrane protein yndD
yndE	BSU17760	SigG regulon	SigG		Spore germination protein YndE
yndF	BSU17770	SigG regulon	SigG		Spore germination protein yndF
sspP	BSU17980	SigG regulon	SigG		Small, acid-soluble spore protein P

Gene name	BSU number	Regulon	Regulator	Mode of action	Description
sspO	BSU17990	SigG regulon	SigG		Small, acid-soluble spore protein O
sspN	BSU18020	SigG regulon	SigG		Small, acid-soluble spore protein N
tlp	BSU18030	SigG regulon	SigG		Small, acid-soluble spore protein Tlp
yozQ	BSU18600	SigG regulon	SigG		Uncharacterized protein yozQ
yoaR	BSU18720	SigG regulon	SigG		Uncharacterized protein yoaR
sspC	BSU19950	SigG regulon	SigG		Small, acid-soluble spore protein C
ypzA	BSU21950	SigG regulon	SigG		Uncharacterized protein ypzA
sspL	BSU22000	SigG regulon	SigG		Small, acid-soluble spore protein L
sspM	BSU22290	SigG regulon	SigG		Small, acid-soluble spore protein M
ypeB	BSU22920	SigG regulon	SigG		Sporulation protein ypeB
sleB	BSU22930	SigG regulon	SigG		Spore cortex-lytic enzyme
lysA	BSU23380	SigG regulon	SigG		Diaminopimelate decarboxylase
spoVAF	BSU23390	SigG regulon	SigG		Stage V sporulation protein AF
spoVAD	BSU23410	SigG regulon	SigG		Stage V sporulation protein AD
spoVAC	BSU23420	SigG regulon	SigG		Stage V sporulation protein AC
spoVAB	BSU23430	SigG regulon	SigG		Stage V sporulation protein AB
spoVAA	BSU23440	SigG regulon	SigG		Stage V sporulation protein AA
sigF	BSU23450	SigG regulon	SigG		RNA polymerase sigma-F factor
spoIIAB	BSU23460	SigG regulon	SigG		Anti-sigma F factor
spoIIAA	BSU23470	SigG regulon	SigG		Anti-sigma F factor antagonist
dacF	BSU23480	SigG regulon	SigG		D-alanyl-D-alanine carboxypeptidase dacF
spoIVB	BSU24230	SigG regulon	SigG		SpoIVB peptidase
yqfX	BSU25080	SigG regulon	SigG		Uncharacterized protein yqfX
yqfU	BSU25110	SigG regulon	SigG		UPF0750 membrane protein yqfU
nfo	BSU25130	SigG regulon	SigG		Probable endonuclease 4
gpr	BSU25540	SigG regulon	SigG		Germination protease
yraG	BSU26950	SigG regulon	SigG		Spore coat protein F-like protein YraG
yraF	BSU26960	SigG regulon	SigG		Spore coat protein F-like protein YraF
adhB	BSU26970	SigG regulon	SigG		Uncharacterized zinc-type alcohol dehydrogenase-like
yraE	BSU26980	SigG regulon	SigG		Uncharacterized protein yraE
yraD	BSU26990	SigG regulon	SigG		Spore coat protein F-like protein YraD
yrrD	BSU27470	SigG regulon	SigG		Uncharacterized protein yrrD
bofC	BSU27750	SigG regulon	SigG		Protein BofC
csbX	BSU27760	SigG regulon	SigG		Alpha-ketoglutarate permease
sspI	BSU28660	SigG regulon	SigG		Small, acid-soluble spore protein I
sspA	BSU29570	SigG regulon	SigG		Small, acid-soluble spore protein A
yteA	BSU30840	SigG regulon	SigG		Uncharacterized protein YteA
yuzA	BSU31380	SigG regulon	SigG		Uncharacterized membrane protein yuzA
yusN	BSU32860	SigG regulon	SigG		Uncharacterized protein yusN
gerAA	BSU33050	SigG regulon	SigG		Spore germination protein A1
gerAB	BSU33060	SigG regulon	SigG		Spore germination protein A2
gerAC	BSU33070	SigG regulon	SigG		Spore germination protein A3
sspJ	BSU33340	SigG regulon	SigG		Small, acid-soluble spore protein J
azoR2	BSU33540	SigG regulon	SigG		FMN-dependent NADH-azoreductase 2
yvdQ	BSU34510	SigG regulon	SigG		Uncharacterized protein yvdQ
cotQ	BSU34520	SigG regulon	SigG		Uncharacterized FAD-linked oxidoreductase yvdP
ctpB	BSU35240	SigG regulon	SigG		Carboxy-terminal processing protease CtpB
gerBA	BSU35800	SigG regulon	SigG		Spore germination protein B1
gerBB	BSU35810	SigG regulon	SigG		Spore germination protein B2
gerBC	BSU35820	SigG regulon	SigG		Spore germination protein B3
pbpG	BSU37510	SigG regulon	SigG		Penicillin-binding protein 2D
rsfA	BSU37620	SigG regulon	SigG		Prespore-specific transcriptional regulator rsfA
yxeD	BSU39590	SigG regulon	SigG		Uncharacterized protein yxeD
yyxA	BSU40360	SigG regulon	SigG		Uncharacterized serine protease yyxA
ccpB	BSU40870	SigG regulon	SigG		Catabolite control protein B
exoA	BSU40880	SigG regulon	SigG		Exodeoxyribonuclease
csfG	BSUNA	SigG regulon	SigG		tRNA modification GTPase MnmE
xpaC	BSU00250	SigW regulon	SigW		Protein xpaC
yaaN	BSU00260	SigW regulon	SigW		Uncharacterized protein yaaN
divIC	BSU00620	SigW regulon	SigW		Cell division protein divIC

Gene name	BSU number	Regulon	Regulator	Mode of action	Description
sigW	BSU01730	SigW regulon	SigW		RNA polymerase sigma factor sigW
rsiW	BSU01740	SigW regulon	SigW		Anti-sigma-W factor rsiW
ybfO	BSU02310	SigW regulon	SigW		Putative hydrolase ybfO
ybfP	BSU02320	SigW regulon	SigW		Uncharacterized HTH-type transcriptional regulator YbfP
ybfQ	BSU02330	SigW regulon	SigW		UPF0176 protein ybfQ
yceC	BSU02890	SigW regulon	SigW		Stress response protein SCP2
yceD	BSU02900	SigW regulon	SigW		General stress protein 16U
yceE	BSU02910	SigW regulon	SigW		Uncharacterized protein YceE
yceF	BSU02920	SigW regulon	SigW		Uncharacterized membrane protein yceF
yceG	BSU02930	SigW regulon	SigW		Uncharacterized protein yceG
yceH	BSU02940	SigW regulon	SigW		Uncharacterized protein yceH
ydbS	BSU04590	SigW regulon	SigW		UPF0699 transmembrane protein ydbS
ydbT	BSU04600	SigW regulon	SigW		UPF0699 transmembrane protein ydbT
pspA	BSU06180	SigW regulon	SigW		Phage shock protein A homolog
ydjO	BSU06270	SigW regulon	SigW		Uncharacterized protein ydjO
ydjP	BSU06280	SigW regulon	SigW		AB hydrolase superfamily protein ydjP
yeaA	BSU06290	SigW regulon	SigW		Uncharacterized protein yeaA
yfhL	BSU08580	SigW regulon	SigW		Uncharacterized protein yfhL
yfhM	BSU08590	SigW regulon	SigW		AB hydrolase superfamily protein yfhM
spo0M	BSU08760	SigW regulon	SigW		Sporulation-control protein spo0M
fabF	BSU11340	SigW regulon	SigW		3-oxoacyl-[acyl-carrier-protein] synthase 2
yjbC	BSU11490	SigW regulon	SigW		Putative acetyltransferase YjbC
spx	BSU11500	SigW regulon	SigW		Regulatory protein spx
yjoB	BSU12420	SigW regulon	SigW		Uncharacterized ATPase YjoB
yknW	BSU14340	SigW regulon	SigW		Uncharacterized protein yknW
yknX	BSU14350	SigW regulon	SigW		Putative efflux system component yknX
yknY	BSU14360	SigW regulon	SigW		Uncharacterized ABC transporter ATP-binding protein
yknZ	BSU14370	SigW regulon	SigW		Uncharacterized ABC transporter permease yknZ
fosB	BSU17840	SigW regulon	SigW		Metallothiol transferase fosB
yoaF	BSU18580	SigW regulon	SigW		Uncharacterized protein yoaF
yoaG	BSU18590	SigW regulon	SigW		UPF0715 membrane protein yoaG
yobJ	BSU18980	SigW regulon	SigW		Uncharacterized protein yobJ
yozO	BSU19290	SigW regulon	SigW		Uncharacterized protein yozO
yqjL	BSU23830	SigW regulon	SigW		Uncharacterized protein yqjL
yqfB	BSU25370	SigW regulon	SigW		Uncharacterized protein yqfB
yqfA	BSU25380	SigW regulon	SigW		UPF0365 protein yqfA
yqeZ	BSU25390	SigW regulon	SigW		Uncharacterized protein yqeZ
yrhJ	BSU27160	SigW regulon	SigW		Probable bifunctional P-450/NADPH-P450 reductase 2
fatR	BSU27170	SigW regulon	SigW		HTH-type transcriptional repressor BscR
yrhH	BSU27180	SigW regulon	SigW		Putative methyltransferase yrhH
ysdB	BSU28830	SigW regulon	SigW		Sigma-w pathway protein ysdB
yteJ	BSU29520	SigW regulon	SigW		Uncharacterized membrane protein yteJ
sppA	BSU29530	SigW regulon	SigW		Putative signal peptide peptidase sppA
ythQ	BSU30000	SigW regulon	SigW		Putative transporter ythQ
ythP	BSU30010	SigW regulon	SigW		Uncharacterized ABC transporter ATP-binding protein
yuaI	BSU31000	SigW regulon	SigW		Uncharacterized N-acetyltransferase YuaI
floT	BSU31010	SigW regulon	SigW		Uncharacterized protein yuaG
yuaF	BSU31020	SigW regulon	SigW		Uncharacterized membrane protein yuaF
racX	BSU34430	SigW regulon	SigW		Probable amino-acid racemase
pbpE	BSU34440	SigW regulon	SigW		Penicillin-binding protein 4*
yvlD	BSU35100	SigW regulon	SigW		Uncharacterized membrane protein yvlD
yvlC	BSU35110	SigW regulon	SigW		Uncharacterized membrane protein yvlC
yvlB	BSU35120	SigW regulon	SigW		Uncharacterized protein yvlB
yvlA	BSU35130	SigW regulon	SigW		Uncharacterized protein yvlA
ywrE	BSU36090	SigW regulon	SigW		Uncharacterized protein ywrE
bcrC	BSU36530	SigW regulon	SigW		Undecaprenyl-diphosphatase BcrC
ywnJ	BSU36540	SigW regulon	SigW		Uncharacterized membrane protein ywnJ
ywbO	BSU38250	SigW regulon	SigW		Uncharacterized protein ywbO
ywbN	BSU38260	SigW regulon	SigW		Probable deferrochelatase/peroxidase EfeN
ywaC	BSU38480	SigW regulon	SigW		GTP pyrophosphokinase ywaC

Gene name	BSU number	Regulon	Regulator	Mode of action	Description
yxzE	BSU38790	SigW regulon	SigW		Uncharacterized protein yxzE
yxjI	BSU38940	SigW regulon	SigW		Uncharacterized protein yxjI

Table S 2 : List of genes regulated more than three folds with respective to their controls with a p-Value of 0.01 (after Benjamin Hochberg correction). The following data was used in the Figure 18 of the main text.

Gene name	BSU number	Up regulated	Down regulated
dnaN	BSU00020		M9_stationary
yaaA	BSU00030		M9_stationary
dacA	BSU00100		M9_stationary
pdxS	BSU00110		M9_stationary
pdxT	BSU00120		M9_stationary
serS	BSU00130		M9_stationary
yaaH	BSU00160	16°C, M9_stationary	
yaaI	BSU00170	51°C	
bofA	BSU00230	16°C	
csfB	BSU00240	16°C	
yabE	BSU00400	16°C	
sspF	BSU00450	16°C	
purR	BSU00470		M9_stationary
yabN	BSU00580		M9_stationary
spoIIE	BSU00640	16°C, M9_stationary	
yabS	BSU00650	16°C, M9_stationary	
yabT	BSU00660	16°C, M9_stationary	
lysS	BSU00820		M9_stationary
rplJ	BSU01040		M9_stationary
rplL	BSU01050		M9_stationary
ybxB	BSU01060		M9_stationary
rplC	BSU01160		M9_stationary
rpsC	BSU01220		M9_stationary
rpmC	BSU01240		M9_stationary
rplN	BSU01260		M9_stationary
rplE	BSU01280		M9_stationary
rpsN1	BSU01290		M9_stationary
rpsH	BSU01300		M9_stationary
rplF	BSU01310		M9_stationary
rplR	BSU01320		M9_stationary
rpsE	BSU01330		M9_stationary
rpmD	BSU01340		M9_stationary
rplO	BSU01350		M9_stationary
secY	BSU01360		M9_stationary
adk	BSU01370		M9_stationary
map	BSU01380		M9_stationary
ybzG	BSU01389		M9_stationary
infA	BSU01390		M9_stationary
rpmJ	BSU01400		M9_stationary
rpsM	BSU01410		M9_stationary
rpsK	BSU01420		M9_stationary
rplQ	BSU01440		M9_stationary
truA	BSU01480		M9_stationary
cwlD	BSU01530	16°C, M9_stationary	
pdaB	BSU01570	16°C, M9_stationary	
ybbA	BSU01600	1.2 M NaCl	M9_stationary
feuC	BSU01610	1.2 M NaCl	M9_stationary
feuB	BSU01620	1.2 M NaCl	M9_stationary
feuA	BSU01630	1.2 M NaCl	M9_stationary
ybbC	BSU01650	M9_stationary	
ybbD	BSU01660	M9_stationary	
skfA	BSU01910	M9_stationary	51°C
skfB	BSU01920	M9_stationary	1.2 M NaCl, 51°C
skfC	BSU01920	M9_stationary	1.2 M NaCl, 51°C
skfE	BSU01950	M9_stationary	51°C
skfF	BSU01960	M9_stationary	51°C
skfG	BSU01970	M9_stationary	51°C

Gene name	BSU number	Up regulated	Down regulated
skfH	BSU01980	M9_stationary	51°C
ybdN	BSU02040		51°C
ybdO	BSU02050		1.2 M NaCl, 51°C, 16°C
csgA	BSU02070	M9_stationary	
cypC	BSU02100	51°C	
ybyB	BSU02110	51°C, 16°C, M9_stationary	
ybfB	BSU02170	51°C	
ybfG	BSU02200	51°C	
purT	BSU02230		M9_stationary
mpr	BSU02240	16°C, M9_stationary	
ybfJ	BSU02250	16°C, M9_stationary	
ybfO	BSU02310		1.2 M NaCl, 51°C
ybfP	BSU02320		1.2 M NaCl, 51°C
gltP	BSU02340	M9_stationary	
gamP	BSU02350		16°C
gamA	BSU02360		16°C
ilvE	BSU02390	M9_stationary	
ybgF	BSU02400		M9_stationary
ybgG	BSU02410		M9_stationary
ycbJ	BSU02520	16°C	51°C
cwlJ	BSU02600	16°C	51°C
lmrB	BSU02670		M9_stationary
lmrA	BSU02680		M9_stationary
estA	BSU02700		M9_stationary
ycdA	BSU02780		16°C, M9_stationary
ycdF	BSU02830	51°C, 16°C	
ycdG	BSU02840	51°C, 16°C	
adcB	BSU02870		M9_stationary
yceD	BSU02900		16°C
yceG	BSU02930		16°C, M9_stationary
yceH	BSU02940		16°C, M9_stationary
naiP	BSU02950		M9_stationary
opuAA	BSU02980		M9_stationary
opuAB	BSU02990		M9_stationary
opuAC	BSU03000		M9_stationary
amhX	BSU03010	M9_stationary	
amyE	BSU03040	M9_stationary	
ldh	BSU03050	51°C	1.2 M NaCl, 16°C
lctP	BSU03060	51°C	
bmr3	BSU03070		M9_stationary
ycgF	BSU03090	16°C	
cah	BSU03180		M9_stationary
ycgM	BSU03200	1.2 M NaCl, 16°C	
ycgN	BSU03210	1.2 M NaCl, 16°C	
ycgT	BSU03270		M9_stationary
nasD	BSU03300		16°C
yckA	BSU03370		16°C
yckB	BSU03380		16°C
yckC	BSU03390	16°C	
yckD	BSU03400	16°C	
nin	BSU03420		51°C, 16°C
nucA	BSU03430		51°C, 16°C
hxlR	BSU03470		16°C
yczE	BSU03580		M9_stationary
tcyC	BSU03590		M9_stationary
tcyB	BSU03600		M9_stationary
tcyA	BSU03610		M9_stationary
yclF	BSU03670	16°C	
yczN	BSU03789		1.2 M NaCl, 51°C
yclO	BSU03810		M9_stationary

Gene name	BSU number	Up regulated	Down regulated
yclP	BSU03820		M9_stationary
yclQ	BSU03830		M9_stationary
ycnB	BSU03840		M9_stationary
ycnC	BSU03850		M9_stationary
nfrA2	BSU03860		16°C
ycnE	BSU03870		16°C
gabD	BSU03910		16°C
yczO	BSU04039	51°C, 16°C, M9_stationary	
ycsF	BSU04050		M9_stationary
ycsG	BSU04060		16°C, M9_stationary
ycsI	BSU04070		M9_stationary
kipI	BSU04080		16°C, M9_stationary
kipA	BSU04090		M9_stationary
kipR	BSU04100		M9_stationary
lipC	BSU04110		M9_stationary
yczI	BSU04120		1.2 M NaCl
ydaC	BSU04180	16°C	
ydaD	BSU04190	51°C, 16°C, M9_stationary	
ydaE	BSU04200	51°C, 16°C, M9_stationary	
ydaG	BSU04220	M9_stationary	
ydzA	BSU04240	M9_stationary	
ydaP	BSU04340	51°C	
ydaS	BSU04370	1.2 M NaCl, 51°C, M9_stationary	
ydaT	BSU04380	51°C, M9_stationary	
gsiB	BSU04400	1.2 M NaCl, 51°C, 16°C, M9_stationary	
ydbD	BSU04430	51°C, M9_stationary	
ydbJ	BSU04490		M9_stationary
ydbK	BSU04500		M9_stationary
ydbN	BSU04530	1.2 M NaCl	M9_stationary
ydbS	BSU04590		M9_stationary
ydbT	BSU04600		M9_stationary
ydcC	BSU04630	16°C, M9_stationary	
rsbU	BSU04700		M9_stationary
rsbV	BSU04710	16°C	
rsbW	BSU04720	16°C	
sigB	BSU04730	16°C	
rsbX	BSU04740	16°C	
int	BSU04800		16°C
immA	BSU04810		16°C
xis	BSU04830	1.2 M NaCl	
ydzL	BSU04839	1.2 M NaCl	
ydcO	BSU04840	1.2 M NaCl	
ydcP	BSU04850	1.2 M NaCl	
ydcQ	BSU04860	1.2 M NaCl	
nicK	BSU04870	1.2 M NaCl	
ydcS	BSU04880	1.2 M NaCl	
ydcT	BSU04890	1.2 M NaCl	
yddA	BSU04900	1.2 M NaCl	
yddB	BSU04910	1.2 M NaCl	
yddC	BSU04920	1.2 M NaCl	
yddD	BSU04930	1.2 M NaCl	
yddE	BSU04940	1.2 M NaCl	
ydeB	BSU05130	16°C, M9_stationary	
ydeC	BSU05150	51°C	
ydgK	BSU05680		M9_stationary
ydhD	BSU05710	M9_stationary	
ydhF	BSU05730	16°C	
phoB	BSU05740	16°C, M9_stationary	
ydhK	BSU05790	51°C	
gmuB	BSU05810	M9_stationary	

Gene name	BSU number	Up regulated	Down regulated
gmuA	BSU05820	M9_stationary	
gmuC	BSU05830	M9_stationary	
gmuD	BSU05840	M9_stationary	
ydiC	BSU05920		M9_stationary
rimI	BSU05930		M9_stationary
gcp	BSU05940		M9_stationary
tatAy	BSU05980	M9_stationary	
tatC2	BSU05990	M9_stationary	
ydjF	BSU06180		51°C, 16°C, M9_stationary
ydjG	BSU06190		51°C, 16°C, M9_stationary
ydjH	BSU06200		1.2 M NaCl, 51°C, 16°C, M9_stationary
ydjI	BSU06210		51°C, 16°C, M9_stationary
ydjM	BSU06250		M9_stationary
ydjN	BSU06260		M9_stationary
ydjO	BSU06270	16°C	
cotA	BSU06300		51°C
yebA	BSU06350		M9_stationary
guaA	BSU06360		M9_stationary
pbuG	BSU06370		M9_stationary
yebC	BSU06380	M9_stationary	16°C
yebD	BSU06390	M9_stationary	
yebE	BSU06400	51°C, M9_stationary	
purE	BSU06420		M9_stationary
purK	BSU06430		M9_stationary
purB	BSU06440		M9_stationary
purC	BSU06450		M9_stationary
yexA	BSU06460		M9_stationary
purQ	BSU06470		M9_stationary
purL	BSU06480		M9_stationary
purF	BSU06490		M9_stationary
purM	BSU06500		M9_stationary
purN	BSU06510		M9_stationary
purH	BSU06520		M9_stationary
purD	BSU06530		M9_stationary
yerA	BSU06560	M9_stationary	
yerD	BSU06590	51°C	
opuE	BSU06660	1.2 M NaCl	
gatA	BSU06680		M9_stationary
gatB	BSU06690		M9_stationary
phrH	BSU06839		16°C
rapH	BSU06839		16°C
yeeK	BSU06850		1.2 M NaCl, 51°C, 16°C
cotJA	BSU06890	16°C, M9_stationary	51°C
cotJB	BSU06900	16°C, M9_stationary	51°C
cotJC	BSU06910	16°C, M9_stationary	51°C
yesJ	BSU06920	16°C, M9_stationary	
yesL	BSU06940	M9_stationary	
yesM	BSU06950	M9_stationary	
yesN	BSU06960	M9_stationary	
yesO	BSU06970	M9_stationary	
yesW	BSU07050	M9_stationary	
yetF	BSU07140	16°C	
yetG	BSU07150		51°C, M9_stationary
yezD	BSU07190		M9_stationary
yetJ	BSU07200		M9_stationary
yfnA	BSU07340		M9_stationary
yfmT	BSU07350		1.2 M NaClM9_stationary
yfmS	BSU07360		1.2 M NaClM9_stationary
yfmG	BSU07480		51°C
yfmF	BSU07490		16°C

Gene name	BSU number	Up regulated	Down regulated
yfmE	BSU07500		16°C
yfmA	BSU07540	16°C	
yflT	BSU07550	51°C, 16°C, M9_stationary	
pel	BSU07560		1.2 M NaCl, 16°C
citM	BSU07610	M9_stationary	
yflN	BSU07620	M9_stationary	
yflJ	BSU07660	16°C, M9_stationary	
yflA	BSU07750	16°C	
treP	BSU07800	M9_stationary	
treA	BSU07810	M9_stationary	
yfkN	BSU07840	1.2 M NaCl	16°C
yfkM	BSU07850	1.2 M NaCl, 51°C, 16°C, M9_stationary	
yfkJ	BSU07880	16°C, M9_stationary	
yfkI	BSU07890	M9_stationary	
yfkE	BSU07920	16°C	
yfzA	BSU08029	M9_stationary	
acoA	BSU08060	M9_stationary	
acoB	BSU08070	M9_stationary	
acoC	BSU08080	M9_stationary	
acoL	BSU08090	M9_stationary	
acoR	BSU08100	M9_stationary	
sspH	BSU08110	M9_stationary	
yfjE	BSU08130	1.2 M NaCl, 51°C	
yfjD	BSU08140	1.2 M NaCl, 51°C	
yfjC	BSU08150	1.2 M NaCl, 51°C	16°C
yfjB	BSU08160	1.2 M NaCl, 51°C	16°C
yfjA	BSU08170	1.2 M NaCl, 51°C	16°C
glvA	BSU08180	M9_stationary	
glvR	BSU08190	M9_stationary	
glvC	BSU08200	M9_stationary	
yfiC	BSU08220		16°C
catD	BSU08230		M9_stationary
catE	BSU08240		M9_stationary
yfiG	BSU08260	M9_stationary	
yfiH	BSU08270	M9_stationary	
yfiI	BSU08280	M9_stationary	
yfiJ	BSU08290	16°C	
yfiY	BSU08440		M9_stationary
yfiZ	BSU08450		M9_stationary
yfhA	BSU08460		M9_stationary
yfhD	BSU08490	M9_stationary	
yfhE	BSU08500	16°C, M9_stationary	
yfhF	BSU08510	51°C	
yfhK	BSU08570	16°C, M9_stationary	
yfhL	BSU08580	M9_stationary	
yfhM	BSU08590	M9_stationary	
csbB	BSU08600	M9_stationary	
fabL	BSU08650		M9_stationary
ygaB	BSU08670	M9_stationary	
ygzB	BSU08740	16°C, M9_stationary	
spo0M	BSU08760		16°C
yhbB	BSU08920	16°C, M9_stationary	
prkA	BSU08970	16°C, M9_stationary	51°C
yhbH	BSU08980	16°C, M9_stationary	
yhbI	BSU08990		M9_stationary
yhbJ	BSU09000		M9_stationary
yhcA	BSU09010		M9_stationary
yhcE	BSU09050		M9_stationary
yhcG	BSU09070		M9_stationary
yhcH	BSU09080		M9_stationary

Gene name	BSU number	Up regulated	Down regulated
yhcI	BSU09090		M9_stationary
yhcJ	BSU09110		M9_stationary
tcyP	BSU09130		M9_stationary
yhcM	BSU09140	M9_stationary	
yhcN	BSU09150		51°C
yhcO	BSU09165		1.2 M NaCl, 51°C
yhcQ	BSU09180		51°C
yhcR	BSU09190	M9_stationary	
yhcS	BSU09200	M9_stationary	
yhcV	BSU09230		1.2 M NaCl, 51°C, 16°C
glpF	BSU09280	M9_stationary	
glpK	BSU09290	M9_stationary	
yhdB	BSU09350		1.2 M NaCl, 51°C, 16°C
lytF	BSU09370		1.2 M NaCl, 16°C, M9_stationary
spoVR	BSU09400	16°C, M9_stationary	
lytE	BSU09420		M9_stationary
yhdF	BSU09450	51°C	
yhdJ	BSU09490	16°C	
yhdN	BSU09530	51°C, 16°C	
yhdR	BSU09570		M9_stationary
yhdX	BSU09630	1.2 M NaCl, 51°C, M9_stationary	
yhdY	BSU09640	51°C	
nhaX	BSU09690	1.2 M NaCl, 51°C, 16°C, M9_stationary	
sspB	BSU09750		1.2 M NaCl, 51°C
yheD	BSU09770	M9_stationary	
yheC	BSU09780	M9_stationary	51°C
yhaX	BSU09830	16°C, M9_stationary	
yhaR	BSU09880	M9_stationary	
yhaL	BSU09940	16°C, M9_stationary	
yhzE	BSU09958		1.2 M NaCl, 51°C
yhzF	BSU10009	16°C, M9_stationary	
serC	BSU10020		M9_stationary
ecsB	BSU10050		16°C
ecsC	BSU10060		16°C
yhgE	BSU10160		M9_stationary
fabHB	BSU10170		51°C, 16°C, M9_stationary
yhfC	BSU10180		16°C
yhfF	BSU10210		16°C
yhfH	BSU10230	16°C, M9_stationary	
lcfB	BSU10270	M9_stationary	
yhfM	BSU10280	16°C, M9_stationary	
yhfN	BSU10290	16°C	
aprE	BSU10300	16°C, M9_stationary	
yhfO	BSU10310	16°C	
yhfS	BSU10350		M9_stationary
yhfT	BSU10360		M9_stationary
bioY	BSU10370		M9_stationary
hemAT	BSU10380		1.2 M NaClM9_stationary
yhfW	BSU10390	16°C	
yhxC	BSU10400	16°C, M9_stationary	51°C
yhzC	BSU10410	M9_stationary	
yhxD	BSU10430	51°C	
ntdR	BSU10560		51°C
addB	BSU10620		16°C
addA	BSU10630		16°C
sbcD	BSU10640		16°C, M9_stationary
gerPF	BSU10670		1.2 M NaCl, 51°C
gerPE	BSU10680		51°C
gerPD	BSU10690		1.2 M NaCl, 51°C
gerPC	BSU10700		1.2 M NaCl, 51°C

Gene name	BSU number	Up regulated	Down regulated
gerPB	BSU10710		1.2 M NaCl, 51°C
gerPA	BSU10720		1.2 M NaCl, 51°C
yisI	BSU10730	M9_stationary	51°C
wprA	BSU10770		1.2 M NaCl
asnO	BSU10790		51°C
yisT	BSU10860	M9_stationary	
yisZ	BSU10910		1.2 M NaCl, 51°C, 16°C
yitA	BSU10920		1.2 M NaCl, 51°C, 16°C
yitB	BSU10930		51°C
comB	BSU10940		1.2 M NaCl, 51°C, 16°C
yitE	BSU10960	16°C, M9_stationary	
yitJ	BSU11010		M9_stationary
yitM	BSU11040	1.2 M NaCl	16°C
yitO	BSU11055	1.2 M NaCl	
yitP	BSU11070	1.2 M NaCl	
nprB	BSU11100	1.2 M NaCl	
yitT	BSU11120	M9_stationary	
ipi	BSU11130	M9_stationary	
yitZ	BSU11180		M9_stationary
argC	BSU11190		M9_stationary
argJ	BSU11200		M9_stationary
argB	BSU11210		M9_stationary
argD	BSU11220		M9_stationary
carA	BSU11230		M9_stationary
carB	BSU11240		M9_stationary
argF	BSU11250		M9_stationary
yjaV	BSU11290	16°C	
fabHA	BSU11330		M9_stationary
appD	BSU11360	M9_stationary	
appB	BSU11390	16°C	
yjbA	BSU11410	16°C, M9_stationary	
trpS	BSU11420		M9_stationary
oppA	BSU11430	16°C, M9_stationary	
oppB	BSU11440	16°C	
oppC	BSU11450	16°C	
oppD	BSU11460	16°C	
oppF	BSU11470	16°C	
yjbC	BSU11490	M9_stationary	
yjbE	BSU11510	16°C, M9_stationary	
coiA	BSU11530		51°C, 16°C
yizD	BSU11549	16°C, M9_stationary	
yjbJ	BSU11570		16°C
yjbQ	BSU11640		M9_stationary
cotO	BSU11730	16°C, M9_stationary	
cotZ	BSU11740		1.2 M NaCl, 51°C
cotY	BSU11750		1.2 M NaCl, 51°C
cotX	BSU11760		1.2 M NaCl, 51°C, M9_stationary
cotW	BSU11770		1.2 M NaCl, 51°C, M9_stationary
cotV	BSU11780		1.2 M NaCl, 51°C, M9_stationary
yjcA	BSU11790	16°C, M9_stationary	
yjzK	BSU11799		1.2 M NaCl, 51°C
yjcZ	BSU11809		1.2 M NaCl, 51°C
spoVIF	BSU11810		1.2 M NaCl, 51°C
yjcD	BSU11820		M9_stationary
yjzE	BSU11839	16°C, M9_stationary	
metI	BSU11870		16°C, M9_stationary
metC	BSU11880		16°C, M9_stationary
yjzF	BSU11928	16°C	
yjzG	BSU11929	16°C	
yjcO	BSU11930	16°C	

Gene name	BSU number	Up regulated	Down regulated
yjcP	BSU11940		1.2 M NaCl
yjcQ	BSU11950		1.2 M NaCl
yjdB	BSU11990	M9_stationary	1.2 M NaCl
yjdH	BSU12050	16°C, M9_stationary	51°C
cotT	BSU12090		1.2 M NaCl, 51°C, 16°C
yjeA	BSU12100	M9_stationary	
yjfA	BSU12110	M9_stationary	1.2 M NaCl
yjfB	BSU12120		M9_stationary
yjgB	BSU12150	M9_stationary	
yjgC	BSU12160	51°C, 16°C	
yjhA	BSU12180		16°C, M9_stationary
yjlB	BSU12270	51°C, M9_stationary	
yjmC	BSU12320	M9_stationary	
yjmD	BSU12330	M9_stationary	
uxuA	BSU12340	M9_stationary	
uxuB	BSU12350	M9_stationary	
exuT	BSU12360	M9_stationary	
yjnA	BSU12400		M9_stationary
yjoA	BSU12410		1.2 M NaCl, 16°C
rapA	BSU12430	M9_stationary	
phrA	BSU12440	M9_stationary	
xtmA	BSU12570	51°C	
xtmB	BSU12580	51°C	
xkdE	BSU12590	51°C	
xkdF	BSU12600	51°C	
xkdG	BSU12610	51°C	
ykzL	BSU12619	51°C	
xkdH	BSU12620	51°C	
xkdI	BSU12630	51°C	
xkdJ	BSU12640	51°C	M9_stationary
ykzM	BSU12649	51°C	
xkdK	BSU12650	51°C	M9_stationary
xkdM	BSU12660	51°C	
xkdN	BSU12671	51°C	
xkzB	BSU12672	51°C	
xkdO	BSU12680	51°C	
xkdP	BSU12690	51°C	
xkdQ	BSU12700	51°C	
xkdR	BSU12710	51°C	
xkdS	BSU12720	51°C	
xkdT	BSU12730	51°C	
xkdU	BSU12740	51°C	
xkzA	BSU12749	51°C	
xkdV	BSU12750	51°C	
xkdW	BSU12760	51°C	
xkdX	BSU12770	51°C	
xepA	BSU12780	51°C	
xhlA	BSU12790	51°C	
xhlB	BSU12800	51°C	
xlyA	BSU12810	51°C	
spoIISB	BSU12820	M9_stationary	
pit	BSU12840		M9_stationary
ykaA	BSU12850		M9_stationary
steT	BSU12860		M9_stationary
fadG	BSU12890	16°C	
htrA	BSU12900		1.2 M NaCl, 16°C
dppA	BSU12920	M9_stationary	
dppB	BSU12930	1.2 M NaClM9_stationary	
dppC	BSU12940	1.2 M NaClM9_stationary	
dppD	BSU12950	M9_stationary	

Gene name	BSU number	Up regulated	Down regulated
dppE	BSU12960	1.2 M NaClM9_stationary	
ykfA	BSU12970	M9_stationary	
ykfB	BSU12980	M9_stationary	
ykfC	BSU12990	M9_stationary	
ykfD	BSU13000	M9_stationary	
ykgA	BSU13020	51°C, 16°C, M9_stationary	
proB	BSU13120		M9_stationary
proA	BSU13130		M9_stationary
ohrA	BSU13140		M9_stationary
ohrB	BSU13160	51°C, 16°C, M9_stationary	
ykzN	BSU13169	16°C, M9_stationary	
metE	BSU13180		M9_stationary
isp	BSU13190	1.2 M NaClM9_stationary	
ykoC	BSU13210	51°C	M9_stationary
ykoD	BSU13220		M9_stationary
ykoE	BSU13230		M9_stationary
ykoF	BSU13240		M9_stationary
ykoJ	BSU13280	M9_stationary	16°C
ykoM	BSU13340	M9_stationary	
ykoW	BSU13420		M9_stationary
ykzP	BSU13509		1.2 M NaCl
ykrP	BSU13520	1.2 M NaCl	
ogt	BSU13540	M9_stationary	
mtnE	BSU13580		M9_stationary
mtnW	BSU13590		M9_stationary
mtnX	BSU13600		M9_stationary
mtnB	BSU13610		M9_stationary
mtnD	BSU13620		M9_stationary
motB	BSU13680		1.2 M NaCl, 16°C
motA	BSU13690		1.2 M NaCl, 16°C
clpE	BSU13700	51°C	
ykvI	BSU13710	16°C, M9_stationary	
queC	BSU13720		M9_stationary
queD	BSU13730		M9_stationary
queE	BSU13740		M9_stationary
ykvP	BSU13780	M9_stationary	
ykvU	BSU13830	16°C, M9_stationary	
stoA	BSU13840	16°C	
ptsG	BSU13890		16°C, M9_stationary
ptsI	BSU13910		M9_stationary
ykwB	BSU13940	M9_stationary	
mcpC	BSU13950		1.2 M NaCl, 16°C
cheV	BSU14010		1.2 M NaCl, 16°C
fadH	BSU14060	16°C, M9_stationary	
ykuL	BSU14130	M9_stationary	
ykuN	BSU14150	1.2 M NaCl, 16°C	51°C, M9_stationary
ykuO	BSU14160	1.2 M NaCl, 16°C	51°C, M9_stationary
ykuP	BSU14170	1.2 M NaCl, 16°C	51°C, M9_stationary
dapH	BSU14180		M9_stationary
ykuR	BSU14190		M9_stationary
cse15	BSU14250	16°C, M9_stationary	51°C
yknX	BSU14350		16°C
yknY	BSU14360		16°C
yknZ	BSU14370		16°C
ykpC	BSU14460	51°C, 16°C	
mreBH	BSU14470	51°C	
abh	BSU14480		1.2 M NaCl
ykqA	BSU14500		M9_stationary
adeC	BSU14520		M9_stationary
ykzV	BSU14569		1.2 M NaCl, 51°C, 16°C, M9_stationary

Gene name	BSU number	Up regulated	Down regulated
pdhA	BSU14580		M9_stationary
pdhB	BSU14590		M9_stationary
pdhC	BSU14600		M9_stationary
pdhD	BSU14610		M9_stationary
ykzW	BSU14629	16°C, M9_stationary	
ykzI	BSU14660	16°C, M9_stationary	
yktD	BSU14690	16°C	
ylaJ	BSU14800	M9_stationary	
ylaK	BSU14810	16°C, M9_stationary	
glsA2	BSU14830	16°C, M9_stationary	
ctaC	BSU14890	M9_stationary	51°C
ctaD	BSU14900	M9_stationary	51°C
ctaE	BSU14910	M9_stationary	51°C
ctaF	BSU14920	M9_stationary	51°C
ctaG	BSU14930	M9_stationary	51°C
ylbA	BSU14940	M9_stationary	
ylbB	BSU14950	16°C	
ylbC	BSU14960	16°C	
ylbJ	BSU15030	16°C, M9_stationary	
ylbN	BSU15070		M9_stationary
ylbO	BSU15090	16°C, M9_stationary	51°C
ylbP	BSU15100	M9_stationary	
spoVD	BSU15170	16°C, M9_stationary	
mraY	BSU15190		M9_stationary
murD	BSU15200		M9_stationary
bpr	BSU15300	M9_stationary	
spoIIGA	BSU15310	16°C, M9_stationary	
sigE	BSU15320	16°C, M9_stationary	
sigG	BSU15330	16°C, M9_stationary	
ylmB	BSU15350	1.2 M NaCl	
ileS	BSU15430		M9_stationary
ylyB	BSU15460		M9_stationary
pyrR	BSU15470		M9_stationary
pyrP	BSU15480		M9_stationary
pyrB	BSU15490		M9_stationary
pyrC	BSU15500		M9_stationary
pyrAA	BSU15510		M9_stationary
pyrAB	BSU15520		M9_stationary
pyrK	BSU15530		M9_stationary
pyrD	BSU15540		M9_stationary
pyrF	BSU15550		M9_stationary
pyrE	BSU15560		M9_stationary
cysH	BSU15570		M9_stationary
cysP	BSU15580		M9_stationary
sat	BSU15590		M9_stationary
cysC	BSU15600		M9_stationary
sumT	BSU15610		M9_stationary
sirB	BSU15620		M9_stationary
sirC	BSU15630		M9_stationary
yloB	BSU15650	16°C, M9_stationary	
thiN	BSU15800		M9_stationary
spoVM	BSU15810	16°C, M9_stationary	
sdaAB	BSU15850	M9_stationary	
fabD	BSU15900		M9_stationary
fabG	BSU15910		M9_stationary
ylqB	BSU15960		1.2 M NaCl, 51°C
rnhB	BSU16060		M9_stationary
ylqG	BSU16070		M9_stationary
ylqH	BSU16080		M9_stationary
flgB	BSU16180		1.2 M NaCl, 16°C

Gene name	BSU number	Up regulated	Down regulated
flgC	BSU16190		1.2 M NaCl, 16°C
fliE	BSU16200		1.2 M NaCl, 16°C
fliF	BSU16210		1.2 M NaCl, 16°C
fliG	BSU16220		1.2 M NaCl, 16°C
fliH	BSU16230		1.2 M NaCl, 16°C, M9_stationary
fliI	BSU16240		1.2 M NaCl, 16°C, M9_stationary
fliJ	BSU16250		1.2 M NaCl, 16°C, M9_stationary
ylxF	BSU16260		1.2 M NaCl, 16°C, M9_stationary
fliK	BSU16270		1.2 M NaCl, 16°C, M9_stationary
ylxG	BSU16280		1.2 M NaCl, 16°C, M9_stationary
flgG	BSU16290		1.2 M NaCl, 16°C, M9_stationary
ylzI	BSU16299		1.2 M NaCl, 16°C, M9_stationary
fliL	BSU16300		1.2 M NaCl, 16°C, M9_stationary
fliM	BSU16310		1.2 M NaCl, 16°C, M9_stationary
fliY	BSU16320		1.2 M NaCl, 16°C, M9_stationary
cheY	BSU16330		1.2 M NaCl, 16°C, M9_stationary
fliZ	BSU16340		1.2 M NaCl, 16°C, M9_stationary
fliP	BSU16350		1.2 M NaCl, 16°C, M9_stationary
fliQ	BSU16360		1.2 M NaCl, 16°C, M9_stationary
fliR	BSU16370		1.2 M NaCl, 16°C, M9_stationary
flhB	BSU16380		1.2 M NaCl, 16°C, M9_stationary
flhA	BSU16390		1.2 M NaCl, 16°C, M9_stationary
flhF	BSU16400		1.2 M NaCl, 16°C, M9_stationary
ylxH	BSU16410		1.2 M NaCl, 16°C, M9_stationary
cheB	BSU16420		1.2 M NaCl, 16°C, M9_stationary
cheA	BSU16430		1.2 M NaCl, 16°C, M9_stationary
cheW	BSU16440		1.2 M NaCl, 16°C, M9_stationary
cheC	BSU16450		1.2 M NaCl, 16°C, M9_stationary
cheD	BSU16460		1.2 M NaCl, 16°C, M9_stationary
sigD	BSU16470		16°C, M9_stationary
ymxH	BSU16720	16°C, M9_stationary	
dpaA	BSU16730		1.2 M NaCl, 51°C, 16°C
dpaB	BSU16740		1.2 M NaCl, 51°C
ymfJ	BSU16880		1.2 M NaCl, 51°C
pbpX	BSU16950		1.2 M NaCl
spoVS	BSU16980	M9_stationary	
tdh	BSU16990	M9_stationary	
kbl	BSU17000	M9_stationary	
cotE	BSU17030	M9_stationary	51°C
ymzD	BSU17060		16°C
pksD	BSU17110		51°C
pksE	BSU17120		51°C
acpK	BSU17130		51°C
pksF	BSU17140		51°C
pksG	BSU17150		51°C
pksH	BSU17160		51°C, 16°C
pksI	BSU17170		51°C, 16°C
pksJ	BSU17180		16°C
pksM	BSU17200		16°C
pksN	BSU17210		16°C
pksR	BSU17220		16°C
ymaG	BSU17310		1.2 M NaCl, 51°C, 16°C, M9_stationary
ymaF	BSU17320	16°C, M9_stationary	
nrdI	BSU17370		M9_stationary
nrdE	BSU17380		M9_stationary
nrdF	BSU17390		M9_stationary
ymaB	BSU17400		M9_stationary
spoVK	BSU17420	16°C	
ynbB	BSU17440		M9_stationary
glnA	BSU17460		M9_stationary

Gene name	BSU number	Up regulated	Down regulated
ynxB	BSU17470	M9_stationary	
yncC	BSU17630	51°C, M9_stationary	
alr2	BSU17640	16°C, M9_stationary	
yncM	BSU17690	M9_stationary	
cotC	BSU17700		1.2 M NaCl
tatAc	BSU17710	M9_stationary	
yndA	BSU17720	16°C, M9_stationary	
ynzB	BSU17740	16°C	
fosB	BSU17840		16°C
tkt	BSU17890		M9_stationary
sirA	BSU17900	16°C, M9_stationary	
cotM	BSU17970		51°C
sspP	BSU17980		1.2 M NaCl, 51°C
sspO	BSU17990		1.2 M NaCl, 51°C
birA	BSU18000		M9_stationary
glmS	BSU18000	M9_stationary	
proH	BSU18000	1.2 M NaCl	
yneN	BSU18010	M9_stationary	
ynzL	BSU18019	16°C, M9_stationary	
sspN	BSU18020	M9_stationary	1.2 M NaCl
tlp	BSU18030	M9_stationary	1.2 M NaCl
ynfC	BSU18110	16°C	
alsT	BSU18120		M9_stationary
yngE	BSU18210	M9_stationary	
yngF	BSU18220	M9_stationary	
yngG	BSU18230	M9_stationary	
yngHB	BSU18239	16°C, M9_stationary	
accC2	BSU18240	16°C, M9_stationary	
yngI	BSU18250	M9_stationary	
yngJ	BSU18260	16°C, M9_stationary	
dacC	BSU18350	M9_stationary	
galM	BSU18360	M9_stationary	
yoeB	BSU18380	M9_stationary	
ggt	BSU18410	M9_stationary	
gltB	BSU18440		M9_stationary
gltA	BSU18450		M9_stationary
proJ	BSU18470	1.2 M NaCl	
yoxD	BSU18500		M9_stationary
yoxC	BSU18510	51°C, 16°C, M9_stationary	
yoxB	BSU18520	16°C, M9_stationary	
yoaA	BSU18530	16°C, M9_stationary	
yoaB	BSU18540	51°C	M9_stationary
yoaC	BSU18550	51°C	M9_stationary
yoaD	BSU18560		M9_stationary
yoaE	BSU18570		M9_stationary
yoaG	BSU18590		16°C
yoaH	BSU18610		1.2 M NaClM9_stationary
yoaJ	BSU18630	1.2 M NaCl	
oxdD	BSU18670		1.2 M NaCl, 51°C
yoaQ	BSU18700	16°C	
yoaS	BSU18730	16°C	
yozG	BSU18740	16°C	
yoaT	BSU18750	16°C	
yoaV	BSU18770	16°C	
yoaW	BSU18780	M9_stationary	
yobB	BSU18820	M9_stationary	
yozY	BSU18908	M9_stationary	
yozM	BSU18960	M9_stationary	
yobJ	BSU18980		16°C
yobN	BSU19020	M9_stationary	

Gene name	BSU number	Up regulated	Down regulated
yobO	BSU19030	M9_stationary	
yobT	BSU19080	51°C	
csk22	BSU19110	16°C, M9_stationary	
yocB	BSU19150	51°C, 16°C, M9_stationary	
yocC	BSU19160		M9_stationary
des	BSU19180	16°C	
yocH	BSU19210		M9_stationary
recQ	BSU19220	16°C	
azoR1	BSU19230		M9_stationary
yocK	BSU19240	16°C, M9_stationary	
yoyB	BSU19259	16°C, M9_stationary	
yozN	BSU19270	16°C, M9_stationary	51°C
yocN	BSU19280	16°C, M9_stationary	51°C
dhaS	BSU19310	M9_stationary	
sqhC	BSU19320	16°C, M9_stationary	
sodF	BSU19330	16°C, M9_stationary	
yojK	BSU19420		16°C
yojJ	BSU19430	M9_stationary	
gerT	BSU19490		51°C
yojB	BSU19510		1.2 M NaCl, 51°C, 16°C
yodC	BSU19550		M9_stationary
yoyD	BSU19579		M9_stationary
yodF	BSU19580		M9_stationary
yodL	BSU19640	16°C, M9_stationary	
yodM	BSU19650	16°C	
yozD	BSU19660	16°C, M9_stationary	
yoyF	BSU19669	16°C, M9_stationary	
yokU	BSU19689	M9_stationary	
kamA	BSU19690	16°C, M9_stationary	
yodP	BSU19700	16°C, M9_stationary	
yodQ	BSU19710	16°C, M9_stationary	
yodR	BSU19720	16°C, M9_stationary	
yodS	BSU19730	16°C, M9_stationary	
yodT	BSU19740	16°C, M9_stationary	
yoyG	BSU19749		1.2 M NaCl, 51°C
cgeC	BSU19770		1.2 M NaCl, 51°C
cgeA	BSU19780		1.2 M NaCl, 51°C
cgeB	BSU19790		1.2 M NaCl, 51°C
yotL	BSU19840	M9_stationary	
yosU	BSU20000		M9_stationary
yorD	BSU20420		51°C
yorB	BSU20440	M9_stationary	
yoqM	BSU20580	M9_stationary	
yonU	BSU20990	M9_stationary	
yonT	BSU21000	M9_stationary	
yonS	BSU21010		1.2 M NaCl, 16°C
yonR	BSU21020		1.2 M NaCl, 16°C
yozP	BSU21310	16°C	
yomK	BSU21330		1.2 M NaCl, 51°C, M9_stationary
bdbB	BSU21440		16°C
sunS	BSU21450		16°C
bdbA	BSU21460		16°C
sunT	BSU21470		16°C
sunA	BSU21480		16°C
yolC	BSU21520	M9_stationary	
yolB	BSU21530		1.2 M NaClM9_stationary
yolA	BSU21540		1.2 M NaClM9_stationary
yokF	BSU21610		1.2 M NaCl, 16°C
yokE	BSU21620		1.2 M NaCl, 16°C
degR	BSU21940		1.2 M NaCl, 16°C

Gene name	BSU number	Up regulated	Down regulated
pbuX	BSU22060		16°C, M9_stationary
xpt	BSU22070		16°C, M9_stationary
kdgT	BSU22090	M9_stationary	
kdgA	BSU22100	M9_stationary	
kduI	BSU22130		16°C
kduD	BSU22140		16°C
yptA	BSU22160	16°C	
ypsA	BSU22190		M9_stationary
yppE	BSU22270	M9_stationary	
yppD	BSU22280	16°C, M9_stationary	
cca	BSU22450		M9_stationary
ypjB	BSU22520	16°C	
qcrC	BSU22540	M9_stationary	
qcrB	BSU22550	M9_stationary	
qcrA	BSU22560	M9_stationary	
ypiF	BSU22570	M9_stationary	
ypiB	BSU22580	M9_stationary	
aroE	BSU22600		M9_stationary
tyrA	BSU22610		M9_stationary
hisC	BSU22620		M9_stationary
trpA	BSU22630		M9_stationary
trpB	BSU22640		51°C, M9_stationary
trpF	BSU22650		51°C, M9_stationary
trpC	BSU22660		51°C, M9_stationary
trpD	BSU22670		51°C, M9_stationary
trpE	BSU22680		51°C, M9_stationary
aroH	BSU22690		M9_stationary
aroB	BSU22700		M9_stationary
aroF	BSU22710		M9_stationary
hepT	BSU22740		M9_stationary
spoIVA	BSU22800	16°C, M9_stationary	51°C
yphB	BSU22850	16°C	
yphA	BSU22860	16°C	
ypzI	BSU22869	M9_stationary	
fni	BSU22870		M9_stationary
serA	BSU23070		M9_stationary
rsiX	BSU23090		1.2 M NaCl
sigX	BSU23100		1.2 M NaCl
spmB	BSU23170	16°C, M9_stationary	
spmA	BSU23180	16°C, M9_stationary	
dacB	BSU23190	16°C, M9_stationary	
ypuD	BSU23300	51°C	
lysA	BSU23380		M9_stationary
sigF	BSU23450	16°C, M9_stationary	
spoIIAB	BSU23460	16°C, M9_stationary	
spoIIAA	BSU23470	16°C, M9_stationary	
dacF	BSU23480	16°C, M9_stationary	
yqzK	BSU23519	16°C, M9_stationary	
spoIIM	BSU23530	16°C, M9_stationary	
proI	BSU23800		M9_stationary
yqjL	BSU23830	M9_stationary	
artM	BSU23960		M9_stationary
artQ	BSU23970		M9_stationary
bmrU	BSU24000	16°C, M9_stationary	
bmr	BSU24010	16°C, M9_stationary	
yqzF	BSU24110	M9_stationary	
prpB	BSU24120	M9_stationary	
prpD	BSU24130	M9_stationary	
mmgD	BSU24140	M9_stationary	
mmgC	BSU24150	M9_stationary	

Gene name	BSU number	Up regulated	Down regulated
mmgB	BSU24160	M9_stationary	
mmgA	BSU24170	M9_stationary	
yqiI	BSU24190	1.2 M NaCl	
yqiH	BSU24200	1.2 M NaCl	
yqiG	BSU24210		16°C
spoIVB	BSU24230		1.2 M NaCl, 51°C
ispA	BSU24280		M9_stationary
xseA	BSU24300		M9_stationary
spoIIIAH	BSU24360	16°C, M9_stationary	
spoIIIAG	BSU24370	16°C, M9_stationary	
spoIIIAF	BSU24380	16°C, M9_stationary	
spoIIIAE	BSU24390	16°C, M9_stationary	
spoIIIAD	BSU24400	16°C, M9_stationary	
spoIIIAC	BSU24410	16°C, M9_stationary	
spoIIIAB	BSU24420	16°C, M9_stationary	
spoIIIAA	BSU24430	16°C, M9_stationary	
yqhV	BSU24440	16°C, M9_stationary	
yqhR	BSU24480	16°C	
yqhQ	BSU24490	M9_stationary	
yqhP	BSU24500	M9_stationary	
yqhO	BSU24510	16°C	
gcvPB	BSU24550	1.2 M NaCl	
gcvPA	BSU24560	1.2 M NaCl	
gcvT	BSU24570	1.2 M NaCl	
yqhH	BSU24580	16°C	
yqhG	BSU24590	16°C	
sinI	BSU24600	16°C, M9_stationary	
tasA	BSU24620		1.2 M NaCl, 51°C
sipW	BSU24630		1.2 M NaCl, 51°C
yqxM	BSU24640		1.2 M NaCl, 51°C
yqzG	BSU24650	16°C, M9_stationary	
yqzE	BSU24660		51°C, 16°C
comGG	BSU24670		51°C, 16°C
comGF	BSU24680		51°C, 16°C
comGE	BSU24690		51°C, 16°C
comGD	BSU24700		51°C, 16°C
comGC	BSU24710		51°C, 16°C
comGB	BSU24720		51°C, 16°C
comGA	BSU24730		51°C, 16°C
corA	BSU24740	51°C, 16°C, M9_stationary	
yqhB	BSU24750	51°C, 16°C, M9_stationary	
rsbRD	BSU24760	16°C	
mgsR	BSU24770	51°C, 16°C, M9_stationary	
yqgY	BSU24780	M9_stationary	
yqgX	BSU24790		16°C
yqgW	BSU24800	M9_stationary	
yqzD	BSU24930		16°C
yqzC	BSU24940		16°C
yqfZ	BSU25060	16°C, M9_stationary	
yqfX	BSU25080		1.2 M NaCl, 51°C
yqfT	BSU25120	M9_stationary	51°C
yqfQ	BSU25150		1.2 M NaCl, 51°C
cccA	BSU25190	M9_stationary	
antE	BSU25220	16°C, M9_stationary	
glyS	BSU25260		M9_stationary
glyQ	BSU25270		M9_stationary
yqfD	BSU25350	16°C, M9_stationary	
yqfC	BSU25360	16°C, M9_stationary	
yqeW	BSU25420	16°C	
mtaB	BSU25430		M9_stationary

Gene name	BSU number	Up regulated	Down regulated
rsmE	BSU25440		M9_stationary
prmA	BSU25450		M9_stationary
dnaJ	BSU25460		M9_stationary
dnaK	BSU25470		M9_stationary
grpE	BSU25480		M9_stationary
yqxA	BSU25520	16°C, M9_stationary	
spoIIP	BSU25530	16°C, M9_stationary	
yqzM	BSU25569	M9_stationary	
comEC	BSU25570		51°C
comEA	BSU25590		51°C, 16°C
comER	BSU25600	16°C, M9_stationary	51°C
yqeM	BSU25610		M9_stationary
nucB	BSU25750		51°C
cisA	BSU25770	16°C	
yqcI	BSU25820		1.2 M NaCl, 51°C, 16°C
phrE	BSU25840	M9_stationary	
yqxJ	BSU25880		16°C
yqxI	BSU25890		16°C
yqaR	BSU26210		1.2 M NaCl
yqaD	BSU26360	M9_stationary	
yqaC	BSU26370	M9_stationary	
yrkD	BSU26550	M9_stationary	
yrzO	BSU26619	51°C	
yrdR	BSU26620	51°C	
czcR	BSU26630	51°C	
cypA	BSU26740	16°C	
yrdC	BSU26760		M9_stationary
yrpD	BSU26820	M9_stationary	1.2 M NaCl
csn	BSU26890	M9_stationary	1.2 M NaCl
yraL	BSU26900	M9_stationary	
yraK	BSU26920	M9_stationary	
yraA	BSU27020		16°C
levE	BSU27060		51°C, 16°C
levD	BSU27070		51°C, 16°C
aapA	BSU27090		M9_stationary
yrhK	BSU27150	51°C	
yrhD	BSU27230	M9_stationary	
yrrT	BSU27280		M9_stationary
pbpI	BSU27310	16°C, M9_stationary	
udk	BSU27330		16°C
yrrO	BSU27340		16°C
yrrN	BSU27350		16°C
yrrM	BSU27360		16°C
alaS	BSU27410		M9_stationary
glnQ	BSU27430	16°C, M9_stationary	
glnH	BSU27440	16°C, M9_stationary	
glnM	BSU27450	16°C, M9_stationary	
glnP	BSU27460	16°C, M9_stationary	
yrzQ	BSU27468	M9_stationary	1.2 M NaCl, 51°C
yrzR	BSU27469	M9_stationary	51°C
yrrD	BSU27470		1.2 M NaCl, 51°C
aspS	BSU27550		M9_stationary
hisS	BSU27560		M9_stationary
yrvJ	BSU27580		16°C
spoVB	BSU27670	16°C, M9_stationary	
yrzE	BSU27690	16°C, M9_stationary	
bofC	BSU27750	16°C, M9_stationary	
csbX	BSU27760	M9_stationary	
yrbE	BSU27770	M9_stationary	16°C
yrzF	BSU27785	M9_stationary	

Gene name	BSU number	Up regulated	Down regulated
coxA	BSU27830	16°C	
nadA	BSU27850		M9_stationary
nadC	BSU27860		M9_stationary
nadB	BSU27870		M9_stationary
nifS	BSU27880		M9_stationary
spoIVFB	BSU27970	16°C, M9_stationary	
spoIVFA	BSU27980	16°C, M9_stationary	
mreC	BSU28020		M9_stationary
mreB	BSU28030		M9_stationary
spoIIB	BSU28060	16°C, M9_stationary	
comC	BSU28070		51°C, 16°C
ysxE	BSU28100	16°C, M9_stationary	51°C
spoVID	BSU28110	16°C, M9_stationary	51°C
lon2	BSU28210	16°C, M9_stationary	
tig	BSU28230		M9_stationary
leuD	BSU28250		M9_stationary
leuC	BSU28260		M9_stationary
leuB	BSU28270		M9_stationary
leuA	BSU28280		M9_stationary
ilvC	BSU28290		M9_stationary
ilvH	BSU28300		M9_stationary
ilvB	BSU28310		M9_stationary
ysnD	BSU28320		51°C
ysnF	BSU28340	51°C, 16°C, M9_stationary	
gerM	BSU28380	16°C, M9_stationary	
gerE	BSU28410		16°C
lysC	BSU28470		16°C, M9_stationary
xsa	BSU28510	M9_stationary	
etfA	BSU28520	M9_stationary	
etfB	BSU28530	M9_stationary	
fadB	BSU28540	M9_stationary	
fadR	BSU28550	M9_stationary	
lcfA	BSU28560	M9_stationary	
pheT	BSU28630		M9_stationary
pheS	BSU28640		M9_stationary
glcD	BSU28680	16°C	
ysfE	BSU28700	M9_stationary	
cstA	BSU28710	M9_stationary	
abfA	BSU28720	M9_stationary	
araQ	BSU28730	M9_stationary	
araP	BSU28740	M9_stationary	
araN	BSU28750	M9_stationary	
egsA	BSU28760	M9_stationary	
araL	BSU28770	M9_stationary	
araD	BSU28780	M9_stationary	
araB	BSU28790	M9_stationary	
araA	BSU28800	M9_stationary	
abnA	BSU28810	M9_stationary	
yscB	BSU28890		1.2 M NaCl
ytxC	BSU28960	16°C	
gapB	BSU29020	M9_stationary	
phoR	BSU29100	M9_stationary	
phoP	BSU29110	M9_stationary	
ytwI	BSU29150		M9_stationary
ytvI	BSU29160	16°C, M9_stationary	
ytrH	BSU29239	16°C, M9_stationary	
ytrI	BSU29240	16°C, M9_stationary	
ytzJ	BSU29249	M9_stationary	
nrnA	BSU29250		16°C
ytlI	BSU29400		M9_stationary

Gene name	BSU number	Up regulated	Down regulated
argH	BSU29440		M9_stationary
ackA	BSU29470		M9_stationary
ytfJ	BSU29500	16°C, M9_stationary	
ytfI	BSU29510	16°C, M9_stationary	
yteJ	BSU29520		16°C, M9_stationary
sppA	BSU29530		16°C, M9_stationary
ppnK2	BSU29540	M9_stationary	
sspA	BSU29570		1.2 M NaCl, 51°C
braB	BSU29600		M9_stationary
hisK	BSU29620	1.2 M NaCl	
yttP	BSU29630	1.2 M NaCl, 16°C, M9_stationary	
tyrS1	BSU29670		16°C, M9_stationary
acsA	BSU29680	M9_stationary	
acuA	BSU29690	M9_stationary	
acuB	BSU29700	M9_stationary	
acuC	BSU29710	M9_stationary	
ytxE	BSU29720		M9_stationary
aroA	BSU29750		M9_stationary
pbuO	BSU29990		M9_stationary
ythQ	BSU30000		16°C
ythP	BSU30010		16°C
ytzE	BSU30020	M9_stationary	
ytzG	BSU30020		M9_stationary
cse60	BSU30080	16°C, M9_stationary	
ytdP	BSU30150	M9_stationary	
ytcQ	BSU30160	M9_stationary	
ytbQ	BSU30180		M9_stationary
bioI	BSU30190		M9_stationary
bioB	BSU30200		M9_stationary
bioD	BSU30210		M9_stationary
bioF	BSU30220		M9_stationary
bioK	BSU30230		M9_stationary
bioW	BSU30240		M9_stationary
msmE	BSU30270	M9_stationary	
amyD	BSU30280	M9_stationary	
amyC	BSU30290	M9_stationary	
melA	BSU30300	M9_stationary	
leuS	BSU30320		M9_stationary
ytvB	BSU30330	M9_stationary	
yttA	BSU30360		16°C
bceB	BSU30370	16°C	
bceA	BSU30380	16°C	
ytrF	BSU30410		M9_stationary
ytrE	BSU30420		M9_stationary
ytrD	BSU30430		M9_stationary
ytrC	BSU30440		M9_stationary
ytrB	BSU30450		M9_stationary
ytrA	BSU30460		M9_stationary
ytqB	BSU30490		M9_stationary
pckA	BSU30560	16°C, M9_stationary	
ytlA	BSU30595		51°C, 16°C
ytlC	BSU30610		51°C, 16°C
ytlD	BSU30620		16°C
ytkC	BSU30640	16°C	
dps	BSU30650	16°C	
ytzI	BSU30659	M9_stationary	
rpmE2	BSU30700	51°C, 16°C	
ytzL	BSU30739		51°C
mntB	BSU30760		16°C
mntA	BSU30770		16°C

Gene name	BSU number	Up regulated	Down regulated
ytcA	BSU30860		51°C, 16°C
cotI	BSU30920		51°C
ytaB	BSU30930	16°C, M9_stationary	
glgP	BSU30940	M9_stationary	
glgA	BSU30950	16°C, M9_stationary	
glgD	BSU30960	16°C, M9_stationary	
glgC	BSU30970	16°C, M9_stationary	
glgB	BSU30980	16°C, M9_stationary	
yuaI	BSU31000		51°C
yuaG	BSU31010		51°C
yuaF	BSU31020		51°C
yubD	BSU31130		M9_stationary
cdoA	BSU31140		1.2 M NaCl, 51°C, 16,
rhaA	BSU31180	M9_stationary	
rhaM	BSU31190	M9_stationary	
yuxG	BSU31220	51°C	
tlpB	BSU31230		M9_stationary
mcpA	BSU31240		1.2 M NaCl, 16°C, M9_stationary
tlpA	BSU31250		1.2 M NaCl, 51°C, 16°C, M9_stationary
mcpB	BSU31260		1.2 M NaCl, 16°C, M9_stationary
tgl	BSU31270		16°C
yuzH	BSU31279	M9_stationary	
yugU	BSU31280	M9_stationary	
yugT	BSU31290	16°C	
yuzI	BSU31319	16°C	
yugN	BSU31330	M9_stationary	
yugM	BSU31340	M9_stationary	
yugJ	BSU31370		M9_stationary
yuzA	BSU31380	M9_stationary	
yugH	BSU31400		16°C
patB	BSU31440		M9_stationary
yufN	BSU31540	M9_stationary	51°C
maeN	BSU31580		M9_stationary
mrpA	BSU31600		M9_stationary
mrpB	BSU31610		M9_stationary
mrpC	BSU31620		M9_stationary
mrpD	BSU31630		M9_stationary
mrpE	BSU31640		M9_stationary
mrpF	BSU31650		M9_stationary
degQ	BSU31720	M9_stationary	
yuzC	BSU31730	16°C, M9_stationary	
yuxH	BSU31740		M9_stationary
yueD	BSU31840	51°C	16°C
yueC	BSU31850	51°C	16°C, M9_stationary
yueB	BSU31860	51°C	16°C, M9_stationary
yukB	BSU31875	51°C	16°C, M9_stationary
yukC	BSU31890		16°C, M9_stationary
yukD	BSU31900	51°C	16°C, M9_stationary
yukE	BSU31910		16°C
yukJ	BSU31945	M9_stationary	
ybdZ	BSU31959	1.2 M NaCl	M9_stationary
dhbF	BSU31960	1.2 M NaCl	M9_stationary
dhbB	BSU31970	1.2 M NaCl	51°C, M9_stationary
dhbE	BSU31980	1.2 M NaCl	51°C, M9_stationary
dhbC	BSU31990	1.2 M NaCl	51°C, M9_stationary
dhbA	BSU32000	1.2 M NaCl, 16°C	51°C, M9_stationary
besA	BSU32010	1.2 M NaCl, 16°C	51°C, M9_stationary
bioYB	BSU32030		M9_stationary
yuiF	BSU32040		M9_stationary
yuiC	BSU32070	16°C	

Gene name	BSU number	Up regulated	Down regulated
yuiB	BSU32080	1.2 M NaClM9_stationary	
yumB	BSU32100	16°C	
guaC	BSU32130		M9_stationary
paiB	BSU32140	16°C	
paiA	BSU32150	16°C	
yutK	BSU32180		M9_stationary
yutJ	BSU32200		M9_stationary
yutH	BSU32270	16°C, M9_stationary	
yunB	BSU32350	16°C	
yunD	BSU32370		M9_stationary
yurJ	BSU32550	1.2 M NaCl	M9_stationary
frlD	BSU32570	1.2 M NaCl	M9_stationary
yurM	BSU32580	1.2 M NaCl	16°C, M9_stationary
yurN	BSU32590	1.2 M NaCl	16°C, M9_stationary
yurO	BSU32600	1.2 M NaCl	16°C, M9_stationary
frlB	BSU32610		16°C, M9_stationary
sspG	BSU32640		1.2 M NaCl, 51°C
yurS	BSU32650		1.2 M NaCl, 51°C
yuzK	BSU32719	1.2 M NaCl, 51°C	
metQ	BSU32730		M9_stationary
metP	BSU32740		M9_stationary
metN	BSU32750		M9_stationary
yusD	BSU32760	M9_stationary	
fadE	BSU32820	M9_stationary	
fadA	BSU32830	M9_stationary	
fadN	BSU32840	M9_stationary	
yuzL	BSU32849	16°C	
mrgA	BSU32990	M9_stationary	
htrB	BSU33000		1.2 M NaCl, 16°C
cssR	BSU33010		16°C
cssS	BSU33020		16°C
yvqJ	BSU33140	M9_stationary	
yvrD	BSU33190		16°C
yvrG	BSU33210		M9_stationary
rsoA	BSU33222	M9_stationary	
sigO	BSU33230	M9_stationary	
yvrJ	BSU33239	M9_stationary	
oxdC	BSU33240	M9_stationary	1.2 M NaCl
yvrL	BSU33250		1.2 M NaCl, 16°C
fhuC	BSU33290		M9_stationary
fhuG	BSU33300		M9_stationary
fhuB	BSU33310		M9_stationary
fhuD	BSU33320		51°C, M9_stationary
yvsH	BSU33330		M9_stationary
sspJ	BSU33340		1.2 M NaCl, 51°C
yvgK	BSU33370	M9_stationary	
yvgN	BSU33400		16°C
yvgO	BSU33410	1.2 M NaCl, 16°C, M9_stationary	
cysI	BSU33430		M9_stationary
cysJ	BSU33440		M9_stationary
cadA	BSU33490		1.2 M NaCl
yvaA	BSU33530	16°C	
azoR2	BSU33540		16°C
est	BSU33620	M9_stationary	
opuBD	BSU33700		M9_stationary
opuBC	BSU33710		16°C, M9_stationary
opuBB	BSU33720		M9_stationary
opuBA	BSU33730		M9_stationary
sdpA	BSU33750		51°C
sdpB	BSU33760		51°C

Gene name	BSU number	Up regulated	Down regulated
sdpI	BSU33780	M9_stationary	51°C
sdpR	BSU33790	M9_stationary	51°C
opuCD	BSU33800		M9_stationary
opuCC	BSU33810		M9_stationary
opuCB	BSU33820		M9_stationary
opuCA	BSU33830		M9_stationary
yvbF	BSU33840		M9_stationary
yvbG	BSU33850	M9_stationary	
yvbJ	BSU33880		1.2 M NaCl, 16°C, M9_stationary
gapA	BSU33940		16°C, M9_stationary
cggR	BSU33950		16°C, M9_stationary
araE	BSU33960	M9_stationary	
yvbW	BSU34010		M9_stationary
ganA	BSU34130	M9_stationary	
cycB	BSU34160	M9_stationary	
lutP	BSU34190	M9_stationary	
sigL	BSU34200	M9_stationary	
epsO	BSU34220		1.2 M NaCl, 51°C, M9_stationary
epsN	BSU34230		1.2 M NaCl, 51°C, M9_stationary
epsM	BSU34240		1.2 M NaClM9_stationary
epsL	BSU34250		1.2 M NaClM9_stationary
epsK	BSU34265		1.2 M NaClM9_stationary
epsJ	BSU34280		1.2 M NaClM9_stationary
epsI	BSU34290		1.2 M NaClM9_stationary
epsH	BSU34300		1.2 M NaClM9_stationary
epsG	BSU34310		1.2 M NaClM9_stationary
epsF	BSU34320		1.2 M NaClM9_stationary
epsE	BSU34330		1.2 M NaClM9_stationary
epsD	BSU34340		1.2 M NaClM9_stationary
epsC	BSU34350		1.2 M NaCl
yveL	BSU34360	16°C	1.2 M NaCl51°C
yveK	BSU34370	16°C	1.2 M NaCl51°C
racX	BSU34430		16°C
pbpE	BSU34440		16°C
yvdJ	BSU34580	M9_stationary	
mdxG	BSU34590	M9_stationary	
mdxF	BSU34600	M9_stationary	
mdxE	BSU34610	M9_stationary	
bbmA	BSU34620	M9_stationary	
yvdB	BSU34660	51°C	
yvdA	BSU34670	51°C, M9_stationary	
cwlO	BSU34800		M9_stationary
yvzA	BSU34830	51°C	16°C
yvcB	BSU34840	51°C	16°C
yvcA	BSU34850		16°C
hisI	BSU34860		M9_stationary
hisF	BSU34870		M9_stationary
hisA	BSU34880		M9_stationary
hisH	BSU34890		M9_stationary
hisB	BSU34900		M9_stationary
hisD	BSU34910		M9_stationary
hisG	BSU34920		M9_stationary
hisZ	BSU34930		M9_stationary
yvnA	BSU35050	M9_stationary	
csbA	BSU35180	16°C, M9_stationary	
ctpB	BSU35240	16°C, M9_stationary	
ftsX	BSU35250		M9_stationary
ftsE	BSU35260		M9_stationary
yvzG	BSU35319		1.2 M NaCl, 16°C, M9_stationary
fliT	BSU35320		1.2 M NaCl, 16°C, M9_stationary

Gene name	BSU number	Up regulated	Down regulated
fliS	BSU35330		1.2 M NaCl, 16°C, M9_stationary
fliD	BSU35340		1.2 M NaCl, 16°C, M9_stationary
yvyC	BSU35350		1.2 M NaCl, 16°C, M9_stationary
hag	BSU35360		1.2 M NaCl
yviE	BSU35390		M9_stationary
flgL	BSU35400		16°C, M9_stationary
flgK	BSU35410		M9_stationary
yvyG	BSU35420		M9_stationary
comFC	BSU35450		51°C
comFB	BSU35460		51°C
comFA	BSU35470		51°C, 16°C
yvyE	BSU35510		16°C
yvhJ	BSU35520		16°C
lytC	BSU35620		16°C, M9_stationary
lytB	BSU35630		16°C, M9_stationary
lytA	BSU35640		16°C, M9_stationary
ggaB	BSU35680		16°C, M9_stationary
ggaA	BSU35690		16°C
tagB	BSU35760	16°C	
tagC	BSU35770	1.2 M NaCl	
lytD	BSU35780		1.2 M NaCl, 16°C, M9_stationary
ywtG	BSU35830	51°C	
pgdS	BSU35860		1.2 M NaCl, 16°C, M9_stationary
rbsR	BSU35910	M9_stationary	16°C
rbsK	BSU35920	M9_stationary	16°C
rbsD	BSU35930	M9_stationary	
rbsA	BSU35940	M9_stationary	
rbsC	BSU35950	M9_stationary	
rbsB	BSU35960	M9_stationary	
ywsB	BSU35970	51°C, 16°C, M9_stationary	
ywsA	BSU35980	M9_stationary	
ywrO	BSU35990		16°C
alsS	BSU36010		M9_stationary
cotB	BSU36050		1.2 M NaCl, 51°C
cotG	BSU36070		1.2 M NaCl, 51°C
ywrE	BSU36090		51°C
ywqJ	BSU36190		16°C
ywqI	BSU36200		16°C
ywqA	BSU36280		M9_stationary
ywpJ	BSU36290		M9_stationary
glcR	BSU36300		M9_stationary
ssbB	BSU36310		51°C, 16°C
fabZ	BSU36370		M9_stationary
rapD	BSU36380	M9_stationary	
flhP	BSU36390		1.2 M NaCl, 16°C
flhO	BSU36400		1.2 M NaCl, 16°C
spoIIID	BSU36420	16°C, M9_stationary	51°C
usd	BSU36430	16°C, M9_stationary	51°C
spoIIQ	BSU36550	16°C, M9_stationary	
ywnC	BSU36610		M9_stationary
ywnA	BSU36630		M9_stationary
ureB	BSU36650	M9_stationary	
csbD	BSU36670	1.2 M NaCl, 51°C, 16°C, M9_stationary	
ywmE	BSU36720	51°C, 16°C, M9_stationary	
spoIID	BSU36750	16°C, M9_stationary	
ywmB	BSU36770		1.2 M NaCl
glyA	BSU36900		M9_stationary
ywlD	BSU36940	16°C	
ywlB	BSU36960	16°C, M9_stationary	
spoIIR	BSU36970	51°C, 16°C, M9_stationary	

Gene name	BSU number	Up regulated	Down regulated
ywkD	BSU37020		M9_stationary
racA	BSU37030	1.2 M NaCl, 16°C, M9_stationary	
ywkB	BSU37040		M9_stationary
maeA	BSU37050		M9_stationary
spo0F	BSU37130	M9_stationary	
pyrG	BSU37150		M9_stationary
fadF	BSU37180	M9_stationary	
ywjC	BSU37210	51°C, 16°C, M9_stationary	
ywjB	BSU37220		M9_stationary
ywjA	BSU37230		M9_stationary
ywiE	BSU37240	51°C, 16°C	
fnr	BSU37310		16°C
sboA	BSU37350	M9_stationary	1.2 M NaCl
albA	BSU37370		16°C
speB	BSU37490		M9_stationary
speE	BSU37500		M9_stationary
rsfA	BSU37620	16°C, M9_stationary	
pta	BSU37660		M9_stationary
ywfG	BSU37690		M9_stationary
bacE	BSU37700		M9_stationary
ywfA	BSU37750	16°C	
rocC	BSU37760	M9_stationary	
rocB	BSU37770	M9_stationary	
rocA	BSU37780	M9_stationary	
rocG	BSU37790	M9_stationary	
spsA	BSU37910		51°C
gerQ	BSU37920	16°C, M9_stationary	51°C
ywdA	BSU38030	1.2 M NaCl	
sacT	BSU38070	16°C, M9_stationary	
ywcI	BSU38080	16°C, M9_stationary	51°C
vpr	BSU38090	M9_stationary	16°C
ywcE	BSU38130	M9_stationary	
qoxD	BSU38140		16°C
qoxC	BSU38150		16°C
ywzA	BSU38180	51°C, 16°C, M9_stationary	
ywcB	BSU38230	M9_stationary	
ywcA	BSU38240	M9_stationary	
ywbO	BSU38250		M9_stationary
efeM	BSU38270		M9_stationary
efeU	BSU38280		M9_stationary
cidA	BSU38320		16°C, M9_stationary
ywbG	BSU38330		M9_stationary
epr	BSU38400		1.2 M NaCl, 16°C, M9_stationary
gspA	BSU38430	51°C, 16°C, M9_stationary	
ywaC	BSU38480	M9_stationary	
ywzH	BSU38499		1.2 M NaCl
dltA	BSU38500		1.2 M NaClM9_stationary
dltB	BSU38510		1.2 M NaClM9_stationary
dltC	BSU38520		1.2 M NaClM9_stationary
dltD	BSU38530		1.2 M NaCl, 16°C, M9_stationary
dltE	BSU38540		1.2 M NaCl, 16°C, M9_stationary
licH	BSU38560	M9_stationary	
licA	BSU38570	M9_stationary	
licC	BSU38580	M9_stationary	
licB	BSU38590	M9_stationary	
yxzF	BSU38610	51°C, 16°C	
katX	BSU38630	M9_stationary	
yxlF	BSU38660	M9_stationary	
yxlE	BSU38670	M9_stationary	
yxlD	BSU38680	51°C, M9_stationary	

Gene name	BSU number	Up regulated	Down regulated
yxlC	BSU38690	M9_stationary	
sigY	BSU38700	M9_stationary	
yxlA	BSU38710		M9_stationary
cydC	BSU38740	16°C	
cydB	BSU38750	51°C, 16°C	
cydA	BSU38760	51°C	
msmX	BSU38810	M9_stationary	
yxkF	BSU38820	M9_stationary	
yxkD	BSU38840		M9_stationary
yxkC	BSU38850		1.2 M NaClM9_stationary
yxjH	BSU38950		M9_stationary
yxjF	BSU38970	16°C, M9_stationary	
scoB	BSU38980	16°C, M9_stationary	
scoA	BSU38990	16°C, M9_stationary	
yxjC	BSU39000	M9_stationary	
yxiS	BSU39040	M9_stationary	
yxiT	BSU39040		1.2 M NaCl
katE	BSU39050	51°C, 16°C, M9_stationary	
citN	BSU39060	M9_stationary	
bglS	BSU39070	M9_stationary	
dbpA	BSU39110		1.2 M NaCl
yxiM	BSU39120		1.2 M NaCl, 16°C
yxzJ	BSU39139		1.2 M NaCl, 16°C
yxiK	BSU39140		1.2 M NaCl, 16°C
yxiJ	BSU39150		1.2 M NaCl, 16°C
yxiI	BSU39160		1.2 M NaCl, 16°C
yxzG	BSU39170		1.2 M NaCl, 16°C
yxiH	BSU39180		1.2 M NaCl, 16°C
yxiG	BSU39190		1.2 M NaCl, 16°C
yxzC	BSU39200		1.2 M NaCl, 16°C
yxiF	BSU39210		1.2 M NaCl, 16°C
yxxG	BSU39220		1.2 M NaCl, 16°C
wapA	BSU39230		1.2 M NaCl, 16°C
yxiE	BSU39250	M9_stationary	
bglH	BSU39260	M9_stationary	
bglP	BSU39270	M9_stationary	16°C
yxiD	BSU39300		16°C
yxiC	BSU39310		16°C
yxiA	BSU39330	M9_stationary	
hutP	BSU39340	M9_stationary	
hutH	BSU39350	M9_stationary	
hutU	BSU39360	M9_stationary	
hutI	BSU39370	M9_stationary	
hutG	BSU39380	M9_stationary	
hutM	BSU39390	M9_stationary	
pdp	BSU39400		16°C
nupC	BSU39410		16°C
deoC	BSU39420		16°C
yxeQ	BSU39460		M9_stationary
yxeP	BSU39470		M9_stationary
yxeO	BSU39480		M9_stationary
yxeN	BSU39490		M9_stationary
yxeM	BSU39500		M9_stationary
yxeL	BSU39510		M9_stationary
yxeK	BSU39520		M9_stationary
yxeE	BSU39580		1.2 M NaCl, 51°C, 16°C, M9_stationary
yxeD	BSU39590		1.2 M NaCl, 51°C
yxeB	BSU39610		M9_stationary
iolH	BSU39690	M9_stationary	
iolG	BSU39700	M9_stationary	

Gene name	BSU number	Up regulated	Down regulated
iolF	BSU39710	M9_stationary	
iolE	BSU39720	M9_stationary	
iolD	BSU39730	M9_stationary	
iolC	BSU39740	M9_stationary	
iolB	BSU39750	M9_stationary	
yxcD	BSU39800		16°C
csbC	BSU39810	51°C, 16°C	
yxbG	BSU39840	51°C	
yxbC	BSU39880	M9_stationary	51°C
yxbB	BSU39890	M9_stationary	51°C
yxbA	BSU39900	M9_stationary	51°C
yxnB	BSU39910	M9_stationary	51°C
asnH	BSU39920	M9_stationary	51°C
yxaM	BSU39930	M9_stationary	51°C
yxaL	BSU39940		1.2 M NaCl
yxaJ	BSU39950		1.2 M NaCl, 16°C, M9_stationary
yxaI	BSU39960		16°C, M9_stationary
yxaH	BSU39970		M9_stationary
qdoI	BSU39980		51°C, M9_stationary
yxzK	BSU40021	51°C	
yyzE	BSU40120	M9_stationary	
yydH	BSU40160		51°C
yydG	BSU40170		51°C
yycP	BSU40270	M9_stationary	
yycO	BSU40280	M9_stationary	
yycN	BSU40290	16°C, M9_stationary	
phrG	BSU40310	M9_stationary	
rocD	BSU40340	M9_stationary	
purA	BSU40420		M9_stationary
dnaC	BSU40440		M9_stationary
yycD	BSU40450	51°C, M9_stationary	
yyzH	BSU40529	51°C, 16°C, M9_stationary	
cotF	BSU40530		1.2 M NaCl, 51°C, 16°C
yybL	BSU40600		M9_stationary
yybK	BSU40610		M9_stationary
yybJ	BSU40620		M9_stationary
yybI	BSU40630	16°C	
yybF	BSU40660		1.2 M NaCl, 16°C, M9_stationary
rpsF	BSU40910		M9_stationary
yyaD	BSU40940	16°C	
yyaC	BSU40950	16°C, M9_stationary	
rnpA	BSU41050		M9_stationary

Table S3: Classification of the significantly regulated genes by K-means clustering according to theie expression profile patterns. The following data was used for the fishcer exact test in Figure 22 in the main text.

Gene name	BSU numbers	Cluster	Log2 ratio data normalized to μ=0.1 condition		
			μ=0.1	NaCl	NaCl+GB
yerD	BSU06590	Cluster 1	-0.01 ± 0.18	1.48 ± 0.16	2.05 ± 0.23
yaaI	BSU00170	Cluster 1	-0.01 ± 0.1	0.49 ± 0.14	2.47 ± 0.3
ybbA	BSU01600	Cluster 1	-0.01 ± 0.1	1.38 ± 0.05	4.19 ± 0.03
feuC	BSU01610	Cluster 1	-0.01 ± 0.14	1.94 ± 0.06	4.88 ± 0.05
feuB	BSU01620	Cluster 1	-0.02 ± 0.28	2.05 ± 0.08	4.88 ± 0.03
feuA	BSU01630	Cluster 1	-0.01 ± 0.11	1.9 ± 0.04	4.89 ± 0.11
btr	BSU01640	Cluster 1	-0.02 ± 0.22	1.34 ± 0.03	2.09 ± 0.13
cypC	BSU02100	Cluster 1	-0.01 ± 0.15	0.11 ± 0.15	1.95 ± 0.26
ybyB	BSU02110	Cluster 1	-0.01 ± 0.07	-0.27 ± 0.17	2.08 ± 0.52
gamP	BSU02350	Cluster 1	-0.03 ± 0.33	-0.91 ± 0.09	2.8 ± 0.56
ycbP	BSU02590	Cluster 1	-0.01 ± 0.19	0.38 ± 0.19	1.61 ± 0.31
ycdF	BSU02830	Cluster 1	-0.01 ± 0.13	1.02 ± 0.11	1.73 ± 0.19
ycgT	BSU03270	Cluster 1	-0.01 ± 0.15	0.66 ± 0.1	1.7 ± 0.08
ydaC	BSU04180	Cluster 1	-0.04 ± 0.4	1.18 ± 0.25	1.56 ± 0.19
ydaD	BSU04190	Cluster 1	-0.03 ± 0.33	2.12 ± 0.19	3.06 ± 0.32
ydaE	BSU04200	Cluster 1	-0.03 ± 0.37	2.03 ± 0.17	2.77 ± 0.31
ydaG	BSU04220	Cluster 1	-0.01 ± 0.12	-0.1 ± 0.12	1.64 ± 0.26
ydaJ	BSU04270	Cluster 1	-0.01 ± 0.16	-0.49 ± 0.09	1.45 ± 0.3
ydaP	BSU04340	Cluster 1	-0.01 ± 0.18	1.24 ± 0.16	2.08 ± 0.23
ydaS	BSU04370	Cluster 1	-0.01 ± 0.14	0.11 ± 0.24	2.1 ± 0.53
ydaT	BSU04380	Cluster 1	-0.01 ± 0.15	0.98 ± 0.16	2.32 ± 0.2
gsiB	BSU04400	Cluster 1	-0.03 ± 0.3	0.49 ± 0.14	2.2 ± 0.28
ydbD	BSU04430	Cluster 1	-0.02 ± 0.29	0.02 ± 0.11	2.13 ± 0.4
fbpB	BSU04530	Cluster 1	-0.01 ± 0.06	1.67 ± 0.17	2.99 ± 0.21
rsbV	BSU04710	Cluster 1	-0.01 ± 0.15	-0.51 ± 0.03	1.45 ± 0.21
yddT	BSU05100	Cluster 1	-0.01 ± 0.19	2.35 ± 0.13	2.67 ± 0.03
ydjJ	BSU06220	Cluster 1	-0.01 ± 0.1	0.68 ± 0.12	1.8 ± 0.2
hmoA	BSU07150	Cluster 1	-0.01 ± 0.02	1.05 ± 0.06	2.36 ± 0.12
yfmH	BSU07470	Cluster 1	-0.05 ± 0.42	2.46 ± 0.1	2.89 ± 0.28
yflT	BSU07550	Cluster 1	-0.01 ± 0.14	0.13 ± 0.2	2.27 ± 0.4
yflS	BSU07570	Cluster 1	-0.02 ± 0.24	-0.35 ± 0.15	1.73 ± 0.16
yflD	BSU07720	Cluster 1	-0.04 ± 0.4	0.15 ± 0.05	1.77 ± 0.32
yflA	BSU07750	Cluster 1	-0.03 ± 0.33	0.33 ± 0.12	1.73 ± 0.29
yfkM	BSU07850	Cluster 1	-0.01 ± 0.2	0.56 ± 0.13	1.77 ± 0.25
yfiB	BSU08210	Cluster 1	-0.01 ± 0.07	0.34 ± 0.11	1.82 ± 0.05
yfiC	BSU08220	Cluster 1	-0.01 ± 0.1	0.23 ± 0.03	1.69 ± 0.03
yfhI	BSU08540	Cluster 1	-0.01 ± 0.11	1.25 ± 0.08	2.11 ± 0.1
yfhK	BSU08570	Cluster 1	-0.02 ± 0.28	-0.23 ± 0.12	1.49 ± 0.24
glpD	BSU09300	Cluster 1	-0.01 ± 0.16	0.06 ± 0.04	1.7 ± 0.17
ygxB	BSU09390	Cluster 1	-0.01 ± 0.16	0.28 ± 0.17	2.21 ± 0.38
lytE	BSU09420	Cluster 1	-0.02 ± 0.22	1.58 ± 0.04	2.18 ± 0.15
yhdF	BSU09450	Cluster 1	-0.02 ± 0.26	0.48 ± 0.12	2.03 ± 0.25
yhdN	BSU09530	Cluster 1	-0.01 ± 0.09	-0.38 ± 0.15	1.34 ± 0.13
nhaX	BSU09690	Cluster 1	-0.01 ± 0.13	0.52 ± 0.19	2.52 ± 0.28
yhxD	BSU10430	Cluster 1	-0.01 ± 0.2	1.08 ± 0.13	3.04 ± 0.43
yhjN	BSU10570	Cluster 1	-0.01 ± 0.19	1.2 ± 0.08	1.77 ± 0.21
yisP	BSU10810	Cluster 1	-0.01 ± 0.09	1.3 ± 0.07	1.81 ± 0.11
yjbB	BSU11480	Cluster 1	-0.01 ± 0.2	1.27 ± 0.06	2.25 ± 0.06
yjbQ	BSU11640	Cluster 1	-0.01 ± 0.04	1.03 ± 0.09	1.86 ± 0.16
yjgB	BSU12150	Cluster 1	-0.01 ± 0.21	1.03 ± 0.18	3.18 ± 0.34
yjgC	BSU12160	Cluster 1	-0.02 ± 0.25	0.56 ± 0.08	2.17 ± 0.29
yjgD	BSU12170	Cluster 1	-0.03 ± 0.3	0.3 ± 0.11	1.98 ± 0.32
yjlB	BSU12270	Cluster 1	-0.03 ± 0.34	0.81 ± 0.08	1.99 ± 0.19
ykgA	BSU13020	Cluster 1	-0.02 ± 0.24	-0.12 ± 0.13	1.61 ± 0.19
metE	BSU13180	Cluster 1	-0.01 ± 0.07	0.59 ± 0.04	1.97 ± 0.16
ykoJ	BSU13280	Cluster 1	-0.01 ± 0.13	1.93 ± 0.03	2.01 ± 0.24
ykrL	BSU13490	Cluster 1	-0.01 ± 0.13	1.51 ± 0.07	1.91 ± 0.16

Gene name	BSU numbers	Cluster	Log2 ratio data normalized to μ=0.1 condition		
			μ=0.1	**NaCl**	**NaCl+GB**
ykrP	BSU13520	Cluster 1	-0.03 ± 0.34	2.9 ± 0.11	3.82 ± 0.09
ykuN	BSU14150	Cluster 1	-0.01 ± 0.11	2.51 ± 0.09	5.55 ± 0.14
ykuO	BSU14160	Cluster 1	-0.01 ± 0.15	2.31 ± 0.11	5.36 ± 0.14
ykuP	BSU14170	Cluster 1	-0.02 ± 0.26	2.22 ± 0.1	5.1 ± 0.07
mreBH	BSU14470	Cluster 1	-0.02 ± 0.29	1.4 ± 0.04	3.02 ± 0.1
slp	BSU14620	Cluster 1	-0.01 ± 0.18	2.64 ± 0.03	3.58 ± 0.23
ylaE	BSU14750	Cluster 1	-0.01 ± 0.17	1.29 ± 0.16	2.21 ± 0.17
ylxP	BSU16640	Cluster 1	-0.01 ± 0.06	-0.44 ± 0.07	1.27 ± 0.24
ynxB	BSU17470	Cluster 1	-0.01 ± 0.15	0.48 ± 0.09	1.78 ± 0.1
ynzF	BSU17480	Cluster 1	-0.03 ± 0.36	0.43 ± 0.05	1.62 ± 0.03
ynzD	BSU17920	Cluster 1	-0.01 ± 0.08	0.81 ± 0.06	2.02 ± 0.1
yoxB	BSU18520	Cluster 1	-0.02 ± 0.22	0.11 ± 0.11	2 ± 0.18
yoaJ	BSU18630	Cluster 1	-0.01 ± 0.08	1.53 ± 0.04	2.17 ± 0.16
yocB	BSU19150	Cluster 1	-0.02 ± 0.23	-0.26 ± 0.07	1.77 ± 0.22
yodC	BSU19550	Cluster 1	-0.01 ± 0.17	0.15 ± 0.04	1.69 ± 0.08
yorD	BSU20420	Cluster 1	-0.01 ± 0.12	0.49 ± 0.05	1.78 ± 0.08
yomL	BSU21320	Cluster 1	-0.01 ± 0.18	1.95 ± 0.02	2.6 ± 0.02
sunA	BSU21480	Cluster 1	-0.03 ± 0.32	1.25 ± 0.07	1.63 ± 0.13
cspD	BSU21930	Cluster 1	-0.02 ± 0.24	-0.24 ± 0.02	1.72 ± 0.26
bmrU	BSU24000	Cluster 1	-0.01 ± 0.09	0.02 ± 0.07	2.02 ± 0.19
bmr	BSU24010	Cluster 1	-0.01 ± 0.14	0.19 ± 0.08	1.9 ± 0.07
yqhB	BSU24750	Cluster 1	-0.01 ± 0.17	0.4 ± 0.08	2.24 ± 0.25
rsbRD	BSU24760	Cluster 1	-0.01 ± 0.21	0.58 ± 0.04	1.95 ± 0.12
yrkA	BSU26610	Cluster 1	-0.01 ± 0.2	2.71 ± 0.04	3.25 ± 0.18
adhA	BSU27010	Cluster 1	-0.01 ± 0.09	0.49 ± 0.02	1.61 ± 0.06
ysnF	BSU28340	Cluster 1	-0.04 ± 0.39	-0.04 ± 0.18	1.94 ± 0.4
ysfC	BSU28680	Cluster 1	-0.01 ± 0.2	1.51 ± 0.02	1.98 ± 0.43
ysfD	BSU28690	Cluster 1	-0.01 ± 0.19	1.3 ± 0.07	1.81 ± 0.51
yugU	BSU31280	Cluster 1	-0.01 ± 0.19	-0.37 ± 0.13	1.61 ± 0.2
yugK	BSU31360	Cluster 1	-0.03 ± 0.31	1.49 ± 0.08	1.8 ± 0.08
mrpA	BSU31600	Cluster 1	-0.01 ± 0.04	2.4 ± 0.04	2.47 ± 0.03
mrpB	BSU31610	Cluster 1	-0.01 ± 0.03	2.37 ± 0.04	2.44 ± 0.02
mrpC	BSU31620	Cluster 1	-0.01 ± 0.07	2.23 ± 0.04	2.28 ± 0.03
mrpD	BSU31630	Cluster 1	-0.01 ± 0.02	2.01 ± 0.03	2.07 ± 0.02
mrpE	BSU31640	Cluster 1	-0.01 ± 0.1	1.62 ± 0.04	1.71 ± 0.07
mrpF	BSU31650	Cluster 1	-0.01 ± 0.04	1.58 ± 0.07	1.63 ± 0.06
mrpG	BSU31660	Cluster 1	-0.01 ± 0.17	1.69 ± 0.05	1.71 ± 0.07
degQ	BSU31720	Cluster 1	-0.01 ± 0.17	2.25 ± 0.19	2.3 ± 0.2
ald	BSU31930	Cluster 1	-0.01 ± 0.11	0.59 ± 0.07	1.67 ± 0.37
dhbF	BSU31960	Cluster 1	-0.04 ± 0.39	3.28 ± 0.03	4.87 ± 0.17
dhbB	BSU31970	Cluster 1	-0.01 ± 0.12	4.31 ± 0.07	5.85 ± 0.28
dhbE	BSU31980	Cluster 1	-0.04 ± 0.36	3.77 ± 0.03	5.46 ± 0.32
dhbC	BSU31990	Cluster 1	-0.03 ± 0.31	4.37 ± 0.04	5.88 ± 0.23
dhbA	BSU32000	Cluster 1	-0.11 ± 0.64	3.69 ± 0.06	5.28 ± 0.25
besA	BSU32010	Cluster 1	-0.01 ± 0.03	1.87 ± 0.06	2.05 ± 0.04
frlD	BSU32570	Cluster 1	-0.09 ± 0.62	1.57 ± 0.06	1.8 ± 0.21
frlM	BSU32580	Cluster 1	-0.12 ± 0.74	1.61 ± 0.06	1.81 ± 0.21
frlN	BSU32590	Cluster 1	-0.1 ± 0.67	1.76 ± 0.06	1.95 ± 0.19
frlO	BSU32600	Cluster 1	-0.06 ± 0.51	1.41 ± 0.05	1.61 ± 0.2
frlB	BSU32610	Cluster 1	-0.06 ± 0.49	1.21 ± 0.08	2.01 ± 0.06
yusV	BSU32940	Cluster 1	-0.01 ± 0.09	0.62 ± 0.07	1.58 ± 0.07
fhuC	BSU33290	Cluster 1	-0.01 ± 0.09	0.98 ± 0.11	2.18 ± 0.1
fhuG	BSU33300	Cluster 1	-0.01 ± 0.03	0.7 ± 0.1	1.97 ± 0.08
fhuD	BSU33320	Cluster 1	-0.01 ± 0.06	0.47 ± 0.02	1.87 ± 0.1
yvgO	BSU33410	Cluster 1	-0.01 ± 0.13	2.31 ± 0.1	3.28 ± 0.44
ywtG	BSU35830	Cluster 1	-0.01 ± 0.21	0.78 ± 0.17	1.88 ± 0.27
ywrC	BSU36110	Cluster 1	-0.01 ± 0.18	0.57 ± 0.02	1.61 ± 0.12
csbD	BSU36670	Cluster 1	-0.02 ± 0.24	0.27 ± 0.22	2.18 ± 0.37
ywmF	BSU36680	Cluster 1	-0.07 ± 0.56	0.19 ± 0.21	3.35 ± 0.39

Gene name	BSU numbers	Cluster	Log2 ratio data normalized to μ=0.1 condition		
			μ=0.1	**NaCl**	**NaCl+GB**
albA	BSU37370	Cluster 1	-0.01 ± 0.16	1.36 ± 0.06	1.71 ± 0.03
albB	BSU37380	Cluster 1	-0.02 ± 0.26	1.21 ± 0.06	1.58 ± 0.04
albC	BSU37390	Cluster 1	-0.02 ± 0.28	1.38 ± 0.08	1.79 ± 0.04
albD	BSU37400	Cluster 1	-0.03 ± 0.32	1.44 ± 0.03	1.77 ± 0.06
albE	BSU37410	Cluster 1	-0.02 ± 0.26	1.56 ± 0.05	1.64 ± 0.03
rocC	BSU37760	Cluster 1	-0.01 ± 0.12	1.42 ± 0.05	2.13 ± 0.32
yxzF	BSU38610	Cluster 1	-0.03 ± 0.32	0.42 ± 0.19	2.23 ± 0.44
yxkO	BSU38720	Cluster 1	-0.02 ± 0.24	1.1 ± 0.16	1.91 ± 0.22
yxiS	BSU39040	Cluster 1	-0.02 ± 0.28	1.03 ± 0.1	1.76 ± 0.17
katE	BSU39050	Cluster 1	-0.01 ± 0.14	1.14 ± 0.12	2.27 ± 0.25
yxeQ	BSU39460	Cluster 1	-0.07 ± 0.5	1.5 ± 0.08	1.59 ± 0.28
yxeO	BSU39480	Cluster 1	-0.04 ± 0.38	1.48 ± 0.06	1.56 ± 0.29
yxeB	BSU39610	Cluster 1	-0.01 ± 0.16	0.83 ± 0.09	2.39 ± 0.06
csbC	BSU39810	Cluster 1	-0.01 ± 0.21	0.49 ± 0.14	1.76 ± 0.24
yxbG	BSU39840	Cluster 1	-0.01 ± 0.12	2.06 ± 0.17	2.7 ± 0.24
yxnA	BSU40000	Cluster 1	-0.01 ± 0.21	0.95 ± 0.16	2.03 ± 0.14
yycD	BSU40450	Cluster 1	-0.03 ± 0.35	-0.1 ± 0.16	2.41 ± 0.25
yybJ	BSU40620	Cluster 1	-0.02 ± 0.24	2.17 ± 0.1	2.09 ± 0.21
sspF	BSU00450	Cluster 2	-0.11 ± 0.67	-2.56 ± 0.17	-2.93 ± 0.24
spoIIE	BSU00640	Cluster 2	-0.04 ± 0.43	-2.94 ± 0.16	-2.97 ± 0.27
yabS	BSU00650	Cluster 2	-0.02 ± 0.24	-2.1 ± 0.06	-2.09 ± 0.17
yabT	BSU00660	Cluster 2	-0.02 ± 0.28	-2.1 ± 0.08	-1.8 ± 0.2
ybaK	BSU01520	Cluster 2	-0.12 ± 0.77	-3.21 ± 0.29	-2.59 ± 0.3
cwlD	BSU01530	Cluster 2	-0.05 ± 0.48	-3.57 ± 0.09	-3.08 ± 0.43
gerD	BSU01550	Cluster 2	-0.06 ± 0.53	-2.09 ± 0.11	-1.9 ± 0.06
pdaB	BSU01570	Cluster 2	-0.03 ± 0.33	-3.11 ± 0.17	-2.41 ± 0.26
csgA	BSU02070	Cluster 2	-0.09 ± 0.65	-4.09 ± 0.4	-2.9 ± 0.37
ybgB	BSU02380	Cluster 2	-0.01 ± 0.19	-1.65 ± 0.06	-1.31 ± 0.03
cwlJ	BSU02600	Cluster 2	-0.07 ± 0.56	-5.2 ± 0.25	-3.71 ± 0.31
ycgL	BSU03190	Cluster 2	-0.1 ± 0.68	-2.05 ± 0.06	-2.27 ± 0.44
yclG	BSU03680	Cluster 2	-0.18 ± 0.92	-5.68 ± 0.08	-5.2 ± 0.04
gerKA	BSU03700	Cluster 2	-0.05 ± 0.48	-1.76 ± 0.22	-1.57 ± 0.17
ydcC	BSU04630	Cluster 2	-0.02 ± 0.28	-2.42 ± 0.12	-2.01 ± 0.32
ydzH	BSU05520	Cluster 2	-0.12 ± 0.74	-4.95 ± 0.27	-3.69 ± 0.23
ydfR	BSU05530	Cluster 2	-0.1 ± 0.67	-4.27 ± 0.05	-3.02 ± 0.23
ydhD	BSU05710	Cluster 2	-0.06 ± 0.5	-3.84 ± 0.34	-3.09 ± 0.48
ydjP	BSU06280	Cluster 2	-0.04 ± 0.38	-1.68 ± 0.09	-1.65 ± 0.14
yeaA	BSU06290	Cluster 2	-0.06 ± 0.51	-2.05 ± 0.08	-1.78 ± 0.25
cotA	BSU06300	Cluster 2	-0.16 ± 0.89	-5.12 ± 0.08	-4.3 ± 0.24
cotJB	BSU06900	Cluster 2	-0.02 ± 0.29	-5.42 ± 0.43	-3.86 ± 0.31
yesJ	BSU06920	Cluster 2	-0.02 ± 0.22	-2.27 ± 0.05	-2.02 ± 0.07
lplD	BSU07130	Cluster 2	-0.02 ± 0.28	-2 ± 0.1	-1.58 ± 0.05
yetF	BSU07140	Cluster 2	-0.04 ± 0.4	-2.36 ± 0.04	-1.87 ± 0.09
yfnE	BSU07300	Cluster 2	-0.15 ± 0.85	-4.91 ± 0.11	-4.01 ± 0.28
yfnD	BSU07310	Cluster 2	-0.17 ± 0.93	-4.86 ± 0.19	-3.97 ± 0.18
yfiM	BSU08320	Cluster 2	-0.23 ± 1.06	-2.67 ± 0.19	-2.4 ± 0.08
yfhE	BSU08500	Cluster 2	-0.04 ± 0.43	-1.68 ± 0.1	-1.25 ± 0.29
sspE	BSU08660	Cluster 2	-0.12 ± 0.76	-3.91 ± 0.03	-3.11 ± 0.29
ygaK	BSU08800	Cluster 2	-0.13 ± 0.77	-3.74 ± 0.1	-3.97 ± 0.06
yhbB	BSU08920	Cluster 2	-0.07 ± 0.54	-3.6 ± 0.19	-2.73 ± 0.38
yhbH	BSU08980	Cluster 2	-0.1 ± 0.69	-4.78 ± 0.14	-3.98 ± 0.17
yhcQ	BSU09180	Cluster 2	-0.07 ± 0.56	-4.44 ± 0.06	-3.15 ± 0.21
phoA	BSU09410	Cluster 2	-0.03 ± 0.38	-2.01 ± 0.01	-2.1 ± 0.06
yheF	BSU09740	Cluster 2	-0.07 ± 0.54	-2.98 ± 0.24	-2.35 ± 0.06
yhaX	BSU09830	Cluster 2	-0.03 ± 0.35	-3.04 ± 0.08	-2.37 ± 0.34
yhaL	BSU09940	Cluster 2	-0.02 ± 0.26	-2.17 ± 0.16	-1.58 ± 0.17
yhfA	BSU10080	Cluster 2	-0.1 ± 0.68	-3.57 ± 0.12	-2.65 ± 0.11
yhfW	BSU10390	Cluster 2	-0.05 ± 0.46	-3.86 ± 0.3	-3.03 ± 0.47
yhxC	BSU10400	Cluster 2	-0.04 ± 0.38	-3.69 ± 0.03	-2.66 ± 0.4

Gene name	BSU numbers	Cluster	Log2 ratio data normalized to μ=0.1 condition		
			μ=0.1	**NaCl**	**NaCl+GB**
yisN	BSU10780	Cluster 2	-0.01 ± 0.15	-2.08 ± 0.06	-1.74 ± 0.14
yitC	BSU10940	Cluster 2	-0.14 ± 0.8	-5.74 ± 0.22	-4.36 ± 0.12
yitE	BSU10960	Cluster 2	-0.05 ± 0.46	-3.28 ± 0.17	-2.77 ± 0.35
yitF	BSU10970	Cluster 2	-0.06 ± 0.48	-2.51 ± 0.08	-1.84 ± 0.08
yitG	BSU10980	Cluster 2	-0.05 ± 0.46	-2.56 ± 0.04	-1.83 ± 0.11
yjzC	BSU11260	Cluster 2	-0.02 ± 0.25	-3.47 ± 0.06	-2.65 ± 0.13
yjaU	BSU11280	Cluster 2	-0.14 ± 0.83	-4.55 ± 0.04	-4.08 ± 0.21
yjzB	BSU11320	Cluster 2	-0.08 ± 0.6	-4.03 ± 0.12	-3.04 ± 0.17
yjaZ	BSU11350	Cluster 2	-0.05 ± 0.45	-1.66 ± 0.04	-1.9 ± 0.06
yjbA	BSU11410	Cluster 2	-0.03 ± 0.37	-2.73 ± 0.11	-2.65 ± 0.36
oppA	BSU11430	Cluster 2	-0.01 ± 0.16	-1.96 ± 0.07	-2.11 ± 0.07
yjbE	BSU11510	Cluster 2	-0.02 ± 0.26	-2.33 ± 0.34	-1.74 ± 0.26
yjdH	BSU12050	Cluster 2	-0.06 ± 0.53	-4.23 ± 0.2	-3.22 ± 0.44
cotT	BSU12090	Cluster 2	-0.09 ± 0.62	-5.41 ± 0.92	-3.96 ± 0.18
ykjA	BSU13060	Cluster 2	-0.08 ± 0.61	-3.18 ± 0.51	-2.82 ± 0.83
ykzD	BSU13290	Cluster 2	-0.1 ± 0.67	-3.56 ± 0.07	-2.96 ± 0.14
ykoS	BSU13380	Cluster 2	-0.04 ± 0.41	-1.72 ± 0.08	-1.34 ± 0.11
ykoT	BSU13390	Cluster 2	-0.04 ± 0.38	-1.76 ± 0.09	-1.55 ± 0.12
ykoU	BSU13400	Cluster 2	-0.05 ± 0.45	-2.65 ± 0.25	-2.1 ± 0.11
sspD	BSU13470	Cluster 2	-0.08 ± 0.61	-3.05 ± 0.1	-2.7 ± 0.19
ykzE	BSU13510	Cluster 2	-0.04 ± 0.43	-6.1 ± 0.34	-4.4 ± 0.14
ykvQ	BSU13790	Cluster 2	-0.11 ± 0.72	-3.16 ± 0.15	-2.31 ± 0.15
ykvU	BSU13830	Cluster 2	-0.01 ± 0.06	-2.8 ± 0.1	-2.4 ± 0.17
stoA	BSU13840	Cluster 2	-0.01 ± 0.03	-1.95 ± 0.06	-1.61 ± 0.04
pbpH	BSU13980	Cluster 2	-0.05 ± 0.44	-1.65 ± 0.08	-1.63 ± 0.01
ldt	BSU14040	Cluster 2	-0.04 ± 0.42	-1.96 ± 0.03	-1.54 ± 0.14
yknT	BSU14250	Cluster 2	-0.08 ± 0.6	-5.14 ± 0.23	-3.76 ± 0.65
ylaK	BSU14810	Cluster 2	-0.03 ± 0.34	-3.48 ± 0.19	-2.79 ± 0.11
ylaM	BSU14830	Cluster 2	-0.02 ± 0.29	-1.99 ± 0.04	-1.97 ± 0.11
ylbJ	BSU15030	Cluster 2	-0.03 ± 0.33	-2.56 ± 0.09	-2.18 ± 0.36
gerR	BSU15090	Cluster 2	-0.04 ± 0.41	-4.34 ± 0.19	-3.5 ± 0.58
spoVD	BSU15170	Cluster 2	-0.04 ± 0.38	-3.37 ± 0.2	-2.4 ± 0.42
sigE	BSU15320	Cluster 2	-0.03 ± 0.33	-2.32 ± 0.14	-1.71 ± 0.27
sigG	BSU15330	Cluster 2	-0.05 ± 0.44	-3.07 ± 0.1	-2.21 ± 0.15
yloB	BSU15650	Cluster 2	-0.02 ± 0.28	-2.92 ± 0.13	-2.1 ± 0.29
ymxH	BSU16720	Cluster 2	-0.02 ± 0.26	-2.84 ± 0.16	-2.51 ± 0.11
tepA	BSU16790	Cluster 2	-0.08 ± 0.61	-2.72 ± 0.2	-2.68 ± 0.2
pbpX	BSU16950	Cluster 2	-0.02 ± 0.28	-1.79 ± 0.1	-1.67 ± 0.24
spoVS	BSU16980	Cluster 2	-0.01 ± 0.2	-1.72 ± 0.08	-1.73 ± 0.14
aprX	BSU17260	Cluster 2	-0.24 ± 1.1	-6.08 ± 0.01	-4.56 ± 0.11
cwlC	BSU17410	Cluster 2	-0.25 ± 1.14	-6.65 ± 0.09	-6.18 ± 0.25
yncD	BSU17640	Cluster 2	-0.07 ± 0.55	-4.35 ± 0.19	-3.09 ± 0.31
cotU	BSU17670	Cluster 2	-0.16 ± 0.9	-3.99 ± 0.43	-3.09 ± 0.23
yndA	BSU17720	Cluster 2	-0.03 ± 0.34	-3.93 ± 0.17	-2.9 ± 0.15
yndD	BSU17750	Cluster 2	-0.08 ± 0.58	-2.07 ± 0.08	-1.52 ± 0.14
yndL	BSU17820	Cluster 2	-0.14 ± 0.82	-4.51 ± 0.08	-3.41 ± 0.24
ynfE	BSU18140	Cluster 2	-0.08 ± 0.58	-3.14 ± 0.39	-2.51 ± 0.35
nrnB	BSU18200	Cluster 2	-0.02 ± 0.27	-1.74 ± 0.03	-1.72 ± 0.11
yngE	BSU18210	Cluster 2	-0.03 ± 0.37	-3.05 ± 0.06	-2.38 ± 0.22
yngF	BSU18220	Cluster 2	-0.05 ± 0.48	-3.89 ± 0.08	-2.81 ± 0.39
yngG	BSU18230	Cluster 2	-0.05 ± 0.46	-4.11 ± 0.12	-2.98 ± 0.43
ynzE	BSU18270	Cluster 2	-0.05 ± 0.45	-1.9 ± 0.11	-1.54 ± 0.07
yngK	BSU18280	Cluster 2	-0.14 ± 0.82	-3.65 ± 0.19	-2.82 ± 0.1
yozQ	BSU18600	Cluster 2	-0.06 ± 0.53	-2.51 ± 0.16	-2.34 ± 0.14
yoaI	BSU18620	Cluster 2	-0.15 ± 0.87	-3.47 ± 0.1	-2.96 ± 0.13
yoaQ	BSU18700	Cluster 2	-0.06 ± 0.51	-3.71 ± 0.12	-2.87 ± 0.29
yobN	BSU19020	Cluster 2	-0.06 ± 0.52	-2.17 ± 0.12	-1.52 ± 0.15
yodI	BSU19610	Cluster 2	-0.17 ± 0.9	-6.14 ± 0.39	-4.54 ± 0.17
yozD	BSU19660	Cluster 2	-0.09 ± 0.66	-4.81 ± 0.17	-3.71 ± 0.41

Gene name	BSU numbers	Cluster	Log2 ratio data normalized to μ=0.1 condition		
			μ=0.1	NaCl	NaCl+GB
yodN	BSU19670	Cluster 2	-0.18 ± 0.95	-5.61 ± 0.07	-4.62 ± 0.23
yotH	BSU19880	Cluster 2	-0.02 ± 0.3	-2.04 ± 0.13	-1.8 ± 0.16
yotG	BSU19890	Cluster 2	-0.01 ± 0.13	-2.25 ± 0.19	-1.82 ± 0.33
yotE	BSU19910	Cluster 2	-0.01 ± 0.15	-1.83 ± 0.19	-1.8 ± 0.2
yotB	BSU19940	Cluster 2	-0.01 ± 0.11	-2.01 ± 0.07	-1.86 ± 0.17
yosX	BSU19970	Cluster 2	-0.02 ± 0.24	-1.78 ± 0.06	-2.12 ± 0.18
yosK	BSU20090	Cluster 2	-0.03 ± 0.34	-2.35 ± 0.17	-1.74 ± 0.19
yosI	BSU20110	Cluster 2	-0.01 ± 0.2	-3.61 ± 0.57	-2.7 ± 0.07
yosH	BSU20120	Cluster 2	-0.02 ± 0.27	-2.39 ± 0.05	-1.95 ± 0.19
yosG	BSU20130	Cluster 2	-0.02 ± 0.25	-2.83 ± 0.12	-2.17 ± 0.27
yosE	BSU20150	Cluster 2	-0.08 ± 0.56	-3.27 ± 0.29	-2.74 ± 0.09
yosD	BSU20160	Cluster 2	-0.02 ± 0.26	-2.07 ± 0.42	-1.99 ± 0.18
yosC	BSU20170	Cluster 2	-0.04 ± 0.38	-1.74 ± 0.11	-1.63 ± 0.29
yosB	BSU20180	Cluster 2	-0.01 ± 0.08	-2.77 ± 0.29	-2.53 ± 0.2
yosA	BSU20190	Cluster 2	-0.05 ± 0.44	-3.73 ± 0.15	-2.9 ± 0.18
yorZ	BSU20200	Cluster 2	-0.01 ± 0.12	-2.56 ± 0.12	-2.39 ± 0.33
yorW	BSU20230	Cluster 2	-0.02 ± 0.28	-2.53 ± 0.43	-2.19 ± 0.23
yorV	BSU20240	Cluster 2	-0.02 ± 0.27	-2.25 ± 0.16	-1.92 ± 0.08
yorJ	BSU20360	Cluster 2	-0.09 ± 0.61	-1.74 ± 0.04	-1.6 ± 0.27
yorI	BSU20370	Cluster 2	-0.11 ± 0.65	-2.2 ± 0.16	-1.96 ± 0.29
yorH	BSU20380	Cluster 2	-0.08 ± 0.55	-2.12 ± 0.31	-2.14 ± 0.22
yorG	BSU20390	Cluster 2	-0.07 ± 0.51	-2.22 ± 0.08	-2.26 ± 0.26
yorF	BSU20400	Cluster 2	-0.09 ± 0.62	-2.43 ± 0.11	-2.66 ± 0.23
yorE	BSU20410	Cluster 2	-0.06 ± 0.5	-2 ± 0.11	-2.32 ± 0.3
yopU	BSU20760	Cluster 2	-0.02 ± 0.25	-2.05 ± 0.24	-1.87 ± 0.13
yopT	BSU20770	Cluster 2	-0.01 ± 0.02	-1.95 ± 0.07	-1.91 ± 0.13
yonT	BSU21000	Cluster 2	-0.16 ± 0.81	-2.1 ± 0.17	-2.32 ± 0.27
yonN	BSU21050	Cluster 2	-0.05 ± 0.43	-2.22 ± 0.46	-1.79 ± 0.16
yonD	BSU21130	Cluster 2	-0.06 ± 0.49	-2.22 ± 0.07	-2.15 ± 0.21
yonC	BSU21140	Cluster 2	-0.06 ± 0.49	-2.56 ± 0.13	-2.44 ± 0.26
yonB	BSU21150	Cluster 2	-0.04 ± 0.4	-2.65 ± 0.04	-2.11 ± 0.21
yonA	BSU21160	Cluster 2	-0.04 ± 0.37	-2.45 ± 0.08	-1.88 ± 0.32
yomZ	BSU21170	Cluster 2	-0.04 ± 0.38	-2.68 ± 0.15	-2.1 ± 0.23
yomY	BSU21180	Cluster 2	-0.04 ± 0.38	-2.92 ± 0.11	-2.18 ± 0.42
yomR	BSU21250	Cluster 2	-0.05 ± 0.47	-2.36 ± 0.11	-1.76 ± 0.18
yomN	BSU21290	Cluster 2	-0.03 ± 0.34	-1.63 ± 0.08	-1.32 ± 0.29
ypzA	BSU21950	Cluster 2	-0.04 ± 0.38	-3.05 ± 0.17	-2.39 ± 0.2
bpsA	BSU22050	Cluster 2	-0.02 ± 0.25	-1.82 ± 0.18	-1.56 ± 0.04
yptA	BSU22160	Cluster 2	-0.04 ± 0.41	-2.56 ± 0.05	-2.69 ± 0.15
yppG	BSU22250	Cluster 2	-0.12 ± 0.75	-4.25 ± 0.08	-3.05 ± 0.3
yppD	BSU22280	Cluster 2	-0.04 ± 0.43	-1.9 ± 0.12	-1.34 ± 0.13
ypeB	BSU22920	Cluster 2	-0.09 ± 0.65	-3.42 ± 0.18	-2.65 ± 0.25
rsiX	BSU23090	Cluster 2	-0.01 ± 0.21	-1.7 ± 0.04	-1.66 ± 0.15
sigX	BSU23100	Cluster 2	-0.01 ± 0.14	-1.57 ± 0.06	-1.68 ± 0.28
spmB	BSU23170	Cluster 2	-0.02 ± 0.21	-3.54 ± 0.33	-2.62 ± 0.58
spmA	BSU23180	Cluster 2	-0.02 ± 0.26	-3.8 ± 0.3	-2.72 ± 0.62
dacB	BSU23190	Cluster 2	-0.03 ± 0.35	-3.4 ± 0.38	-2.71 ± 0.43
spoVAF	BSU23390	Cluster 2	-0.08 ± 0.59	-2.55 ± 0.05	-2.09 ± 0.08
spoVAF	BSU23400	Cluster 2	-0.07 ± 0.54	-3.42 ± 0.15	-2.53 ± 0.15
spoVAB	BSU23430	Cluster 2	-0.02 ± 0.27	-3.24 ± 0.33	-2.33 ± 0.21
spoIIM	BSU23530	Cluster 2	-0.02 ± 0.24	-2.06 ± 0.02	-1.79 ± 0.21
bkdR	BSU24100	Cluster 2	-0.02 ± 0.24	-1.67 ± 0.05	-1.86 ± 0.14
yqiQ	BSU24120	Cluster 2	-0.04 ± 0.42	-1.96 ± 0.12	-1.88 ± 0.2
mmgE	BSU24130	Cluster 2	-0.05 ± 0.47	-2.74 ± 0.08	-2.4 ± 0.54
mmgD	BSU24140	Cluster 2	-0.04 ± 0.38	-3.17 ± 0.07	-2.61 ± 0.71
mmgC	BSU24150	Cluster 2	-0.06 ± 0.48	-3.28 ± 0.07	-2.66 ± 0.79
mmgB	BSU24160	Cluster 2	-0.04 ± 0.4	-3.46 ± 0.11	-2.65 ± 0.94
mmgA	BSU24170	Cluster 2	-0.03 ± 0.35	-3.36 ± 0.08	-2.73 ± 0.82
spoIIIAA	BSU24430	Cluster 2	-0.03 ± 0.35	-4.01 ± 0.3	-2.81 ± 0.21

Gene name	BSU numbers	Cluster	Log2 ratio data normalized to μ=0.1 condition		
			μ=0.1	NaCl	NaCl+GB
yqhO	BSU24510	Cluster 2	-0.05 ± 0.45	-3.17 ± 0.1	-3.2 ± 0.31
yqhH	BSU24580	Cluster 2	-0.05 ± 0.46	-3.25 ± 0.22	-2.43 ± 0.23
sinI	BSU24600	Cluster 2	-0.04 ± 0.38	-2.19 ± 0.06	-2.36 ± 0.16
tasA	BSU24620	Cluster 2	-0.03 ± 0.31	-1.9 ± 0.09	-1.81 ± 0.09
yqgO	BSU24880	Cluster 2	-0.05 ± 0.47	-2.64 ± 0.12	-1.99 ± 0.44
yqfQ	BSU25150	Cluster 2	-0.04 ± 0.4	-3.67 ± 0.17	-2.93 ± 0.09
yqfD	BSU25350	Cluster 2	-0.02 ± 0.24	-2.1 ± 0.14	-1.58 ± 0.12
yqxA	BSU25520	Cluster 2	-0.03 ± 0.31	-2.64 ± 0.13	-2.01 ± 0.28
spoIIP	BSU25530	Cluster 2	-0.05 ± 0.47	-3.05 ± 0.18	-2.58 ± 0.27
gpr	BSU25540	Cluster 2	-0.05 ± 0.46	-3 ± 0.08	-2.45 ± 0.28
cwlH	BSU25710	Cluster 2	-0.13 ± 0.79	-6.98 ± 0.42	-5.9 ± 0.48
yrkF	BSU26530	Cluster 2	-0.01 ± 0.19	-1.53 ± 0.11	-1.83 ± 0.12
yrkC	BSU26560	Cluster 2	-0.12 ± 0.75	-2.69 ± 0.03	-1.95 ± 0.11
cypA	BSU26740	Cluster 2	-0.06 ± 0.49	-3.55 ± 0.06	-3.22 ± 0.26
adhB	BSU26970	Cluster 2	-0.04 ± 0.41	-2.88 ± 0.17	-2.14 ± 0.07
yraE	BSU26980	Cluster 2	-0.04 ± 0.4	-4.12 ± 0.15	-2.97 ± 0.3
yraD	BSU26990	Cluster 2	-0.03 ± 0.3	-4.01 ± 0.31	-2.98 ± 0.19
pbpI	BSU27310	Cluster 2	-0.01 ± 0.15	-2.9 ± 0.15	-2.03 ± 0.11
yrzK	BSU27570	Cluster 2	-0.08 ± 0.62	-2.92 ± 0.08	-2.19 ± 0.17
spoVB	BSU27670	Cluster 2	-0.01 ± 0.13	-2.25 ± 0.06	-1.74 ± 0.09
yrbG	BSU27680	Cluster 2	-0.06 ± 0.5	-2.57 ± 0.33	-2.42 ± 0.34
yrbD	BSU27810	Cluster 2	-0.06 ± 0.51	-3.16 ± 0.14	-2.34 ± 0.22
coxA	BSU27830	Cluster 2	-0.07 ± 0.55	-3.03 ± 0.09	-2.76 ± 0.21
spoIVFA	BSU27980	Cluster 2	-0.02 ± 0.23	-1.73 ± 0.11	-1.68 ± 0.23
gerM	BSU28380	Cluster 2	-0.02 ± 0.25	-4.18 ± 0.34	-3.06 ± 0.56
gerE	BSU28410	Cluster 2	-0.07 ± 0.57	-3 ± 0.08	-2.25 ± 0.09
lcfA	BSU28560	Cluster 2	-0.01 ± 0.05	-1.84 ± 0.1	-1.5 ± 0.08
sspI	BSU28660	Cluster 2	-0.04 ± 0.39	-2.78 ± 0.15	-2.42 ± 0.21
ytvI	BSU29160	Cluster 2	-0.03 ± 0.32	-2.95 ± 0.23	-2.18 ± 0.35
ytrI	BSU29240	Cluster 2	-0.01 ± 0.2	-2.5 ± 0.22	-2.06 ± 0.47
ytpI	BSU29260	Cluster 2	-0.04 ± 0.42	-1.58 ± 0.1	-1.74 ± 0.16
yteV	BSU30080	Cluster 2	-0.01 ± 0.18	-2.68 ± 0.15	-2.12 ± 0.04
ytzC	BSU30470	Cluster 2	-0.08 ± 0.6	-4.25 ± 0.1	-3.01 ± 0.3
ytkC	BSU30640	Cluster 2	-0.2 ± 1	-6.58 ± 0.24	-5.26 ± 0.11
ythB	BSU30720	Cluster 2	-0.06 ± 0.49	-2.91 ± 0.15	-2.13 ± 0.16
ytdA	BSU30850	Cluster 2	-0.11 ± 0.72	-3.48 ± 0.24	-2.62 ± 0.11
glgP	BSU30940	Cluster 2	-0.04 ± 0.37	-2.67 ± 0.17	-2.57 ± 0.07
glgA	BSU30950	Cluster 2	-0.04 ± 0.38	-3.04 ± 0.19	-2.77 ± 0.19
glgD	BSU30960	Cluster 2	-0.04 ± 0.38	-3.1 ± 0.23	-2.8 ± 0.18
glgC	BSU30970	Cluster 2	-0.04 ± 0.37	-3.19 ± 0.22	-2.78 ± 0.22
glgB	BSU30980	Cluster 2	-0.05 ± 0.47	-3.48 ± 0.12	-2.86 ± 0.28
yugT	BSU31290	Cluster 2	-0.06 ± 0.48	-2.97 ± 0.05	-2.55 ± 0.24
yugF	BSU31420	Cluster 2	-0.06 ± 0.5	-2.45 ± 0.05	-1.79 ± 0.15
yueG	BSU31790	Cluster 2	-0.03 ± 0.35	-1.83 ± 0.11	-1.63 ± 0.1
yutH	BSU32270	Cluster 2	-0.04 ± 0.41	-1.95 ± 0.06	-1.57 ± 0.12
lytH	BSU32340	Cluster 2	-0.04 ± 0.39	-2.4 ± 0.02	-1.86 ± 0.05
yunB	BSU32350	Cluster 2	-0.07 ± 0.57	-3.2 ± 0.03	-2.52 ± 0.21
yunC	BSU32360	Cluster 2	-0.07 ± 0.56	-2.8 ± 0.12	-2.55 ± 0.02
yurZ	BSU32720	Cluster 2	-0.07 ± 0.55	-3.87 ± 0.03	-2.84 ± 0.19
gerAB	BSU33060	Cluster 2	-0.07 ± 0.56	-2.55 ± 0.21	-1.98 ± 0.24
gerAC	BSU33070	Cluster 2	-0.04 ± 0.38	-1.87 ± 0.08	-1.55 ± 0.03
oxdC	BSU33240	Cluster 2	-0.03 ± 0.36	-2.05 ± 0.08	-2.38 ± 0.15
azoR2	BSU33540	Cluster 2	-0.04 ± 0.42	-2.22 ± 0.08	-2.34 ± 0.03
yvaC	BSU33550	Cluster 2	-0.03 ± 0.33	-1.81 ± 0.07	-1.42 ± 0.32
yvfO	BSU34120	Cluster 2	-0.02 ± 0.27	-1.64 ± 0.13	-1.25 ± 0.09
slrR	BSU34380	Cluster 2	-0.06 ± 0.52	-1.75 ± 0.17	-1.94 ± 0.26
cotQ	BSU34520	Cluster 2	-0.13 ± 0.78	-3.54 ± 0.06	-2.86 ± 0.13
cotR	BSU34530	Cluster 2	-0.17 ± 0.91	-6.26 ± 0.05	-4.52 ± 0.37
ctpB	BSU35240	Cluster 2	-0.05 ± 0.45	-3.51 ± 0.18	-2.58 ± 0.27

Gene name	BSU numbers	Cluster	Log2 ratio data normalized to μ=0.1 condition		
			μ=0.1	NaCl	NaCl+GB
ywrK	BSU36030	Cluster 2	-0.19 ± 0.97	-6.87 ± 0.17	-5.28 ± 0.2
ywrJ	BSU36040	Cluster 2	-0.15 ± 0.85	-3.21 ± 0.06	-3.21 ± 0.12
cotB	BSU36050	Cluster 2	-0.19 ± 0.97	-5.9 ± 0.07	-4.24 ± 0.32
cotH	BSU36060	Cluster 2	-0.14 ± 0.81	-5.16 ± 0.15	-3.79 ± 0.26
spoIID	BSU36750	Cluster 2	-0.03 ± 0.35	-3.18 ± 0.12	-2.23 ± 0.45
ywkF	BSU36990	Cluster 2	-0.08 ± 0.61	-2.54 ± 0.13	-2.43 ± 0.16
ywjD	BSU37200	Cluster 2	-0.08 ± 0.58	-3.36 ± 0.2	-2.61 ± 0.44
ywhL	BSU37440	Cluster 2	-0.27 ± 1.16	-4 ± 0.11	-3.76 ± 0.12
ywhK	BSU37450	Cluster 2	-0.27 ± 1.18	-4.7 ± 0.04	-4.32 ± 0.08
thrZ	BSU37560	Cluster 2	-0.02 ± 0.28	-1.83 ± 0.17	-1.54 ± 0.15
spsL	BSU37810	Cluster 2	-0.1 ± 0.67	-3.46 ± 0.27	-3.18 ± 0.23
spsK	BSU37820	Cluster 2	-0.12 ± 0.75	-3.97 ± 0.09	-3.28 ± 0.29
spsJ	BSU37830	Cluster 2	-0.12 ± 0.74	-4.37 ± 0.07	-3.44 ± 0.27
spsI	BSU37840	Cluster 2	-0.15 ± 0.85	-4.28 ± 0.03	-3.39 ± 0.2
spsG	BSU37850	Cluster 2	-0.15 ± 0.83	-4.81 ± 0.16	-3.39 ± 0.23
ywcA	BSU38240	Cluster 2	-0.02 ± 0.29	-1.99 ± 0.05	-1.44 ± 0.14
ywbA	BSU38390	Cluster 2	-0.03 ± 0.34	-2.02 ± 0.07	-1.92 ± 0.1
ywaF	BSU38440	Cluster 2	-0.05 ± 0.46	-1.75 ± 0.11	-1.66 ± 0.13
yxlE	BSU38670	Cluster 2	-0.02 ± 0.24	-1.72 ± 0.08	-1.61 ± 0.06
yxlC	BSU38690	Cluster 2	-0.01 ± 0.13	-1.61 ± 0.05	-1.47 ± 0.1
sigY	BSU38700	Cluster 2	-0.01 ± 0.14	-1.65 ± 0.02	-1.48 ± 0.09
cydC	BSU38740	Cluster 2	-0.01 ± 0.13	-1.58 ± 0.08	-1.73 ± 0.22
yxjF	BSU38970	Cluster 2	-0.04 ± 0.39	-2.68 ± 0.07	-2.24 ± 0.24
scoB	BSU38980	Cluster 2	-0.05 ± 0.46	-3.36 ± 0.09	-2.72 ± 0.21
scoA	BSU38990	Cluster 2	-0.05 ± 0.44	-4.38 ± 0.03	-3.49 ± 0.58
yxjC	BSU39000	Cluster 2	-0.06 ± 0.49	-4.72 ± 0.49	-3.32 ± 0.39
yxiM	BSU39120	Cluster 2	-0.01 ± 0.17	-2.54 ± 0.05	-2.5 ± 0.07
yxzI	BSU39130	Cluster 2	-0.02 ± 0.27	-2.4 ± 0.13	-2.08 ± 0.19
yxiK	BSU39140	Cluster 2	-0.02 ± 0.26	-2.2 ± 0.15	-2 ± 0.2
yxiJ	BSU39150	Cluster 2	-0.01 ± 0.11	-2.71 ± 0.18	-2.65 ± 0.16
yxiI	BSU39160	Cluster 2	-0.02 ± 0.27	-2.68 ± 0.08	-2.51 ± 0.12
yxzG	BSU39170	Cluster 2	-0.01 ± 0.17	-3.04 ± 0.07	-3.04 ± 0.07
yxiH	BSU39180	Cluster 2	-0.02 ± 0.25	-2.79 ± 0.17	-2.71 ± 0.26
yxiG	BSU39190	Cluster 2	-0.01 ± 0.17	-3.58 ± 0.08	-3.6 ± 0.08
yxzC	BSU39200	Cluster 2	-0.01 ± 0.13	-3.89 ± 0.06	-3.89 ± 0.02
yxiF	BSU39210	Cluster 2	-0.01 ± 0.11	-3.99 ± 0.14	-4.02 ± 0.17
yxxG	BSU39220	Cluster 2	-0.01 ± 0.19	-4.23 ± 0.09	-4.19 ± 0.64
wapA	BSU39230	Cluster 2	-0.01 ± 0.18	-4.78 ± 0.07	-4.85 ± 0.09
bglH	BSU39260	Cluster 2	-0.14 ± 0.76	-1.89 ± 0.08	-2.01 ± 0.34
bglP	BSU39270	Cluster 2	-0.11 ± 0.7	-1.85 ± 0.04	-1.88 ± 0.27
yycP	BSU40270	Cluster 2	-0.06 ± 0.52	-2.75 ± 0.06	-2.05 ± 0.14
yycO	BSU40280	Cluster 2	-0.07 ± 0.54	-2.73 ± 0.07	-2.05 ± 0.07
yycN	BSU40290	Cluster 2	-0.03 ± 0.31	-1.62 ± 0.02	-1.44 ± 0.11
ybbC	BSU01650	Cluster 3	-0.06 ± 0.51	-1.72 ± 0.03	-2.18 ± 0.04
nagZ	BSU01660	Cluster 3	-0.06 ± 0.52	-1.84 ± 0.03	-2.24 ± 0.04
amiE	BSU01670	Cluster 3	-0.05 ± 0.46	-1.82 ± 0.06	-2.23 ± 0.03
murP	BSU01680	Cluster 3	-0.05 ± 0.48	-1.76 ± 0.02	-2.19 ± 0.03
murR	BSU01690	Cluster 3	-0.06 ± 0.53	-1.52 ± 0.03	-1.89 ± 0.08
murQ	BSU01700	Cluster 3	-0.09 ± 0.63	-1.38 ± 0.04	-1.75 ± 0.09
yceK	BSU02970	Cluster 3	-0.01 ± 0.11	-1.16 ± 0.04	-1.8 ± 0.05
ycgG	BSU03100	Cluster 3	-0.04 ± 0.39	-1.31 ± 0.07	-1.66 ± 0.11
putR	BSU03230	Cluster 3	-0.01 ± 0.2	-0.2 ± 0.06	-2.05 ± 0.15
lipC	BSU04110	Cluster 3	-0.13 ± 0.78	-1.82 ± 0.06	-2.21 ± 0.11
ydeK	BSU05230	Cluster 3	-0.02 ± 0.26	-0.47 ± 0.06	-1.84 ± 0.11
pdaA	BSU07980	Cluster 3	-0.06 ± 0.52	-0.92 ± 0.02	-1.66 ± 0.2
ssuC	BSU08850	Cluster 3	-0.04 ± 0.41	-0.2 ± 0.12	-1.84 ± 0.29
bcaP	BSU09460	Cluster 3	-0.01 ± 0.09	-1.52 ± 0.1	-1.91 ± 0.2
yhdJ	BSU09490	Cluster 3	-0.01 ± 0.21	0.35 ± 0.11	-1.52 ± 0.15
fabHB	BSU10170	Cluster 3	-0.15 ± 0.86	-0.78 ± 0.02	-2.3 ± 0.38

Gene name	BSU numbers	Cluster	Log2 ratio data normalized to μ=0.1 condition		
			μ=0.1	**NaCl**	**NaCl+GB**
yhfH	BSU10230	Cluster 3	-0.04 ± 0.41	-0.88 ± 0.13	-1.9 ± 0.17
yisY	BSU10900	Cluster 3	-0.06 ± 0.52	-1.07 ± 0.03	-2.03 ± 0.11
appF	BSU11370	Cluster 3	-0.01 ± 0.21	-0.64 ± 0.04	-1.63 ± 0.06
appF	BSU11380	Cluster 3	-0.02 ± 0.22	-1.08 ± 0.09	-1.66 ± 0.12
pdaC	BSU12100	Cluster 3	-0.03 ± 0.3	-2.29 ± 0.02	-2.89 ± 0.09
yjnA	BSU12400	Cluster 3	-0.05 ± 0.47	-0.57 ± 0.15	-1.77 ± 0.27
yknU	BSU14320	Cluster 3	-0.02 ± 0.22	-1 ± 0.01	-2.48 ± 0.05
yknV	BSU14330	Cluster 3	-0.03 ± 0.3	-1.1 ± 0.03	-2.38 ± 0.13
nprE	BSU14700	Cluster 3	-0.01 ± 0.04	0.03 ± 0.05	-2.18 ± 0.18
fosB	BSU17840	Cluster 3	-0.01 ± 0.18	-1.47 ± 0.13	-1.83 ± 0.18
sirA	BSU17900	Cluster 3	-0.02 ± 0.31	-1.18 ± 0.07	-1.62 ± 0.16
alsT	BSU18120	Cluster 3	-0.01 ± 0.19	0.69 ± 0.03	-1.19 ± 0.14
des	BSU19180	Cluster 3	-0.05 ± 0.44	-2.8 ± 0.02	-3.91 ± 0.14
yopX	BSU20730	Cluster 3	-0.03 ± 0.3	-0.72 ± 0.08	-1.68 ± 0.14
yopW	BSU20740	Cluster 3	-0.02 ± 0.22	-0.14 ± 0.26	-1.77 ± 0.28
yonX	BSU20970	Cluster 3	-0.01 ± 0.13	-1.07 ± 0.1	-1.83 ± 0.15
yonP	BSU21030	Cluster 3	-0.03 ± 0.36	-1.21 ± 0.22	-1.97 ± 0.05
pstS	BSU24990	Cluster 3	-0.01 ± 0.19	-1.07 ± 0.26	-1.75 ± 0.14
nucB	BSU25750	Cluster 3	-0.03 ± 0.35	-1.5 ± 0.07	-2.3 ± 0.06
yraJ	BSU26920	Cluster 3	-0.01 ± 0.14	-0.41 ± 0.09	-1.75 ± 0.12
yraI	BSU26930	Cluster 3	-0.01 ± 0.13	-0.52 ± 0.04	-2.02 ± 0.12
spoIIB	BSU28060	Cluster 3	-0.03 ± 0.32	-1.69 ± 0.11	-2.22 ± 0.18
mutTA	BSU30630	Cluster 3	-0.09 ± 0.64	-1.07 ± 0.11	-1.93 ± 0.13
kapD	BSU31470	Cluster 3	-0.08 ± 0.59	-1.43 ± 0.02	-1.92 ± 0.11
yuzF	BSU31820	Cluster 3	-0.08 ± 0.61	-0.43 ± 0.04	-2.02 ± 0.1
yuiC	BSU32070	Cluster 3	-0.03 ± 0.33	-0.35 ± 0.05	-1.8 ± 0.25
yusW	BSU32950	Cluster 3	-0.05 ± 0.48	-1.27 ± 0.06	-1.64 ± 0.11
opuCD	BSU33800	Cluster 3	-0.01 ± 0.16	-1.34 ± 0.04	-1.72 ± 0.09
opuCC	BSU33810	Cluster 3	-0.01 ± 0.08	-1.52 ± 0.06	-2.01 ± 0.08
opuCB	BSU33820	Cluster 3	-0.01 ± 0.15	-1.53 ± 0.05	-2.24 ± 0.05
opuCA	BSU33830	Cluster 3	-0.01 ± 0.12	-1.58 ± 0.09	-2.81 ± 0.03
epsB	BSU34360	Cluster 3	-0.01 ± 0.02	-1.17 ± 0.2	-2.26 ± 0.23
bacA	BSU37740	Cluster 3	-0.01 ± 0.12	0.75 ± 0.04	-1.23 ± 0.06
sacT	BSU38070	Cluster 3	-0.03 ± 0.37	-2.7 ± 0.06	-3.32 ± 0.25
ywcI	BSU38080	Cluster 3	-0.04 ± 0.42	-3.54 ± 0.15	-4.38 ± 0.34
cydB	BSU38750	Cluster 3	-0.01 ± 0.15	-1.42 ± 0.15	-1.75 ± 0.21
yybI	BSU40630	Cluster 3	-0.05 ± 0.44	-1.99 ± 0.05	-2.45 ± 0.13
yyaD	BSU40940	Cluster 3	-0.01 ± 0.16	-0.98 ± 0.12	-1.65 ± 0.09
yaaH	BSU00160	Cluster 4	-0.04 ± 0.4	-3.59 ± 0.07	-1.48 ± 0.39
gin	BSU00240	Cluster 4	-0.09 ± 0.65	-4.1 ± 0.11	-2.81 ± 0.33
yabG	BSU00430	Cluster 4	-0.15 ± 0.85	-6.13 ± 0.37	-3.59 ± 0.25
yabP	BSU00600	Cluster 4	-0.01 ± 0.15	-1.68 ± 0.06	-0.99 ± 0.11
ybxH	BSU02080	Cluster 4	-0.1 ± 0.68	-4.25 ± 0.74	-2.71 ± 0.46
gltP	BSU02340	Cluster 4	-0.01 ± 0.12	-1.89 ± 0.05	-0.88 ± 0.17
lmrB	BSU02670	Cluster 4	-0.01 ± 0.1	-1.63 ± 0.07	-0.65 ± 0.12
lmrA	BSU02680	Cluster 4	-0.01 ± 0.06	-1.75 ± 0.06	-1.01 ± 0.16
ycgH	BSU03110	Cluster 4	-0.1 ± 0.66	-5.07 ± 0.67	-2.85 ± 0.43
ycgI	BSU03120	Cluster 4	-0.05 ± 0.45	-2.53 ± 0.35	-1.5 ± 0.43
yckD	BSU03400	Cluster 4	-0.07 ± 0.55	-3.86 ± 0.17	-2.17 ± 0.56
yclF	BSU03670	Cluster 4	-0.01 ± 0.18	-2.4 ± 0.05	-1.64 ± 0.16
glcU	BSU03920	Cluster 4	-0.08 ± 0.62	-5.34 ± 0.49	-3.11 ± 0.35
gdh	BSU03930	Cluster 4	-0.1 ± 0.67	-5.53 ± 0.08	-3.42 ± 0.48
cotP	BSU05550	Cluster 4	-0.18 ± 0.94	-5.99 ± 0.2	-3.93 ± 0.35
ydgA	BSU05560	Cluster 4	-0.12 ± 0.75	-7.73 ± 0.42	-3.92 ± 0.4
ydgB	BSU05570	Cluster 4	-0.16 ± 0.89	-7.36 ± 0.45	-4.08 ± 0.38
ydhF	BSU05730	Cluster 4	-0.04 ± 0.42	-3.09 ± 0.12	-1.91 ± 0.26
phoB	BSU05740	Cluster 4	-0.05 ± 0.45	-3.55 ± 0.14	-2.03 ± 0.29
ydhU/1	BSU05890	Cluster 4	-0.06 ± 0.53	-4.02 ± 0.11	-2.53 ± 0.05
yeeK	BSU06850	Cluster 4	-0.13 ± 0.77	-5.59 ± 0.26	-3.46 ± 0.36

Gene name	BSU numbers	Cluster	Log2 ratio data normalized to μ=0.1 condition		
			μ=0.1	**NaCl**	**NaCl+GB**
cotJA	BSU06890	Cluster 4	-0.07 ± 0.55	-7.31 ± 0.69	-4.33 ± 0.62
cotJC	BSU06910	Cluster 4	-0.06 ± 0.51	-7.33 ± 0.72	-4.33 ± 0.61
yesL	BSU06940	Cluster 4	-0.01 ± 0.09	-2.72 ± 0.1	-1.27 ± 0.1
yesM	BSU06950	Cluster 4	-0.01 ± 0.05	-2.62 ± 0.04	-1.5 ± 0.16
yesN	BSU06960	Cluster 4	-0.01 ± 0.02	-2.47 ± 0.13	-1.43 ± 0.18
yesO	BSU06970	Cluster 4	-0.02 ± 0.27	-3.12 ± 0.1	-1.83 ± 0.27
yesP	BSU06980	Cluster 4	-0.01 ± 0.16	-4.05 ± 0.14	-2.06 ± 0.31
yesQ	BSU06990	Cluster 4	-0.02 ± 0.21	-3.77 ± 0.12	-2 ± 0.22
yesR	BSU07000	Cluster 4	-0.02 ± 0.24	-2.59 ± 0.08	-1.55 ± 0.17
yesS	BSU07010	Cluster 4	-0.01 ± 0.14	-3.02 ± 0.06	-1.6 ± 0.19
yesT	BSU07020	Cluster 4	-0.01 ± 0.16	-3.01 ± 0.14	-1.49 ± 0.14
yesU	BSU07030	Cluster 4	-0.02 ± 0.29	-2.83 ± 0.09	-1.34 ± 0.11
yesV	BSU07040	Cluster 4	-0.01 ± 0.17	-3.12 ± 0.04	-1.38 ± 0.1
yesW	BSU07050	Cluster 4	-0.01 ± 0.15	-2.91 ± 0.25	-1.35 ± 0.19
yesX	BSU07060	Cluster 4	-0.01 ± 0.13	-2.52 ± 0.18	-1.26 ± 0.11
yesY	BSU07070	Cluster 4	-0.01 ± 0.15	-2.77 ± 0.04	-1.37 ± 0.16
yesZ	BSU07080	Cluster 4	-0.01 ± 0.19	-2.54 ± 0.11	-1.32 ± 0.15
lplA	BSU07100	Cluster 4	-0.01 ± 0.07	-2.01 ± 0.08	-0.56 ± 0.08
lplB	BSU07110	Cluster 4	-0.03 ± 0.33	-2.1 ± 0.1	-0.74 ± 0.08
yfnH	BSU07270	Cluster 4	-0.18 ± 0.96	-8 ± 0.55	-4.61 ± 0.38
yfnG	BSU07280	Cluster 4	-0.17 ± 0.91	-7.3 ± 0.37	-4.46 ± 0.35
yfnF	BSU07290	Cluster 4	-0.15 ± 0.86	-7.22 ± 0.22	-4.38 ± 0.28
yfkR	BSU07780	Cluster 4	-0.01 ± 0.21	-1.67 ± 0.06	-1.03 ± 0.03
yfkQ	BSU07790	Cluster 4	-0.06 ± 0.48	-2.53 ± 0.11	-1.64 ± 0.19
treP	BSU07800	Cluster 4	-0.01 ± 0.09	-1.68 ± 0.11	-1.05 ± 0.09
yfkD	BSU07930	Cluster 4	-0.05 ± 0.48	-1.94 ± 0.01	-0.58 ± 0.3
sspH	BSU08110	Cluster 4	-0.01 ± 0.16	-2.15 ± 0.04	-0.82 ± 0.09
yfiG	BSU08260	Cluster 4	-0.01 ± 0.08	-1.64 ± 0.03	-1.11 ± 0.06
yfhD	BSU08490	Cluster 4	-0.07 ± 0.55	-3.94 ± 0.1	-2.43 ± 0.25
sspK	BSU08550	Cluster 4	-0.06 ± 0.51	-4.33 ± 0.41	-2.63 ± 0.33
yfhS	BSU08640	Cluster 4	-0.23 ± 1.1	-4.34 ± 0.5	-2.87 ± 0.37
katA	BSU08820	Cluster 4	-0.01 ± 0.1	-2.19 ± 0.02	-1.08 ± 0.04
prkA	BSU08970	Cluster 4	-0.04 ± 0.38	-6.15 ± 0.28	-3.46 ± 0.7
yhcN	BSU09150	Cluster 4	-0.09 ± 0.65	-5.8 ± 0.34	-2.92 ± 0.36
yhcN	BSU09160	Cluster 4	-0.13 ± 0.79	-7.84 ± 0.56	-3.74 ± 0.35
yhcO	BSU09170	Cluster 4	-0.12 ± 0.75	-8.01 ± 0.05	-3.82 ± 0.39
yhcV	BSU09230	Cluster 4	-0.07 ± 0.58	-5.61 ± 0.03	-3.18 ± 0.34
yhdB	BSU09350	Cluster 4	-0.08 ± 0.6	-7.45 ± 0.64	-3.59 ± 0.26
yhdC	BSU09360	Cluster 4	-0.05 ± 0.43	-2.38 ± 0.13	-1.45 ± 0.04
spoVR	BSU09400	Cluster 4	-0.06 ± 0.52	-5.14 ± 0.18	-3.26 ± 0.59
sspB	BSU09750	Cluster 4	-0.11 ± 0.73	-7.41 ± 0.49	-3.24 ± 0.41
yheD	BSU09770	Cluster 4	-0.09 ± 0.62	-5.77 ± 0.36	-3.48 ± 0.51
yheC	BSU09780	Cluster 4	-0.07 ± 0.57	-6.51 ± 0.17	-3.68 ± 0.54
yhfD	BSU10190	Cluster 4	-0.27 ± 1.14	-7.89 ± 0.36	-4.96 ± 0.49
yhfM	BSU10280	Cluster 4	-0.07 ± 0.55	-3.09 ± 0.05	-1.55 ± 0.25
yhjQ	BSU10600	Cluster 4	-0.05 ± 0.47	-2.32 ± 0.28	-1.28 ± 0.22
yhjR	BSU10610	Cluster 4	-0.11 ± 0.71	-6.12 ± 0.4	-3.65 ± 0.45
gerPF	BSU10670	Cluster 4	-0.12 ± 0.77	-6.38 ± 0.21	-3.69 ± 0.37
gerPE	BSU10680	Cluster 4	-0.13 ± 0.79	-5 ± 0.17	-3.09 ± 0.22
gerPD	BSU10690	Cluster 4	-0.11 ± 0.7	-5 ± 0.18	-3.03 ± 0.17
gerPC	BSU10700	Cluster 4	-0.14 ± 0.8	-4.91 ± 0.33	-3.23 ± 0.19
gerPB	BSU10710	Cluster 4	-0.13 ± 0.78	-5.25 ± 0.24	-3.26 ± 0.32
gerPA	BSU10720	Cluster 4	-0.15 ± 0.85	-5.53 ± 0.09	-3.34 ± 0.32
yisJ	BSU10740	Cluster 4	-0.11 ± 0.7	-2.99 ± 0.09	-1.91 ± 0.11
asnO	BSU10790	Cluster 4	-0.1 ± 0.67	-6.4 ± 0.39	-3.75 ± 0.4
yisZ	BSU10910	Cluster 4	-0.14 ± 0.8	-5.98 ± 0.27	-3.26 ± 0.12
yitA	BSU10920	Cluster 4	-0.12 ± 0.75	-5.03 ± 0.08	-2.94 ± 0.09
yitB	BSU10930	Cluster 4	-0.14 ± 0.82	-6.34 ± 0.24	-4.07 ± 0.25
yjaV	BSU11290	Cluster 4	-0.06 ± 0.52	-4.72 ± 0.34	-2.9 ± 0.52

Gene name	BSU numbers	Cluster	Log2 ratio data normalized to μ=0.1 condition		
			μ=0.1	**NaCl**	**NaCl+GB**
cotO	BSU11730	Cluster 4	-0.05 ± 0.47	-4.92 ± 0.24	-3.23 ± 0.47
cotZ	BSU11740	Cluster 4	-0.16 ± 0.88	-9.1 ± 0.38	-4.27 ± 0.36
cotY	BSU11750	Cluster 4	-0.19 ± 0.98	-9.63 ± 0.6	-4.3 ± 0.38
cotX	BSU11760	Cluster 4	-0.33 ± 1.34	-10.89 ± 0.5	-5.37 ± 0.48
cotW	BSU11770	Cluster 4	-0.38 ± 1.44	-10.05 ± 0.46	-5.1 ± 0.46
cotV	BSU11780	Cluster 4	-0.34 ± 1.36	-10.99 ± 0.49	-5.4 ± 0.5
yjcA	BSU11790	Cluster 4	-0.04 ± 0.41	-4.99 ± 0.4	-3.26 ± 0.34
yjzK	BSU11800	Cluster 4	-0.15 ± 0.84	-5.71 ± 0.58	-3.74 ± 0.16
spoVIF	BSU11810	Cluster 4	-0.19 ± 0.98	-9.43 ± 0.69	-4.53 ± 0.42
yjfA	BSU12110	Cluster 4	-0.02 ± 0.27	-5.43 ± 0.09	-2.8 ± 0.08
yjmC	BSU12320	Cluster 4	-0.03 ± 0.35	-4.89 ± 0.17	-2.96 ± 0.49
yjmD	BSU12330	Cluster 4	-0.02 ± 0.29	-3.66 ± 0.16	-2.43 ± 0.17
uxuA	BSU12340	Cluster 4	-0.02 ± 0.27	-3.92 ± 0.15	-2.47 ± 0.22
yjmF	BSU12350	Cluster 4	-0.02 ± 0.23	-3.32 ± 0.07	-2.11 ± 0.27
exuT	BSU12360	Cluster 4	-0.03 ± 0.34	-3.53 ± 0.05	-2.19 ± 0.27
ykzH	BSU13050	Cluster 4	-0.05 ± 0.45	-2.37 ± 0.41	-1.64 ± 0.2
ykoM	BSU13340	Cluster 4	-0.01 ± 0.1	-1.94 ± 0.15	-0.96 ± 0.08
ykoP	BSU13360	Cluster 4	-0.11 ± 0.71	-4.56 ± 0.28	-3.03 ± 0.09
ykoV	BSU13410	Cluster 4	-0.04 ± 0.4	-3.76 ± 0.16	-2.41 ± 0.09
ykvI	BSU13710	Cluster 4	-0.01 ± 0.2	-2.12 ± 0.13	-1.41 ± 0.16
ykvP	BSU13780	Cluster 4	-0.15 ± 0.87	-5.04 ± 0.09	-2.66 ± 0.24
ykvZ	BSU13870	Cluster 4	-0.03 ± 0.32	-1.65 ± 0.07	-1 ± 0.23
splA	BSU13920	Cluster 4	-0.01 ± 0.2	-1.6 ± 0.1	-0.72 ± 0.19
splB	BSU13930	Cluster 4	-0.03 ± 0.37	-1.93 ± 0.04	-1.1 ± 0.13
mcpC	BSU13950	Cluster 4	-0.13 ± 0.73	-4.42 ± 0.06	-1.44 ± 0.11
fruR	BSU14380	Cluster 4	-0.03 ± 0.35	-1.68 ± 0.16	-0.71 ± 0.03
abh	BSU14480	Cluster 4	-0.02 ± 0.26	-2.78 ± 0.12	-1.92 ± 0.18
ylaJ	BSU14800	Cluster 4	-0.03 ± 0.37	-2.6 ± 0.01	-1.41 ± 0.11
ylbD	BSU14970	Cluster 4	-0.14 ± 0.81	-4.39 ± 0.12	-2.95 ± 0.3
ylbE	BSU14980	Cluster 4	-0.14 ± 0.82	-4.88 ± 0.13	-2.98 ± 0.25
spoIIGA	BSU15310	Cluster 4	-0.04 ± 0.4	-2.63 ± 0.17	-1.8 ± 0.26
ylyA	BSU15440	Cluster 4	-0.08 ± 0.6	-3.9 ± 0.14	-2.68 ± 0.28
spoVM	BSU15810	Cluster 4	-0.08 ± 0.61	-4.62 ± 0.15	-2.69 ± 0.41
flgB	BSU16180	Cluster 4	-0.01 ± 0.08	-3.59 ± 0.08	-1 ± 0.01
flgC	BSU16190	Cluster 4	-0.01 ± 0.12	-2.95 ± 0.12	-0.9 ± 0.03
fliZ	BSU16340	Cluster 4	-0.01 ± 0.17	-1.64 ± 0.05	-0.48 ± 0.04
spoVFA	BSU16730	Cluster 4	-0.15 ± 0.83	-7.87 ± 0.53	-3.99 ± 0.3
spoVFB	BSU16740	Cluster 4	-0.15 ± 0.85	-7.29 ± 0.19	-3.96 ± 0.31
ymfJ	BSU16880	Cluster 4	-0.09 ± 0.65	-7.14 ± 0.29	-3.76 ± 0.43
cotE	BSU17030	Cluster 4	-0.13 ± 0.77	-7.42 ± 0.51	-3.88 ± 0.63
ymaG	BSU17310	Cluster 4	-0.03 ± 0.35	-5.04 ± 1.26	-3.37 ± 0.56
ymaF	BSU17320	Cluster 4	-0.04 ± 0.42	-4.76 ± 0.26	-3.28 ± 0.05
spoVK	BSU17420	Cluster 4	-0.1 ± 0.69	-4.87 ± 0.13	-3.11 ± 0.33
yndM	BSU17830	Cluster 4	-0.09 ± 0.64	-4.13 ± 0.25	-2.38 ± 0.43
cotM	BSU17970	Cluster 4	-0.13 ± 0.79	-4.77 ± 0.11	-2.95 ± 0.25
sspP	BSU17980	Cluster 4	-0.12 ± 0.75	-5.29 ± 0.17	-2.92 ± 0.06
sspO	BSU17990	Cluster 4	-0.11 ± 0.71	-6.38 ± 0.45	-3.41 ± 0.23
sspN	BSU18020	Cluster 4	-0.11 ± 0.71	-5.85 ± 0.11	-3.5 ± 0.32
tlp	BSU18030	Cluster 4	-0.09 ± 0.65	-5.21 ± 0.18	-3 ± 0.28
ynfC	BSU18110	Cluster 4	-0.01 ± 0.1	-1.94 ± 0.09	-0.93 ± 0.13
yngH	BSU18240	Cluster 4	-0.05 ± 0.46	-4.52 ± 0.05	-3.11 ± 0.44
yngI	BSU18250	Cluster 4	-0.03 ± 0.37	-5.57 ± 0.39	-3.26 ± 0.6
yngJ	BSU18260	Cluster 4	-0.02 ± 0.3	-5.6 ± 0.28	-3.29 ± 0.54
yngL	BSU18290	Cluster 4	-0.09 ± 0.64	-3.39 ± 0.33	-2.23 ± 0.25
iseA	BSU18380	Cluster 4	-0.12 ± 0.69	-5.14 ± 0.03	-3.57 ± 0.18
oxdD	BSU18670	Cluster 4	-0.12 ± 0.76	-6.58 ± 0.56	-3.43 ± 0.39
yozF	BSU18710	Cluster 4	-0.03 ± 0.36	-2.29 ± 0.05	-1.56 ± 0.16
yoaR	BSU18720	Cluster 4	-0.09 ± 0.62	-4.31 ± 0.29	-2.52 ± 0.23
yobW	BSU19110	Cluster 4	-0.07 ± 0.57	-5.32 ± 0.95	-3.28 ± 0.42

Gene name	BSU numbers	Cluster	Log2 ratio data normalized to μ=0.1 condition		
			μ=0.1	NaCl	NaCl+GB
yozN	BSU19270	Cluster 4	-0.07 ± 0.56	-4.98 ± 0.23	-2.66 ± 0.6
yocN	BSU19280	Cluster 4	-0.09 ± 0.65	-4.16 ± 0.46	-2.43 ± 0.51
sqhC	BSU19320	Cluster 4	-0.04 ± 0.42	-4.1 ± 0.17	-2.31 ± 0.33
sodF	BSU19330	Cluster 4	-0.07 ± 0.54	-4.35 ± 0.05	-2.54 ± 0.38
gerT	BSU19490	Cluster 4	-0.15 ± 0.84	-5.43 ± 0.23	-3.41 ± 0.24
yojC	BSU19500	Cluster 4	-0.13 ± 0.78	-4.07 ± 0.95	-2.69 ± 0.27
yojB	BSU19510	Cluster 4	-0.14 ± 0.83	-6.74 ± 0.11	-3.38 ± 0.2
kamA	BSU19690	Cluster 4	-0.09 ± 0.64	-5.12 ± 0.35	-3.22 ± 0.69
yodP	BSU19700	Cluster 4	-0.09 ± 0.63	-5.37 ± 0.21	-3.21 ± 0.68
yodQ	BSU19710	Cluster 4	-0.05 ± 0.47	-4.5 ± 0.25	-2.88 ± 0.52
yodR	BSU19720	Cluster 4	-0.07 ± 0.56	-6.06 ± 0.44	-3.29 ± 0.76
yodS	BSU19730	Cluster 4	-0.07 ± 0.57	-6.59 ± 0.52	-3.17 ± 0.51
yodT	BSU19740	Cluster 4	-0.06 ± 0.52	-6.81 ± 0.25	-3.31 ± 0.73
cgeE	BSU19750	Cluster 4	-0.02 ± 0.25	-2.82 ± 0.06	-0.88 ± 0.1
cgeD	BSU19760	Cluster 4	-0.13 ± 0.77	-6.95 ± 0.47	-4.12 ± 0.33
cgeC	BSU19770	Cluster 4	-0.2 ± 0.99	-8.3 ± 0.18	-4.48 ± 0.41
cgeA	BSU19780	Cluster 4	-0.3 ± 1.26	-10.05 ± 0.61	-4.45 ± 0.42
cgeB	BSU19790	Cluster 4	-0.27 ± 1.18	-9.4 ± 0.38	-4.22 ± 0.44
yodU	BSU19810	Cluster 4	-0.15 ± 0.86	-7.44 ± 0.39	-4.4 ± 0.38
yotN	BSU19820	Cluster 4	-0.11 ± 0.73	-5.71 ± 0.65	-3 ± 0.61
yotM	BSU19830	Cluster 4	-0.01 ± 0.12	-3.11 ± 0.12	-1.46 ± 0.34
yotK	BSU19850	Cluster 4	-0.03 ± 0.31	-2.39 ± 0.29	-1.6 ± 0.21
yotJ	BSU19860	Cluster 4	-0.05 ± 0.46	-3 ± 0.63	-1.81 ± 0.05
yotF	BSU19900	Cluster 4	-0.01 ± 0.08	-2.78 ± 0.15	-1.7 ± 0.17
yotD	BSU19920	Cluster 4	-0.01 ± 0.21	-2.03 ± 0.19	-1.24 ± 0.46
sspC	BSU19950	Cluster 4	-0.09 ± 0.65	-6.19 ± 0.91	-3.14 ± 0.12
yosW	BSU19980	Cluster 4	-0.04 ± 0.38	-2.41 ± 0.41	-1.45 ± 0.55
yosQ	BSU20050	Cluster 4	-0.07 ± 0.53	-2.09 ± 0.05	-1.13 ± 0.23
nrdEB	BSU20060	Cluster 4	-0.05 ± 0.45	-2.33 ± 0.15	-1.69 ± 0.04
yosM	BSU20070	Cluster 4	-0.07 ± 0.51	-2.44 ± 0.13	-1.78 ± 0.34
yosL	BSU20080	Cluster 4	-0.07 ± 0.5	-3.29 ± 0.19	-2.2 ± 0.14
yosJ	BSU20100	Cluster 4	-0.01 ± 0.13	-4.02 ± 0.7	-2.71 ± 0.36
yosF	BSU20140	Cluster 4	-0.03 ± 0.33	-3.37 ± 0.16	-2.29 ± 0.22
yorY	BSU20210	Cluster 4	-0.01 ± 0.11	-2.83 ± 0.79	-1.17 ± 0.38
yorX	BSU20220	Cluster 4	-0.05 ± 0.42	-1.79 ± 0.1	-0.69 ± 0.04
mtbP	BSU20250	Cluster 4	-0.03 ± 0.32	-3.98 ± 0.8	-2.16 ± 0.27
yorT	BSU20260	Cluster 4	-0.04 ± 0.36	-4.04 ± 1.31	-2.34 ± 0.23
yorS	BSU20270	Cluster 4	-0.02 ± 0.25	-2.79 ± 0.47	-1.76 ± 0.11
yorR	BSU20280	Cluster 4	-0.02 ± 0.25	-2.95 ± 0.14	-1.41 ± 0.05
yorP	BSU20300	Cluster 4	-0.02 ± 0.26	-1.64 ± 0.51	-0.73 ± 0.12
yonU	BSU20990	Cluster 4	-0.04 ± 0.43	-1.79 ± 0.1	-1.24 ± 0.13
yonO	BSU21040	Cluster 4	-0.02 ± 0.24	-1.95 ± 0.2	-1.27 ± 0.06
yonK	BSU21060	Cluster 4	-0.08 ± 0.54	-3.18 ± 0.44	-1.86 ± 0.55
yonJ	BSU21070	Cluster 4	-0.1 ± 0.63	-3.05 ± 0.11	-1.94 ± 0.18
yonH	BSU21090	Cluster 4	-0.04 ± 0.41	-2.57 ± 0.11	-1.64 ± 0.28
yonF	BSU21110	Cluster 4	-0.06 ± 0.46	-1.72 ± 0.05	-0.71 ± 0.13
yomX	BSU21190	Cluster 4	-0.04 ± 0.38	-2.75 ± 0.06	-1.89 ± 0.3
yomW	BSU21200	Cluster 4	-0.04 ± 0.42	-2.73 ± 0.06	-1.76 ± 0.27
yomV	BSU21210	Cluster 4	-0.06 ± 0.51	-2.86 ± 0.07	-1.81 ± 0.29
yomU	BSU21220	Cluster 4	-0.06 ± 0.51	-2.77 ± 0.02	-1.91 ± 0.32
yomT	BSU21230	Cluster 4	-0.08 ± 0.6	-3.23 ± 0.21	-1.92 ± 0.27
yomS	BSU21240	Cluster 4	-0.07 ± 0.55	-2.59 ± 0.38	-1.87 ± 0.25
yomQ	BSU21260	Cluster 4	-0.05 ± 0.44	-1.67 ± 0.03	-0.89 ± 0.07
yomP	BSU21270	Cluster 4	-0.01 ± 0.2	-1.9 ± 0.13	-1.28 ± 0.3
yomM	BSU21300	Cluster 4	-0.03 ± 0.31	-2.01 ± 0.09	-1.03 ± 0.22
yomE	BSU21390	Cluster 4	-0.12 ± 0.68	-3.16 ± 0.25	-2.31 ± 0.38
yomD	BSU21400	Cluster 4	-0.08 ± 0.59	-1.69 ± 0.16	-1.24 ± 0.34
blyA	BSU21410	Cluster 4	-0.07 ± 0.53	-2.59 ± 0.35	-1.64 ± 0.28
cotD	BSU22200	Cluster 4	-0.34 ± 1.36	-4.34 ± 0.04	-2.79 ± 0.2

Gene name	BSU numbers	Cluster	Log2 ratio data normalized to μ=0.1 condition		
			μ=0.1	NaCl	NaCl+GB
ypqA	BSU22240	Cluster 4	-0.14 ± 0.81	-5.42 ± 0.17	-3.33 ± 0.18
sspM	BSU22290	Cluster 4	-0.04 ± 0.4	-5.97 ± 0.29	-3.01 ± 0.11
spoIVA	BSU22800	Cluster 4	-0.04 ± 0.42	-5.12 ± 0.23	-3.28 ± 0.67
seaA	BSU22850	Cluster 4	-0.04 ± 0.42	-2.02 ± 0.03	-1.37 ± 0.35
yphA	BSU22860	Cluster 4	-0.03 ± 0.36	-2.55 ± 0.05	-1.16 ± 0.3
ypfB	BSU22900	Cluster 4	-0.01 ± 0.16	-1.88 ± 0.05	-1.23 ± 0.18
sleB	BSU22930	Cluster 4	-0.1 ± 0.69	-6.26 ± 0.13	-3.21 ± 0.42
ypzC	BSU23320	Cluster 4	-0.04 ± 0.4	-2.37 ± 0.04	-1.47 ± 0.25
ypzD	BSU23350	Cluster 4	-0.17 ± 0.92	-8.9 ± 0.21	-5.25 ± 0.2
ypuA	BSU23370	Cluster 4	-0.02 ± 0.23	-1.6 ± 0.06	-0.95 ± 0.17
spoVAD	BSU23410	Cluster 4	-0.08 ± 0.58	-4.76 ± 0.08	-2.97 ± 0.09
spoVAC	BSU23420	Cluster 4	-0.11 ± 0.7	-5.3 ± 0.37	-3.48 ± 0.35
spoVAA	BSU23440	Cluster 4	-0.1 ± 0.67	-6.77 ± 0.41	-3.53 ± 0.51
dacF	BSU23480	Cluster 4	-0.06 ± 0.51	-5.72 ± 0.34	-3.47 ± 0.56
artR	BSU23960	Cluster 4	-0.01 ± 0.13	-1.76 ± 0.05	-0.89 ± 0.07
artQ	BSU23970	Cluster 4	-0.02 ± 0.23	-1.71 ± 0.03	-0.93 ± 0.09
artP	BSU23980	Cluster 4	-0.02 ± 0.29	-1.93 ± 0.05	-1.04 ± 0.09
spoIVB	BSU24230	Cluster 4	-0.11 ± 0.72	-5.36 ± 0.1	-3.45 ± 0.26
spoIIIAH	BSU24360	Cluster 4	-0.03 ± 0.34	-4.22 ± 0.2	-2.79 ± 0.49
spoIIIAG	BSU24370	Cluster 4	-0.02 ± 0.3	-4.5 ± 0.38	-2.85 ± 0.65
spoIIIAF	BSU24380	Cluster 4	-0.03 ± 0.37	-4.2 ± 0.31	-2.79 ± 0.53
spoIIIAE	BSU24390	Cluster 4	-0.02 ± 0.29	-3.58 ± 0.33	-2.24 ± 0.23
spoIIIAD	BSU24400	Cluster 4	-0.03 ± 0.34	-4.18 ± 0.51	-2.56 ± 0.41
spoIIIAC	BSU24410	Cluster 4	-0.03 ± 0.31	-4.17 ± 0.46	-2.78 ± 0.62
spoIIIAB	BSU24420	Cluster 4	-0.02 ± 0.24	-3.9 ± 0.66	-2.7 ± 0.33
yqhV	BSU24440	Cluster 4	-0.02 ± 0.27	-4.94 ± 0.4	-2.97 ± 0.73
yqhR	BSU24480	Cluster 4	-0.05 ± 0.47	-2.98 ± 0.41	-1.68 ± 0.16
yqhG	BSU24590	Cluster 4	-0.02 ± 0.28	-2.27 ± 0.04	-1.31 ± 0.15
yqzG	BSU24650	Cluster 4	-0.05 ± 0.45	-4.9 ± 0.34	-2.56 ± 0.38
yqfX	BSU25080	Cluster 4	-0.11 ± 0.72	-6.97 ± 0.05	-3.34 ± 0.33
yqfT	BSU25120	Cluster 4	-0.12 ± 0.76	-5.49 ± 0.21	-3.48 ± 0.4
yqfC	BSU25360	Cluster 4	-0.06 ± 0.5	-3.78 ± 0.31	-2.57 ± 0.28
comER	BSU25600	Cluster 4	-0.06 ± 0.52	-5.85 ± 0.39	-3.71 ± 0.47
spoIVCB	BSU25760	Cluster 4	-0.11 ± 0.7	-6.26 ± 0.16	-3.83 ± 0.55
yqcI	BSU25820	Cluster 4	-0.17 ± 0.92	-5.34 ± 0.15	-2.37 ± 0.23
yqaO	BSU26240	Cluster 4	-0.1 ± 0.65	-2.1 ± 0.21	-1.34 ± 0.12
yqaN	BSU26250	Cluster 4	-0.1 ± 0.68	-2.39 ± 0.23	-1.38 ± 0.14
yraG	BSU26950	Cluster 4	-0.07 ± 0.55	-4.15 ± 0.2	-2.77 ± 0.13
yraF	BSU26960	Cluster 4	-0.08 ± 0.6	-4.52 ± 0.09	-3.04 ± 0.15
yrrI	BSU27420	Cluster 4	-0.01 ± 0.16	-2.34 ± 0.06	-1.54 ± 0.03
glnQ	BSU27430	Cluster 4	-0.08 ± 0.59	-5.63 ± 0.34	-2.86 ± 0.64
glnH	BSU27440	Cluster 4	-0.06 ± 0.53	-5.56 ± 0.26	-3.05 ± 0.62
glnM	BSU27450	Cluster 4	-0.06 ± 0.51	-5.13 ± 0.16	-3.01 ± 0.57
glnP	BSU27460	Cluster 4	-0.06 ± 0.53	-4.99 ± 0.29	-2.95 ± 0.53
yrrD	BSU27470	Cluster 4	-0.06 ± 0.52	-4.85 ± 0.26	-2.58 ± 0.21
yrzE	BSU27690	Cluster 4	-0.02 ± 0.3	-4.24 ± 0.14	-2.33 ± 0.43
ysxE	BSU28100	Cluster 4	-0.05 ± 0.45	-5.56 ± 0.22	-3.15 ± 0.61
spoVID	BSU28110	Cluster 4	-0.05 ± 0.44	-5.91 ± 0.59	-3.15 ± 0.63
lonB	BSU28210	Cluster 4	-0.05 ± 0.47	-4.62 ± 0.06	-2.96 ± 0.43
ysnD	BSU28320	Cluster 4	-0.09 ± 0.64	-6.18 ± 0.24	-3.21 ± 0.27
ysfE	BSU28700	Cluster 4	-0.01 ± 0.18	-1.83 ± 0.14	-1.22 ± 0.01
cstA	BSU28710	Cluster 4	-0.01 ± 0.13	-1.86 ± 0.05	-0.98 ± 0.09
abfA	BSU28720	Cluster 4	-0.01 ± 0.2	-2.92 ± 0.02	-1.46 ± 0.13
araQ	BSU28730	Cluster 4	-0.01 ± 0.15	-3.34 ± 0.04	-1.6 ± 0.09
araP	BSU28740	Cluster 4	-0.01 ± 0.17	-3.29 ± 0.11	-1.63 ± 0.09
araN	BSU28750	Cluster 4	-0.01 ± 0.19	-3.19 ± 0.05	-1.58 ± 0.09
araM	BSU28760	Cluster 4	-0.01 ± 0.18	-3.24 ± 0.12	-1.73 ± 0.13
araL	BSU28770	Cluster 4	-0.01 ± 0.18	-3.22 ± 0.02	-1.71 ± 0.1
araD	BSU28780	Cluster 4	-0.02 ± 0.24	-3.03 ± 0.08	-1.77 ± 0.1

Gene name	BSU numbers	Cluster	Log2 ratio data normalized to μ=0.1 condition		
			μ=0.1	NaCl	NaCl+GB
araB	BSU28790	Cluster 4	-0.02 ± 0.24	-2.95 ± 0.05	-1.62 ± 0.12
araA	BSU28800	Cluster 4	-0.01 ± 0.17	-4.11 ± 0.05	-1.95 ± 0.06
abnA	BSU28810	Cluster 4	-0.02 ± 0.23	-6.61 ± 0.24	-2.49 ± 0.14
ytfJ	BSU29500	Cluster 4	-0.06 ± 0.5	-5.9 ± 0.34	-3.7 ± 0.44
ytfI	BSU29510	Cluster 4	-0.06 ± 0.49	-4.51 ± 0.19	-3.08 ± 0.51
sspA	BSU29570	Cluster 4	-0.13 ± 0.77	-5.56 ± 0.11	-3.82 ± 0.5
ytzH	BSU29910	Cluster 4	-0.04 ± 0.39	-3.04 ± 0.18	-2.06 ± 0.15
yteT	BSU30100	Cluster 4	-0.02 ± 0.22	-1.67 ± 0.08	-0.53 ± 0.1
ytcQ	BSU30160	Cluster 4	-0.03 ± 0.35	-2.5 ± 0.03	-0.77 ± 0.09
ytcP	BSU30170	Cluster 4	-0.03 ± 0.3	-3 ± 0.08	-0.87 ± 0.08
msmE	BSU30270	Cluster 4	-0.01 ± 0.05	-2.41 ± 0.07	-1.44 ± 0.09
amyD	BSU30280	Cluster 4	-0.01 ± 0.04	-2.4 ± 0.14	-1.45 ± 0.07
amyC	BSU30290	Cluster 4	-0.01 ± 0.11	-2.51 ± 0.07	-1.5 ± 0.06
melA	BSU30300	Cluster 4	-0.01 ± 0.05	-1.84 ± 0.07	-1.22 ± 0.05
ytmA	BSU30590	Cluster 4	-0.12 ± 0.73	-5.88 ± 0.37	-3.68 ± 0.31
ytlA	BSU30600	Cluster 4	-0.13 ± 0.79	-6.68 ± 0.52	-3.8 ± 0.25
ytlC	BSU30610	Cluster 4	-0.13 ± 0.78	-6.31 ± 0.37	-3.81 ± 0.36
ytlD	BSU30620	Cluster 4	-0.09 ± 0.63	-4.49 ± 0.31	-3.11 ± 0.12
ythA	BSU30710	Cluster 4	-0.06 ± 0.49	-3.92 ± 0.15	-2.41 ± 0.18
ythB	BSU30730	Cluster 4	-0.11 ± 0.73	-6.72 ± 0.17	-3.84 ± 0.38
yteA	BSU30840	Cluster 4	-0.09 ± 0.66	-5.44 ± 0.28	-3.33 ± 0.16
ytcA	BSU30860	Cluster 4	-0.14 ± 0.83	-7.13 ± 0.36	-3.3 ± 0.36
ytcB	BSU30870	Cluster 4	-0.13 ± 0.79	-4.93 ± 0.11	-3.16 ± 0.34
ytcC	BSU30880	Cluster 4	-0.16 ± 0.9	-7.03 ± 0.4	-3.42 ± 0.41
ytxO	BSU30890	Cluster 4	-0.14 ± 0.82	-6.1 ± 0.14	-3.51 ± 0.38
cotS	BSU30900	Cluster 4	-0.15 ± 0.87	-6.6 ± 0.13	-3.62 ± 0.44
cotSA	BSU30910	Cluster 4	-0.13 ± 0.8	-7.35 ± 0.35	-3.56 ± 0.44
cotI	BSU30920	Cluster 4	-0.16 ± 0.88	-8.79 ± 0.31	-3.79 ± 0.38
yubC	BSU31140	Cluster 4	-0.12 ± 0.77	-5.47 ± 0.14	-3.55 ± 0.09
mcpB	BSU31260	Cluster 4	-0.02 ± 0.24	-2.78 ± 0.1	-0.82 ± 0.04
tgl	BSU31270	Cluster 4	-0.1 ± 0.69	-4.85 ± 0.23	-2.93 ± 0.29
yugS	BSU31300	Cluster 4	-0.04 ± 0.39	-1.67 ± 0.08	-0.85 ± 0.09
yuzC	BSU31730	Cluster 4	-0.05 ± 0.47	-4.92 ± 0.27	-3.38 ± 0.87
yutG	BSU32280	Cluster 4	-0.08 ± 0.62	-5.9 ± 0.72	-3.6 ± 0.46
sspG	BSU32640	Cluster 4	-0.31 ± 1.3	-10.36 ± 0.3	-6.5 ± 0.45
yurS	BSU32650	Cluster 4	-0.15 ± 0.86	-9.23 ± 0.32	-5.72 ± 0.48
fadM	BSU32850	Cluster 4	-0.17 ± 0.92	-5.58 ± 0.62	-3.84 ± 0.46
yusN	BSU32860	Cluster 4	-0.09 ± 0.62	-4.44 ± 0.31	-3 ± 0.27
gerAA	BSU33050	Cluster 4	-0.07 ± 0.57	-3.47 ± 0.07	-2.22 ± 0.27
sspJ	BSU33340	Cluster 4	-0.12 ± 0.77	-6.73 ± 0.07	-3.5 ± 0.42
cadA	BSU33490	Cluster 4	-0.04 ± 0.41	-3.2 ± 0.12	-0.92 ± 0.26
araE	BSU33960	Cluster 4	-0.04 ± 0.38	-2.63 ± 0.09	-1.05 ± 0.15
lacA	BSU34130	Cluster 4	-0.01 ± 0.15	-2.38 ± 0.01	-1.46 ± 0.05
yvfM	BSU34140	Cluster 4	-0.01 ± 0.15	-2.08 ± 0.09	-1.09 ± 0.07
yvfL	BSU34150	Cluster 4	-0.01 ± 0.13	-2.1 ± 0.06	-1.12 ± 0.12
cycB	BSU34160	Cluster 4	-0.01 ± 0.19	-2.15 ± 0.07	-1.17 ± 0.1
lutP	BSU34190	Cluster 4	-0.01 ± 0.15	-1.62 ± 0.08	-0.78 ± 0.13
yveA	BSU34470	Cluster 4	-0.1 ± 0.68	-5.14 ± 0.17	-2.64 ± 0.54
yvdQ	BSU34510	Cluster 4	-0.06 ± 0.5	-4.96 ± 0.11	-2.89 ± 0.15
lytD	BSU35780	Cluster 4	-0.01 ± 0.18	-3.73 ± 0.02	-1.73 ± 0.05
gerBA	BSU35800	Cluster 4	-0.07 ± 0.53	-3.52 ± 0.47	-2.25 ± 0.16
ywsA	BSU35980	Cluster 4	-0.01 ± 0.17	-2.17 ± 0.05	-1.29 ± 0.24
cotG	BSU36070	Cluster 4	-0.46 ± 1.63	-11.42 ± 0.56	-5.71 ± 0.64
spoIIID	BSU36420	Cluster 4	-0.11 ± 0.73	-7.24 ± 0.66	-4.26 ± 0.7
usd	BSU36430	Cluster 4	-0.09 ± 0.63	-7.57 ± 0.67	-3.99 ± 0.65
spoIIQ	BSU36550	Cluster 4	-0.04 ± 0.41	-4.25 ± 0.25	-2.92 ± 0.51
ywlB	BSU36960	Cluster 4	-0.01 ± 0.13	-1.7 ± 0.07	-0.67 ± 0.22
acdA	BSU37170	Cluster 4	-0.02 ± 0.27	-1.74 ± 0.04	-0.97 ± 0.06
fadF	BSU37180	Cluster 4	-0.01 ± 0.13	-1.61 ± 0.03	-0.61 ± 0.07

Gene name	BSU numbers	Cluster	Log2 ratio data normalized to μ=0.1 condition		
			μ=0.1	**NaCl**	**NaCl+GB**
ywjE	BSU37190	Cluster 4	-0.11 ± 0.71	-4.62 ± 0.27	-2.88 ± 0.29
pbpG	BSU37510	Cluster 4	-0.08 ± 0.58	-4 ± 0.26	-2.37 ± 0.37
rsfA	BSU37620	Cluster 4	-0.04 ± 0.43	-4.56 ± 0.2	-3.09 ± 0.61
spsF	BSU37860	Cluster 4	-0.17 ± 0.9	-5.59 ± 0.09	-3.63 ± 0.32
spsE	BSU37870	Cluster 4	-0.18 ± 0.91	-5.74 ± 0.11	-3.54 ± 0.33
spsD	BSU37880	Cluster 4	-0.14 ± 0.79	-5.62 ± 0.26	-3.76 ± 0.27
spsC	BSU37890	Cluster 4	-0.13 ± 0.77	-5.45 ± 0.21	-3.57 ± 0.23
spsB	BSU37900	Cluster 4	-0.16 ± 0.87	-6.25 ± 0.11	-3.79 ± 0.36
spsA	BSU37910	Cluster 4	-0.15 ± 0.86	-6.44 ± 0.3	-3.91 ± 0.3
gerQ	BSU37920	Cluster 4	-0.06 ± 0.5	-6.93 ± 0.59	-3.87 ± 0.66
ywaC	BSU38480	Cluster 4	-0.02 ± 0.23	-1.64 ± 0.05	-1.04 ± 0.31
licH	BSU38560	Cluster 4	-0.05 ± 0.43	-2.56 ± 0.13	-1.45 ± 0.16
licA	BSU38570	Cluster 4	-0.04 ± 0.4	-2.52 ± 0.09	-1.35 ± 0.16
licC	BSU38580	Cluster 4	-0.04 ± 0.41	-2.46 ± 0.03	-1.23 ± 0.14
licB	BSU38590	Cluster 4	-0.02 ± 0.29	-2.17 ± 0.09	-1.15 ± 0.15
citH	BSU39060	Cluster 4	-0.05 ± 0.44	-4.98 ± 0.18	-2.97 ± 0.65
yxeE	BSU39580	Cluster 4	-0.21 ± 1.01	-8.85 ± 0.27	-4.37 ± 0.42
yxeD	BSU39590	Cluster 4	-0.13 ± 0.77	-6.37 ± 0.11	-3.94 ± 0.44
cotF	BSU40530	Cluster 4	-0.11 ± 0.74	-7.89 ± 0.33	-4.22 ± 0.28
yyaC	BSU40950	Cluster 4	-0.03 ± 0.37	-3.16 ± 0.08	-1.99 ± 0.28
proJ	BSU18470	Cluster 5	-0.01 ± 0.19	2.21 ± 0.04	0.26 ± 0.13
proH	BSU18480	Cluster 5	-0.02 ± 0.23	2.14 ± 0.05	0.19 ± 0.12
ybfF	BSU02190	Cluster 5	-0.03 ± 0.36	1.86 ± 0.06	1.42 ± 0.15
ybfG	BSU02200	Cluster 5	-0.01 ± 0.18	2.24 ± 0.06	0.3 ± 0.15
purT	BSU02230	Cluster 5	-0.01 ± 0.09	1.3 ± 0.01	-0.32 ± 0.12
ybfM	BSU02280	Cluster 5	-0.01 ± 0.03	1.25 ± 0.06	-0.53 ± 0.03
psd	BSU02290	Cluster 5	-0.01 ± 0.08	1.36 ± 0.04	-0.3 ± 0.07
ybfN	BSU02300	Cluster 5	-0.06 ± 0.49	1.67 ± 0.13	0.68 ± 0.03
ybgF	BSU02400	Cluster 5	-0.03 ± 0.33	1.81 ± 0.09	-0.26 ± 0.34
rtpA	BSU02530	Cluster 5	-0.02 ± 0.22	2 ± 0.12	1.04 ± 0.16
phoD	BSU02620	Cluster 5	-0.03 ± 0.31	1.66 ± 0.11	0.78 ± 0.09
natA	BSU02750	Cluster 5	-0.01 ± 0.1	1.88 ± 0.1	1.04 ± 0.09
opuAA	BSU02980	Cluster 5	-0.01 ± 0.11	1.62 ± 0.04	-0.2 ± 0.26
ldh	BSU03050	Cluster 5	-0.08 ± 0.57	2.22 ± 0.02	1.99 ± 0.15
lctP	BSU03060	Cluster 5	-0.12 ± 0.69	2.83 ± 0.06	2.55 ± 0.14
putB	BSU03200	Cluster 5	-0.02 ± 0.25	3.86 ± 0.12	-1.04 ± 0.05
putC	BSU03210	Cluster 5	-0.01 ± 0.13	3.56 ± 0.07	-0.63 ± 0.05
putP	BSU03220	Cluster 5	-0.01 ± 0.07	1.97 ± 0.09	-0.75 ± 0.02
nasD	BSU03300	Cluster 5	-0.02 ± 0.22	1.61 ± 0.11	0.64 ± 0.2
srfAA	BSU03480	Cluster 5	-0.05 ± 0.44	2.28 ± 0.05	1.71 ± 0.15
srfAB	BSU03490	Cluster 5	-0.05 ± 0.48	2.44 ± 0.02	1.66 ± 0.09
comS	BSU03500	Cluster 5	-0.03 ± 0.37	2.53 ± 0.15	1.75 ± 0.07
srfAC	BSU03510	Cluster 5	-0.05 ± 0.45	2.09 ± 0.06	1.46 ± 0.21
srfAD	BSU03520	Cluster 5	-0.05 ± 0.44	2.25 ± 0.05	1.36 ± 0.25
sfp/2	BSU03570	Cluster 5	-0.01 ± 0.15	1.7 ± 0.03	1.01 ± 0.15
ycsF	BSU04050	Cluster 5	-0.01 ± 0.14	1.64 ± 0.03	0.37 ± 0.02
ycsI	BSU04070	Cluster 5	-0.01 ± 0.17	1.92 ± 0.1	0.79 ± 0.05
kipI	BSU04080	Cluster 5	-0.01 ± 0.19	2.04 ± 0.05	0.95 ± 0.11
kipA	BSU04090	Cluster 5	-0.02 ± 0.22	1.79 ± 0.05	0.76 ± 0.03
kipR	BSU04100	Cluster 5	-0.01 ± 0.11	2.06 ± 0.05	1.11 ± 0.04
mutT	BSU04330	Cluster 5	-0.01 ± 0.19	1.87 ± 0.1	1.13 ± 0.11
ydbJ	BSU04490	Cluster 5	-0.01 ± 0.03	1.66 ± 0.08	0.83 ± 0.03
ydbL	BSU04510	Cluster 5	-0.01 ± 0.21	1.97 ± 0.13	0.14 ± 0.13
ydcO	BSU04840	Cluster 5	-0.03 ± 0.33	1.8 ± 0.13	0.05 ± 0.09
ydcP	BSU04850	Cluster 5	-0.04 ± 0.39	2.04 ± 0.09	0.11 ± 0.13
ydcQ	BSU04860	Cluster 5	-0.02 ± 0.29	1.75 ± 0.11	0.47 ± 0.06
ydcS	BSU04880	Cluster 5	-0.03 ± 0.34	1.65 ± 0.07	0.46 ± 0.11
yddD	BSU04930	Cluster 5	-0.1 ± 0.63	2.03 ± 0.12	0.64 ± 0.02
conE	BSU04940	Cluster 5	-0.01 ± 0.07	1.7 ± 0.13	0.32 ± 0.17

Gene name	BSU numbers	Cluster	Log2 ratio data normalized to μ=0.1 condition		
			μ=0.1	**NaCl**	**NaCl+GB**
yddF	BSU04950	Cluster 5	-0.02 ± 0.24	2.02 ± 0.14	0.24 ± 0.14
yddG	BSU04960	Cluster 5	-0.04 ± 0.38	1.85 ± 0.21	-0.15 ± 0.05
yddJ	BSU04990	Cluster 5	-0.01 ± 0.08	1.97 ± 0.11	0.81 ± 0.07
lrpB	BSU05060	Cluster 5	-0.02 ± 0.24	1.93 ± 0.1	0.43 ± 0.1
ydeG	BSU05190	Cluster 5	-0.01 ± 0.06	1.59 ± 0.06	1.23 ± 0.12
ydgK	BSU05680	Cluster 5	-0.01 ± 0.07	2.21 ± 0.06	0.64 ± 0.28
ydhB	BSU05690	Cluster 5	-0.01 ± 0.15	0.75 ± 0.04	-0.91 ± 0.14
pbuE	BSU05800	Cluster 5	-0.06 ± 0.51	2.14 ± 0.06	1.3 ± 0.04
ydjM	BSU06250	Cluster 5	-0.02 ± 0.3	2.51 ± 0.13	1.47 ± 0.18
ydjN	BSU06260	Cluster 5	-0.02 ± 0.27	2.49 ± 0.06	1.44 ± 0.13
opuE	BSU06660	Cluster 5	-0.01 ± 0.16	3.5 ± 0.08	1.66 ± 0.33
yetL	BSU07220	Cluster 5	-0.01 ± 0.03	2.1 ± 0.1	1.09 ± 0.11
yfmQ	BSU07380	Cluster 5	-0.02 ± 0.24	1.31 ± 0.09	-0.47 ± 0.18
yfmG	BSU07480	Cluster 5	-0.01 ± 0.12	2.51 ± 0.16	1.49 ± 0.1
ltaS	BSU07710	Cluster 5	-0.01 ± 0.12	1.68 ± 0.05	1.07 ± 0.08
yfkN	BSU07840	Cluster 5	-0.01 ± 0.11	2.66 ± 0.02	0.63 ± 0.03
yfjC	BSU08150	Cluster 5	-0.01 ± 0.09	2.08 ± 0.09	1.31 ± 0.04
yfjB	BSU08160	Cluster 5	-0.01 ± 0.12	2.2 ± 0.04	1.35 ± 0.05
yfjA	BSU08170	Cluster 5	-0.01 ± 0.16	2.64 ± 0.03	1.52 ± 0.11
yfiQ	BSU08360	Cluster 5	-0.02 ± 0.22	2.45 ± 0.06	1.05 ± 0.05
yhaT	BSU09860	Cluster 5	-0.01 ± 0.14	1.86 ± 0.08	0.58 ± 0.07
yhjC	BSU10460	Cluster 5	-0.06 ± 0.51	1.53 ± 0.08	0.58 ± 0.15
yhjP	BSU10590	Cluster 5	-0.01 ± 0.15	1.71 ± 0.05	0.35 ± 0.14
yisV	BSU10880	Cluster 5	-0.01 ± 0.13	1.59 ± 0.02	0.03 ± 0.05
yitM	BSU11040	Cluster 5	-0.05 ± 0.45	2.81 ± 0.11	1.27 ± 0.21
yitM	BSU11050	Cluster 5	-0.04 ± 0.42	4.21 ± 0.07	2.65 ± 0.15
yitO	BSU11060	Cluster 5	-0.04 ± 0.42	4.1 ± 0.11	2.59 ± 0.13
yitP	BSU11070	Cluster 5	-0.06 ± 0.49	4.09 ± 0.14	2.69 ± 0.06
nprB	BSU11100	Cluster 5	-0.01 ± 0.18	2.52 ± 0.06	1.6 ± 0.13
yjcD	BSU11820	Cluster 5	-0.01 ± 0.07	1.78 ± 0.11	1.32 ± 0.28
yjdJ	BSU12070	Cluster 5	-0.01 ± 0.16	1.62 ± 0.09	0.57 ± 0.16
ctaO	BSU12080	Cluster 5	-0.04 ± 0.41	2.75 ± 0.07	0.94 ± 0.33
xkdB	BSU12520	Cluster 5	-0.02 ± 0.28	3.06 ± 0.08	0.25 ± 0.22
xkdC	BSU12530	Cluster 5	-0.03 ± 0.37	2.05 ± 0.05	-0.55 ± 0.09
xkdD	BSU12540	Cluster 5	-0.01 ± 0.12	1.34 ± 0.12	-0.42 ± 0.05
xtrA	BSU12550	Cluster 5	-0.02 ± 0.26	2.58 ± 0.06	-0.08 ± 0.12
xpf	BSU12560	Cluster 5	-0.06 ± 0.5	3.18 ± 0.09	0.07 ± 0.12
xtmA	BSU12570	Cluster 5	-0.03 ± 0.32	1.94 ± 0.03	-0.15 ± 0.19
xtmB	BSU12580	Cluster 5	-0.01 ± 0.21	2.14 ± 0.04	-0.01 ± 0.13
xkdE	BSU12590	Cluster 5	-0.02 ± 0.23	2.18 ± 0.07	0.02 ± 0.16
xkdF	BSU12600	Cluster 5	-0.02 ± 0.29	1.72 ± 0.06	-0.47 ± 0.13
xkdG	BSU12610	Cluster 5	-0.02 ± 0.29	1.57 ± 0.02	-0.5 ± 0.14
xkdH	BSU12620	Cluster 5	-0.03 ± 0.32	1.75 ± 0.05	-0.32 ± 0.12
xkdI	BSU12630	Cluster 5	-0.02 ± 0.29	1.66 ± 0.05	-0.47 ± 0.13
xkdJ	BSU12640	Cluster 5	-0.02 ± 0.28	1.69 ± 0.06	-0.28 ± 0.13
xkdK	BSU12650	Cluster 5	-0.03 ± 0.37	1.73 ± 0.09	-0.53 ± 0.15
xkdM	BSU12660	Cluster 5	-0.03 ± 0.33	1.73 ± 0.04	-0.55 ± 0.13
xkdM	BSU12670	Cluster 5	-0.02 ± 0.27	1.48 ± 0.16	-0.85 ± 0.18
xkdO	BSU12680	Cluster 5	-0.02 ± 0.25	1.64 ± 0.05	-0.82 ± 0.06
xkdP	BSU12690	Cluster 5	-0.02 ± 0.22	1.8 ± 0.2	-0.78 ± 0.08
xkdQ	BSU12700	Cluster 5	-0.03 ± 0.34	1.87 ± 0.03	-0.68 ± 0.06
xkdR	BSU12710	Cluster 5	-0.02 ± 0.26	1.68 ± 0.06	-0.41 ± 0.05
xkdS	BSU12720	Cluster 5	-0.02 ± 0.27	1.79 ± 0.01	-0.76 ± 0.06
xkdT	BSU12730	Cluster 5	-0.01 ± 0.21	1.77 ± 0.06	-0.63 ± 0.04
xkdU	BSU12740	Cluster 5	-0.02 ± 0.3	1.75 ± 0.07	-0.58 ± 0.09
xkdV	BSU12750	Cluster 5	-0.04 ± 0.39	1.71 ± 0.03	-0.75 ± 0.13
xkdW	BSU12760	Cluster 5	-0.04 ± 0.38	1.99 ± 0.04	-0.54 ± 0.16
xkdX	BSU12770	Cluster 5	-0.05 ± 0.44	1.92 ± 0.05	-0.64 ± 0.14
xepA	BSU12780	Cluster 5	-0.02 ± 0.27	1.8 ± 0.03	-0.58 ± 0.11

Gene name	BSU numbers	Cluster	Log2 ratio data normalized to μ=0.1 condition		
			μ=0.1	**NaCl**	**NaCl+GB**
xhlA	BSU12790	Cluster 5	-0.04 ± 0.42	1.94 ± 0.06	-0.25 ± 0.15
xhlB	BSU12800	Cluster 5	-0.03 ± 0.37	2 ± 0.06	-0.16 ± 0.09
xlyA	BSU12810	Cluster 5	-0.03 ± 0.37	1.89 ± 0.06	-0.03 ± 0.06
ohrA	BSU13140	Cluster 5	-0.01 ± 0.17	1.86 ± 0.08	1.43 ± 0.14
ykwD	BSU13970	Cluster 5	-0.04 ± 0.38	2.24 ± 0.04	1.85 ± 0.09
ylbG	BSU15000	Cluster 5	-0.01 ± 0.1	1.6 ± 0.02	0.95 ± 0.14
bpr	BSU15300	Cluster 5	-0.01 ± 0.17	2.13 ± 0.17	1.04 ± 0.16
ylmA	BSU15340	Cluster 5	-0.01 ± 0.08	2.17 ± 0.02	1.16 ± 0.07
mutS	BSU17040	Cluster 5	-0.01 ± 0.14	1.71 ± 0.07	0.83 ± 0.03
mutL	BSU17050	Cluster 5	-0.01 ± 0.21	1.67 ± 0.08	0.85 ± 0.11
ynzC	BSU17880	Cluster 5	-0.04 ± 0.41	2.06 ± 0.03	1.62 ± 0.22
penP	BSU18800	Cluster 5	-0.01 ± 0.07	1.71 ± 0.04	0.26 ± 0.1
yocC	BSU19160	Cluster 5	-0.01 ± 0.21	2.94 ± 0.03	2.29 ± 0.3
yocH	BSU19210	Cluster 5	-0.02 ± 0.22	2.63 ± 0.06	2.01 ± 0.09
yojE	BSU19480	Cluster 5	-0.02 ± 0.21	1.76 ± 0.1	0.66 ± 0.22
yosU	BSU20000	Cluster 5	-0.04 ± 0.42	2.41 ± 0.06	0.88 ± 0.56
bdbB	BSU21440	Cluster 5	-0.01 ± 0.07	1.74 ± 0.1	1.48 ± 0.05
sunS	BSU21450	Cluster 5	-0.01 ± 0.11	1.66 ± 0.15	1.49 ± 0.14
bdbA	BSU21460	Cluster 5	-0.01 ± 0.11	1.8 ± 0.16	1.45 ± 0.1
sunT	BSU21470	Cluster 5	-0.01 ± 0.08	2 ± 0.19	1.34 ± 0.19
yolD	BSU21510	Cluster 5	-0.02 ± 0.3	1.6 ± 0.16	0.12 ± 0.35
ypuE	BSU23290	Cluster 5	-0.01 ± 0.15	1.73 ± 0.23	0.89 ± 0.1
yqjM	BSU23820	Cluster 5	-0.01 ± 0.09	1.54 ± 0.06	-0.68 ± 0.05
yqiK	BSU24180	Cluster 5	-0.01 ± 0.03	3.03 ± 0.03	0.68 ± 0.09
yqiI	BSU24190	Cluster 5	-0.01 ± 0.18	6.91 ± 0.13	2.1 ± 0.11
yqiH	BSU24200	Cluster 5	-0.43 ± 1.31	4.41 ± 0.09	-0.19 ± 0.29
lipM	BSU24530	Cluster 5	-0.01 ± 0.07	1.6 ± 0.01	0.91 ± 0.15
gcvPB	BSU24550	Cluster 5	-0.02 ± 0.26	1.86 ± 0.04	1.47 ± 0.06
gcvPA	BSU24560	Cluster 5	-0.01 ± 0.21	1.81 ± 0.04	1.42 ± 0.07
gcvT	BSU24570	Cluster 5	-0.03 ± 0.31	1.73 ± 0.08	1.45 ± 0.08
yqgB	BSU25040	Cluster 5	-0.01 ± 0.16	1.68 ± 0.05	0.89 ± 0.17
yqxJ	BSU25880	Cluster 5	-0.01 ± 0.06	3.24 ± 0.13	1.64 ± 0.21
yqxI	BSU25890	Cluster 5	-0.02 ± 0.28	3.04 ± 0.09	1.22 ± 0.16
yqbD	BSU26150	Cluster 5	-0.03 ± 0.35	1.71 ± 0.16	0.36 ± 0.08
yqbC	BSU26160	Cluster 5	-0.01 ± 0.18	1.78 ± 0.05	0.68 ± 0.09
yrdR	BSU26620	Cluster 5	-0.03 ± 0.31	1.92 ± 0.02	0.89 ± 0.08
yrhP	BSU27100	Cluster 5	-0.02 ± 0.28	3.74 ± 0.02	1.79 ± 0.5
yrhO	BSU27110	Cluster 5	-0.01 ± 0.15	1.84 ± 0.06	1.29 ± 0.12
comC	BSU28070	Cluster 5	-0.04 ± 0.39	2.37 ± 0.22	2.02 ± 0.19
tcyN	BSU29340	Cluster 5	-0.01 ± 0.18	2.02 ± 0.04	0.76 ± 0.16
tcyM	BSU29350	Cluster 5	-0.01 ± 0.03	2.18 ± 0.16	0.77 ± 0.25
tcyL	BSU29360	Cluster 5	-0.02 ± 0.23	2.05 ± 0.02	0.55 ± 0.31
tcyK	BSU29370	Cluster 5	-0.01 ± 0.11	2.31 ± 0.16	0.57 ± 0.56
tcyJ	BSU29380	Cluster 5	-0.01 ± 0.15	1.69 ± 0.08	0.19 ± 0.24
ytmI	BSU29390	Cluster 5	-0.02 ± 0.24	3.42 ± 0.08	1.17 ± 0.49
ytlI	BSU29400	Cluster 5	-0.01 ± 0.12	1.78 ± 0.1	0.41 ± 0.27
ackA	BSU29470	Cluster 5	-0.01 ± 0.14	1.92 ± 0.05	1.33 ± 0.25
ytvA	BSU30340	Cluster 5	-0.01 ± 0.1	1.6 ± 0.11	1.29 ± 0.05
yttB	BSU30350	Cluster 5	-0.07 ± 0.51	2.01 ± 0.11	0.92 ± 0.1
mntB	BSU30760	Cluster 5	-0.02 ± 0.29	1.64 ± 0.05	1.48 ± 0.13
mntA	BSU30770	Cluster 5	-0.02 ± 0.25	1.7 ± 0.03	1.57 ± 0.03
gbsB	BSU31050	Cluster 5	-0.01 ± 0.17	2 ± 0.05	1.28 ± 0.1
gbsA	BSU31060	Cluster 5	-0.01 ± 0.12	2.15 ± 0.05	1.33 ± 0.06
yuxJ	BSU31480	Cluster 5	-0.01 ± 0.02	1.59 ± 0.04	0.74 ± 0.1
yuiH	BSU32020	Cluster 5	-0.01 ± 0.13	1.59 ± 0.08	0.91 ± 0.09
yuiB	BSU32080	Cluster 5	-0.02 ± 0.27	0.92 ± 0.09	-0.81 ± 0.37
yuiA	BSU32090	Cluster 5	-0.02 ± 0.23	0.92 ± 0.18	-0.93 ± 0.46
lip	BSU02700	Cluster 5	-0.01 ± 0.14	1.94 ± 0.03	1.22 ± 0.05
lipA	BSU32330	Cluster 5	-0.01 ± 0.14	1.94 ± 0.03	1.22 ± 0.05

Gene name	BSU numbers	Cluster	Log2 ratio data normalized to μ=0.1 condition		
			μ=0.1	**NaCl**	**NaCl+GB**
pucA	BSU32510	Cluster 5	-0.02 ± 0.28	1.75 ± 0.13	0.35 ± 0.12
pucG	BSU32520	Cluster 5	-0.02 ± 0.25	1.72 ± 0.09	0.98 ± 0.04
pucF	BSU32530	Cluster 5	-0.02 ± 0.29	2.75 ± 0.06	1.96 ± 0.04
yusR	BSU32900	Cluster 5	-0.02 ± 0.22	1.68 ± 0.05	0.64 ± 0.07
rghR	BSU33660	Cluster 5	-0.01 ± 0.11	2.17 ± 0.04	0.89 ± 0.07
yvaO	BSU33670	Cluster 5	-0.01 ± 0.07	2.34 ± 0.03	0.85 ± 0.13
sdpA	BSU33750	Cluster 5	-0.02 ± 0.23	2.68 ± 0.11	1.87 ± 0.1
sdpB	BSU33760	Cluster 5	-0.02 ± 0.22	2.85 ± 0.19	2.08 ± 0.07
sdpC	BSU33770	Cluster 5	-0.03 ± 0.33	1.7 ± 0.03	0.94 ± 0.09
yvbF	BSU33840	Cluster 5	-0.01 ± 0.09	2.03 ± 0.04	-0.4 ± 0.08
padC	BSU34400	Cluster 5	-0.01 ± 0.2	2.59 ± 0.06	1.35 ± 0.06
yveG	BSU34410	Cluster 5	-0.02 ± 0.24	3.01 ± 0.02	1.82 ± 0.03
yveF	BSU34420	Cluster 5	-0.03 ± 0.31	3.1 ± 0.06	1.97 ± 0.1
sacB	BSU34450	Cluster 5	-0.02 ± 0.28	2.45 ± 0.02	1.71 ± 0.14
yvdB	BSU34660	Cluster 5	-0.01 ± 0.12	1.46 ± 0.08	-0.21 ± 0.14
yvdA	BSU34670	Cluster 5	-0.01 ± 0.17	1.34 ± 0.03	-0.28 ± 0.03
yvkC	BSU35190	Cluster 5	-0.02 ± 0.27	1.87 ± 0.09	0.87 ± 0.12
capE	BSU35870	Cluster 5	-0.03 ± 0.34	1.75 ± 0.13	1.4 ± 0.12
capA	BSU35880	Cluster 5	-0.02 ± 0.25	2.18 ± 0.04	0.89 ± 0.02
capC	BSU35890	Cluster 5	-0.01 ± 0.07	2.07 ± 0.03	0.92 ± 0.11
capB	BSU35900	Cluster 5	-0.01 ± 0.12	2.01 ± 0.07	0.49 ± 0.09
alsD	BSU36000	Cluster 5	-0.01 ± 0.21	2.31 ± 0.02	0.82 ± 0.14
alsS	BSU36010	Cluster 5	-0.02 ± 0.23	1.99 ± 0.07	0.35 ± 0.15
ywqG	BSU36220	Cluster 5	-0.02 ± 0.21	1.6 ± 0.02	1.26 ± 0.06
ptpZ	BSU36240	Cluster 5	-0.01 ± 0.09	2.36 ± 0.03	2.13 ± 0.19
glcR	BSU36300	Cluster 5	-0.01 ± 0.07	1.83 ± 0.05	1.29 ± 0.17
ssbB	BSU36310	Cluster 5	-0.02 ± 0.24	1.66 ± 0.24	0.98 ± 0.28
mscL	BSU36360	Cluster 5	-0.02 ± 0.21	2 ± 0.04	0.87 ± 0.02
ywpB	BSU36370	Cluster 5	-0.02 ± 0.25	2.74 ± 0.09	1.28 ± 0.2
ywnB	BSU36620	Cluster 5	-0.01 ± 0.06	1.86 ± 0.01	0.82 ± 0.08
ywmC	BSU36740	Cluster 5	-0.08 ± 0.58	1.63 ± 0.15	0.35 ± 0.11
sboA	BSU37350	Cluster 5	-0.03 ± 0.34	1.37 ± 0.11	-0.29 ± 0.21
sboX	BSU37360	Cluster 5	-0.02 ± 0.24	1.64 ± 0.14	0.06 ± 0.14
sacP	BSU38050	Cluster 5	-0.03 ± 0.35	1.67 ± 0.06	0.66 ± 0.06
sacX	BSU38410	Cluster 5	-0.03 ± 0.32	2.95 ± 0.07	2.34 ± 0.04
sacY	BSU38420	Cluster 5	-0.01 ± 0.1	2.08 ± 0.05	1.6 ± 0.05
ywaD	BSU38470	Cluster 5	-0.02 ± 0.22	2.04 ± 0.09	-0.6 ± 0.05
yxlA	BSU38710	Cluster 5	-0.04 ± 0.41	2.2 ± 0.11	1.1 ± 0.29
yxeL	BSU39510	Cluster 5	-0.05 ± 0.44	1.59 ± 0.09	1.45 ± 0.34
yxeK	BSU39520	Cluster 5	-0.04 ± 0.37	1.83 ± 0.12	1.46 ± 0.44
yxeA	BSU39620	Cluster 5	-0.12 ± 0.69	1.74 ± 0.17	0.52 ± 0.05
yxdM	BSU39630	Cluster 5	-0.01 ± 0.17	2.17 ± 0.01	1.12 ± 0.06
yxdL	BSU39640	Cluster 5	-0.02 ± 0.25	2.07 ± 0.06	0.75 ± 0.1
yxbD	BSU39870	Cluster 5	-0.06 ± 0.5	1.7 ± 0.15	0.22 ± 0.23
yxaD	BSU40020	Cluster 5	-0.01 ± 0.1	2.78 ± 0.07	1.94 ± 0.11
yxaA	BSU40040	Cluster 5	-0.02 ± 0.26	2.4 ± 0.03	1.63 ± 0.06
yydJ	BSU40140	Cluster 5	-0.01 ± 0.21	1.76 ± 0.04	1.4 ± 0.1
yydG	BSU40170	Cluster 5	-0.01 ± 0.15	3.03 ± 0.21	2.34 ± 0.1
yydF	BSU40180	Cluster 5	-0.02 ± 0.26	2.3 ± 0.18	1.95 ± 0.16
yycS	BSU40240	Cluster 5	-0.01 ± 0.04	2.3 ± 0.09	1.39 ± 0.02
yybM	BSU40590	Cluster 5	-0.01 ± 0.14	1.88 ± 0.17	1.68 ± 0.14
yybL	BSU40600	Cluster 5	-0.02 ± 0.27	2.42 ± 0.23	2.2 ± 0.23
yybK	BSU40610	Cluster 5	-0.01 ± 0.05	2.26 ± 0.16	2.03 ± 0.3
yyaN	BSU40800	Cluster 5	-0.01 ± 0.13	1.67 ± 0.02	0.39 ± 0.37
ccpB	BSU40870	Cluster 5	-0.01 ± 0.01	2.15 ± 0.02	0.54 ± 0.1
pckA	BSU30560	Cluster 6	-0.11 ± 0.71	-1.38 ± 0.02	0.48 ± 0.08
gapB	BSU29020	Cluster 6	-0.27 ± 1.09	-2.69 ± 0.04	0.53 ± 0.13
ybdO	BSU02050	Cluster 6	-0.05 ± 0.46	-1.43 ± 0.04	0.37 ± 0.16
glpQ	BSU02130	Cluster 6	-0.01 ± 0.1	-0.72 ± 0.11	0.91 ± 0.22

Gene name	BSU numbers	Cluster	Log2 ratio data normalized to μ=0.1 condition		
			μ=0.1	**NaCl**	**NaCl+GB**
glpT	BSU02140	Cluster 6	-0.01 ± 0.06	-1.3 ± 0.12	1.23 ± 0.2
gamA	BSU02360	Cluster 6	-0.02 ± 0.29	-1.27 ± 0.07	2.57 ± 0.41
yckE	BSU03410	Cluster 6	-0.23 ± 0.98	-3.5 ± 0.05	-0.6 ± 1.08
dctP	BSU04470	Cluster 6	-0.01 ± 0.12	-1.14 ± 0.07	0.63 ± 0.08
iolT	BSU06230	Cluster 6	-0.02 ± 0.23	-2.89 ± 0.06	0.46 ± 0.22
purH	BSU06520	Cluster 6	-0.03 ± 0.3	-1.44 ± 0.17	0.2 ± 0.14
yfmT	BSU07350	Cluster 6	-0.02 ± 0.22	-4.27 ± 0.09	-0.25 ± 0.11
yfmS	BSU07360	Cluster 6	-0.01 ± 0.18	-4.02 ± 0.08	-0.21 ± 0.11
acoA	BSU08060	Cluster 6	-0.04 ± 0.37	-2.65 ± 0.27	1.3 ± 0.29
acoB	BSU08070	Cluster 6	-0.03 ± 0.34	-2.78 ± 0.3	1.17 ± 0.26
acoC	BSU08080	Cluster 6	-0.04 ± 0.37	-2.87 ± 0.28	1.14 ± 0.25
acoL	BSU08090	Cluster 6	-0.04 ± 0.41	-2.42 ± 0.35	1.24 ± 0.3
malA	BSU08180	Cluster 6	-0.01 ± 0.07	-1.7 ± 0.06	-0.08 ± 0.08
glvR	BSU08190	Cluster 6	-0.01 ± 0.09	-1.91 ± 0.05	-0.47 ± 0.07
malP	BSU08200	Cluster 6	-0.01 ± 0.11	-2.56 ± 0.04	-0.48 ± 0.13
csbB	BSU08600	Cluster 6	-0.01 ± 0.06	-0.87 ± 0.1	0.74 ± 0.13
yhcM	BSU09140	Cluster 6	-0.05 ± 0.44	-2.29 ± 0.1	-0.2 ± 0.18
glpF	BSU09280	Cluster 6	-0.01 ± 0.13	-2.93 ± 0.05	0.63 ± 0.23
glpK	BSU09290	Cluster 6	-0.01 ± 0.21	-1.95 ± 0.07	0.87 ± 0.15
lytF	BSU09370	Cluster 6	-0.01 ± 0.08	-3.8 ± 0.07	-0.12 ± 0.07
yhaR	BSU09880	Cluster 6	-0.01 ± 0.14	-1.6 ± 0.09	-0.37 ± 0.1
hemAT	BSU10380	Cluster 6	-0.01 ± 0.15	-3.48 ± 0.21	-0.5 ± 0.03
yjbC	BSU11490	Cluster 6	-0.01 ± 0.13	-1.74 ± 0.05	-0.19 ± 0.19
cwlQ	BSU11570	Cluster 6	-0.01 ± 0.09	-2.07 ± 0.09	-0.36 ± 0.05
yjcP	BSU11940	Cluster 6	-0.02 ± 0.25	-2.01 ± 0.12	0.83 ± 0.2
yjcQ	BSU11950	Cluster 6	-0.02 ± 0.21	-1.18 ± 0.08	0.54 ± 0.09
manP	BSU12010	Cluster 6	-0.02 ± 0.25	-1.45 ± 0.03	0.9 ± 0.12
manA	BSU12020	Cluster 6	-0.01 ± 0.14	-1.14 ± 0.03	0.77 ± 0.03
yjfB	BSU12120	Cluster 6	-0.01 ± 0.21	-3.57 ± 0.07	-0.53 ± 0.12
rapA	BSU12430	Cluster 6	-0.01 ± 0.14	-1.63 ± 0.1	0.48 ± 0.31
phrA	BSU12440	Cluster 6	-0.02 ± 0.22	-1.5 ± 0.07	0.53 ± 0.2
ykoW	BSU13420	Cluster 6	-0.01 ± 0.11	-2.75 ± 0.14	-0.32 ± 0.03
motB	BSU13680	Cluster 6	-0.18 ± 0.86	-4.3 ± 0.02	-0.74 ± 0.1
motA	BSU13690	Cluster 6	-0.17 ± 0.83	-4.58 ± 0.05	-0.69 ± 0.05
ptsG	BSU13890	Cluster 6	-0.07 ± 0.52	-2.8 ± 0.13	0.39 ± 0.23
ptsH	BSU13900	Cluster 6	-0.07 ± 0.52	-2.25 ± 0.22	0.04 ± 0.21
ptsI	BSU13910	Cluster 6	-0.03 ± 0.36	-1.92 ± 0.16	0.05 ± 0.23
cheV	BSU14010	Cluster 6	-0.11 ± 0.67	-3.8 ± 0.11	-0.88 ± 0.01
ykzI	BSU14660	Cluster 6	-0.09 ± 0.63	-3.16 ± 0.11	-0.82 ± 0.28
ylqB	BSU15960	Cluster 6	-0.05 ± 0.47	-3.38 ± 0.04	0.98 ± 0.14
rnhB	BSU16060	Cluster 6	-0.01 ± 0.11	-2.35 ± 0.07	0.15 ± 0.07
ylqG	BSU16070	Cluster 6	-0.01 ± 0.12	-2.05 ± 0.07	0.29 ± 0.09
ylqH	BSU16080	Cluster 6	-0.01 ± 0.2	-1.33 ± 0.12	0.63 ± 0.08
trmFO	BSU16130	Cluster 6	-0.01 ± 0.21	-1.68 ± 0.15	-0.13 ± 0.04
fliE	BSU16200	Cluster 6	-0.01 ± 0.07	-3.67 ± 0.11	-0.98 ± 0.03
fliF	BSU16210	Cluster 6	-0.01 ± 0.05	-3.49 ± 0.06	-0.94 ± 0.07
fliG	BSU16220	Cluster 6	-0.01 ± 0.1	-3.44 ± 0.15	-0.9 ± 0.1
fliH	BSU16230	Cluster 6	-0.01 ± 0.17	-3.18 ± 0.1	-0.79 ± 0.12
fliI	BSU16240	Cluster 6	-0.01 ± 0.04	-3.18 ± 0.14	-0.83 ± 0.06
fliJ	BSU16250	Cluster 6	-0.01 ± 0.05	-3.12 ± 0.07	-0.71 ± 0.06
ylxF	BSU16260	Cluster 6	-0.01 ± 0.1	-3.17 ± 0.15	-0.6 ± 0.11
fliK	BSU16270	Cluster 6	-0.01 ± 0.13	-3.19 ± 0.18	-0.48 ± 0.08
ylxG	BSU16280	Cluster 6	-0.01 ± 0.13	-3.3 ± 0.11	-0.64 ± 0.04
flgE	BSU16290	Cluster 6	-0.01 ± 0.19	-3.17 ± 0.06	-0.66 ± 0.06
fliL	BSU16300	Cluster 6	-0.01 ± 0.18	-3.01 ± 0.12	-0.61 ± 0.04
fliM	BSU16310	Cluster 6	-0.02 ± 0.22	-3.01 ± 0.18	-0.68 ± 0.03
fliY	BSU16320	Cluster 6	-0.02 ± 0.21	-2.99 ± 0.14	-0.67 ± 0.04
cheY	BSU16330	Cluster 6	-0.01 ± 0.18	-3 ± 0.13	-0.57 ± 0.08
fliP	BSU16350	Cluster 6	-0.01 ± 0.18	-3.12 ± 0.06	-0.66 ± 0.08

Gene name	BSU numbers	Cluster	Log2 ratio data normalized to μ=0.1 condition		
			μ=0.1	NaCl	NaCl+GB
fliQ	BSU16360	Cluster 6	-0.01 ± 0.17	-2.8 ± 0.1	-0.31 ± 0.03
fliR	BSU16370	Cluster 6	-0.01 ± 0.18	-2.87 ± 0.1	-0.21 ± 0.06
flhB	BSU16380	Cluster 6	-0.01 ± 0.15	-2.59 ± 0.12	-0.19 ± 0.15
flhA	BSU16390	Cluster 6	-0.01 ± 0.2	-2.38 ± 0.12	-0.03 ± 0.08
flhF	BSU16400	Cluster 6	-0.01 ± 0.19	-2.51 ± 0.13	-0.24 ± 0.1
ylxH	BSU16410	Cluster 6	-0.02 ± 0.23	-2.22 ± 0.09	-0.03 ± 0.13
cheB	BSU16420	Cluster 6	-0.02 ± 0.22	-2.21 ± 0.14	-0.07 ± 0.14
cheA	BSU16430	Cluster 6	-0.02 ± 0.29	-2.25 ± 0.07	-0.26 ± 0.11
cheW	BSU16440	Cluster 6	-0.03 ± 0.33	-1.71 ± 0.05	0.05 ± 0.07
cheC	BSU16450	Cluster 6	-0.02 ± 0.27	-1.65 ± 0.04	0.07 ± 0.09
cheD	BSU16460	Cluster 6	-0.02 ± 0.23	-1.63 ± 0.06	0.05 ± 0.12
sigD	BSU16470	Cluster 6	-0.01 ± 0.13	-1.29 ± 0.05	0.39 ± 0.05
tdh	BSU16990	Cluster 6	-0.01 ± 0.11	-1.83 ± 0.06	-0.15 ± 0.1
kbl	BSU17000	Cluster 6	-0.01 ± 0.09	-1.91 ± 0.02	-0.1 ± 0.14
yncC	BSU17630	Cluster 6	-0.01 ± 0.2	-1 ± 0.04	0.92 ± 0.15
yoxC	BSU18510	Cluster 6	-0.02 ± 0.29	-0.63 ± 0.12	1.31 ± 0.19
yoaH	BSU18610	Cluster 6	-0.01 ± 0.16	-3.35 ± 0.11	-0.07 ± 0.03
pps	BSU18830	Cluster 6	-0.01 ± 0.07	-1.05 ± 0.06	0.92 ± 0.04
yobO	BSU19030	Cluster 6	-0.01 ± 0.11	-1.65 ± 0.07	-0.27 ± 0.18
yojJ	BSU19430	Cluster 6	-0.02 ± 0.3	-2.08 ± 0.07	-0.05 ± 0.23
yojA	BSU19520	Cluster 6	-0.02 ± 0.25	-1.77 ± 0.12	-0.07 ± 0.06
yorQ	BSU20290	Cluster 6	-0.01 ± 0.04	-1.94 ± 0.52	-0.54 ± 0.2
yorO	BSU20310	Cluster 6	-0.01 ± 0.17	-1.95 ± 0.47	-0.04 ± 0.23
yonS	BSU21010	Cluster 6	-0.01 ± 0.14	-2.29 ± 0.03	0.46 ± 0.09
yonR	BSU21020	Cluster 6	-0.01 ± 0.17	-2.18 ± 0.13	0.51 ± 0.17
yomK	BSU21330	Cluster 6	-0.02 ± 0.23	-2.57 ± 0.25	0.49 ± 0.09
yodH	BSU19600	Cluster 6	-0.01 ± 0.16	-1.89 ± 0.09	0.22 ± 0.04
yolB	BSU21530	Cluster 6	-0.01 ± 0.16	-1.89 ± 0.09	0.22 ± 0.04
yolA	BSU21540	Cluster 6	-0.01 ± 0.19	-1.77 ± 0.08	0.2 ± 0.06
pbuX	BSU22060	Cluster 6	-0.01 ± 0.08	-2.82 ± 0.25	0.09 ± 0.15
xpt	BSU22070	Cluster 6	-0.01 ± 0.17	-2.53 ± 0.16	-0.13 ± 0.21
corA	BSU24740	Cluster 6	-0.03 ± 0.34	-0.6 ± 0.13	1.11 ± 0.27
mgsR	BSU24770	Cluster 6	-0.02 ± 0.25	-1.25 ± 0.18	1.56 ± 0.38
yqbF	BSU26130	Cluster 6	-0.01 ± 0.17	-1.79 ± 0.19	0.22 ± 0.11
yqaR	BSU26210	Cluster 6	-0.01 ± 0.2	-1.49 ± 0.06	0.5 ± 0.02
yscB	BSU28890	Cluster 6	-0.02 ± 0.25	-3.38 ± 0.19	-0.08 ± 0.14
yteS	BSU30110	Cluster 6	-0.01 ± 0.19	-2.33 ± 0.14	-0.25 ± 0.24
yteR	BSU30120	Cluster 6	-0.07 ± 0.5	-2.14 ± 0.05	-0.28 ± 0.15
yteR	BSU30130	Cluster 6	-0.07 ± 0.52	-2.77 ± 0.08	-0.4 ± 0.12
yteP	BSU30140	Cluster 6	-0.09 ± 0.58	-2.08 ± 0.15	-0.31 ± 0.17
ytdP	BSU30150	Cluster 6	-0.01 ± 0.12	-2.31 ± 0.07	-0.31 ± 0.07
tlpB	BSU31230	Cluster 6	-0.01 ± 0.05	-2.41 ± 0.09	-0.34 ± 0.1
mcpA	BSU31240	Cluster 6	-0.02 ± 0.29	-3.64 ± 0.04	0.44 ± 0.14
tlpA	BSU31250	Cluster 6	-0.06 ± 0.47	-0.94 ± 0.2	0.92 ± 0.14
yuzA	BSU31380	Cluster 6	-0.01 ± 0.17	-1.6 ± 0.2	0.33 ± 0.3
yvbJ	BSU33880	Cluster 6	-0.01 ± 0.12	-2.03 ± 0.09	-0.53 ± 0.18
fliT	BSU35320	Cluster 6	-0.02 ± 0.22	-3.62 ± 0.05	-0.56 ± 0.06
fliS	BSU35330	Cluster 6	-0.02 ± 0.23	-3.62 ± 0.04	-0.59 ± 0.03
fliD	BSU35340	Cluster 6	-0.01 ± 0.16	-3.81 ± 0.09	-0.61 ± 0.08
yvyC	BSU35350	Cluster 6	-0.01 ± 0.17	-3.66 ± 0.23	-0.47 ± 0.06
hag	BSU35360	Cluster 6	-0.08 ± 0.56	-5.91 ± 0.02	-0.76 ± 0.05
flgL	BSU35400	Cluster 6	-0.01 ± 0.11	-2.08 ± 0.11	-0.06 ± 0.07
flgK	BSU35410	Cluster 6	-0.01 ± 0.11	-2.1 ± 0.07	-0.05 ± 0.07
yvyG	BSU35420	Cluster 6	-0.01 ± 0.06	-1.97 ± 0.15	0.04 ± 0.12
flgM	BSU35430	Cluster 6	-0.01 ± 0.12	-2.33 ± 0.09	-0.19 ± 0.09
yvyF	BSU35440	Cluster 6	-0.01 ± 0.09	-1.66 ± 0.13	-0.42 ± 0.05
lytC	BSU35620	Cluster 6	-0.01 ± 0.11	-1.24 ± 0.09	0.86 ± 0.13
lytB	BSU35630	Cluster 6	-0.01 ± 0.05	-1.03 ± 0.17	0.94 ± 0.07
lytA	BSU35640	Cluster 6	-0.01 ± 0.08	-1.05 ± 0.11	0.99 ± 0.09

Gene name	BSU numbers	Cluster	Log2 ratio data normalized to μ=0.1 condition		
			μ=0.1	**NaCl**	**NaCl+GB**
pgdS	BSU35860	Cluster 6	-0.01 ± 0.13	-3.81 ± 0.02	-0.56 ± 0.05
rbsR	BSU35910	Cluster 6	-0.01 ± 0.13	-2.05 ± 0.1	-0.4 ± 0.13
rbsK	BSU35920	Cluster 6	-0.01 ± 0.1	-2.15 ± 0.06	-0.39 ± 0.22
rbsD	BSU35930	Cluster 6	-0.01 ± 0.11	-2.51 ± 0.03	-0.55 ± 0.21
rbsA	BSU35940	Cluster 6	-0.01 ± 0.16	-2.71 ± 0.13	-0.63 ± 0.26
rbsC	BSU35950	Cluster 6	-0.01 ± 0.14	-2.77 ± 0.1	-0.66 ± 0.32
rbsB	BSU35960	Cluster 6	-0.01 ± 0.08	-2.9 ± 0.1	-0.67 ± 0.33
ywsB	BSU35970	Cluster 6	-0.01 ± 0.09	-1.89 ± 0.12	0.09 ± 0.25
flhP	BSU36390	Cluster 6	-0.01 ± 0.07	-2.39 ± 0.02	-0.06 ± 0.02
flhO	BSU36400	Cluster 6	-0.01 ± 0.1	-2.48 ± 0.04	-0.14 ± 0.07
ywmE	BSU36720	Cluster 6	-0.03 ± 0.34	-0.8 ± 0.25	1.27 ± 0.28
ywkB	BSU37040	Cluster 6	-0.03 ± 0.36	-0.99 ± 0.16	0.81 ± 0.28
ywjC	BSU37210	Cluster 6	-0.07 ± 0.57	-1.65 ± 0.08	0.81 ± 0.44
ywcE	BSU38130	Cluster 6	-0.01 ± 0.19	-1.65 ± 0.13	-0.36 ± 0.33
ywzA	BSU38180	Cluster 6	-0.04 ± 0.39	-0.85 ± 0.11	1.52 ± 0.29
epr	BSU38400	Cluster 6	-0.01 ± 0.12	-5.35 ± 0.05	-1.47 ± 0.09
yxkH	BSU38800	Cluster 6	-0.01 ± 0.09	-2.2 ± 0.11	0.53 ± 0.05
msmX	BSU38810	Cluster 6	-0.01 ± 0.17	-1.87 ± 0.06	0.53 ± 0.06
yxkC	BSU38850	Cluster 6	-0.02 ± 0.27	-2.07 ± 0.06	0.66 ± 0.22
iolJ	BSU39670	Cluster 6	-0.01 ± 0.2	-1.5 ± 0.08	0.49 ± 0.04
iolI	BSU39680	Cluster 6	-0.02 ± 0.24	-1.53 ± 0.07	0.59 ± 0.02
iolH	BSU39690	Cluster 6	-0.02 ± 0.24	-1.38 ± 0.06	0.68 ± 0.03
iolG	BSU39700	Cluster 6	-0.02 ± 0.23	-1.4 ± 0.08	0.65 ± 0.03
iolF	BSU39710	Cluster 6	-0.02 ± 0.22	-1.18 ± 0.07	0.81 ± 0.03
iolE	BSU39720	Cluster 6	-0.02 ± 0.25	-1.03 ± 0.1	0.84 ± 0.06
iolD	BSU39730	Cluster 6	-0.02 ± 0.23	-1.17 ± 0.03	0.71 ± 0.09
iolC	BSU39740	Cluster 6	-0.01 ± 0.21	-1.04 ± 0.05	0.92 ± 0.07
iolB	BSU39750	Cluster 6	-0.01 ± 0.21	-1.11 ± 0.03	0.93 ± 0.06
iolA	BSU39760	Cluster 6	-0.03 ± 0.31	-0.9 ± 0.11	1.17 ± 0.17
yxaH	BSU39970	Cluster 6	-0.02 ± 0.29	-1.72 ± 0.09	0.1 ± 0.1
qdoI	BSU39980	Cluster 6	-0.02 ± 0.3	-2.14 ± 0.15	-0.21 ± 0.05

9. AFFIDAVIT / ERKLÄRUNG

Hiermit erkläre ich, dass diese Arbeit bisher von mir weder an der Mathematisch-Naturwissenschaftlichen Fakultät der Ernst-Moritz-Arndt-Universität Greifswald noch einer anderen wissenschaftlichen Einrichtung zum Zwecke der Promotion eingereicht wurde.

Ferner erkläre ich, dass ich diese Arbeit selbständig verfasst und keine anderen als die darin angegebenen Hilfsmittel und Hilfen benutzt und keine Textabschnitte eines Dritten ohne Kennzeichnung übernommen habe.

Greifswald, date: 24.04.2014 Praveen Kumar Sappa

10. CURRICULUM VITAE

Personal Details

Name	Praveen Kumar Sappa
Date of Birth	05.08.1986
Place of Birth	Tadepalligudem
Nationality	Indian

Educational Qualifications

1. Higher Secondary School (2001-2003): Vikas Junior college, Rajahmundry, India

3. Bachelor in Science (2003-2006): Andhra University, Visakhapatnam, India

4. Masters in Biotechnology (2006-2008): University of Hyderabad, Hyderabad, India

Doctoral Study (since 08/2008): Doctoral student at Interfakultary Institute for Genetics and Functional Genomics, Dept. of Functional Genomics, Ernst-Moritz-Arndt-University, Greifswald, Germany

Greifswald, Date: 24.04.2014 Praveen Kumar Sappa

11. SCIENTIFIC CONTRIBUTIONS

11.1 PUBLICATIONS

Liebal UW*, **Sappa PK***, Millat T, Steil L, Homuth G, Völker U, Wolkenhauer O.
Proteolysis of beta-galactosidase following SigmaB activation in *Bacillus subtilis*.
Mol Biosyst. 2012 Jun;8(6):1806-14. doi: 10.1039/c2mb25031d. Epub 2012 Apr 17.
*Equal contribution

Nicolas P, Mäder U, Dervyn E, Rochat T, Leduc A, Pigeonneau N, Bidnenko E, Marchadier E, Hoebeke M, Aymerich S, Becher D, Bisicchia P, Botella E, Delumeau O, Doherty G, Denham EL, Fogg MJ, Fromion V, Goelzer A, Hansen A, Härtig E, Harwood CR, Homuth G, Jarmer H, Jules M, Klipp E, Le Chat L, Lecointe F, Lewis P, Liebermeister W, March A, Mars RA, Nannapaneni P, Noone D, Pohl S, Rinn B, Rügheimer F, **Sappa PK**, Samson F, Schaffer M, Schwikowski B, Steil L, Stülke J, Wiegert T, Devine KM, Wilkinson AJ, van Dijl JM, Hecker M, Völker U, Bessières P, Noirot P.
Condition-dependent transcriptome reveals high-level regulatory architecture in *Bacillus subtilis*.
Science. 2012 Mar 2;335(6072):1103-6. doi: 10.1126/science.1206848.

Maass S, Sievers S, Zühlke D, Kuzinski J, **Sappa PK**, Muntel J, Hessling B, Bernhardt J, Sietmann R, Völker U, Hecker M, Becher D.
Efficient, global-scale quantification of absolute protein amounts by integration of targeted mass spectrometry and two-dimensional gel-based proteomics.
Anal Chem. 2011 Apr 1;83(7):2677-84. doi: 10.1021/ac1031836. Epub 2011 Mar 11.

Iuga C, Seicean A, Iancu C, Buiga R, **Sappa PK**, Völker U, Hammer E.
Proteomic identification of potential prognostic biomarkers in resectable pancreatic ductal adenocarcinoma.
Sumbitted

Simple method to inhibit the activity of nonspecific proteases during sporulation in *B. subtilis* for shotgun proteomic analysis.
Sappa PK, Steil L, Völker U.

Manuscript under preperation.

Kohlstedt M, **Sappa PK**, Meyer H, Maaß S, Zaprasis A, Hoffmann T, Becker J, Mäder U, Steil L, Hecker M, Stülke J, Bremer E, Lalk M, Völker U and, Wittmann C.
Systems-wide regulation of carbon core metabolism of *Bacillus subtilis* under conditions of osmotic stress and osmoprotection.
Manuscript under preparation.

Hoffmann T, Bleisteiner M, **Sappa PK**, Mäder U, Steil L, Völker U and Bremer E.
Point mutations that render the osmotically controlled *proHJ* promoter of *Bacillus subtilis* hyperactive.
Manuscript under preparation.

11.2 POSTERS

Transcriptome Analysis of Batch and Fed-Batch Fermentations.
Sappa PK, Knoke B, Mäder U, Steil L, Reuss M, Hecker M, and Völker U.
2009, May, Vienna, Austria.

Absolute quantitation of central carbon metabolic proteins in Osmotic stressed *Bacillus subtilis* - deployment of QconCAT strategy.
Sappa PK, Kohlstedt M, Meyer H, Burian M, Mäder U, Hoffmann T, Lalk M, Bremer E, Wittmann C, Völker U.
EuPA-BSPR 2012, June, Glasgow, UK. (awarded Deutsche Gesellschaft für Proteomforschung travel scholarship)

Multi-omics based investigation of central carbon metabolism of glucose starved *Bacillus subtilis* under osmotic stress and osmoprotection.
Sappa PK, Kohlstedt M, Meyer H, Burian M, Mäder U, Hoffmann T, Lalk M, Bremer E, Wittmann C, Völker U.
Proteome forum Berlin - 2013, April, Berlin, Germany. (awarded Deutsche Gesellschaft für Proteomforschung travel scholarship)

12. ACKNOWLEDGEMENTS

I am greatly thankful to Prof. Uwe Völker for giving me this wonderful opportunity to pursue my doctoral studies. I would like to express my gratitude for his immense support at work and beyond which made my stay in Greifswald a great pleasure. His remarkable professional and straightforward approach at sorting out things is a striking quality that I deeply admire.

I would like to especially thank Leif Steil for his support and guidance throughout my work in the lab. He was the one person I used to depend on for advice regardless of the kind of problem and he never gave up without a tough fight. I am extremely thankful to Ulrike Mäder for her timely guidance and help through several collaborative projects I was involved. Her meticulous approach towards the details really helped me to correct my mistakes several times. I would also like to thank Elke Hammer, Frank Schmidt and George Homuth for their helpful discussions and advices. It was my great pleasure working with Dhople and learning key aspects of mass spectrometry from his remarkable experience.

I would like to thank Ulf Leibal (from Rostock), Michael Kohlstedt (from Braunschweig), Hanna Meyer and Sandra Maß for not only being my collaborators but also for their incredible welcoming and friendly relationship. The great fun we had on several business trips was priceless. I would like to thank all the people involved in BaCell-SysMO phase I and phase II for their collaboration and BMBF (Bundesministerium für Bildung und Forschung) for the financial support.

I am greatly thankful to all my friends, current and former colleagues in the lab for creating a wonderful environment at work place. I would like to thank especially Marc Schaffer, Marc Burian, Tej, Priyanka, Hermann, Nico, Henrike, Kristin, Martin, Ravi, Lars, Manu, Gourav, Annette, Franzi, Stefan, Tobi, Abdullah, Malek and all other members in the lab. I would like to thank all the TA's for their timely help especially Anja, Jette and Katrin.

Last but not least I am indebted to my parents, my sister and my wife for their infinite care, love and support throughout my life.